UNIVERSIDADE FEDERAL DO RIO GRANDE DO SUL
INSTITUTO DE CIÊNCIAS BÁSICAS DA SAÚDE
PROGRAMA DE PÓS-GRADUAÇÃO EM CIÊNCIAS BIOLÓGICAS: BIOQUÍMICA

JÚLIO SANTOS TERRA MACHADO

ALTERAÇÕES EM COMPONENTES INIBITÓRIOS AO LONGO DO NEURODESENVOLVIMENTO: EFEITOS PREVENTIVOS DO RESVERATROL EM MODELO ANIMAL DE TEA

TESE DE DOUTORADO

Porto Alegre
2022

JÚLIO SANTOS TERRA MACHADO

ALTERAÇÕES EM COMPONENTES INIBITÓRIOS AO LONGO DO NEURODESENVOLVIMENTO: EFEITOS PREVENTIVOS DO RESVERATROL EM MODELO ANIMAL DE TEA

Tese apresentada ao Instituto de Ciências Básicas da Saúde da Universidade Federal do Rio Grande do Sul como requisito parcial para a obtenção do título de Doutor em Bioquímica.

Orientadora: Prof.ª Dr.ª Carmem Gottfried
Coorientadora: Prof.ª Dr.ª Mellanie Fontes Dutra

Porto Alegre

2022

CIP - Catalogação na Publicação

Machado, Júlio
Alterações em componentes inibitórios ao longo do neurodesenvolvimento: efeitos preventivos do resveratrol em modelo animal de TEA / Júlio Machado. -- 2022.
263 f.
Orientadora: Carmem Gottfried.

Coorientadora: Mellanie Fontes-Dutra.

Tese (Doutorado) -- Universidade Federal do Rio Grande do Sul, Instituto de Ciências Básicas da Saúde, Programa de Pós-Graduação em Ciências Biológicas: Bioquímica, Porto Alegre, BR-RS, 2022.

1. Transtorno do Espectro Autista. 2. Ácido Valproico. 3. Resveratrol. 4. Modelo Animal. 5. Neurodesenvolvimento. I. Gottfried, Carmem, orient. II. Fontes-Dutra, Mellanie, coorient. III. Título.

Elaborada pelo Sistema de Geração Automática de Ficha Catalográfica da UFRGS com os dados fornecidos pelo(a) autor(a).

Júlio Santos Terra Machado

Alterações em componentes inibitórios ao longo do neurodesenvolvimento: efeitos preventivos do resveratrol em modelo animal de TEA

Tese apresentada ao Instituto de Ciências Básicas da Saúde da Universidade Federal do Rio Grande do Sul como requisito parcial para a obtenção do título de Doutor em Bioquímica.

Aprovado em: 25 de abril de 2022.

BANCA EXAMINADORA

_____

Rachel Krolow Santos Silva Bast - UFRGS

_____

Eloísa da Silveira Loss - UFRGS

_____

Marcelo Farina - UFSC

_____

Carmem Gottfried – UFRGS (Orientadora)

Agradecimentos

Inicialmente, agradeço à minha orientadora, professora Carmem Gottfried, pela oportunidade e pelo acolhimento desde 2014. Obrigado por todo incentivo e amparo durante diferentes fases da minha vida acadêmica, proporcionando contatos com múltiplos aspectos do conhecimento e fomentando novas descobertas dentro do GETTEA. Ao Victorio, por abrir as portas do laboratório e por todos os ensinamentos sobre TEA.

Às agências de fomento CNPq, CAPES, Instituto Nacional de Ciência e Tecnologia em NeuroImunoModulação (INCT-NIM) e Fundo de Incentivo à Pesquisa e Eventos (FIPE-HCPA) pelo financiamento.

Ao PPG Bioquímica, por viabilizar um local de aprendizado e discussão de alto nível, proporcionado pela presença de professores altamente qualificados e competentes. À secretaria do PPG, sempre disponível para auxiliar os alunos em quaisquer situações. Aos trabalhadores da recepção e do biotério, responsáveis por manter o ambiente tão acolhedor e produtivo.

Agradeço a todos os ICs (Bibi, Wal, Marília, Giovanna, Bárbara, ...) PGs (Mauro, Gustavo, Gui Cordenonsi, Josemar, Brum, Darling, Gui, Bruna, Mell, Iohanna, ...) pela parceria ao longo dos anos. Agradeço à Mell pela amizade e pela coorientação ao longo do TCC e do doutorado, sem as tuas contribuições e ajudas nos momentos mais críticos não teria sido possível realizar tantas conquistas científicas. Gio, obrigado por ter aceitado fazer parte de um dos momentos mais importantes da minha formação, me concedendo a honra de coorientar um TCC de altíssima qualidade. Bruna, obrigado por todos os momentos de diversão e pelas *playlists* variadas (emo a canto gregoriano). Mauro, muito obrigado pela parceria, ensinamentos de PCR e por ter me feito desenvolver tolerância à cafeína depois das 6 jarras diárias. Iohanna, muito obrigado por ser essa grande amiga durante todos esses anos, sempre me ajudando em qualquer circunstância (experimento, escritas de relatórios, artigos, surtos), com certeza tu foi uma parte fundamental pra que essa tese existisse. A duplinha “Corda e Caçamba” fez o seu nome e, apesar de todas as angústias, produziu conhecimentos incríveis, num ambiente de muito respeito, amizade e admiração.

Às amigas biomédicas Amanda, Bruna, Brenda e Deb por todos os momentos de apoio desde a faculdade (nas situações mais tenebrosas possíveis) e por todos os momentos de felicidade, especialmente nossas jantas maravilhosas.

Aos meus pais, meu agradecimento pelo amor incondicional, pelo apoio irrestrito e por proporcionarem toda a base necessária para que eu pudesse realizar meus estudos da melhor forma possível. A todos os meus familiares, muita gratidão por toda união, amor e afeto, é um privilégio fazer parte de uma família tão alegre e apoiadora, onde todos possuem uns pelos outros um sentimento tão pleno de fraternidade.

À minha amiga-irmã Vitória, quero agradecer por ser esse porto seguro, sempre pronta para aguentar os desabafos mais tenebrosos, realizar os favores mais maçantes (vide revisar inglês de páginas e páginas...) mas também por compartilhar de momentos felizes desde o princípio dos tempos. Aproveito para agradecer também ao meu querido Nonino, lenda do horror/realismo fantástico/mágico latinoamericano e da contenção dos (meus) surtos diários.

Ao Marcos, agradeço por ser esse irmão de longa data, disposto sempre ao que de melhor (ou pior) a Fernandes é capaz de oferecer. À Taís, por ser simplesmente Amiga Desde Sempre, fundamental para conversas ininterruptas no trajeto Porto Alegre – São Simão.

Aos meus queridos Bruno e Mariana, não sei o que teria sido dos períodos de isolamento sem as videochamadas de sexta, apenas agradecer por tantos anos de muita amizade e apoio desses seres humanos incríveis.

Às queridas Marina e Fernanda, amigas que sempre se fazem presentes de alguma forma, sempre prontas pra conversar sobre a vida e ouvir desabafos.

Ao André, por nunca medir esforços para ajudar os amigos, teu coração é do tamanho do mundo (e a tua capacidade de crítica também!). Ao Vitor, por ter o astral capaz de animar qualquer um, tu é uma pessoa que realmente inspira os que estão ao teu redor a seguir em frente com muita determinação (e teimosia). Ao Frê, pela paz e tranquilidade de quem sabe que vai dar tudo certo no final, já que sempre vai existir tua casa em São Simão pra gente se reunir, dar risada e recarregar as baterias.

Aos animais de experimentação e a todos que acreditam no potencial da ciência brasileira.

“As janelas estavam tapadas, completamente fechadas com tijolos. Para evitar que alguém entrasse ou que algo saísse?”

Mariana Enríquez

SUMÁRIO

PARTE I

RESUMO

O transtorno do espectro autista (TEA) é uma desordem multifatorial complexa cuja fisiopatologia ainda não é completamente compreendida. Entretanto, algumas características, como as alterações nos componentes inibitórios encefálicos, se evidenciam nessa desordem. Dentre os principais fatores de risco ambientais para o TEA se destaca a exposição ao ácido valproico (VPA) durante a gestação, de forma que se utilizou o modelo animal baseado nessa abordagem para a obtenção dos dados experimentais. No Capítulo I, realizou-se um compilado de dados da literatura sobre o papel de fatores de transcrição (FTs) em diferentes desordens do neurodesenvolvimento; além disso, foram feitas análises, utilizando ferramentas de bioinformática, dos principais locais de expressão, bem como dos momentos de pico de expressão e das possíveis rotas de interação entre os FTs, incluindo os possíveis prejuízos induzidos pelo VPA. Essa análise contribuiu para a identificação de diversas hipóteses que poderiam estar associadas com danos observados na vida pós-natal. Sabendo-se que o VPA possui características pró-inflamatórias e pró-oxidantes, o resveratrol (RSV), polifenol com características anti-inflamatórias, antioxidantes e neuroprotetoras, surge como uma estratégia interessante de contraposição dessas características, viabilizando um estudo importante de vias envolvidas no TEA. No Capítulo II, foi possível observar que o VPA induziu vastas alterações na composição neuronal do córtex pré-frontal medial (CPFm) e, em menor escala, no hipocampo (HC), além de reduzir a expressão de receptor $GABA_A$ e das proteínas sinápticas neuroliguina-2 e gefirina. O tratamento com RSV foi capaz de prevenir, de forma geral, as alterações em neurônios totais e interneurônios GABAérgicos (IGs) no CPFm, porém não no HC. Além disso, o RSV também teve um efeito similar ao VPA na expressão de proteínas sinápticas no CPFm. Análises de bancos de dados de modelos animais em idade embrionária ressaltam alterações na maquinaria transcricional, metabolismo de carboidratos, metabolismo mitocondrial e ciclo celular, via da WNT, via da NOTCH e outros, sugerindo, junto ao Capítulo I, hipóteses referentes às ações do VPA e do RSV. No Capítulo III, foi observada uma expansão do dano hipocampal induzida pela exposição ao VPA, com descontinuidade do giro denteado e descompactação de CA1, além de alterações disseminadas na composição neuronal em todas as sub-regiões do HC. O RSV preveniu a alteração morfológica, além de equilibrar diversos parâmetros associados a IGs e neurônios totais. A exposição ao VPA induziu alterações na expressão de PTEN, AKT e CK2, não prevenidas por RSV. A partir destes dados, conclui-se que a exposição ao VPA pode desencadear alterações em etapas iniciais do desenvolvimento embrionário, com consequentes alterações pós-natais. Em animais jovens, foram observadas alterações em IGs, sinapses e receptor $GABA_A$. Em animais adultos, o HC se destaca como uma região fortemente alterada, indicando um provável agravamento ao longo da vida. É provável que a ação preventiva do RSV ocorra por oposição ao VPA em vias de regulação da transcrição, metabolismo e outras, conforme apontam os Capítulos I e II. Dessa forma, observa-se que uma intervenção precoce é capaz de mudar o panorama de evolução da desordem, abrindo horizontes para estudos de novas abordagens no TEA.

Palavras-chave: transtorno do espectro autista, modelo animal, ácido valproico, resveratrol, interneurônios GABAérgicos, sinapses, fatores de transcrição.

ABSTRACT

Autism spectrum disorder (ASD) is a complex multifactorial disorder whose pathophysiology is not yet fully understood. However, some characteristics, such as changes in brain inhibitory components, emerge in this disorder. Among the main environmental risk factors for ASD, exposure to valproic acid (VPA) during pregnancy stands out, so the animal model based on this approach was used to obtain the experimental data. In Chapter I, a compilation of data from the literature on the role of transcription factors (TFs) in different neurodevelopmental disorders was carried out, in addition, analyzes were conducted, using bioinformatics tools, of the main sites of expression, as well as the moments of peak expression and possible routes of interaction among TFs, including possible damage induced by VPA. This analysis contributed to the identification of several hypotheses that could be associated with the damage observed in postnatal life. Knowing that VPA has pro-inflammatory and pro-oxidant characteristics, resveratrol (RSV), a polyphenol with anti-inflammatory, antioxidant, and neuroprotective characteristics, appears as an interesting strategy to counteract these characteristics, enabling an important study of the pathways involved in ASD. In Chapter II, it was possible to observe that VPA induced vast changes in the neuronal composition of the medial prefrontal cortex (mPFC) and, to a lesser extent, in the hippocampus (HC), in addition to reducing the expression of $GABA_A$ receptor and synaptic proteins neuroligin-2 and gephyrin. Treatment with RSV was able to generally prevent changes in total neurons and GABAergic interneurons (GIs) in mPFC, but not in the HC. Furthermore, RSV also had a similar effect to VPA on the expression of synaptic proteins in the mPFC. Database analyzes of animal models at embryonic age highlight changes in transcriptional machinery, carbohydrate metabolism, mitochondrial metabolism, cell cycle, WNT pathway, NOTCH pathway, and others, suggesting, together with Chapter I, hypotheses regarding the actions of VPA and the RSV. In Chapter III, an expansion of the hippocampal damage induced by exposure to VPA was observed, with discontinuity of the dentate gyrus and decompaction of the CA1, in addition to widespread changes in neuronal composition in all HC subregions. RSV prevented the morphological change, in addition to balancing several parameters associated with IGs and total neurons. Exposure to VPA induced changes in the expression of PTEN, AKT and CK2, not prevented by RSV. From these data, it is concluded that exposure to VPA can trigger changes in early stages of embryonic development, with consequent postnatal changes. In young animals, changes were observed in GIs, synapses, and $GABA_A$ receptor. In adult animals, the HC stands out as a strongly altered region, indicating a probable worsening throughout life. It is likely that the preventive action of RSV occurs in opposition to VPA in transcriptional, metabolic, and other regulatory pathways, as indicated in Chapters I and II. In this way, it is observed that an early intervention can change the course of the disorder, opening horizons for studies of new approaches in ASD.

Keywords: Autism Spectrum Disorder, animal model, valproic acid, resveratrol, GABAergic interneurons, synapses, transcription factors.

LISTA DE ABREVIATURAS

AChE – Acetilcolinesterase

ADDM – Monitoramento de Autismo e Desordens do Desenvolvimento, do inglês *Autism and Developmental Disabilities Monitoring*

ADHD – Transtorno do déficit de atenção e hiperatividade, do inglês *attention deficit hyperactivity disorder*

ADNP – Fator neuroprotetor homeobox atividade-dependente, do inglês *activity-dependent neuroprotector homeobox fator*

AIM – Ativação imune materna, em inglês MIA (*maternal immune activation*)

AKT – RAC (família Rho)-alfa serina/treonina-proteína cinase, do inglês *RAC (Rho family)-alpha serine/threonine-protein kinase*

AMPA – Receptor de ácido α-amino-3-hidroxi-5-metil-4-isoxazolepropiônico, do inglês *α-amino-3-hydroxy-5-methyl-4-isoxazolepropionic acid receptor*

AMPK – Proteína cinase ativada por AMP, do inglês *AMP-activated kinase protein*

ANOVA – Análise de variância

ARE – Elementos responsivos ao álcool, do inglês *alcohol responsive elements*

ARIDB1 – Proteína 1B contendo domínio interativo rico em AT, do inglês *AT-rich interactive domain-containing protein 1B*

ARX – Proteína homeobox associada a aristaless, do inglês *aristaless related homeobox protein*

ATP – Adenosina trifosfato

ATP6 – Subunidade 6 da membrana da ATP sintase codificada mitocondrialmente, do inglês *mitochondrially encoded ATP synthase membrane subunit 6*

AWARD – Autism Wellbeing And Research Development

BAF – Fator dependente de ATP associado a BRG1/BRM, do inglês *ATP-dependent BRG1/BRM associated factor*

BCL-2 – Proteína envolvida no linfoma de células B 2, do inglês, *B-cell lymphoma 2 associated protein*

BNDF – Fator neurotrófico derivado do cérebro, do inglês *brain-derived neurotrophic factor*

BSA – Albumina sérica bovina, do inglês *bovine serum albumine*

BTBR – Cepa de camundongo BTBR T+Itpr3tf/J, um modelo genético de TEA

CA – Cornu ammonis

CACNA1A – subunidade alfa1 A do canal de cálcio dependente de voltagem, do inglês *calcium voltage-gated channel subunit alpha1 A*

CAPES – Coordenação de Aperfeiçoamento de Pessoal de Nível Superior

CB – Calbindina, quando CB+ ou CB^{+} interneurônio GABAérgico positivo para calbindina

CCa – Córtex cingulado anterior, em inglês **aCC** (*anterior cingulate cortex*)

CCL2 – Ligante do motivo C-C de quimiocina 2, do inglês *C-C motif chemokine ligand 2*

CDC – Centro de Controle e Prevenção de Doenças, do inglês *Centers for Disease Control and Prevention*

CEUA – Comissão de Ética no Uso de Animais

CHD8 – Proteína de ligação ao cromodomínio-helicase-DNA 8, do inglês *chromodomain-helicase-DNA-binding protein 8*

CI – Córtex infra-límbico, em inglês **IL** (*infra-limbic cortex*)

circRNA – RNA circular

CK2 – Caseína Cinase 2, do inglês *casein kinase 2*

CMM – Centro de Microscopia e Microanálises

CMV – Citomegalovírus

CNPq – Conselho Nacional de Desenvolvimento Científico e Tecnológico

CONCEA – Conselho Nacional de Controle de Experimentação Animal

COVID-19 – Doença causada pelo coronavírus – 19, do inglês *coronavirus disease – 19*

COX2 – Ciclo-oxigenase 2

CPFm – Córtex pré-frontal medial, em inglês **mPFC** (*medial prefrontal cortex*)

CPL – Córtex pré-límbico, em inglês **PrL** (*pre-limbic cortex*)

CREAL – Centro de Reprodução e Experimentação de Animais de Laboratório

CTIP2 – Proteína que interage com COUP-TF 2, do inglês *COUP-TF-interacting protein 2*

CTNAP2 – Proteína tipo 2 associada à contactina, do inglês *contactin associated protein 2*

CXCL12 – Quimiocina C-X-C com motivo 12, do inglês *C-X-C motif chemokine 12*

CXCR4 – Receptor de quimiocinas C-X-C do tipo 4, do inglês *C-X-C chemokine receptor type 4*

DAPI – 4',6'-diamino-2-fenil-indol

DCV – Doenças cardiovasculares

DLX – Proteína distal-less homeobox, do inglês *homebox distal-less protein*

DMSO – Dimetilsulfóxido

DNA – Ácido desoxirribonucleico, do inglês *desoxirribonucleic acid*

DNs – Desordens do neurodesenvolvimento

DS – Base de dados, do inglês *database*

DSM – Manual de Diagnóstico e Estatística de Transtornos Mentais, do inglês *Diagnostic and Statistical Manual of Mental Disorders*

E/I – Balanço excitatório/inibitório

EDTA – Ácido etilenodiamino tetra-acético, do inglês *ethylenediamine tetra-acetic acid*

EG – Eminência gangliônica, em inglês **GE** (*ganglionic eminence)*

EGC – Eminência gangliônica central, em inglês **CGE** (*central ganglionic eminence*)

EGM – Eminência gangliônica medial

EGR2 – Proteína de crescimento precoce 2, do inglês *early growth response protein 2*

EN2 – Proteína homebox engrailed-2, do inglês *engrailed-2 homebox protein*

EROs – Espécies reativas de oxigênio, do inglês *reactive species of oxygen*

EUA – Estados Unidos da América

FEV – Proteína Variante Fifth Ewing, do inglês *fifth ewing variant protein*

FMRP – Regulador transcricional FMRP 1, do inglês *FMRP translational regulator 1*

FOXP3 – Fator de transcrição forkhead box P3, do inglês *forkhead box P3 transcription factor*

FT – Fator de transcrição, em inglês **TF** *transcription fator*

GABA – Ácido gama-aminobutírico

GAD – Glutamato descarboxilase

GATA3 – Fator de transcrição que reconhece sequências de nucleotídeos G-A-T-A em promotores de genes alvo 3, do inglês *GATA binding protein 3*

GD – Giro Denteado, em inglês **DG** (*dentate gyrus*)

GDE – Gene diferencialmente expresso, em inglês **DEG** (*differentially expressed gene*)

GETTEA – Grupo de Estudos Translacionais em Transtorno do Espectro Autista

GFAP – Proteína ácida fibrilar glial, do inglês *glial fibrillary acidic protein*

GLT1 – Transportador astrocítico de glutamato 1, do inglês *astrocytic glutamate transporter 1*

GO – Ontologia genética, do inglês *gene ontology*

GS – Glutamina sintetase

GSK3β – Glicogênio sintase cinase 3 beta, do inglês *glycogen synthase kinase 3 beta*

GTF – Fator de transcrição geral, do inglês *general transcription fator*

GWAS – estudos de associação ampla do genoma, do inglês *Genome wide association studies*

HC – Hipocampo

HDAC – Desacetilase de histonas, do inglês *histone deacetylase*

HES1 – Fator de transcrição Hes1 da família BHLH, do inglês *Hes family BHLH transcription factor 1*

HIPPO – Via biológica caracterizada pela proteína cinase *hippo*

HOXA1 – Proteína homeobox A1, do inglês *homeobox protein HOX-A1*

HOXB1 – Proteína homeobox B1, do inglês *homeobox protein HOX-B1*

HPLC – Cromatografia líquida de alta eficiência, do inglês *high-performance liquid chromatography*

HRP – Peroxidase do rabanete, do inglês *horseradish peroxidase*

HSF1 – Fator de choque térmico 1, do inglês *heat shock factor 1*

ICBS – Instituto de Ciências Básicas de Saúde

IG – Interneurônio GABAérgico, em inglês **GI** (*GABAergic interneuron*)

IL – Interleucina

INCT-NIM – Instituto Nacional de Ciência e Tecnologia – Neuroimunomodulação

IUPAC – União Internacional de Química Pura e Aplicada, do inglês *International Union of Pure and Applied Chemistry*

JAK – Janus cinase, do inglês *janus kinase*

KCC2 – Cotransportador de cloreto e potássio 2, do inglês *potassium chloride cotransporter 2*

KO – Nocaute, do inglês *knockout*

LHX6 – Fator LIM homeobox 6, do inglês *LIM homeobox 6 factor*

LPS – Lipopolissacarídeo

MAP/ERK – Via da Ras-Raf-MEK-ERK, do inglês *Ras-Raf-MEK-ERK pathway*

MAZ – Proteína dedo de zinco associada a MYC, do inglês *myc associated zinc finger protein*

MECP2 – Proteína de ligação a metil–CpG 2, do inglês *methyl-cpg binding protein 2*

miRNA – micro RNA

mTOR – Alvo da rapamicina em mamíferos, do inglês *mammalian target of rapamycin*

mTORC1 – Complexo 1 da mTOR

NADPH – Nicotinamida adenina dinucleotídeo fosfato

NeuN – Proteína neuronal nuclear, do inglês *neuronal nuclear protein*

NEUROD1 – Fator de diferenciação neuronal 1, do inglês *neuronal differentiation factor 1*

NGN2 – Neurogenina-2

NIH – National Institute of Health

NK – Linfócito exterminador natural, do inglês *natural killer*

NKX2.1 – Fator de transcrição homebox 1 NK2, do inglês *NK2 homeobox 1 transcription factor*

NKκB – Fator nuclear kappa B, do inglês *nuclear factor kappa B*

NOTCH – Via biológica caracterizada pelo receptor *notch*

OXTR – Receptor de oxitocina, do inglês *oxytocin receptor*

PAX – Fator de transcrição paired box, do inglês *paired box transcription fator*

PBS – Tampão fosfato-salina, do inglês *phosphate buffered salin*

PGC – Coativador do receptor ativado por proliferadores de peroxissomo gama, do inglês, *peroxisome proliferator-activated receptor gamma coactivator*

PITX3 – Proteína homeobox 3 da hipófise, do inglês *pituitary homeobox 3*

POUF – Fator de transcrição da classe de domínio POU, do inglês *POU domain class transcription factor*

PPR-γ – Receptor ativado por proliferadores de peroxissomo gama, do inglês *peroxisome proliferator-activated receptor gamma*

PSD95 – Proteína da densidade pós-sináptica 95, do inglês, *postsynaptic density protein 95*

PTEN – Fosfatase homóloga à tensina, do inglês *phosphatase and tensin homologue*

PV – Parvalbumina, quando PV+ ou PV^{+} interneurônio GABAérgico positivo para parvalbumina

RARB – Receptor de ácido retinóico beta, do inglês *retinoic acid receptor beta*

REST – Fator de transcrição silenciador de RE-1, do inglês *RE1-silencing transcription factor*

RMf – Ressonância Magnética funcional

RNA – Ácido ribonucleico, do inglês *ribonucleic acid*

RNA-Seq – Sequenciamento de RNA, do inglês *RNA-sequencing*

ROR-γT – Receptor gama órfão relacionado a RAR, do inglês, *RAR-related orphan receptor gamma*

RSV – Resveratrol

RT-qPCR – Reação em cadeia da polimerase quantitativa precedida de transcrição reversa, do inglês *quantitative polymerase chain reaction preceded by reverse transcription*

SAF – Síndrome alcoólica fetal

SDS – Dodecil sulfato de sódio, do inglês *sodium dodecyl sulfate*

SFARI – Simons Foundation Autism Research Initiative

SHANK3 – Proteína com SH3 e múltiplos domínios repetidos de anquirina 3, do inglês *SH3 and multiple ankyrin repeat domains 3 protein*

SHH – Proteína Sonic - porco espinho, do inglês *sonic hedgehog protein*

SHOX – Fator homeobox relacionado à baixa estatura, do inglês *short stature homeobox containing gene*

SIRT – Sirtuína

SLC25A12 – Membro 12 da família 25 de carreadores de soluto, do inglês *solute carrier family 25 member 12*

SNC – Sistema nervoso central

SOM – Somatostatina, quando SOM+ ou SOM^{+} interneurônio GABAérgico positivo para somatostatina

SOX – Fator de transcrição associado a SRY-box, do inglês *SRY-box transcription factor*

SP1 – Fator de transcrição Sp1, do inglês *Sp1 transcription factor*

SPTH – Síndrome de Pitt Hopkins

STAT – Transdutor de sinal e ativador da transcrição, do inglês *signal transducer and activator of transcription*

T-bet – Fator 21 de transcrição da T-Box, do inglês *T-Box transcription factor 21*

TBR1 – Fator de transcrição do cérebro 1 associado a T-box, do inglês *T-Box brain transcription factor 1*

TCF4 – Fator de transcrição 4, do inglês *transcription fator 4*

TEA – Transtorno do Espectro Autista, em inglês ASD (*Autism Spectrum Disorder*)

TGF – Fator de transformação do crescimento beta, do inglês *transforming growth factor beta*

Th – T *helper*

TLR – Receptor toll-like, do inglês *toll-like receptor*

TNF – Fator de necrose tumoral, do inglês *tumoral necrosis fator*

TRIS/HCl – Tampão tris(hidroximetil)aminometano/ácido clorídrico

TTBS – Tampão salina com TRIS e polissorbato 20 (Tween 20)

UFRGS – Universidade Federal do Rio Grande do Sul

V1aR – Receptor de vasopressina 1ª, do inglês *vasopressin receptor 1ª*

VGLUT – Transportador vesicular 1 de glutamato, do inglês *vesicular glutamate transporter 1*

VPA – Ácido Valproico, do inglês *valproic acid*

WNT – Via biológica cuja sigla em inglês contém letras das palavras *Wingless* (drosófilas mutantes sem asas) e *Int* (denominação do gene mutante que causa a ausência de asas)

ZNF292 – Proteína dedo de zinco 292, do inglês *zinc finger protein 292*

LISTA DE FIGURAS

1. INTRODUÇÃO

1.1 Transtorno do Espectro Autista

O Transtorno do Espectro Autista (TEA) é uma desordem do neurodesenvolvimento caracterizada, segundo o Manual Diagnóstico e Estatístico de Transtornos Mentais - 5ª edição (AMERICAN PSYCHIATRIC ASSOCIATION, 2013) (DSM-5), por prejuízos de comunicação e interação social, além de comportamentos repetitivos ou estereotipados. Além disso, diversas comorbidades já foram descritas no contexto do TEA, incluindo alterações sensoriais, distúrbios gastrointestinais, ansiedade e epilepsia (VEENSTRA-VANDERWEELE; BLAKELY, 2011). Em relação à última, se estima que até 30% dos indivíduos com TEA apresentam epilepsia ou alterações eletrofisiológicas como convulsões (SPENCE; SCHNEIDER, 2009).

Diversas hipóteses buscam explicar os mecanismos neurobiológicos subjacentes à desordem. Uma das principais sugere a existência de um desequilíbrio entre excitação e inibição no encéfalo de indivíduos com TEA, com prevalência da excitação sobre a inibição (E/I) (UZUNOVA; PALLANTI; HOLLANDER, 2016). A principal implicação dessa característica, além dos distúrbios eletrofisiológicos, seria a alteração no padrão de conectividade encefálica: redução na conectividade entre diferentes regiões, prejudicando a integração e aumentando o processamento local (BELMONTE *et al.*, 2004). O hiperprocessamento local, por sua vez, possivelmente induz uma sobrecarga que converte estímulos não nocivos em nocivos, condição comum no TEA (MARKRAM; MARKRAM, 2010).

Historicamente, a primeira utilização do termo “autismo” foi feita em 1911 pelo psiquiatra suíço Paul Eugen Bleuler ao descrever o comportamento retraído e “distante da realidade” apresentado por crianças diagnosticadas com esquizofrenia (BLEULER; BLEULER, 1986). Posteriormente, em 1926, a psiquiatra russa Grunya Sukhareva utilizou a denominação “autismo” para caracterizar indivíduos com prejuízos sociais e estereotipias, sendo a primeira descrição detalhada da desordem no formato similar à concepção vigente atualmente (SSUCHAREWA, 1926).

Na década de 1940, Leo Kanner e Hans Asperger, psiquiatras austríacos, realizaram importantes contribuições para a descrição do autismo: Kanner estudou crianças com prejuízos de interação social e linguagem, denominando essas características de “autismo infantil precoce” (KANNER, 1943), enquanto Asperger descreveu a “psicopatia autista” em crianças, definida por dificuldades de estabelecimento de vínculos sociais, foco seletivo, presença de alterações motoras e

outras características (ASPERGER, 1944). Apesar do pioneirismo, Kanner é responsável pela criação do conceito errôneo de “mãe geladeira”, onde atribuía o surgimento do autismo às mães “afetivamente frias” – a popularização dessa hipótese, além de prejudicar os estudos sobre o tema, ainda gerou intenso sofrimento para as famílias envolvidas (KANNER, 1949). Asperger, por sua vez, foi complacente com o regime nazista, conforme apontam estudos mais recentes, inclusive encaminhando crianças para a clínica *Am Spiegelgrund* (BARON-COHEN, 2018; CZECH, 2018), onde tinha ciência de que fariam parte da “Ação T4”, a iniciativa nazista de eliminar pessoas com deficiência física e/ou mental e portadores de doenças consideradas incuráveis (ROTZOLL *et al.*, 2010).

1.2 Epidemiologia do TEA

A prevalência mundial do transtorno é estimada em 1 a cada 160 crianças (ELSABBAGH *et al.*, 2012), entretanto, a ausência de dados epidemiológicos consistentes em diversos países é um dos componentes que dificulta essa estimativa. Na América Latina, alguns países apresentam dados preliminares ou de estudos-piloto sobre a prevalência, incluindo: Maracaibo, Venezuela (17/10.000) (MONTIEL-NAVA; PEÑA, 2008), San Isidro, Argentina (13,1/10.000) (LEJARRAGA *et al.*, 2008), Atibaia, Brasil (27,2/10.000) (PAULA *et al.*, 2011), Quito, Equador (11/10.000) (DEKKERS *et al.*, 2015) e Guanajuato, México (87/10.000) (FOMBONNE *et al.*, 2016). As discrepâncias observadas entre esses países provavelmente se devem às diferenças e limitações metodológicas de cada estudo.

Nos EUA, os primeiros estudos de prevalência datam da década de 1970, quando a prevalência apontada foi de 3,1/10.000 crianças (TREFFERT, 1970). Os dados mais recentes do Centro de Controle e Prevenção de Doenças (CDC, do inglês *Center for Disease Control and Prevention*) (referentes ao ano de 2018), obtidos pela Rede de Monitoramento de Autismo e Desordens do Desenvolvimento (ADDM, do inglês *Autism and Developmental Disabilities Monitoring*), apontam 230/10.000 crianças até 8 anos de idade, o equivalente a 1/44 (MAENNER *et al.*, 2021). Esse dado indica um importante aumento na prevalência nas últimas décadas – em 2000, ano do primeiro acompanhamento da ADDM, a prevalência estimada era de 67/10.000 (RICE, 2007). Ainda, interessantemente, os mesmos dados indicam que a incidência em indivíduos do sexo masculino é aproximadamente quatro vezes maior do que no sexo feminino. Existem diversas hipóteses para as diferenças

observadas entre os sexos, incluindo a ação da testosterona durante a vida fetal (BARON-COHEN *et al.*, 2011), um potencial efeito protetivo da presença de dois cromossomos X (visto que vários alelos associados com risco de TEA estão localizados nesse cromossomo) (WERLING; GESCHWIND, 2015), além do subdiagnóstico em pessoas do sexo feminino, tendo em vista que as características muitas vezes não se enquadram nos padrões estabelecidos pelos manuais (FERRI; ABEL; BRODKIN, 2018).

O aumento da prevalência ao longo dos anos se deve, em grande parte, às alterações nos critérios diagnósticos do TEA. Segundo um acompanhamento feito na Dinamarca com todos os nascidos vivos entre 1980 e 1991, 60% do aumento na prevalência se deve a mudanças no diagnóstico (HANSEN; SCHENDEL; PARNER, 2015). Nos EUA, uma projeção aponta que 54% do aumento na prevalência se deva a fatores como ampliação do diagnóstico e conscientização social (WEINTRAUB, 2011). De modo geral, uma parcela relevante (cerca de 40%) da variação epidemiológica nos últimos anos está associada a fatores desconhecidos ou não especificados.

1.3 Fatores de risco para o desenvolvimento de TEA

O TEA é considerado uma desordem de etiologia multifatorial, tendo diversos fatores de risco, tanto genéticos quanto ambientais. A interação entre esses fatores é fundamental para definir o fenótipo de cada indivíduo, questão que possivelmente contribui para a heterogeneidade do transtorno.

1.3.1 Fatores Genéticos

Os valores de herdabilidade e concordância para TEA entre gêmeos monozigóticos chegam a mais de 90% (ROSENBERG, R. E. *et al.*, 2009; SANDIN *et al.*, 2017), demonstrando a relevância do componente genético para a desordem. Dentre os principais genes alterados no TEA, destacam-se os que codificam proteínas associadas com a estrutura sináptica (neuroliguinas, neurexinas, SHANK (GUANG *et al.*, 2018)), transportadores de glutamato/aspartato (SLC25A12 (TURUNEN *et al.*, 2008)), reguladores de transcrição (FTs) (CHD8 (SUGATHAN *et al.*, 2014)), MECP2 (WEN *et al.*, 2017), fatores de transcrição (ARX (SHERR, 2003), HOXA1, HOXB1 (INGRAM *et al.*, 2000)), canais de cálcio (CACNA1A (DAMAJ *et al.*, 2015)), receptores de oxitocina (OXTR (LOPARO; WALDMAN, 2015)) e outros. Um amplo estudo recente identificou alterações em 102 genes no TEA, a maioria

demonstrando um padrão alto de expressão desde o princípio do desenvolvimento encefálico, além de envolvimento na formação sináptica e no desenvolvimento de neurônios excitatórios e inibitórios (SATTERSTROM *et al.*, 2020). Recentemente, componentes como miRNA (SCHEPICI *et al.*, 2019), lncRNA (COGILL *et al.*, 2018) e circRNA (CHEN, Y. J. *et al.*, 2020) vêm emergindo, não apenas no contexto de alterações em vias biológicas como também em alternativas promissoras de biomarcadores (ainda inexistentes no TEA) (SALLOUM-ASFAR *et al.*, 2021), tendo em vista que podem ser obtidos de fluidos biológicos como plasma e saliva (YERI *et al.*, 2017). Finalmente, evidências relacionadas a aspectos epigenéticos, especialmente alterações no padrão de metilação e modificação de histonas, já foram descritos no TEA (ESHRAGHI *et al.*, 2018). Tendo em consideração que diferentes fatores exógenos podem induzir alterações epigenéticas, é provável que esse seja um possível elo entre os aspectos genéticos e ambientais (CAVALLI; HEARD, 2019).

1.3.2 Fatores Ambientais

Os fatores de risco ambientais associados ao TEA contemplam um grupo diverso de variáveis, as quais, majoritariamente, estão associadas a alterações ocasionadas durante o período gestacional ou perinatal. Cabe ressaltar, inicialmente, a existência de um grave equívoco nesse tema: a teoria de que o processo de imunização poderia ser um fator de risco. Essa hipótese foi ventilada após a publicação, em periódico de alto impacto, de um artigo (já retratado) que associava a vacina tríplice viral ao desencadeamento de autismo – o trabalho, além de conter diversos erros metodológicos, ainda era produto de forte conflito de interesse. Uma ampla gama de evidências demonstra que não existe qualquer tipo de associação nesse aspecto (DESTEFANO; SHIMABUKURO, 2019; EGGERTSON, 2010; FOLB *et al.*, 2004).

A ativação imunitária materna (AIM), caracterizada pela ativação imunológica em resposta a um agente infeccioso durante a gestação (MINAKOVA; WARNER, 2018), já foi associada com diferentes desordens psiquiátricas, especialmente TEA e esquizofrenia (BROWN; CONWAY, 2019). A liberação de sinalizadores pró-inflamatórios como IL-1β, IL-6, IL-17 e TNF-α (MINAKOVA; WARNER, 2018), além da ativação de receptores do tipo Toll (TLR, do inglês *Toll-like receptor*) (HAN *et al.*, 2021) são alguns dos principais fatores que medeiam os efeitos da AIM no

embrião/feto. Ainda, condições que não envolvem a presença de patógenos como as doenças autoimunes e a obesidade também podem ser consideradas fatores de risco, uma vez que há uma ativação inflamatória basal, além disso, especialmente no caso das doenças autoimunes, pode ocorrer a passagem placentária de autoanticorpos anti-cérebro (BRIMBERG *et al.*, 2013).

Durante o primeiro trimestre gestacional, os agentes virais são os principais fatores de risco, especialmente os vírus *citomegalovírus* (CMV) e *rubella* – já existem hipóteses que indicam que o *Sars-CoV-2* poderia estabelecer o mesmo tipo de associação, porém ainda não há estudos conclusivos sobre esse tema (STEINMAN, 2020). A infecção pelo vírus causador da rubéola, além de alterar os parâmetros inflamatórios, também é capaz de ocasionar a rubéola congênita, uma vez que o vírus é capaz de ultrapassar a barreira placentária (ROBERTSON *et al.*, 2003). As principais consequências para o feto são danos cardíacos e oftalmológicos, além de atrasos no desenvolvimento neurológico, incluindo alterações na fala, pontos que estabelecem sobreposição com TEA (BERGER; NAVAR-BOGGAN; OMER, 2011). Foi observado, em fetos, que essa condição causava uma extensa ativação de linfócitos NK, T (PARKER *et al.*, 2020) e microglia (GANGULI; CHAVALI, 2021) – interessantemente, estudos da década de 1970 nos EUA apontam que o TEA era duzentas vezes mais prevalente em crianças com rubéola congênita, demonstrando uma importante associação (CHESS, 1971). De forma similar, o CMV também é capaz de causar surdez e alterações visuais no feto (STAGNO *et al.*, 1977) e, além disso, a infecção congênita por CMV foi relacionada com um aumento de dez vezes na prevalência de TEA (GENTILE *et al.*, 2017).

Durante os últimos dois trimestres da gestação, a espécie do patógeno não parece ser um fator diferencial para o risco de TEA. Nesse período, especialmente, infecções bacterianas de origem geniturinária, são capazes de induzir importantes respostas imunológicas mediadas por fatores como IL-1β, IL-4, IL-5, IL-10, TNF-α, TNF-β, IFN-γ, já identificados tanto no plasma materno quanto no fluido amniótico fetal e no plasma de neonatos com TEA (FONTES-DUTRA *et al.*, 2020). A presença de moléculas como lipopolissacarídeo (LPS) e enterotoxina A nos microrganismos contribui para a resposta imunológica exacerbada. Interessantemente, a exposição gestacional ao LPS é um dos modelos mais consolidados de indução de características do tipo autista em animais (PATTERSON, 2011).

Diversos fatores químicos e farmacológicos também apresentam risco importante durante o período gestacional. A talidomida foi um dos primeiros teratógenos amplamente estudados, segundo estimativas de um estudo sueco a prevalência de TEA entre indivíduos expostos durante a gestação era cinquenta vezes maior do que na população geral, além disso, esses indivíduos possuíam diversas alterações nos nervos cranianos, indicando lesão inicial no tronco encefálico (RODIER *et al.*, 1996). O consumo de etanol durante o período gestacional está associado com o desenvolvimento da síndrome alcoólica fetal (SAF), uma desordem marcada pelas malformações craniofaciais e alterações cerebrais (VORGIAS; BERNSTEIN, 2022), interessantemente a prevalência de TEA na SAF é duas vezes maior que na população em geral (STEVENS *et al.*, 2013; VORGIAS; BERNSTEIN, 2022). A principal hipótese para explicar essa associação é a de que o etanol promove amplas alterações no padrão de metilação do DNA, impactando na expressão de genes fundamentais para o neurodesenvolvimento como BDNF, VGLUT, GFAP e outros (BASAVARAJAPPA; SUBBANNA, 2016).

Finalmente, o ácido valproico (VPA) (IUPAC: ácido 2-propionil pentanoico), um fármaco amplamente utilizado como anticonvulsivante, estabilizador de humor e no tratamento de enxaqueca, também já demonstrou relação importante com o TEA (quando utilizado durante o período gestacional) (CHRISTENSEN *et al.*, 2013). O mecanismo de ação desse fármaco está associado a diversas atividades, incluindo o bloqueio de canais iônicos, inibição da GABA transaminase e succinato semialdeído desidrogenase (aumentando a disponibilidade de GABA) e inibição de desacetilases de histonas (HDACs) (RAHMAN; NGUYEN, 2022). O VPA é capaz de atingir seu pico de absorção uma a duas horas após a ingesta oral na forma de comprimidos revestidos, tendo uma meia-vida de eliminação de dez a dezesseis horas, a qual se mantém mesmo em indivíduos que realizam uso contínuo (GUGLER; VON UNRUH, 2012). Além disso, o VPA é capaz de atravessar barreiras biológicas como a hematoencefálica (CORNFORD; DIEP; PARDRIDGE, 1985) e a placentária (FOWLER; EADIE; DICKINSON, 1989). Em estudo feito com macacos rhesus, foi observado que, quinze minutos após a injeção intravenosa de VPA fêmea prenhe, os fetos já apresentavam concentrações séricas do fármaco similares às maternas – em análise tecidual, se observou uma ampla distribuição nos tecidos fetais, inclusive no cérebro (ainda que inferior ao observado em outros tecidos) (DICKINSON *et al.*, 1980).

Um estudo dinamarquês de 2013 que acompanhou todos os nascidos vivos entre 1996 e 2006 demonstrou que a utilização de VPA durante a gestação, especialmente no primeiro trimestre, aumentou o risco de desenvolvimento de TEA em 3 a 4,9 vezes, associação que não foi observada em outros anticonvulsivantes (CHRISTENSEN *et al.*, 2013). As evidências dessa associação, entretanto, já eram descritas desde o final dos anos 1980: diversos estudos apontaram a presença de alterações do neurodesenvolvimento (ARDINGER *et al.*, 1988), além de características do tipo autista (CHRISTIANSON; CHESTER; KROMBERG, 1994; GAIL WILLIAMS; HERSH, 1997) em crianças diagnosticadas com a síndrome fetal do valproato. Além disso, a exposição intraútero ao VPA é capaz de elevar o risco de malformações, especialmente espinha bífida, demonstrando uma importante ação deletéria em aspectos de fechamento do tubo neural (KOREN *et al.*, 2006). A partir dessas observações, no final da década de 1990, Rodier e colaboradores sugeriram que o VPA poderia ser utilizado como uma forma de induzir características do tipo autista em animais, de forma a viabilizar diversas análises translacionais (RODIER *et al.*, 1996).

1.4 Modelo animal de TEA induzido por VPA

O trabalho visionário de Rodier e colaboradores em 1996 demonstrou que a exposição pré-natal de roedores ao VPA induzia alterações nos núcleos motores dos nervos cranianos, dano similar ao identificado na autópsia de um indivíduo com TEA no mesmo estudo (RODIER *et al.*, 1996). Posteriormente, Schneider e colaboradores demonstraram que ratos expostos ao VPA intraútero apresentavam atrasos no desenvolvimento, prejuízos sociais e estereotipias, elementos característicos do TEA (SCHNEIDER; PRZEWŁOCKI, 2005). Além disso, as características comportamentais eram mais presentes em animais machos (SCHNEIDER *et al.*, 2008), outro aspecto de alta translacionalidade. Finalmente, um estudo do mesmo grupo demonstrou que o enriquecimento ambiental era capaz de atenuar os comportamentos do tipo autista observados nos roedores (SCHNEIDER; TURCZAK; PRZEWŁOCKI, 2006). Essas constatações iniciais já demonstravam que o modelo possuía as três validades preconizadas (WILLNER, 1986): A) de face, pois reproduziu as características comportamentais do transtorno; B) construto, pois se observou que o mesmo fármaco que induz aumento de risco para TEA em humanos foi capaz de induzir característica do tipo TEA em roedores e C) preditiva, pois um

tratamento similar (enriquecimento ambiental), foi capaz de trazer benefícios tanto em humanos quanto no modelo animal (ARONOFF; HILLYER; LEON, 2016; SCHNEIDER; TURCZAK; PRZEWŁOCKI, 2006).

Inicialmente, a principal abordagem em relação aos efeitos do VPA era restrita aos seus efeitos deletérios no fechamento do tubo neural. Diversas hipóteses contribuem para explicar esse efeito: a inibição das HDACs provavelmente induz vasta alteração na expressão gênica, ocasionando a transcrição inadequada de genes como o sinalizador de apoptose BCL-2 (GURVICH *et al.*, 2005), o fator de transcrição HOXA1 (STODGELL *et al.*, 2006) e os genes associados à ativação da via da WNT (WILTSE, 2005). Além disso, o VPA interfere na cadeia transportadora de elétrons (WELLS *et al.*, 2010) e é convertido em metabólitos altamente reativos (como o ((E)-2,4-dieno VPA), os quais depletam os estoques de NADPH, consequentemente induzindo aumento na produção de espécies reativas de oxigênio (EROs) (LLOYD; SILLS, 2013). Finalmente, o VPA também parece ser capaz de antagonizar os efeitos do folato, alterando enzimas envolvidas no metabolismo desse nutriente (LLOYD; SILLS, 2013).

O desequilíbrio E/I no sistema nervoso central (SNC) – especialmente prevalência disfuncional da excitação - é uma das principais hipóteses associadas com a neurobiologia do TEA (RUBENSTEIN; MERZENICH, 2003). Diversas alterações nos neurotransmissores glutamato e GABA já foram identificadas no modelo animal induzido por VPA (ZIEMINSKA *et al.*, 2018). No córtex cerebral, o VPA foi capaz de, de forma geral, aumentar a expressão de genes associados à sinalização glutamatérgica (como canais iônicos), além de aumentar em cem vezes a expressão de proteínas sinápticas glutamatérgicas, enquanto exercia um efeito diferente nos genes associados ao GABA no córtex, HC e cerebelo (aumentando a expressão de três genes e diminuindo a expressão de outros três) (LENART *et al.*, 2020). Efeitos aumentados do glutamato também foram observados nas projeções glutamatérgicas no núcleo da rafe, as quais elevavam a frequência de disparos dos neurônios serotoninérgicos locais, condição que possivelmente possui associação com o comportamento do tipo ansioso observado nos animais (WANG, R. *et al.*, 2018). A expressão aumentada de receptores AMPA no CPFm de animais VPA foi associada com aspectos comportamentais, uma vez que a utilização de um antagonista específico trouxe resultados benéficos (KIM *et al.*, 2019). Em relação ao GABA, diferentes estudos apontam para uma redução na expressão e/ou atividade

da enzima glutamato descarboxilase (GAD) (WEI *et al.*, 2016; WIN-SHWE *et al.*, 2018), além de prejuízo na transmissão sináptica GABAérgica (BANERJEE *et al.*, 2013). Componentes do receptor $GABA_A$ também apresentam expressão reduzida no modelo VPA (LI *et al.*, 2017), paralelamente, a utilização de agonistas $GABA_A$ e $GABA_B$ foi capaz de restabelecer diversos parâmetros comportamentais (YANG; YANG; YIN, 2021).

Nos aspectos relativos à citoarquitetura e sinapse, o modelo VPA também apresenta importantes alterações: presença de hiperplasticidade sináptica em regiões como CPFm (RINALDI; PERRODIN; MARKRAM, 2008) e neocórtex (SILVA *et al.*, 2009), aumento de sinapses glutamatérgicas excitatórias (KIM *et al.*, 2013) (possivelmente induzida por mudanças no perfil de expressão de MECP2 (KIM *et al.*, 2016)) e redução na expressão de proteínas ancoradoras como SHANK3 (LIU *et al.*, 2016). Histologicamente, há descrições de redução na quantidade de neurônios de Purkinje no cerebelo, além de volume reduzido dessa região (INGRAM *et al.*, 2000), enquanto na amígdala ocorre um aumento de celularidade e massa (ECKER; BOOKHEIMER; MURPHY, 2015; MARKRAM *et al.*, 2008). Finalmente, no neocórtex, o VPA é capaz de induzir alterações na proliferação neuronal, levando a modificações na organização das camadas corticais (FUJIMURA *et al.*, 2016).

Finalmente, no nosso grupo de pesquisa, já observamos que a exposição pré-natal ao VPA foi capaz de induzir alterações sociais (inclusive em comportamentos de alta complexidade como o do tipo empático), estereotipias, mudanças em aspectos sensoriais (tanto em relação a estímulos nocivos e não nocivos) e comportamentos do tipo ansioso. Assim, de maneira geral, os animais replicam não só as características centrais como também outras que são comumente associadas ao transtorno. Ainda, já observamos alterações no metabolismo hipocampal do glutamato (BRISTOT SILVESTRIN *et al.*, 2013) e em aspectos oxidativos no fígado (BAMBINI-JUNIOR *et al.*, 2011), expressão diferencial de miRNA (HIRSCH *et al.*, 2018), prejuízo na distribuição de interneurônios parvalbumina-positivos associada à modificações na organização das camadas corticais na área somatossensorial (FONTES-DUTRA *et al.*, 2018) e, por fim, aumento na permeabilidade da barreira hematoencefálica e alterações na reatividade astrocitária e no padrão de expressão de aquaporinas em diferentes regiões corticais e subcorticais (DECKMANN *et al.*, 2021). O conjunto observado reforça as validades do modelo para além de questões comportamentais, demonstrando sua translacionalidade.

1.5 Resveratrol

O *trans*-resveratrol - 3,4′,5-triidroxiestilbeno (RSV) é um composto polifenólico da família do estilbenos presente em diversos alimentos, tais como amendoim, soja e uva (BURNS *et al.*, 2002). O vinho tinto também é um alimento rico nesse componente, uma vez que a maior concentração de RSV na uva se encontra na casca (SOUTO *et al.*, 2001). Nas plantas, o RSV possui papel de fitoalexina, estabelecendo defesas contra danos abióticos e bióticos, incluindo exposição a raios ultravioleta e luz visível, além de infecções bacterianas e fúngicas (HASAN; BAE, 2017).

Em doenças cardiovasculares (DCV), o RSV já demonstrou efeitos benéficos na arteriosclerose, hipertensão, isquemia, enfarto agudo do miocárdio e insuficiência cardíaca (BONNEFONT-ROUSSELOT, 2016). Os principais mecanismos associados a essa proteção são a capacidade antioxidante do RSV, especialmente via neutralização direta de radicais hidroxil e superóxido, reduzindo a peroxidação lipídica (PINYAEV *et al.*, 2019). Além disso, o RSV é capaz de aumentar a disponibilidade de óxido nítrico, melhorando a função endotelial, via estimulação da expressão e da atividade da enzima dimetilargininase (FROMBAUM *et al.*, 2012).

A ação anti-inflamatória do RSV é outra característica de relevância, especialmente em contextos como a diabetes, obesidade, dislipidemias, câncer e DCV. O RSV é capaz de modular componentes importantes do sistema imunológico como o fator nuclear kappa B (NFκB), citocinas (IL-1β, IL-6, IL-8, IL-17), fatores de necrose e crescimento tumoral (TNF-α, TGF-β), quimiocina CCL2 e prostaglandina PGE2; além de receptores do TLR, receptores de citocina e a sinalização por JAK/STAT (COUTINHO *et al.*, 2018). A ação do RSV ativando as enzimas SIRT (desacetilases de histonas) também contribui para a ação anti-inflamatória, possivelmente através da inibição das rotas associadas ao TNF-α (ZHU *et al.*, 2011) e ao PPR-γ (KALLIORA *et al.*, 2019).

Recentemente, o RSV tem se destacado no contexto de desordens neuropsiquiátricas. Na doença de Alzheimer, o RSV foi capaz de mitigar o declínio cognitivo (WITTE *et al.*, 2014), além de aumentar a eliminação de peptídeos β amilóides através da ativação de SIRT e AMPK (YANG; BAGIT; MACPHERSON, 2021), de forma similar, na doença de Parkinson, o RSV é capaz de atenuar disfunções motoras e reduzir o conteúdo de α-sinucleína via ativação das SIRT (GUO *et al.*, 2016). Na esquizofrenia, o uso de RSV como adjuvante da terapia com

risperidona trouxe melhoras nos sintomas negativos em humanos (SAMAEI *et al.*, 2020) e, em modelos animais, foi capaz de melhorar aspectos cognitivos e motores possivelmente por uma modulação de BDNF via SIRT no HC (NIU; CAO; JI, 2020).

No TEA, o tratamento adjunto de RSV com risperidona reduziu parâmetros de hiperatividade (HENDOUEI *et al.*, 2020), enquanto no modelo BTBR T+ Itpr3tf/J (BTBR) (um modelo genético, no qual os animais apresentam alterações na formação do corpo caloso e características comportamentais do tipo autista) o RSV foi capaz de atenuar múltiplos parâmetros de ativação imunológicas, incluindo sinalização via JAK/STAT, COX-2, receptores TLR, receptores de quimiocinas e desregulação Th1, Th2 e Th17 (AHMAD *et al.*, 2018c; BAKHEET *et al.*, 2016). No nosso grupo de pesquisa, já observamos que o tratamento com RSV intraútero no modelo VPA foi capaz de prevenir prejuízos sociais e sensoriais, estereotipias, expressão alterada de miRNA (miR134-5p) e alterações na citoarquitetura cortical (BAMBINI-JUNIOR *et al.*, 2014; DECKMANN *et al.*, 2021; HIRSCH *et al.*, 2018). Em um estudo piloto, o uso do RSV em crianças com TEA foi capaz de melhorar parâmetros de irritabilidade, favorecendo o estabelecimento de comportamentos sociais (Marchezan et al., *manuscrito submetido*). Dessa forma, é possível observar o potencial do RSV como uma ferramenta importante no estudo do TEA, uma vez que esse composto é capaz de contrapor e prevenir diversas das alterações induzidas pelo VPA intraútero (além de ter resultados positivos em outros modelos), viabilizando um estudo mais amplo das vias biológicas e mecanismos fisiopatológicos envolvidos no TEA.

1.6 Fatores de transcrição

FTs são proteínas com capacidade de interagir com o DNA, modulando a expressão gênica. Em seres humanos, mais de 1600 fatores de transcrição já foram descritos (LAMBERT *et al.*, 2018) e sua classificação usualmente está associada com a natureza do domínio de interação com o DNA. A extensa maioria dos FTs está incluída em três famílias: Domínio Básico, Domínio Coordenado por Zinco e Domínio Hélice-Dupla-Hélice (WINGENDER *et al.*, 2015).

Os estudos pioneiros sobre o papel de FTs ocorreram em drosófilas, especialmente nos anos 1970, onde foram observados os primeiros indícios de que algumas proteínas eram capazes de interferir na ação das RNA polimerases (KAUFFMAN, 1971) e nos anos 1980, quando se observou que alterações nos FTs,

especialmente da classe *Hox*, eram capazes de causar vasta alterações no desenvolvimento como duplo tórax e crescimento ectópico de pernas (KAUFMAN; LEWIS; WAKIMOTO, 1980; WEATHERBEE *et al.*, 1998). Atualmente, diversos estudos já demonstram o amplo papel dos FTs em diversos processos biológicos, em doenças como o câncer e diabetes (LEE; YOUNG, 2013) e em desordens neuropsiquiátricas (CHEN *et al.*, 2013; FORREST *et al.*, 2018).

As desordens do neurodesenvolvimento (DNs) associadas a fatores genéticos específicos definidos são mais raras, porém normalmente apresentam alterações mais contundentes. A proteína MECP2 é um FT que possui a capacidade de reprimir a expressão gênica através da ligação a domínios metilados do DNA (IP; MELLIOS; SUR, 2018). Mutações específicas em MECP2 estão associadas à síndrome de Rett, segunda maior causa de deficiência intelectual em mulheres (ROSENBERG; PASCUAL, 2014). Estudos em modelos animais apontam que a depleção de MECP2 induz alterações no conteúdo e na expressão de receptores de GABA e glutamato (CALFA *et al.*, 2015; EL-KHOURY *et al.*, 2014), perda da organização do córtex somatossensorial (LEE; TSYTSAREV; ERZURUMLU, 2017) modificações em sistemas de sinalização serotoninérgica (VOGELGESANG *et al.*, 2018), além de funcionalidade reduzida de células gliais como astrócitos e oligodendrócitos (SHARMA *et al.*, 2015). Mutações em FTs como SOX5 (LAMB *et al.*, 2012), SOX9 (KWOK *et al.*, 1995), SOX10 (PINGAULT *et al.*, 1998), SOX11 (KOSHO; MIYAKE; CAREY, 2014), TCF4 (AMIEL *et al.*, 2007; BROCKSCHMIDT *et al.*, 2007; ZWEIER *et al.*, 2007), GTF2i (MORRIS, 2017) e outros também já foram descritos no contexto de desordens mais raras.

Além de questões genéticas, os FTs também podem sofrer interferências de fatores ambientais, condição que pode ser crítica durante o período gestacional, uma vez que a maioria dos FTs apresenta seu pico de expressão durante o desenvolvimento intraútero (CARDOSO-MOREIRA *et al.*, 2019).

No contexto da AIM, já foi observado aumento embrionário na expressão de PAX6 e de STAT3, ocasionando alterações no padrão de expressão dos marcadores de camadas corticais CTIP2 e TBR1 (BEN-REUVEN; REINER, 2019; ZUIKI *et al.*, 2017). Outros FTs como REST e ARX também apresentam alterações em modelos de AIM, resultando em danos associados à sinalização de GABA e à funcionalidade de neurônios parvalbumina positivos (PV+) (CORRADINI *et al.*, 2018; NAKAMURA *et al.*, 2019).

Certos teratógenos como o etanol e o VPA também estabelecem efeitos importantes nos FTs. O etanol é capaz de alterar a expressão de PAX6 em murinos (ARONNE *et al.*, 2008), induzindo alteração de diferenciação celular via modulação de POU5F1 e SOX2 (SÁNCHEZ-ALVAREZ *et al.*, 2013). Em peixe-zebra, a exposição ao etanol reduziu a expressão de SOX2 (SARMAH *et al.*, 2020), prejudicando o processo de gastrulação. Em relação ao VPA, estudo *in vitro* com precursores hipocampais demonstrou que a exposição das células a esse fármaco induziu aumento na expressão de NEUROD1, um FT essencial para diferenciação celular (HSIEH *et al.*, 2004). Em roedores, a exposição embrionária ou intraútero ao VPA induziu alterações na linha do tempo de expressão de diversos FTs incluindo POU3F1, SOX4, EGR2, NGN2, NEUROD1 e PAX6 (KIM *et al.*, 2014; OKADA *et al.*, 2005). Em relação ao PAX6, a alteração não pôde ser observada quando a indução foi feita utilizando valpromida, um análogo do VPA sem efeito inibidor de HDACs, indicando uma possível via determinante para a expressão desse FT (KIM *et al.*, 2014). Além disso, a alteração em PAX6 foi associada com decréscimo na expressão de HES1, um FT essencial para a diferenciação de progenitores da região subventricular (KAWADA *et al.*, 2018).

No contexto do TEA, estudos de associação ampla do genoma (do inglês, *Genome wide association studies* - GWAS) já foram capazes de demonstrar que FTs como TBR1, ADNP e PAX5 fazem parte do conjunto de genes cujas alterações estão associadas com um risco aumentado de desenvolvimento da desordem (O'ROAK *et al.*, 2014). Mudanças no padrão de expressão desses FTs já foram relacionadas, especialmente em modelos animais, com malformações corticais (VEGAS *et al.*, 2018; ZAWERTON *et al.*, 2020), prejuízos na autofagia (SRAGOVICH; MERENLENDER-WAGNER; GOZES, 2017), maturação e migração celular (HELSMOORTEL *et al.*, 2014; MOLLINEDO *et al.*, 2019), além de expressão alterada de marcadores das camadas corticais (OHTSUKA *et al.*, 2013).

Outro aspecto consolidado no TEA que possui influência dos FTs são as alterações neuroimunológicas. No modelo animal BTBR, já foram observadas diversas mudanças no padrão de expressão de FTs como FOXP3, GATA3, STAT3, T-Bet e RORγt, as quais, de forma geral, foram associados com desequilíbrios imunológicos que favoreciam cascatas pró inflamatórios e prejudicavam vias regulatórias (AHMAD *et al.*, 2018a, 2018e; AHMAD *et al.*, 2017; BAKHEET *et al.*,

2017; DECKMANN *et al.*, 2018). Resultados similares foram observados em monócitos provenientes de pacientes com TEA.

1.7 Interneurônios inibitórios

Os interneurônios GABAérgicos (IGs) representam um pequeno percentual dos neurônios totais, alcançando cerca de 10-15% da população total no HC e 20-30% no neocórtex em humanos, enquanto os demais 70-90% correspondem majoritariamente a neurônios glutamatérgicos excitatórios (PELKEY *et al.*, 2017). Entretanto, a diversidade de formas, funções e circuitos associados a essas células ressalta a sua relevância para o funcionamento do SNC. Em relação à classificação, os interneurônios podem ser subdivididos através de características morfológicas, fisiológicas ou através de marcadores histológicos. No presente trabalho, optou-se pela utilização de marcadores histológicos como critério de diferenciação (MIHALJEVIĆ *et al.*, 2019).

Cerca de 40% da população de IGs é composta por neurônios PV+, sendo essa a maior subpopulação do encéfalo. Os neurônios somatostatina-positivos (SOM+) compõem aproximadamente 30% da população total, enquanto outros marcadores diversos ocupam os demais 30%, incluindo os IGs calbindina-positivos (CB+) (KELSOM; LU, 2013). Todos esses IGs se originam da eminência gangliônica (EG) e, posteriormente, realizam rotas de migração para o córtex e regiões subcorticais, entretanto, a localização, o tempo de proliferação e os fatores envolvidos no desenvolvimento diferem entre cada subpopulação (FAUX *et al.*, 2012). A extensa maioria dos IGs se origina na EG medial e inicia suas rotas de migração por volta do dia embrionário (E) 12,5 em ratos (KELSOM; LU, 2013). O processo de migração para regiões como córtex e HC inicia numa organização tangencial e finaliza com uma disposição radial, onde os IGs tendem a ser organizar laminarmente, integrando as diferentes camadas ou subáreas dessas regiões. Os neurônios excitatórios, diferentemente, se originam diretamente das regiões paraventriculares e subventriculares do córtex e de uma área de proliferação celular no limite dorsal do telencéfalo, estabelecendo usualmente uma rota de migração curta (GUO, J.; ANTON, 2014; SUN *et al.*, 2015).

Os neurônios PV+ apresentam a expressão constitutiva da proteína ligadora de cálcio parvalbumina e podem ser subclassificados, conforme a morfologia, em células candelabro (do inglês, *chandelier cell*) e células em cesta dupla (do inglês,

double basket cell) (ASCOLI *et al.*, 2008; KAWAGUCHI; SHINDOU, 1998). Uma das principais características dos PV+ é o seu disparo rápido (do inglês, *fast spiking*) (KAWAGUCHI; KUBOTA, 1997), o que viabiliza a geração das ondas gama, um padrão eletrofisiológico essencial para diversos processos cognitivos, uma vez que possibilita a integração entre diferentes regiões encefálicas (ANTONOUDIOU *et al.*, 2020). A presença de sinapses elétricas (além de químicas) entre os próprios neurônios PV+ contribui para promover uma ampla sincronização (GALARRETA; HESTRIN, 2002). A inibição promovida pelos PV+ é direcionada principalmente a segmentos iniciais do axônio (CONTRERAS; HINES; HINES, 2019) e, além disso, estima-se que cada PV+ seja capaz de inibir quase todos os neurônios piramidais adjacentes (PACKER; YUSTE, 2011), demonstrando seu importante papel na circuitaria encefálica.

Alterações em neurônios PV+ já foram descritas em diversas desordens, especial TEA e esquizofrenia. Em relação à última, já existem estudos *post mortem* demonstrando redução na densidade de neurônios PV+ no CPFm (KAAR *et al.*, 2019), além de reduzida marcação da rede perineuronal (ENWRIGHT *et al.*, 2016) e reduzida expressão de FTs associados ao desenvolvimento de interneurônios como PV+ e SOM+ (VOLK; EDELSON; LEWIS, 2016). No TEA, estudos sobre PV+ em humanos ainda são incipientes, porém diversas análises em modelos animais já demonstram evidências importantes. No modelo VPA, já foi observado alteração na disposição dos PV+ no córtex somatossensorial, mudanças de densidade no estriado (SAWADA; KAMIYA; AOKI, 2021), além de desbalanço na expressão de canais essenciais para a funcionalidade dos PV+ como KCN1 e HCN1 (LAUBER; FILICE; SCHWALLER, 2016). Em animais expostos a AIM houve redução de PV+ no córtex frontal (VOJTECHOVA *et al.*, 2021), além de alteração na expressão gênica da parvalbumina (NAKAMURA *et al.*, 2021). Em modelos genéticos como o nocaute (do inglês, *knockout* – KO) para *Ctnap2* observou-se redução na quantidade de PV+ no HC, ocasionando perda de inibição em CA1 e impactos nas oscilações gama (PATERNO *et al.*, 2021), enquanto no modelo KO para *Engrailed-2* (EN2) houve uma redução na densidade de PV+ no prosencéfalo (PROVENZANO *et al.*, 2020).

Os neurônios SOM+ apresentam imunorreatividade para o neuropeptídeo somatostatina e podem ser classificados morfologicamente em células de Martinotti e células não Martinotti (incluindo células em cesta, células em buquê duplo, do

inglês *double bouquet cells* e outras) (RIEDEMANN, 2019). A somatostatina, por si só, possui importantes efeitos inibitórios, estabelecendo uma sinalização de efeito mais lento e a longo prazo, típica dos neuropeptídeos (LIGUZ-LECZNAR; URBAN-CIECKO; KOSSUT, 2016). Entretanto, as peculiaridades dos SOM+ independem da ação direta da somatostatina. A alta atividade de disparo basal (mesmo sem estímulo sináptico) aliada a alta conectividade local, especialmente nos dendritos dos neurônios glutamatérgicos, torna os SOM+ importantes controladores das circuitarias locais (diferente dos PV+, que estão mais associados com integração de regiões encefálicas) (URBAN-CIECKO; BARTH, 2016). Além disso, os SOM+ já se mostraram essenciais para a regulação de diversos comportamentos de alta complexidade como aprendizado e memória aversiva (KVITSIANI *et al.*, 2013; LOVETT-BARRON *et al.*, 2014; PI *et al.*, 2013).

No contexto de transtornos psiquiátricos, as principais descrições envolvendo os SOM+ ocorrem na epilepsia e na esquizofrenia. Em um modelo de síndrome de Dravet, uma forma infantil de epilepsia acompanhada de prejuízo cognitivo e características do tipo TEA, houve redução na excitabilidade de neurônios SOM+, consequentemente acarretando prejuízos inibitórios subsequentes (TAI *et al.*, 2014), além disso animais KO para somatostatina apresentam episódios de convulsão mais severos (BUCKMASTER *et al.*, 2002). No HC, a perda de SOM+ induzida por epilepsia do lobo temporal prejudica a inibição no giro denteado, causando sobrecarga na circuitaria local (HOFMANN *et al.*, 2016) – interessantemente, reduzidos níveis de somatostatina já foram identificados no HC de pacientes com epilepsia do lobo temporal (ROBBINS *et al.*, 1991). Na esquizofrenia, já se identificou redução na expressão gênica de somatostatina e no número de SOM+ no córtex pré-frontal (VOLK; EDELSON; LEWIS, 2016), no HC (KONRADI *et al.*, 2011) e na amígdala (PANTAZOPOULOS *et al.*, 2017) em análise *post mortem* de pacientes. No TEA, a literatura a respeito do papel dos SOM+ é restrita.

Os neurônios CB+ expressam a proteína ligadora de cálcio calbindina e, na sua maioria, são classificados morfologicamente como células em buquê duplo (DEL RÍO; DEFELIPE, 1995). Apesar de representarem uma subpopulação menor, os CB+ participam de circuitos importantes como o processamento do córtex somatossensorial, sendo modulados pelos interneurônios positivos para peptídeo vasoativo intestinal (STAIGER *et al.*, 2004), além de integrarem a rede HC-amígdala, contribuindo para a consolidação de memórias emocionais (BIENVENU *et al.*, 2012).

No TEA, há descrição de redução do número de neurônios de Purkinje positivos para calbindina no cerebelo (WHITNEY *et al.*, 2008) e aumento da densidade de CB+ no giro denteado do HC (LAWRENCE *et al.*, 2010) em análises *post mortem*, enquanto no modelo VPA houve redução na expressão de calbindina no verme cerebelar (MAIN; KULESZA, 2017). No modelo de TEA por KO do receptor ativador de plasminogênio tipo uroquinase, os animais apresentaram redução de 50% na quantidade de CB+ no córtex frontoparietal (POWELL *et al.*, 2003).

Uma ampla gama de aspectos regula o ciclo de vida e os aspectos funcionais dos IGs desde a sua origem na EG até a disposição final nas diferentes regiões encefálica. Os FTs fatores DLX 1 e 2 possuem papel importante na migração dessas células para o córtex (ANDERSON *et al.*, 1997), na manutenção da expressão da enzima glutamato descarboxilase (responsável pela síntese de GABA) (LE *et al.*, 2017) e na expressão das proteínas de membrana neuropilinas (LE *et al.*, 2007), essenciais para outro tipo de sinalização ao longo da migração, enquanto os fatores DLX 5 e 6 parecem ter uma associação específica com o desenvolvimento apropriado dos interneurônios PV+ (WANG *et al.*, 2010). Outro fator importante da mesma classe é o ARX, o qual já demonstrou, através de estudos com animais KO, ser essencial para a distribuição correta dos interneurônios PV+ ao longo das camadas corticais (MARSH *et al.*, 2016; SHERR, 2003), característica alterada no córtex sensorial de animais do modelo animal de TEA.

Os fatores LHX6 e SOX6 também possuem papel importante na formação das camadas corticais, sobrevivência dos interneurônios PV+ e SOM+ (VOLK *et al.*, 2012; VOLK; EDELSON; LEWIS, 2014) e manutenção de suas peculiaridades eletrofisiológicas (BATISTA-BRITO *et al.*, 2009). Alterações já foram descritas principalmente em esquizofrenia (VOLK *et al*., 2012).

Outros fatores como a quimiocina CXCL12, secretada pelas células da meninge, e seu receptor CXCR4 já foram descritos como fundamentais para a mudança no padrão de migração tangencial para radial (induzindo a laminação cortical) (ABE *et al.*, 2015; LI *et al.*, 2008), concomitante a esse estabelecimento de camadas ocorre o aumento da expressão da proteína KCC2, a qual promove a troca da característica excitatória do GABA para inibitória (KELSOM; LU, 2013).

Ao longo da vida adulta, outros aspectos se tornam fundamentais para os IGs, incluindo as rotas de sinalização da AKT/GSK3β e da CK2/PTEN (WEI; HAN, 2020). A perda de AKT em modelos animais induziu ampla redução do número de IGs

corticais (CARRIERE *et al.*, 2020), enquanto a inibição de AKT ocasionou uma perda direcionada de PV+ no HC (CHANG *et al.*, 2016). Ainda, a inibição da rota AKT/GSK3β ocasionou apoptose de interneurônios em estágios imaturos, levando à perda celular (WEI; HAN, 2020). Em relação à PTEN, o KO dessa proteína foi capaz de induzir mudanças na proporção de PV+ e SOM+ (CUPOLILLO *et al.*, 2016; LUGO *et al.*, 2014; SHIN; SANTI; HUANG, 2021) - interessantemente, o KO seletivo de PTEN nesses IGs induziu características do tipo autista (SHIN; SANTI; HUANG, 2021). Finalmente, apesar de não haver associação direta de CK2 com IGs, já existem evidências de que essa proteína exerce papel importante na sinalização gabaérgica no HC (KIM *et al.*, 2020; QIN *et al.*, 2021).

1.8 Córtex pré-frontal medial

Em roedores, o CPFm possui importante homologia com o córtex dorsolateral de primatas (apesar de ainda existirem debates sobre os limites anatômicos dessas regiões) (LAUBACH *et al.*, 2018). O CPFm é uma área integrativa associada a diversos comportamentos complexos, incluindo autorreferenciamento, perspectiva (D'ARGEMBEAU *et al.*, 2007), interação social (GROSSMANN, 2013), tomada de decisão e memória (EUSTON; GRUBER; MCNAUGHTON, 2012). O CPFm estabelece rotas de conectividade com diversas regiões, incluindo amígdala basolateral, HC, estriado, claustro, área tegmental ventral, substância negra periaquedutal, tálamo e outras regiões do córtex (ANASTASIADES; CARTER, 2021), característica que o torna uma região fundamental para a cognição.

O CPFm de roedores pode ser dividido em três sub-regiões distintas através de critérios neuroanatômicos e de conectividade: córtex cingulado anterior (CCa), córtex pré-límbico (CPL) e córtex infralímbico (CI) (ÖNGÜR; PRICE, 2000). O CCa possui papel relevante em comportamentos associados à sociabilidade: já se observou, em humanos, que a exposição a situações que demandam mensuração de expectativas sociais ativa diferencialmente essa região (SOMERVILLE; HEATHERTON; KELLEY, 2006). Além disso, vários atributos associados à chamada "cognição social" como atribuição de valores às atitudes, identificação e correção de erros, tomada de decisão, empatia e outros (APPS; RUSHWORTH; CHANG, 2016; LAVIN *et al.*, 2013) possuem associação com o CCa. Finalmente, a intensa conectividade como o HC se mostra fundamental para o estabelecimento de memórias associadas ao contexto (WANG; JOHN; BARBAS, 2021), elemento

importante para a sociabilidade. O CPL e o CI, por sua vez, apresentam intensa associação com a amígdala: enquanto o CPL promove o contexto de medo e a busca por recompensas, o CI inibe esse tipo de comportamento (CAPUZZO; FLORESCO, 2020; RIAZ *et al.*, 2019). Em situações como a dor crônica, por exemplo, diversas modificações, especialmente eletrofisiológicas, ocorrem no CPL e no CI, ressaltando o papel dessas regiões em contextos de memória aversiva (THOMPSON; NEUGEBAUER, 2019).

Tendo em vista os prejuízos sociais característicos do TEA, o CPFm se destaca como uma região de interesse nessa desordem. Em animais KO para SHANK3, um consolidado modelo de TEA, se observou alteração na estrutura sináptica (JACOT-DESCOMBES *et al.*, 2020) no CPFm e dessincronização da conectividade com outras regiões (PAGANI *et al.*, 2019). Além disso, a deleção específica de SHANK3 no CCa foi capaz de, por si só, induzir prejuízos sociais, os quais foram restabelecidos após a restauração da expressão de SHANK3 nessa região (GUO *et al.*, 2019).

No modelo VPA, já se observou aumento da conectividade e plasticidade em neurônios da camada V do CPFm (RINALDI; PERRODIN; MARKRAM, 2008), complementarmente, outro estudo demonstrou aumento da facilitação por pulso pareado e potenciação de longo prazo nessa região, além da exacerbação de memórias aversivas (SUI; CHEN, 2012). Em arganazes-do-campo expostos intrauterinamente ao VPA, houve alteração na expressão de MECP2 e receptor de vasopressina (V1aR) no CPFm, bem como diversos prejuízos sociais (interessantemente, o estabelecimento de vínculo monogâmico, típico desses animais, não foi prejudicado) (SAILER *et al.*, 2019).

Em indivíduos com TEA, diversos estudos de ressonância magnética funcional (RMf) já demonstraram alterações na ativação de regiões homólogas ao CPFm em diferentes contextos. Durante tarefas executivas, indivíduos com TEA demonstraram ativação aumentada do córtex pré-frontal (GILBERT *et al.*, 2008), característica que também foi observada quando os indivíduos eram expostos a situações de identificação de erros (GOLDBERG *et al.*, 2011). Além disso, as alterações nessa região foram mais proeminentes em homens do que em mulheres (TRAKOSHIS *et al.*, 2020). Em conjunto, esses estudos ressaltam o papel de alterações do CPFm no prejuízo em funções cognitivas associadas com TEA.

1.9 Hipocampo

O HC é uma estrutura subcortical classicamente associada com processos que envolvem a formação, consolidação e evocação de memórias (MIRY; LI; CHEN, 2021). A porção dorsal dessa região em roedores pode ser dividida em quatro sub-regiões: três divisões do *cornu ammonis* (CA1, CA2 e CA3) e giro denteado (GD) (PAXINOS; WATSON, 2004). Além de diferenças anatômicas, essas sub-regiões também apresentam diferenças de conectividade e funcionalidade – a região entre o GD e o hilo, por exemplo, é um dos locais onde ocorre neurogênese durante períodos mais tardios da vida pós-natal (GONÇALVES; SCHAFER; GAGE, 2016).

A sociabilidade demanda várias funções executadas pelo HC, especialmente a memória social, a qual possibilita a antecipação de demandas e a interpretação adequada de estímulos externos (TZAKIS; HOLAHAN, 2019). A integração do HC com áreas como o CPFm e a amígdala é fundamental para a adição de componentes emocionais ao contexto social, viabilizando processos de atenção e tomada de decisão (RUBIN *et al.*, 2014).

Em modelos animais de TEA, mudanças profundas na expressão gênica do HC já foram identificadas nos modelos BTBR e KO para o gene EN-2 ($EN2^{-/-}$): 153 genes em comum para os modelos foram identificados como alterados, sendo que no modelo BTBR, grupos de genes associados à microglia estavam enriquecidos, enquanto no modelo $EN2^{-/-}$ sinapses GABA e glutamatérgicas, além de elementos associados à FMRP (proteína associado à síndrome do X frágil, do inglês *fragile x mental retardation protein*) e à epilepsia constavam nos grupos de genes alterados no HC (PROVENZANO *et al.*, 2016). No modelo VPA, já foi observada alteração no metabolismo glutamatérgico do HC em animais adultos (BRISTOT SILVESTRIN *et al.*, 2013)

Em indivíduos com TEA, já foram observadas alterações anatômicas no HC como aumento da assimetria (RICHARDS *et al.*, 2020) e descrições divergentes entre aumento e diminuição de volume dependendo do estudo (SCHUMANN *et al.*, 2004). Interessantemente, o formato do HC em análises por RMf já foi sugerido como um possível marcador para o TEA (CHADDAD *et al.*, 2017). Finalmente, diversas vertentes apontam o HC como um potencial organizador de “mapas cognitivos”, integrando memória social e espacial, questões intrinsecamente associadas com o TEA (BANKER *et al.*, 2021).

2. JUSTIFICATIVAS E HIPÓTESES

Apesar da alta prevalência e dos avanços científicos a nível de pesquisa básica e clínica, o TEA segue como uma desordem cujas vias biológicas envolvidas ainda não foram propriamente elucidadas, porém baseando-se nos dados já existentes sobre esse assunto tanto em modelos animais quanto em humanos espera-se que:

1) O VPA induza alguma alteração funcional ao longo do desenvolvimento dos IGs e das sinapses, por alterar fatores envolvidos nesses processos, principalmente através do seu papel modulador da expressão gênica.
2) Essas modificações acabem induzindo alguma alteração na composição neuronal no CPFm e HC, alterando as redes neuronais em que estão envolvidos.
3) Essas alterações possam ter associação com as mudanças na expressão dos FTs durante o período embrionário, especialmente pela ampla descrição da literatura sobre os seus papéis no TEA e em desordens correlatas.
4) Essas alterações se perpetuem ao longo do desenvolvimento, ocasionando mudanças estruturais com efeitos a longo prazo.

3. OBJETIVOS

3.1. OBJETIVO GERAL

Elucidar aspectos associados com a maturação, funcionalidade e citoarquitetura dos IGs PV+, SOM+ e CB+, além do conteúdo sináptico e outros fatores associados em diferentes fases do desenvolvimento no modelo animal de autismo induzido por exposição pré-natal ao VPA, bem como os potenciais efeitos do RSV nesses aspectos desde o período embrionário até a idade adulta.

3.2. OBJETIVOS ESPECÍFICOS

Capítulo I:

- Revisão, através de buscas na literatura e ferramentas de bioinformática, do papel dos FTs em diferentes DNs, sugerindo possíveis mecanismos biológicos comuns e convergentes nesses transtornos;

Capítulo II:

- Analisar, em bancos de dados de embriões de modelos de TEA, possíveis vias e rotas alteradas em regiões-chave para o desenvolvimento de componentes inibitórios como os IGs;
- Analisar, em animais jovens do modelo VPA, aspectos qualitativos e quantitativos referentes à disposição e organização dos IGs no CPFm e no HC;
- Quantificar, em animais jovens do modelo VPA, o imunoconteúdo de proteínas sinápticas no CPFm e no HC;
- Quantificar, em animais jovens do modelo VPA, o imunoconteúdo de receptores GABAérgicos no CPFm e no HC;
- Analisar potenciais efeitos preventivos do RSV nos aspectos citados anteriormente em animais jovens do modelo VPA.

Capítulo III:

- Analisar, em animais adultos do modelo VPA, aspectos qualitativos e quantitativos referentes à disposição e organização dos IGs no HC;
- Analisar, em animais adultos do modelo VPA, aspectos morfológicos do HC;
- Quantificar, em animais adultos do modelo VPA, o imunoconteúdo de proteínas de sinalização celular no HC através da técnica de western blotting;
- Analisar potenciais efeitos preventivos do RSV nos aspectos citados anteriormente em animais adultos do modelo VPA.

PARTE II

CAPÍTULO I

Artigo publicado**:**

"*Transcription factors in neurodevelopmental and associated psychiatric disorders: a potential convergence for genetic and environmental risk factors*"

Acesso na íntegra somente em:

International Journal of Developmental Neuroscience 2021; 81(7):545-578.
DOI: https://doi.org/10.1002/jdn.10141

Transcription Factors in Neurodevelopmental and Associated Psychiatric Disorders: A Potential Convergence for Genetic and Environmental Risk Factors

Júlio Santos-Terra*[1,2,3,4], Iohanna Deckmann[1,2,3,4], Mellanie Fontes-Dutra[1,2,3,4], Gustavo Brum Schwingel[1,2,3,4], Victorio Bambini-Junior*[1,3,4,5], Carmem Gottfried*[1,2,3,4]

[1] Translational Research Group in Autism Spectrum Disorders (GETTEA), Universidade Federal do Rio Grande do Sul (UFRGS), Porto Alegre, Brazil.

[2] Department of Biochemistry, Universidade Federal do Rio Grande do Sul (UFRGS), Porto Alegre, Brazil.

[3] National Institute of Science and Technology on Neuroimmunomodulation (INCT-NIM), Oswaldo Cruz Institute, Oswaldo Cruz Foundation, Rio de Janeiro, Brazil.

[4] Autism Wellbeing And Research Development (AWARD) Institute, BR-UK-CA

[5] School of Pharmacology and Biomedical Sciences, University of Central Lancashire, Preston, United Kingdom.

*CORRESPONDING AUTHORS:

JS-T (juliosterra@gmail.com), CG (cgottfried@ufrgs.br)

Departamento de Bioquímica, ICBS, Universidade Federal do Rio Grande do Sul, Ramiro Barcelos 2600 – 21111. CEP: 90035-003 Porto Alegre-RS, Brazil.

Abstract

Neurodevelopmental disorders (NDDs) are a heterogeneous and highly prevalent group of psychiatric conditions marked by impairments in the nervous system. Their onset occurs during gestation, and the alterations are observed throughout the postnatal life. Although many genetic and environmental risk factors have been described in this context, the interactions between them challenge the understanding of the pathways associated with NDDs. Transcription factors (TFs) – a group of over 1,600 proteins that can interact with DNA, regulating gene expression through modulation of RNA synthesis, represent a point of convergence for different risk factors. In addition, TFs organize critical processes like angiogenesis, blood-brain barrier formation, myelination, neuronal migration, immune activation, and many others in a time and location-dependent way. In this review, we summarize

important TF alterations in NDD and associated disorders, along with specific impairments observed in animal models, and, finally, establish hypotheses to explain how these proteins may be critical mediators in the context of genome-environment interactions.

Key Words: Transcription Factors; Neurodevelopmental Disorders; Psychiatric Disorders; Environment-Genome Interaction; Transcription; Animal Model.

Capítulo II

Artigo Aceito para publicação:

"*Resveratrol prevents cytoarchitectural and interneuronal alterations in the animal model of ASD induced by valproic acid*"

International Journal of Molecular Sciences

International Journal of
Molecular Sciences

MDPI

Article

Resveratrol Prevents Cytoarchitectural and Interneuronal Alterations in the Valproic Acid Rat Model of Autism

Júlio Santos-Terra [1,2,3,4], Iohanna Deckmann [1,2,3,4], Giovanna Carello-Collar [1,2,3], Gustavo Della-Flora Nunes [1,2,3], Guilherme Bauer-Negrini [1,2,3,4], Gustavo Brum Schwingel [1,2,3,4], Mellanie Fontes-Dutra [1,2,3,4], Rudimar Riesgo [1,3,4,5] and Carmem Gottfried [1,2,3,4,*]

1 Translational Research Group in Autism Spectrum Disorder—GETTEA, Universidade Federal do Rio Grande do Sul (UFRGS), Porto Alegre 90040-060, Brazil; juliosterra@gmail.com (J.S.-T.); iohanna.deckmann@gmail.com (I.D.); giovannacollar@gmail.com (G.C.-C.); gustavodfnunes@gmail.com (G.D.-F.N.); negrini.guilherme@gmail.com (G.B.-N.); brumschwingel@gmail.com (G.B.S.); dutra.mellanie@gmail.com (M.F.-D.); rriesgo@hcpa.edu.br (R.R.)
2 Department of Biochemistry, Universidade Federal do Rio Grande do Sul (UFRGS), Porto Alegre 90040-060, Brazil
3 National Institute of Science and Technology in Neuroimmunomodulation—INCT-NIM, Rio de Janeiro 21040-900, Brazil
4 Autism Wellbeing and Research Development—AWARD—Initiative BR-UK-CA, Porto Alegre 90040-060, Brazil
5 Child Neurology Unit, Department of Pediatrics, Hospital de Clínicas de Porto Alegre, Porto Alegre 90035-903, Brazil
* Correspondence: cgottfried@ufrgs.br

check for updates

Citation: Santos-Terra, J.; Deckmann, I.; Carello-Collar, G.; Nunes, G.D.-F.; Bauer-Negrini, G.; Schwingel, G.B.; Fontes-Dutra, M.; Riesgo, R.; Gottfried, C. Resveratrol Prevents Cytoarchitectural and Interneuronal Alterations in the Valproic Acid Rat Model of Autism. *Int. J. Mol. Sci.* **2022**, *23*, 4075. https://doi.org/10.3390/ijms23084075

Academic Editor: Dominique Delmas

Received: 16 March 2022
Accepted: 2 April 2022
Published: 7 April 2022

Publisher's Note: MDPI stays neutral with regard to jurisdictional claims in published maps and institutional affiliations.

Abstract: Autism spectrum disorder (ASD) is a prevalent neurodevelopmental disorder characterized by several alterations, including disorganized brain cytoarchitecture and excitatory/inhibitory (E/I) imbalance. We aimed to analyze aspects associated with the inhibitory components in ASD, using bioinformatics to develop notions about embryonic life and tissue analysis for postnatal life. We analyzed microarray and RNAseq datasets of embryos from different ASD models, demonstrating that regions involved in neuronal development are affected. We evaluated the effect of prenatal treatment with resveratrol (RSV) on the neuronal organization and quantity of parvalbumin-positive (PV+), somatostatin-positive (SOM+), and calbindin-positive (CB+) GABAergic interneurons, besides the levels of synaptic proteins and GABA receptors in the medial prefrontal cortex (mPFC) and hippocampus (HC) of the ASD model induced by valproic acid (VPA). VPA increased the total number of neurons in the mPFC, while it reduced the number of SOM+ neurons, as well as the proportion of SOM+, PV+, and CB+ neurons (subregion-specific manner), with preventive effects of RSV. In summary, metabolic alterations or gene expression impairments could be induced by VPA, leading to extensive damage in the late developmental stages. By contrast, due to its antioxidant, neuroprotective, and opposite action on histone properties, RSV may avoid damages induced by VPA.

Keywords: autism spectrum disorder; valproic acid; resveratrol; interneuron; synapse; GABA receptor

1. Introduction

Autism spectrum disorder (ASD) is a neurodevelopmental disorder described as a behavioral dyad composed of (a) communication and social interaction impairments and (b) stereotyped or repetitive patterns of behavior [1]. Besides that, ASD presents a high prevalence (1:44 in children up to 8 years old in the USA) [2] and heterogeneity among individuals [3], resulting in a challenge for clinical diagnosis [4,5] and public health policies [6].

Epilepsy and other electrophysiological abnormalities are among the most prevalent ASD comorbidities, affecting up to 1/3 of the individuals with ASD [7–9]. This evidence

leads to the most consolidated hypothesis regarding ASD pathophysiology—that the imbalance between excitation and inhibition is probably associated with impairments in the inhibitory component [10–12]. Interneurons are crucial for the inhibition of neural circuits [13]. Although they represent only 10–15% of the total neurons in the hippocampus (HC) [14] and 20–30% in the neocortex in humans [15], the high diversity of cellular shapes, populations, and functional properties highlight their importance in the brain [16,17]. Parvalbumin-positive (PV+) and somatostatin-positive (SOM+) interneurons comprise the majority of the GABAergic interneurons (40% and 30% in the cortex, respectively), followed by several smaller populations, including calbindin-positive (CB+) interneurons [16,18]. While SOM+ neurons contribute to the regulation of the local excitatory input integration in cortical regions [19], PV+ neurons are implicated in the integration among different regions [20] and between the hemispheres [21]. Moreover, changes in PV+ neuron inputs [22,23] and the intrinsic features of this subpopulation [24,25] are observed in animal models of ASD, while evidence regarding SOM+ is still incipient. In addition, dysfunctions in other inhibitory components of the E/I balance have already been described in ASD, such as decreased levels of GABA receptor subunits in the parietal cortex and cerebellum in postmortem analysis [26] and synaptic alterations (e.g., reduced pruning [27] and mutations in the genes of PSD-95, gephyrin, and neuroligins [28,29]).

Recently, neuroimmune aspects have emerged as important factors involved in triggering neurodevelopmental disorders. For example, maternal immune activation (MIA) induces ASD-like features, changes in the cytokine profile (especially IL-6), and imbalances in lymphocyte populations [30,31]. In addition, it is observed to alter the expression of genes associated with neurodevelopment, such as genes involved with migration, function, and placement of interneurons [32–34]. Similarly, prenatal exposure to valproic acid (VPA) in rodents, a well-established model of autism [35–39], induces interneuronal alterations in sensory areas [36] and HC [40,41]. Furthermore, those animals show alterations in the profile of brain and peripheral cytokines [42] and a reduction of T CD4 + lymphocytes in the lymph nodes [43], indicating a possible involvement of the neuroimmune axis in the VPA model.

Therefore, molecules that prenatally modulate the immune system may hold promise in preventing neurodevelopmental alterations. For example, MR-39, an agonist of the FRP2 receptor, modulates the expression of lipoxin A4 in hippocampal tissues of BTBR and VPA animals, also improving social behavior impairments [44]. Following this line, trans-resveratrol (RSV, 3,5,4′-trihydroxystilbene) has been studied in the context of schizophrenia [45], attention deficit hyperactivity disorder [46], and ASD due to its antioxidant, anti-inflammatory, and neuroprotective effects [47]. The mechanisms associated with the neuroprotective effects of polyphenols, in general, involve scavenging of reactive species of oxygen (and others), modulation of inflammatory cytokines, reduction of the aggregation of amyloid proteins, among several other effects [48]. Interestingly, prenatal treatment with RSV prevented behavioral and molecular impairments in the VPA model [35,36,38]. However, it remains unknown whether RSV exerts any preventive effect on the quantity of GABAergic interneurons and on the laminar organization in the cortex and HC. Thus, we aimed to evaluate RNA-Seq and microarray library datasets in order to identify altered biological pathways in the embryos from an ASD animal model. Subsequently, we aimed to verify which of these pathways could be modulated by RSV; another further goal of this study was to investigate the possible preventive effects of RSV in the VPA model related to GABAergic interneuron proportion and placement; synaptic proteins, and GABA receptor expression in the medial prefrontal cortex (mPFC) and HC from juvenile rats.

2. Results

2.1. Big Data Evaluation: Early Metabolic Alterations, Cell Cycle Dysfunctions, and Progressive Impairments in Embryos or Progenitor Cells from ASD-Associated Animal Models

In order to create insights regarding cortical embryonic alterations in the VPA model, we refined five datasets (DS) library repositories (Figure S2). The descriptions of the DS are summarized in Table 1.

Table 1. Description of the datasets analyzed.

Reference	Animal Model/Sample	Embryonic Day	Method
Balmer et al., 2014 (DS1)	Neural differentiated hESC exposed to VPA	6 h and 4 days after VPA exposure	Microarray
Canales et al., 2021 (DS2)	MIA Poly(I:C), mouse cortex	E12.5, E14.5, and E17.5	RNA-Seq
Cui et al., 2020 (DS3)	Cortical organoids exposed to VPA	5 days after exposure	RNA-Seq
Kalish et al., 2021 (DS4)	MIA Poly(I:C), mouse brain	E14 and E18	RNA-Seq (single-cell)
Oskvig et al., 2012 (DS5)	MIA Poly(I:C), rat cortex	E15	Microarray

These analyses helped conduct the evaluation of the experimental results, enabling the creation of more grounded hypotheses about the changes identified in postnatal life. In DS2, we observed an enrichment of differentially expressed genes (DEGs) for pathways associated with carbohydrate metabolism, hypoxia response, and sensory organ development six hours after MIA induction at E12.5 (besides other expected alterations like sensory organ development represented by the eye). Interestingly, 1.83% of these DEGs had an ortholog described in the SFARI database. At E14.5, the lipid, purine, and mitochondrial metabolism were associated with upregulated genes, while the protein dynamics (including histone modification and ubiquitination), cell cycle, nucleic acid metabolism, and response to reactive oxygen species were associated with downregulated genes. Moreover, the cell adhesion, extracellular matrix, synapse, and GABA/glutamate pathways were associated with upregulated DEGs (5.52% of these genes had an ortholog described in the SFARI database). At E18.5, mitochondrial and purine metabolism were still associated with upregulated genes, together with cell adhesion, extracellular matrix, synapse, glutamate metabolism, MAP/ERK, and adenylyl cyclase/cAMP signaling. Protein dynamics (including histone modification and ubiquitination), cell cycle, and nucleic acid metabolism were still associated with downregulated genes, together with WNT, Notch, and Hippo signaling, GABAergic neuron differentiation, and neuronal migration. Of note, 7.6% of the DEGs had an ortholog described in the Simons Foundation Autism Research Initiative (SFARI) database.

In DS5, at E15, upregulated genes were associated with mitochondrial and nucleic acid metabolism, ubiquitination regulation, and cell cycle. On the other hand, downregulated genes were associated with RNA metabolism, gene expression, histone modifications, GABAergic neurons differentiation, and neuronal migration. Interestingly, 5.15% of the DEGs had an ortholog described in the SFARI database.

In DS4, at E14.5, the DEGs identified in different subregions, including cortical subplate, cortical layers, subventricular zone, ganglionic eminence, and neural cells such as interneurons and radial glia, pointed to enriched pathways associated with mitochondrial metabolism, nucleic acid metabolism, protein dynamics, and cell cycle. Of note, 4.45–9.93% of the DEGs had an ortholog described in the SFARI database, depending on the brain region and cell type. At E18.5, the same regions and cells, and also other cortical layers and oligodendrocytes, presented a higher restricted pattern of alterations, especially in the mitochondrial metabolism and protein translation and metabolism. Around 2.91–7.47% of the DEGs had an ortholog described in the SFARI database, except for one region (ganglionic eminence) and one cell (radial glia), which did not present any match with SFARI.

In DS1, the neural cells exposed to VPA demonstrated, after six hours, DEGs associated with nucleic acid metabolism, cell cycle, MAP/ERK, and adenylyl cyclase/cAMP signaling, and neuronal migration, with 5.84% of the DEGs presenting an ortholog described in the SFARI database. After four days, the DEGs were associated with the same pathways, and WNT and Notch signaling, extracellular matrix, cell adhesion, and response to hypoxia. Interestingly, 7.42% of the DEGs had an ortholog described in the SFARI database.

Finally, in DS3, the organoids exposed to VPA demonstrated upregulation of genes associated with carbohydrate and lipid metabolism, ion transport, and cell adhesion. The downregulated genes were associated with nucleic acid and protein metabolism, eye development, synapse, and the WNT pathway. Only 6.36% of the DEGs had an ortholog described in the SFARI database.

2.2. The RSV Treatment Prevented the Neuronal Number Alterations Induced by VPA in the mPFC

The absolute numbers of total neurons (NeuN + DAPI) and interneurons (CB+ NeuN + DAPI, PV+ NeuN + DAPI, and SOM+ NeuN + DAPI) were counted in each area. The ratio between the number of each interneuron and total neurons is a measurement of the proportion between the inhibitory (interneuron) and excitatory components (the majority of the total neurons). This is done in each subarea of the mPFC and in the mPFC as a whole. The RSV was able to prevent the increased number of total neurons induced by VPA (Figure 1A, interaction factor: $F(1, 12) = 14.56$, $p = 0.0025$; Cont-VPA ppost-hoc = 0.0361; RSV-VPA ppost-hoc = 0.0627; RSV + VPA-VPA = 0.0016); the decreased ratio of PV+ interneurons (Figure 1E, interaction factor: $F(1, 13) = 9.314$, $p = 0.0093$; Cont-VPA ppost-hoc = 0.006; RSV-VPA ppost-hoc = 0.0065; RSV + VPA-VPA = 0.0436); and the decreased number of SOM+ interneurons (Figure 1F, interaction factor: $F(1, 12) = 12.39$, $p = 0.0042$; Cont-VPA ppost-hoc = 0.0008; RSV-VPA ppost-hoc = 0.0030; RSV + VPA-VPA = 0.0074) as well as the SOM+ ratio (Figure 1G, interaction factor: $F(1, 12) = 33.09$, $p < 0.0001$; Cont-VPA ppost-hoc < 0.0001; RSV-VPA ppost-hoc = 0.0002; RSV + VPA-VPA < 0.0001). PV+ number (Figure 1B), CB+ number (Figure 1D) and CB+ ratio (Figure 1E) did not present significant differences among groups.

2.3. The RSV Treatment Prevented the Increased Total Number of Neurons in the Deeper Layers and Whole PrL and IL

The data in Table 2 show that RSV was able to prevent the VPA-induced total neuron increase in deeper layers of PrL (Pre-Limbic Cortex), in the whole PrL, in deeper layers of IL (Infra Limbic Cortex), and in the whole IL. In the upper layers of PrL, a difference between the VPA and VPA-RSV groups was observed. In the deeper layers of aCC (anterior cingulate cortex) and whole aCC, RSV decreased the number of neurons. In the upper layers of IL and aCC, no significant differences were found.

2.4. The VPA Induced Alterations in PV+ Number and Ratio in Different Layers of the aCC and PrL

The data in Table 3 show that VPA decreased the number of PV+ neurons in the superficial layers of aCC, without RSV prevention. Interestingly, RSV prevented the VPA-induced decrease in PV+ ratio observed in the superficial layers of aCC. The PV+ ratio in the deeper layers of aCC was decreased by VPA, with partial prevention by RSV. When observing the whole aCC, the VPA decreased the PV+ ratio, which was prevented by RSV. In the superficial layers of PrL, the RSV prevented the VPA-induced increase in PV+ number. Regarding the ratio, a tendency was found in the interaction, and differences were identified in the isolated factors. In all the other regions, no differences were found among groups. Illustrative images of PV+ neurons are presented in Figure 2A.

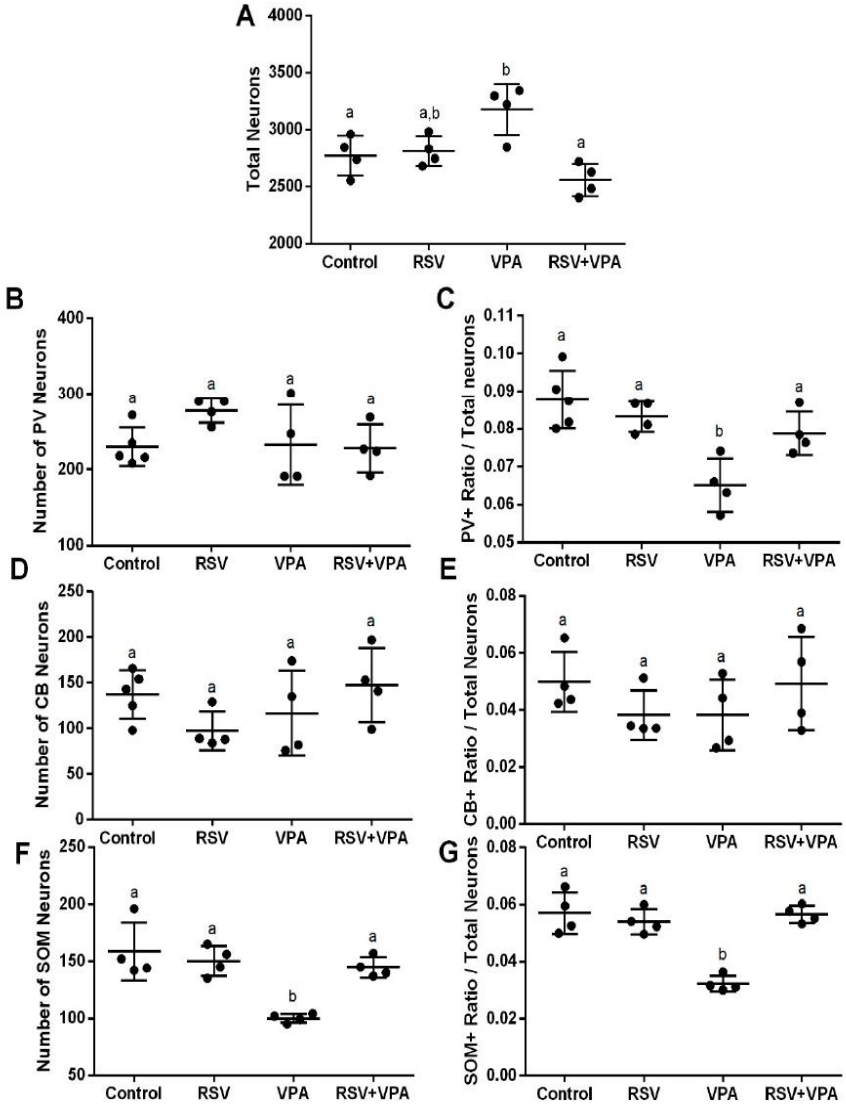

Figure 1. RSV prevents the increase in the number of total neurons, the reduction in the PV+ ratio, and the reduction in the number and ratio of SOM+ induced by VPA in the whole mPFC. (**A**) Quantification of total neurons. (**B**) Quantification of CB+ interneurons. (**C**) Quantification of ratio of CB+ interneurons/total neurons. (**D**) Quantification of PV+ interneurons. (**E**) Quantification of ratio of PV+ interneurons/total neurons (**F**) Quantification of SOM+ interneurons. (**G**) Quantification of the ratio of SOM+ interneurons/total neurons. Values are shown as mean ± standard deviation. Statistical analysis: two-way ANOVA followed by Bonferroni, $p < 0.05$ was considered significant. NCON: 5, NRSV: 4, NVPA: 4, NRSV + VPA:4 CB+NeuN+DAPI, and PV+NeuN+DAPI; N_{CON}: 4, N_{RSV}: 4, N_{VPA}: 4, $N_{RSV + VPA}$:4 and SOM+NeuN+DAPI. Different letters indicate significant differences in the post-test when interaction was significant ($p < 0.05$).

Table 2. Distribution profile of total neurons in the mPFC.

	Mean ± SD	F (DFn. DFd); *p*-Value	Pairwise Comparisons	
Total Neurons aCC (II/III)	CON: 336.00 ± 39.75 RSV: 321.00 ± 42.35 VPA: 371.25 ± 59.35 RSV + VPA: 318.75 ± 41.60	Interaction: F (1, 12) = 0.6523 p = 0.4350 VPA: F (1, 12) = 0.5052 p = 0.4908 RSV: F (1, 12) = 2.113 p = 0.1717	CON vs. RSV:	>0.9999
			CON vs. VPA:	>0.9999
			CON vs. RSV + VPA:	>0.9999
			RSV vs. VPA:	0.9108
			RSV vs. RSV + VPA:	>0.9999
			VPA vs. RSV + VPA:	0.8147
Total Neurons aCC (IV/V)	CON: 555.25 ± 76.01 RSV: 513.00 ± 13.71 VPA: 650.25 ± 49.85 RSV + VPA: 506.75 ± 39.78	Interaction: F (1, 12) = 4.086 p = 0.0661 # VPA: F (1, 12) = 3.140 p = 0.1018 RSV: F (1, 12) = 13.75 p = 0.0030 **	CON vs. RSV:	>0.9999
			CON vs. VPA:	0.1197
			CON vs. RSV + VPA:	>0.9999
			RSV vs. VPA:	0.0132 *
			RSV vs. RSV + VPA:	>0.9999
			VPA vs. RSV + VPA:	0.0096 **
Total Neurons Whole aCC	CON: 891.25 ± 104.45 RSV: 834.00 ± 51,153 VPA: 1021.00 ± 107.97 RSV + VPA: 825.50 ± 71.11	Interaction: F (1, 12) = 2.546 p = 0.1365 VPA: F (1, 12) = 1.960 p = 0.1868 RSV: F (1, 12) = 8.482 p = 0.0130 *	CON vs. RSV:	>0.9999
			CON vs. VPA:	0.3342
			CON vs. RSV + VPA:	>0.9999
			RSV vs. VPA:	0.0606 #
			RSV vs. RSV + VPA:	>0.9999
			VPA vs. RSV + VPA:	0.0469 *
Total Neurons PrL (II/III)	CON: 368.25 ± 55.12 RSV: 363.50 ± 14.91 VPA: 404.75 ± 28.15 RSV + VPA: 325.75 ± 13.25	Interaction: F (1, 12) = 5.214 p = 0.0414 * VPA: F (1, 12) = 0.001478 p = 0.9700 RSV: F (1, 12) = 6.633 p = 0.0243 *	CON vs. RSV:	>0.9999
			CON vs. VPA:	0.8305
			CON vs. RSV + VPA:	0.5360
			RSV vs. VPA:	0.5882
			RSV vs. RSV + VPA:	0.7594
			VPA vs. RSV + VPA:	0.0296 *
Total Neurons PrL (IV/V)	CON: 572.50 ± 22.10 RSV: 611.25 ± 62.50 VPA: 693.00 ± 49.22 RSV + VPA: 536.00 ± 49.43	Interaction: F (1, 12) = 16.54 p = 0.0016 ** VPA: F (1, 12) = 0.8838 p = 0.3657 RSV: F (1, 12) = 6.036 p = 0.0302 *	CON vs. RSV:	>0.9999
			CON vs. VPA:	0.0244 *
			CON vs. RSV + VPA:	>0.9999
			RSV vs. VPA:	0.2004
			RSV vs. RSV + VPA:	0.2832
			VPA vs. RSV + VPA:	0.0036 **
Total Neurons Whole PrL	CON: 940.75 ± 63.10 RSV: 974.75 ± 76.61 VPA: 1097.75 ± 61.32 RSV + VPA: 861.75 ± 60.10	Interaction: F (1, 12) = 16.93 p = 0.0014 ** F (1, 12) = 0.4497 p = 0.5152 F (1, 12) = 9.478 p = 0.0096 **	CON vs. RSV:	>0.9999
			CON vs. VPA:	0.0326 *
			CON vs. RSV + VPA:	0.6861
			RSV vs. VPA:	>0.1268
			RSV vs. RSV + VPA:	0.1884
			VPA vs. RSV + VPA:	0.0016 **

Table 2. *Cont.*

	Mean ± SD	F (DFn. DFd); *p*-Value	Pairwise Comparisons	
Total Neurons IL (II/III)	CON: 348.75 ± 47.98 RSV: 355.75 ± 26.98 VPA: 363.25 ± 20.85 RSV + VPA: 315.25 ± 17.41	Interaction: F (1, 12) =3.49 p = 0.0880 # VPA: F (1, 12) = 0.7707 p = 0.3972 RSV: F (1, 12) = 1.917 p =0.1914	CON vs. RSV:	>0.9999
			CON vs. VPA:	>0.9999
			CON vs. RSV + VPA:	0.8139
			RSV vs. VPA:	>0.9999
			RSV vs. RSV + VPA:	0.4623
			VPA vs. RSV + VPA:	0.2447
Total Neurons IL (IV/V)	CON: 593.75 ± 39.22 RSV: 646.00 ± 26.24 VPA: 696.50 ± 51.39 RSV + VPA: 557.00 ± 54.16	Interaction: F (1, 12) = 18.75 p = 0.0010 ** VPA: F (1, 12) = 0.1041 p = 0.7525 RSV: F (1, 12) = 3.858 p = 0.0731 #	CON vs. RSV:	0.7209
			CON vs. VPA:	0.0387 *
			CON vs. RSV + VPA:	>0.9999
			RSV vs. VPA:	0.7910
			RSV vs. RSV + VPA:	0.0904 #
			VPA vs. RSV + VPA:	0.0047 **
Total Neurons Whole IL	CON: 942.50 ± 27.47 RSV: 1001.75 ± 35.08 VPA: 1059.75 ± 66.74 RSV + VPA: 872.75 ± 53.72	Interaction: F (1, 12) = 26.01 p = 0.0003 *** VPA: F (1, 12) = 0.05921 p = 0.8119 RSV: F (1, 12) = 7.000 p = 0.0213	CON vs. RSV:	0.6496
			CON vs. VPA:	0.0297 *
			CON vs. RSV + VPA:	0.3820
			RSV vs. VPA:	0.6908
			RSV vs. RSV + VPA:	0.0158 *
			VPA vs. RSV + VPA:	0.0008 ***

II/III, upper cortical layers; IV/V, deeper cortical layers; aCC, anterior cingulate cortex; IL, infralimbic cortex; mPFC, medial prefrontal cortex; PrL, prelimbic cortex; SD, standard deviation. $p < 0.05$ considered significant. * $p < 0.05$. ** $p < 0.01$, *** $p < 0.001$, # trend. Statistical analyses: two-way ANOVA parametric test followed by Bonferroni. N_{CON}: 4. N_{RSV}: 4. N_{VPA}: 4. $N_{RSV + VPA}$: 4.

Table 3. Distribution profile of PV neurons in the mPFC.

	Mean ± SD	F (DFn. DFd); *p*-Value	Pairwise Comparisons	
PV Total aCC (II/III)	CON: 30.200 ± 2.863564 RSV: 28.750 ± 5.560276 VPA: 21.250 ± 7.274384 RSV + VPA: 25.000 ± 0.816	Interaction: F (1, 13) = 1.292 p = 0.2761 VPA: F (1, 13) = 7.709 p = 0.0157 * RSV: F (1, 13) = 0.2528 p = 0.6235	CON vs. RSV:	>0.9999
			CON vs. VPA:	0.0830
			CON vs. RSV + VPA:	0.7351
			RSV vs. VPA:	0.2497
			RSV vs. RSV + VPA:	>0.9999
			VPA vs. RSV + VPA:	>0.9999
PV Ratio aCC (II/III)	CON: 0.0804 ± 0.005 RSV: 0.0812 ± 0.017 VPA: 0.0506 ± 0.009 RSV + VPA: 0.0777 ± 0.005	Interaction: F (1, 13) = 6.862 p = 0.0212 * VPA: F (1, 13) = 11.06 p = 0.0055 ** RSV: F (1, 13) = 7.772 p = 0.0154 *	CON vs. RSV:	0.9999
			CON vs. VPA:	0.0050 **
			CON vs. RSV + VPA:	0.9999
			RSV vs. VPA:	0.0061 **
			RSV vs. RSV + VPA:	0.9999
			VPA vs. RSV + VPA:	0.0152 *
PV Total aCC (IV/V)	CON: 51.800 ± 8.55 RSV: 50.500 ± 13.89 VPA: 36.750 ± 15.37 RSV + VPA: 49.500 ± 10.96	Interaction: F (1, 13) = 1.391 p = 0.2593 VPA: F (1, 13) = 1.816 p = 0.2009 RSV: F (1, 13) = 0.9240 p = 0.3540	CON vs. RSV:	0.9999
			CON vs. VPA:	0.5361
			CON vs. RSV + VPA:	0.9999
			RSV vs. VPA:	0.8135
			RSV vs. RSV + VPA:	0.9999
			VPA vs. RSV + VPA:	0.9834

Table 3. *Cont.*

	Mean ± SD	F (DFn. DFd); *p*-Value	Pairwise Comparisons	
PV Ratio aCC (IV/V)	CON: 0.107 ± 0.0145 RSV: 0.0856 ± 0.01586 VPA: 0.0548 ± 0.0168 RSV + VPA: 0.0840 ± 0.019	Interaction: F (1, 13) = 9.992 p = 0.0075 ** VPA: F (1, 13) = 11.16 p = 0.0053 ** RSV: F (1, 13) = 0.2128 p = 0.6522	CON vs. RSV:	0.4297
			CON vs. VPA:	0.0024
			CON vs. RSV + VPA:	0.3398
			RSV vs. VPA:	0.1270
			RSV vs. RSV + VPA:	>0.9999
			VPA vs. RSV + VPA:	0.1606
PV Total Whole aCC	CON: 82.000 ± 11.25 RSV: 78.500 ± 16.60 VPA: 59.750 ± 23.60 RSV + VPA:74.500 ± 10.87	Interaction: F (1, 13) = 1.354 p = 0.2655 VPA: F (1, 13) = 2.801 p = 0.1181 RSV: F (1, 13) = 0.5144 p = 0.4859	CON vs. RSV:	0.9999
			CON vs. VPA:	0.3593
			CON vs. RSV + VPA:	0.9999
			RSV vs. VPA:	0.7401
			RSV vs. RSV + VPA:	0.9999
			VPA vs. RSV + VPA:	0.9999
PV Ratio Whole aCC	CON: 0.094 ± 0.009 RSV: 0.084 ± 0.014 VPA: 0.053 ± 0.012 RSV + VPA 0.081 ± 0.011	Interaction: F (1, 13) = 11.45 p = 0.0049 ** VPA: F (1, 13) = 14.87 p = 0.0020 ** RSV: F (1, 13) = 2.065 p = 0.1744	CON vs. RSV:	0.9999
			CON vs. VPA:	0.0009 ***
			CON vs. RSV + VPA:	0.6141
			RSV vs. VPA:	0.0177 *
			RSV vs. RSV + VPA:	0.9999
			VPA vs. RSV + VPA:	0.0330 *
PV Total PrL (II/III)	CON: 28.400 ± 2.88 RSV:24.500 ± 7.04 VPA: 38.750 ± 3.77 RSV + VPA:26.250 ± 6.94	Interaction: F (1, 13) = 4.159 p = 0.0483 * VPA: F (1, 13) = 7.359 p = 0.0178 * RSV: F (1, 13) = 7.675 p = 0.0159 *	CON vs. RSV:	0.9999
			CON vs. VPA:	0.0257 *
			CON vs. RSV + VPA:	0.9999
			RSV vs. VPA:	0.0138 *
			RSV vs. RSV + VPA:	0.9999
			VPA vs. RSV + VPA:	0.0335 *
PV Ratio PrL (II/III)	CON: 0.072 ± 0.004 RSV: 0.066 ± 0.009 VPA: 0.087 ± 0.003 RSV + VPA 0.070 ± 0.007	Interaction: F (1, 13) = 2.679 p = 0.0930 # VPA: F (1, 13) = 7.172 p = 0.0190 * RSV: F (1, 13) = 15.25 p = 0.0018 **	CON vs. RSV:	0.7397
			CON vs. VPA:	0.0474 *
			CON vs. RSV + VPA:	0.9999
			RSV vs. VPA:	0.0033 **
			RSV vs. RSV + VPA:	0.9999
			VPA vs. RSV + VPA:	0.0128 *
PV Total PrL (IV/V)	CON: 49.200 ± 7.82 RSV: 56.000 ± 6.83 VPA: 50.750 ± 5.12 RSV + VPA: 48.750 ± 12.57	Interaction: F (1, 13) = 1.129 p = 0.3072 VPA: F (1, 13) = 0.4738 p = 0.5033 RSV: F (1, 13) = 0.3360 p = 0.5720	CON vs. RSV:	>0.9999
			CON vs. VPA:	>0.9999
			CON vs. RSV + VPA:	>0.9999
			RSV vs. VPA:	>0.9999
			RSV vs. RSV + VPA:	>0.9999
			VPA vs. RSV + VPA:	>0.9999
PV Ratio PrL (IV/V)	CON: 0.096 ± 0.020 RSV:0.084 ± 0.009 VPA: 0.068 ± 0.010 RSV + VPA:0.082 ± 0.020	Interaction: F (1, 13) = 2.460 p = 0.1408 VPA: F (1, 13) = 3.640 p = 0.0787 # RSV: F (1, 13) = 0.001322 p = 0.9715	CON vs. RSV:	0.9999
			CON vs. VPA:	0.1520
			CON vs. RSV + VPA:	0.9999
			RSV vs. VPA:	0.9999
			RSV vs. RSV + VPA:	0.9999
			VPA vs. RSV + VPA:	0.9999

Table 3. *Cont.*

	Mean ± SD	F (DFn. DFd); *p*-Value	Pairwise Comparisons	
PV Total Whole PrL	CON: 74.400 ± 8.82 RSV: 80.500 ± 13.52 VPA: 86.500 ± 9.000 RSV + VPA: 75.000 ± 17.92	Interaction: F (1, 13) = 2.051 p = 0.1758 VPA: F (1, 13) = 0.2884 p = 0.6003 RSV: F (1, 13) = 0.1930 p = 0.6676	CON vs. RSV:	>0.9999
			CON vs. VPA:	>0.9999
			CON vs. RSV + VPA:	>0.9999
			RSV vs. VPA:	>0.9999
			RSV vs. RSV + VPA:	>0.9999
			VPA vs. RSV + VPA:	>0.9999
PV Ratio Whole PrL	CON: 0.088 ± 0.013 RSV:0.078 ± 0.006 VPA: 0.072 ± 0.001 RSV + VPA:0.077 ± 0.014	Interaction: F (1, 13) = 2.101 p = 0.1709 VPA: F (1, 13) = 2.834 p = 0.1161 RSV: F (1, 13) = 0.3874 p = 0.5444	CON vs. RSV:	0.9372
			CON vs. VPA:	0.2425
			CON vs. RSV + VPA:	0.7067
			RSV vs. VPA:	0.9999
			RSV vs. RSV + VPA:	0.9999
			VPA vs. RSV + VPA:	0.9999
PV Total IL (II/III)	CON: 28.800 ± 5.90 RSV: 29.250 ± 10.25 VPA: 33.750 ± 5.12 RSV + VPA: 25.000 ± 4.69	Interaction: F (1, 13) = 1.936 p = 0.1875 VPA: F (1, 13) = 0.01121 p = 0.9173 RSV: F (1, 13) = 1.576 p = 0.2315	CON vs. RSV:	>0.9999
			CON vs. VPA:	>0.9999
			CON vs. RSV + VPA:	>0.9999
			RSV vs. VPA:	>0.9999
			RSV vs. RSV + VPA:	>0.9999
			VPA vs. RSV + VPA:	0.5473
PV Ratio IL (II/III)	CON: 0.082 ± 0.010 RSV: 0.070 ± 0.015 VPA: 0.070 ± 0.010 RSV + VPA: 0.075 ± 0.008	Interaction: F (1, 13) = 2.644 p = 0.1279 VPA: F (1, 13) = 0.4062 p = 0.5350 RSV: F (1, 13) = 0.3412 p = 0.5691	CON vs. RSV:	0.7940
			CON vs. VPA:	0.7443
			CON vs. RSV + VPA:	>0.9999
			RSV vs. VPA:	>0.9999
			RSV vs. RSV + VPA:	>0.9999
			VPA vs. RSV + VPA:	>0.9999
PV Total IL (IV/V)	CON: 45.40 ± 9.50 RSV: 56.00 ± 28.25 VPA: 48.00 ± 12.355 RSV + VPA: 53.50 ± 11.80	Interaction: F (1, 13) = 0.1646 p = 0.6915 VPA: F (1, 13) = 0.001360 p = 0.9711 RSV: F (1, 13) = 1.171 p = 0.2989	CON vs. RSV:	>0.9999
			CON vs. VPA:	>0.9999
			CON vs. RSV + VPA:	>0.9999
			RSV vs. VPA:	>0.9999
			RSV vs. RSV + VPA:	>0.9999
			VPA vs. RSV + VPA:	>0.9999
PV Ratio IL (IV/V)	CON:0.080 ± 0.020 RSV: 0.073 ± 0.031 VPA: 0.067 ± 0.016 RSV + VPA: 0.081 ± 0.020	Interaction: F (1, 13) = 1.046 p = 0.3251 VPA: F (1, 13) = 0.04663 p = 0.8324 RSV: F (1, 13) = 0.1055 p = 0.7504	CON vs. RSV:	>0.9999
			CON vs. VPA:	>0.9999
			CON vs. RSV + VPA:	>0.9999
			RSV vs. VPA:	>0.9999
			RSV vs. RSV + VPA:	>0.9999
			VPA vs. RSV + VPA:	>0.9999
PV Total Whole IL	CON: 74.60 ± 8.50 RSV: 80.50 ± 13.52 VPA: 81.75 ± 15.25 RSV + VPA: 77.50 ± 15.25	Interaction: F (1, 13) = 0.6249 p = 0.4434 VPA: F (1, 13) = 0.1045 p = 0.7517 RSV: F (1, 13) = 0.01651 p = 0.8997	CON vs. RSV:	>0.9999
			CON vs. VPA:	>0.9999
			CON vs. RSV + VPA:	>0.9999
			RSV vs. VPA:	>0.9999
			RSV vs. RSV + VPA:	>0.9999
			VPA vs. RSV + VPA:	>0.9999

Table 3. *Cont.*

	Mean ± SD	F (DFn. DFd); *p*-Value	Pairwise Comparisons	
PV Ratio Whole IL	CON: 0.082 ± 0.015 RSV: 0.072 ± 0.024 VPA: 0.068 ± 0.013 RSV + VPA: 0.079 ± 0.013	Interaction: F (1, 13) = 1.533 $p = 0.2376$ VPA: F (1, 13) = 0.1634 $p = 0.6926$ RSV: F (1, 13) = 0.006546 $p = 0.9367$	CON vs. RSV:	>0.9999
			CON vs. VPA:	>0.9999
			CON vs. RSV + VPA:	>0.9999
			RSV vs. VPA:	>0.9999
			RSV vs. RSV + VPA:	>0.9999
			VPA vs. RSV + VPA:	>0.9999

II/III, upper cortical layers; IV/V, deeper cortical layers; aCC, anterior cingulate cortex; IL, infralimbic cortex; mPFC, medial prefrontal cortex; PrL, prelimbic cortex; PV, parvalbumin-positive interneuron; SD, standard deviation. $p < 0.05$ was considered significant. * $p < 0.05$. ** $p < 0.01$, *** $p < 0.001$, # trend. Statistical analyses: two-way ANOVA parametric test followed by Bonferroni. N_{CON}: 4. N_{RSV}: 4. N_{VPA}: 4. $N_{RSV + VPA}$: 4.

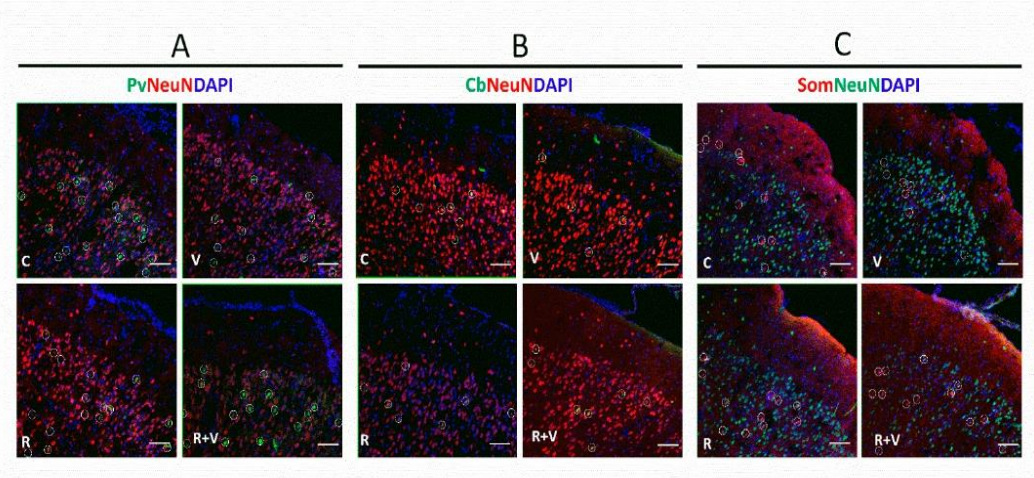

Figure 2. Representative immunofluorescence images of total neurons, PV+, CB+, and SOM+ in the mPFC. Representative images of the aCC, upper layers (II/III). (**A**) Pv, parvalbumin (green); NeuN (red); DAPI (blue). (**B**) Cb, calbindin (green); NeuN (red); DAPI (blue). (**C**) Som, somatostatin (red); NeuN (green); DAPI (blue). Scale bar: 50 µm. The respective interneurons are highlighted within white circles. aCC, anterior cingulate cortex; CB, calbindin-neurons; mPFC, medial frontal cortex; PV, parvalbumin-neurons; SOM, somatostatin-neurons.

2.5. The VPA Induced Alterations in CB+ Ratio in the Upper Layers of aCC, PrL, and IL

The data in Table 4 show that RSV prevented the decreased CB+ ratio induced by VPA in the superficial layers of aCC, but not in the superficial layers of PrL and IL. The differences found in the CB+ number in the superficial layers of aCC, ratio in the whole aCC, ratio in the whole PrL, and ratio in the IL were not associated with any specific factor after the post-hoc test. Illustrative images of PV+ neurons are presented in Figure 2B.

Table 4. Distribution profile of CB neurons in the mPFC.

	Mean ± SD	F (DFn. DFd); *p*-Value	Pairwise Comparisons	
CB Total aCC (II/III)	CON: 19.20 ± 6.87 RSV: 16.75 ± 2.50 VPA: 13.25 ± 6.70 RSV + VPA: 21.75 ± 3.59	Interaction: F (1, 13) = 6.023 p = 0.0290 * VPA: F (1, 13) = 0.03959 p = 0.8454 RSV: F (1, 13) = 2.327 p = 0.1511	CON vs. RSV:	0.9999
			CON vs. VPA:	0.7519
			CON vs. RSV + VPA:	0.9999
			RSV vs. VPA:	0.9999
			RSV vs. RSV + VPA:	0.5430
			VPA vs. RSV + VPA:	0.1006
CB Ratio aCC (II/III)	CON: 0.057 ± 0.005 RSV: 0.050 ± 0.006 VPA: 0.034 ± 0.010 RSV + VPA: 0.064 ± 0.014	Interaction: F (1, 13) = 18.31 p = 0.0009 *** VPA: F (1, 13) = 1.081 p = 0.3175 RSV: F (1, 13) = 6.006 p = 0.0292	CON vs. RSV:	0.9999
			CON vs. VPA:	0.0117 *
			CON vs. RSV + VPA:	0.9999
			RSV vs. VPA:	0.1905
			RSV vs. RSV + VPA:	0.2626
			VPA vs. RSV + VPA:	0.0028 **
CB Total aCC (IV/V)	CON: 22.00 ± 7.25 RSV: 17.00 ± 4.45 VPA: 22.75 ± 10.00 RSV + VPA: 22.5 ± 9.95	Interaction: F (1, 13) = 0.4352 p = 0.5210 VPA: F (1, 13) = 0.7193 p = 0.4117 RSV: F (1, 13) = 0.5220 p = 0.4828	CON vs. RSV:	0.9999
			CON vs. VPA:	0.9999
			CON vs. RSV + VPA:	0.9999
			RSV vs. VPA:	0.9999
			RSV vs. RSV + VPA:	0.9999
			VPA vs. RSV + VPA:	0.9999
CB Ratio aCC (IV/V)	CON: 0.059 ± 0.024 RSV: 0.037 ± 0.012 VPA: 0.039 ± 0.011 RSV + VPA: 0.042 ± 0.020	Interaction: F (1, 13) = 2.304 p = 0.1530 VPA:F (1, 13) = 0.7381 p = 0.4058 RSV:F (1, 13) = 1.381 p = 0.2610	CON vs. RSV:	0.4334
			CON vs. VPA:	0.6472
			CON vs. RSV + VPA:	0.9794
			RSV vs. VPA:	0.9999
			RSV vs. RSV + VPA:	0.9999
			VPA vs. RSV + VPA:	0.9999
CB Total Whole aCC	CON: 37.2 ± 13.92 RSV: 28.25 ± 8.15 VPA: 38.75 ± 19.77 RSV + VPA: 39.25 ± 17.40	Interaction: F (1, 13) = 0.4000 p = 0.5381 VPA: F (1, 13) = 0.7055 p = 0.4161 RSV: (1, 13) = 0.3198 p = 0.5813	CON vs. RSV:	0.9999
			CON vs. VPA:	0.9999
			CON vs. RSV + VPA:	0.9999
			RSV vs. VPA:	0.9999
			RSV vs. RSV + VPA:	0.9999
			VPA vs. RSV + VPA:	0.9999
CB Ratio Whole aCC	CON: 0.058 ± 0.014 RSV: 0.042 ± 0.009 VPA: 0.038 ± 0.010 RSV + VPA 0.051 ± 0.017	Interaction: F (1, 13) = 5.701 p = 0.0328 * VPA: F (1, 13) = 0.9515 p = 0.3471 RSV: F (1, 13) = 0.03555 p = 0.8534	CON vs. RSV:	0.5037
			CON vs. VPA:	0.1775
			CON vs. RSV + VPA:	0.9999
			RSV vs. VPA:	0.9999
			RSV vs. RSV + VPA:	0.9999
			VPA vs. RSV + VPA:	0.9213
CB Total PrL (II/III)	CON: 26.20 ± 7.35 RSV: 18.25 ± 1.70 VPA: 16.00 ± 9.75 RSV + VPA:19.25 ± 5.45	Interaction: F (1, 13) = 2.859 p = 0.1147 VPA: F (1, 13) = 1.929 p = 0.1882 RSV: F (1, 13) = 0.5036 p = 0.4905	CON vs. RSV:	0.6284
			CON vs. VPA:	0.2603
			CON vs. RSV + VPA:	0.9078
			RSV vs. VPA:	0.9999
			RSV vs. RSV + VPA:	0.9999
			VPA vs. RSV + VPA:	0.9999

Table 4. *Cont.*

	Mean ± SD	F (DFn. DFd); *p*-Value	Pairwise Comparisons	
CB Ratio PrL (II/III)	CON: 0.079 ± 0.025 RSV: 0.059 ± 0.009 VPA: 0.034 ± 0.015 RSV + VPA: 0.057 ± 0.016	Interaction: F (1, 13) = 6.149 p = 0.0276 VPA: F (1, 13) = 7.593 p = 0.0164 RSV: F (1, 13) = 0.01238 p = 0.9131	CON vs. RSV:	0.6541
			CON vs. VPA:	0.0132
			CON vs. RSV + VPA:	0.4615
			RSV vs. VPA:	0.4187
			RSV vs. RSV + VPA:	0.9999
			VPA vs. RSV + VPA:	0.5849
CB Total PrL (IV/V)	CON: 23.20 ± 4.35 RSV: 19.00 ± 4.95 VPA: 26.75 ± 14.05 RSV + VPA: 33.2 ± 7.65	Interaction: F (1, 13) = 1,748 p = 0.2089 VPA: F (1, 13) = 4.837 p = 0.0709 # RSV: F (1, 13) = 0.04947 p = 0.8275	CON vs. RSV:	0.9999
			CON vs. VPA:	0.9999
			CON vs. RSV + VPA:	0.6120
			RSV vs. VPA:	0.9999
			RSV vs. RSV + VPA:	0.1830
			VPA vs. RSV + VPA:	0.9999
CB Ratio PrL (IV/V)	CON: 0.054 ± 0.018 RSV: 0.034 ± 0.009 VPA: 0.041 ± 0.017 RSV + VPA: 0.050 ± 0.014	Interaction: F (1, 13) = 3.755 p = 0.0747 VPA F (1, 13) = 0.04387 p = 0.8373 RSV: F (1, 13) = 0.6898 p = 0.4212	CON vs. RSV:	0.3931
			CON vs. VPA:	0.9999
			CON vs. RSV + VPA:	0.9999
			RSV vs. VPA:	0.9999
			RSV vs. RSV + VPA:	0.9763
			VPA vs. RSV + VPA:	0.9999
CB Total Whole PrL	CON: 51.00 ± 7.87 RSV: 36.25 ± 6.95 VPA: 42.75 ± 19.25 RSV + VPA:52.25 ± 7.90	interaction: F (1, 12) = 3.243 p = 0.0969 VPA: F (1, 12) = 0.3312 p = 0.5756 RSV: F (1, 12) = 0.1520 p = 0.7035	CON vs. RSV:	0.8841
			CON vs. VPA:	0.9999
			CON vs. RSV + VPA:	0.9999
			RSV vs. VPA:	0.9999
			RSV vs. RSV + VPA:	0.7124
			VPA vs. RSV + VPA:	0.9999
CB Ratio Whole PrL	CON: 0.062 ± 0.016 RSV: 0.043 ± 0.08 VPA: 0.038 ± 0.016 RSV + VPA: 0.052 ± 0.014	Interaction: F (1, 13) = 5.736 p = 0.0324 * VPA: F (1, 13) = 0.4439 p = 0.5169 RSV: F (1, 13) = 0.2759 p = 0.6082	CON vs. RSV:	0.3221
			CON vs. VPA:	0.2670
			CON vs. RSV + VPA:	0.9999
			RSV vs. VPA:	0.9999
			RSV vs. RSV + VPA:	0.9999
			VPA vs. RSV + VPA:	0.9999
CB Total IL (II/III)	CON: 18.75 ± 5.50 RSV: 14.25 ± 4.70 VPA: 14.25 ± 7.00 RSV + VPA: 26.00 ± 11.5	Interaction: F (1, 11) = 3.947 p = 0.0662 # VPA: F (1, 11) = 7.953 p = 0.4461 RSV: F (1, 11) = 12.79 p = 0.4471	CON vs. RSV:	0.9999
			CON vs. VPA:	0.9999
			CON vs. RSV + VPA:	0.9999
			RSV vs. VPA:	0.9999
			RSV vs. RSV + VPA:	0.4421
			VPA vs. RSV + VPA:	0.4421
CB Ratio IL (II/III)	CON: 0.069 ± 0.018 RSV: 0.043 ± 0.013 VPA: 0.031 ± 0.007 RSV + VPA: 0.060 ± 0.023	Interaction: F (1, 13) = 13.42 p = 0.0029 ** VPA: F (1, 13) = 1.476 p = 0.2460 RSV: F (1, 13) = 0.01159 p = 0.9159	CON vs. RSV:	0.1364
			CON vs. VPA:	0.0216 *
			CON vs. RSV + VPA:	0.9999
			RSV vs. VPA:	0.9999
			RSV vs. RSV + VPA:	0.6924
			VPA vs. RSV + VPA:	0.1324

Table 4. *Cont.*

	Mean ± SD	F (DFn. DFd); *p*-Value	Pairwise Comparisons	
CB Total IL (IV/V)	CON: 29.00 ± 10.90 RSV: 19.00 ± 6.13 VPA: 26.25.00 ± 6.18 RSV + VPA: 30.00 ± 8.25	Interaction: F (1, 13) = 3.990 p = 0.0672 # VPA: F (1, 13) = 1,271 p = 0.2800 RSV: F (1, 13) = 0.5051 p = 0.4898	CON vs. RSV:	0.4251
			CON vs. VPA:	0.9999
			CON vs. RSV + VPA:	0.9999
			RSV vs. VPA:	0.9999
			RSV vs. RSV + VPA:	0.3037
			VPA vs. RSV + VPA:	0.9999
CB Ratio IL (IV/V)	CON: 0.045 ± 0.010 RSV: 0.035 ± 0.013 VPA: 0.040 ± 0.010 RSV + VPA: 0.048 ± 0.014	Interaction: F (1, 12) = 2.805 p = 0.1198 VPA: F (1, 12) = 0.3000 p = 0.5939 RSV: F (1, 12) = 0.07687 p = 0.7863	CON vs. RSV:	0.9999
			CON vs. VPA:	0.9999
			CON vs. RSV + VPA:	0.9999
			RSV vs. VPA:	0.9999
			RSV vs. RSV + VPA:	0.8522
			VPA vs. RSV + VPA:	0.9999
CB Total Whole IL	CON: 44.25 ± 9.45 RSV: 33.00 ± 9.70 VPA: 40.25 ± 12.00 RSV + VPA: 55.00 ± 18.65	Interaction: F (1, 13) = 5.378 p = 0.0597 # VPA: F (1, 13) = 0.7738 p = 0.3950 RSV: F (1, 13) = 0.01655 p = 0.8996	CON vs. RSV:	0.5925
			CON vs. VPA:	0.9999
			CON vs. RSV + VPA:	0.9999
			RSV vs. VPA:	0.9999
			RSV vs. RSV + VPA:	0.2766
			VPA vs. RSV + VPA:	0.9303
CB Ratio Whole IL	CON: 0.64 ± 0.027 RSV: 0.39 ± 0.011 VPA: 0.36 ± 0.008 RSV + VPA: 0.53 ± 0.018	Interaction: F (1, 13) = 5.736 p = 0.0324 * VPA: F (1, 13) = 0.4439 p = 0.5169 RSV: F (1, 13) = 0.2759 p = 0.6082	CON vs. RSV:	0.3221
			CON vs. VPA:	0.2670
			CON vs. RSV + VPA:	0.9999
			RSV vs. VPA:	0.9999
			RSV vs. RSV + VPA:	0.9999
			VPA vs. RSV + VPA:	0.9999

II/III, upper cortical layers; IV/V, deeper cortical layers; aCC, anterior cingulate cortex; CB, calbindin-positive interneuron; IL, infralimbic cortex; mPFC, medial prefrontal cortex; PrL, prelimbic cortex; SD, standard deviation. $p < 0.05$ considered significant. * $p < 0.05$, ** $p < 0.01$, *** $p < 0.001$, # trend. Statistical analyses: two-way ANOVA parametric test followed by Bonferroni. N_{CON}: 5. N_{RSV}: 4. N_{VPA}: 4. $N_{RSV + VPA}$: 4.

2.6. The RSV Prevented the Widespread Impairments Induced by VPA in SOM+ Neurons

The data in Table 5 show that RSV prevented the VPA-induced decrease in SOM+ number and ratio in the superficial layers of aCC. The RSV was also able to prevent the decreased SOM+ number and ratio induced by VPA in the deeper layers of aCC. These results reflected a preventive effect of RSV in the whole aCC in both decreased SOM+ number and ratio. The RSV was also able to prevent the VPA-induced SOM+ ratio decrease in the superficial layers of PrL. In the deeper layers of PrL, RSV + VPA did not differ from any other group, but RSV prevented the reduction in the SOM+ ratio. In the whole PrL, RSV + VPA did not differ from any other group for the SOM+ number, but a prevention was observed in the ratio. In the superficial layers of IL, VPA decreased the numbers of SOM+ neurons. Regarding the ratio, a tendency was found in the interaction, and relevant differences were identified in the isolated factors. In the deeper layers of IL, RSV prevented the VPA-induced decrease of SOM+ neurons in both number and ratio. In the whole IL, RSV prevented the reductions in the SOM+ number and ratio. Illustrative images of PV+ neurons are presented in Figure 2C.

Table 5. Distribution profile of SOM neurons in the mPFC.

	Mean ± SD	F (DFn. DFd); *p*-Value	Pairwise Comparisons	
SOM Total aCC (II/III)	CON: 18.5 ± 2.65 RSV: 17.5 ± 0.5 VPA: 12 ± 2.50 RSV + VPA: 18.75 ± 2.00	Interaction: F (1, 12) = 13.66 p = 0.0031 ** VPA: F (1, 12) = 6.270 p = 0.0277 * RSV: F (1, 12) = 7.521 p = 0.0178 *	CON vs. RSV:	>0.9999
			CON vs. VPA:	0.0053 **
			CON vs. RSV + VPA:	>0.9999
			RSV vs. VPA:	0.0179 *
			RSV vs. RSV + VPA:	>0.9999
			VPA vs. RSV + VPA:	0.0040 **
SOM Ratio aCC (II/III)	CON: 0.060 ± 0.009 RSV: 0.059 ± 0.008 VPA: 0.034 ± 0.007 RSV + VPA: 0.068 ± 0.002	Interaction: F (1, 12) = 25.14 p = 0.0003 *** VPA: F (1, 12) = 6.460 p = 0.0259 * RSV: F (1, 12) = 22.93 p = 0.0004 ***	CON vs. RSV:	>0.9999
			CON vs. VPA:	0.0011 **
			CON vs. RSV + VPA:	0.8282
			RSV vs. VPA:	0.0014 **
			RSV vs. RSV + VPA:	0.6359
			VPA vs. RSV + VPA:	<0.0001 ****
SOM Total aCC (IV/V)	CON: 33.25 ± 5.56 RSV: 30.50 ± 3.70 VPA: 21.00 ± 1.15 RSV + VPA: 31.25 ± 2.63	Interaction: F (1, 12) = 12.64 p = 0.0040 ** VPA: F (1, 12) = 9.888 p = 0.0085 ** RSV: F (1, 12) = 4.206 p = 0.0628 *	CON vs. RSV:	>0.9999
			CON vs. VPA:	0.0029 **
			CON vs. RSV + VPA:	>0.9999
			RSV vs. VPA:	0.0191 *
			RSV vs. RSV + VPA:	>0.9999
			VPA vs. RSV + VPA:	0.0113 *
SOM Ratio aCC (IV/V)	CON: 0.060 ± 0.010 RSV: 0.060 ± 0.008 VPA: 0.036 ± 0.007 RSV + VPA: 0.062 ± 0.005	Interaction: F (1, 12) = 15.49 p = 0.0020 ** VPA: F (1, 12) = 11.03 p = 0.0061 ** RSV: F (1, 12) = 13.84 p = 0.0029 **	CON vs. RSV:	0.9999
			CON vs. VPA:	0.0015 **
			CON vs. RSV + VPA:	0.9999
			RSV vs. VPA:	0.0019 **
			RSV vs. RSV + VPA:	0.9999
			VPA vs. RSV + VPA:	0.0009 ***
SOM Total Whole aCC	CON: 51.75 ± 4.20 RSV: 48.00 ± 4.00 VPA: 33.00 ± 1.15 RSV + VPA: 50.00 ± 4.32	Interaction: F (1, 12) = 31.75 p = 0.0001 *** VPA: F (1, 12) = 20.69 p = 0.0007 *** RSV: F (1, 12) = 12.94 p = 0.0037 **	CON vs. RSV:	>0.9999
			CON vs. VPA:	<0.0001 ****
			CON vs. RSV + VPA:	>0.9999
			RSV vs. VPA:	0.0005 ***
			RSV vs. RSV + VPA:	>0.9999
			VPA vs. RSV + VPA:	0.0002 ***
SOM Ratio Whole aCC	CON: 0.058 ± 0.006 RSV: 0.056 ± 0.007 VPA: 0.033 ± 0.005 RSV + VPA: 0.061 ± 0.005	Interaction: F (1, 12) = 23.64 p = 0.0004 *** VPA: F (1, 12) = 14.87 p = 0.0023 ** RSV: F (1, 12) = 21.35 p = 0.0006 ***	CON vs. RSV:	>0.9999
			CON vs. VPA:	0.0003 ***
			CON vs. RSV + VPA:	>0.9999
			RSV vs. VPA:	0.0004 ***
			RSV vs. RSV + VPA:	>0.9999
			VPA vs. RSV + VPA:	0.0001 ***
SOM Total PrL (II/III)	CON: 19.75 ± 8.25 RSV: 18.25 ± 1.55 VPA: 12.50 ± 0.70 RSV + VPA: 17.25 ± 1.90	Interaction: F (1, 12) = 2.825 p = 0.1186 VPA: F (1, 12) = 2.825 p = 0.1186 RSV: F (1, 12) = 0.2721 p = 0.6114	CON vs. RSV:	>0.9999
			CON vs. VPA:	0.2097
			CON vs. RSV + VPA:	>0.9999
			RSV vs. VPA:	0.8721
			RSV vs. RSV + VPA:	>0.9999
			VPA vs. RSV + VPA:	0.8721

Table 5. *Cont.*

	Mean ± SD	F (DFn. DFd); *p*-Value	Pairwise Comparisons	
SOM Ratio PrL (II/III)	CON: 0.053 ± 0.016 RSV: 0.047 ± 0.003 VPA: 0.032 ± 0.004 RSV + VPA: 0.049 ± 0.007	Interaction: F (1, 12) = 8.612 p = 0.0125 * VPA: F (1, 12) = 2.893 p = 0.1147 RSV: F (1, 12) = 3.103 p = 0.1036	CON vs. RSV:	>0.9999
			CON vs. VPA:	0.0396 *
			CON vs. RSV + VPA:	>0.9999
			RSV vs. VPA:	0.1841
			RSV vs. RSV + VPA:	>0.9999
			VPA vs. RSV + VPA:	0.0366 *
SOM Total PrL (IV/V)	CON: 37.00 ± 5.90 RSV: 34.25 ± 5.75 VPA: 21.25 ± 3.86 RSV + VPA: 29.25 ± 2.63	Interaction: F (1, 12) = 5.170 p = 0.0422 ** VPA: F (1, 12) = 19.26 p = 0.0009 *** RSV: F (1, 12) = 1.233 p = 0.2886	CON vs. RSV:	>0.9999
			CON vs. VPA:	0.0030 **
			CON vs. RSV + VPA:	0.2334
			RSV vs. VPA:	0.0129 *
			RSV vs. RSV + VPA:	0.9636
			VPA vs. RSV + VPA:	0.2037
SOM Ratio PrL (IV/V)	CON: 0.064 ± 0.008 RSV: 0.056 ± 0.008 VPA: 0.032 ± 0.007 RSV + VPA: 0.055 ± 0.005	Interaction: F (1, 12) = 18.82 p = 0.0010 VPA: F (1, 12) = 22.16 p = 0.0005 *** RSV: F (1, 12) = 4.211 p = 0.0626 #	CON vs. RSV:	0.7919
			CON vs. VPA:	0.0002 ***
			CON vs. RSV + VPA:	0.5095
			RSV vs. VPA:	0.0027**
			RSV vs. RSV + VPA:	>0.9999
			VPA vs. RSV + VPA:	0.0042 **
SOM Total Whole PrL	CON: 56.75 ± 12.55 RSV: 51.50 ± 7.25 VPA: 33.75 ± 3.40 RSV + VPA: 46.50 ± 2.00	Interaction: F (1, 12) = 5.739 p = 0.0338 * VPA: F (1, 12) = 13.89 p = 0.0029 ** RSV: F (1, 12) = 0.9963 p = 0.3379	CON vs. RSV:	>0.9999
			CON vs. VPA:	0.0059 **
			CON vs. RSV + VPA:	0.4661
			RSV vs. VPA:	0.0353 *
			RSV vs. RSV + VPA:	>0.9999
			VPA vs. RSV + VPA:	0.2012
SOM Ratio Whole PrL	CON: 0.060 ± 0.011 RSV: 0.053 ± 0.006 VPA: 0.031 ± 0.004 RSV + VPA: 0.054 ± 0.005	Interaction: F (1, 12) = 18.37 p = 0.0011 ** VPA: F (1, 12) = 15.21 p = 0.0021 ** RSV: F (1, 12) = 4.905 p = 0.0469 *	CON vs. RSV:	>0.9999
			CON vs. VPA:	0.0005 ***
			CON vs. RSV + VPA:	>0.9999
			RSV vs. VPA:	0.0059 **
			RSV vs. RSV + VPA:	>0.9999
			VPA vs. RSV + VPA:	0.0037 **
SOM Total IL (II/III)	CON: 15.50 ± 1.75 RSV: 17.00 ± 2.45 VPA: 11.50 ± 2.50 RSV + VPA: 15.25 ± 1.50	Interaction: F (1, 12) = 1,152 p = 0.3043 VPA: F (1, 12) = 7.521 p = 0.0178 * RSV: F (1, 12) = 6.270 p = 0.0277 *	CON vs. RSV:	>0.9999
			CON vs. VPA:	0.1163
			CON vs. RSV + VPA:	>0.9999
			RSV vs. VPA:	0.0179 *
			RSV vs. RSV + VPA:	>0.9999
			VPA vs. RSV + VPA:	0.1587
SOM Ratio IL (II/III)	CON: 0.045 ± 0.007 RSV: 0.048 ± 0.008 VPA: 0.032 ± 0.006 RSV + VPA: 0.048 ± 0.004	Interaction: F (1, 12) = 4.503 p = 0.0553 # VPA: F (1, 12) = 3.938 p = 0.0706 # RSV: F (1, 12) = 9.410 p = 0.0098 **	CON vs. RSV:	>0.9999
			CON vs. VPA:	0.0794 #
			CON vs. RSV + VPA:	>0.9999
			RSV vs. VPA:	0.0230 *
			RSV vs. RSV + VPA:	>0.9999
			VPA vs. RSV + VPA:	0.0193 *

Table 5. *Cont.*

	Mean ± SD	F (DFn. DFd); *p*-Value	Pairwise Comparisons	
SOM Total IL (IV/V)	CON: 34.50 ± 7.15 RSV: 33.75 ± 1.00 VPA: 21.75 ± 3.00 RSV + VPA: 33.00 ± 1.45	Interaction: F (1, 12) = 9.167 p = 0.0105 * VPA: F (1, 12) = 11,60 p = 0.0052 ** RSV: F (1, 12) = 7.019 p = 0.0212 *	CON vs. RSV:	>0.9999
			CON vs. VPA:	0.0040 **
			CON vs. RSV + VPA:	>0.9999
			RSV vs. VPA:	0.0064 **
			RSV vs. RSV + VPA:	>0.9999
			VPA vs. RSV + VPA:	0.0103*
SOM Ratio IL (IV/V)	CON: 0.058 ± 0.011 RSV: 0.052 ± 0.002 VPA: 0.032 ± 0.003 RSV + VPA: 0.059 ± 0.005	Interaction: F (1, 12) = 29.00 p = 0.0002 *** VPA: F (1, 12) = 9.617 p = 0.0092 ** RSV: F (1, 12) = 12.21 p = 0.0044 **	CON vs. RSV:	>0.9999
			CON vs. VPA:	0.0004 ***
			CON vs. RSV + VPA:	>0.9999
			RSV vs. VPA:	0.0033 **
			RSV vs. RSV + VPA:	0.7939
			VPA vs. RSV + VPA:	0.0002 ***
SOM Total Whole IL	CON: 50.00 ± 8.70 RSV: 50.75 ± 3.30 VPA: 33.25 ± 4.71 RSV + VPA: 48.25 ± 2.63	Interaction: F (1, 12) = 6.840 p = 0.0226 * VPA: F (1, 12) = 12.48 p = 0.0041 ** RSV: F (1, 12) = 8.356 p = 0.0136 *	CON vs. RSV:	>0.9999
			CON vs. VPA:	0.0057 **
			CON vs. RSV + VPA:	>0.9999
			RSV vs. VPA:	0.0041 **
			RSV vs. RSV + VPA:	>0.9999
			VPA vs. RSV + VPA:	0.0128 *
SOM Ratio Whole IL	CON: 0.053 ± 0.008 RSV: 0.051 ± 0.003 VPA: 0.032 ± 0.003 RSV + VPA: 0.055 ± 0.001	Interaction: F (1, 12) = 31.96 p = 0.0001 *** VPA: F (1, 12) = 12.93 p = 0.0037 ** RSV: F (1, 12) = 21.75 p = 0.0005 ***	CON vs. RSV:	>0.9999
			CON vs. VPA:	0.0002 ***
			CON vs. RSV + VPA:	>0.9999
			RSV vs. VPA:	0.0005 ***
			RSV vs. RSV + VPA:	>0.9999
			VPA vs. RSV + VPA:	<0.0001 ****

II/III, upper cortical layers; IV/V, deeper cortical layers; aCC, anterior cingulate cortex; IL, infralimbic cortex; mPFC, medial prefrontal cortex; PrL, prelimbic cortex; SD, standard deviation; SOM, somatostatin-positive interneuron. $p < 0.05$ was considered significant. * $p < 0.05$, ** $p < 0.01$, *** $p < 0.001$, **** $p < 0.0001$, # trend. Statistical analyses: two-way ANOVA parametric test followed by Bonferroni. N_{CON}: 4. N_{RSV}: 4. N_{VPA}: 4. $N_{RSV + VPA}$: 4.

2.7. Both VPA and RSV Changed the Levels of Synaptic Proteins, whereas the Level of $GABA_A$ Was Affected Only by VPA

The protein quantification shows that VPA decreased $GABA_A$, without RSV prevention (VPA: F (1, 12) = 16.00, p = 0.0018) (Figure 3A). Both RSV and VPA decreased gephyrin (Interaction: F (1, 12) = 21.56, p = 0.006; Cont-RSV ppost-hoc = 0.0031; Cont-VPApost-hoc = 0.0001; Cont-RSV + VPApost-hoc = 0.0029) (Figure 3C) and neuroligin-2 (Interaction: F (1, 12) = 10.77, p = 0.0066; Cont-RSV ppost-hoc = 0.0220, Cont-VPApost-hoc = 0.0172; Cont-RSV + VPA ppost-hoc = 0.1128) (Figure 3D). No differences were observed among groups for $GABA_B$ (Figure 3B), PSD-95 (Figure 3E), and synaptophysin (Figure 3F).

2.8. The VPA Decreased the Number of Total Neurons and Altered the Ratio of Interneurons in the DG, without Full Prevention by RSV

The VPA decreased the number of total neurons in DG (Interaction: F (1, 12) = 7.441, p = 0.0183; Cont-VPApost-hoc = 0.0166) (Figure 4A), in PV+ ratio (VPA: F (1, 12) = 5.732, p = 0.0339) (Figure 4C), and in CB+ ratio (VPA: F (1, 11) = 5.709, p = 0.0359) (Figure 4E), and increased the SOM+ ratio (Interaction: F (1, 12) = 4.840, p = 0.0481; Cont-VPA ppost-hoc = 0.0023; RSV-VPA ppost-hoc= 0.0024; RSV + VPA-VPA ppost-hoc = 0.054) (Figure 4G). No differences were observed in the number of PV+ (Figure 4B), CB+ (Figure 4D), and SOM+ neurons (Figure 4F) among groups. Illustrative images of total neurons, PV+, CB+, and SOM+ are presented in Figure 5A–C.

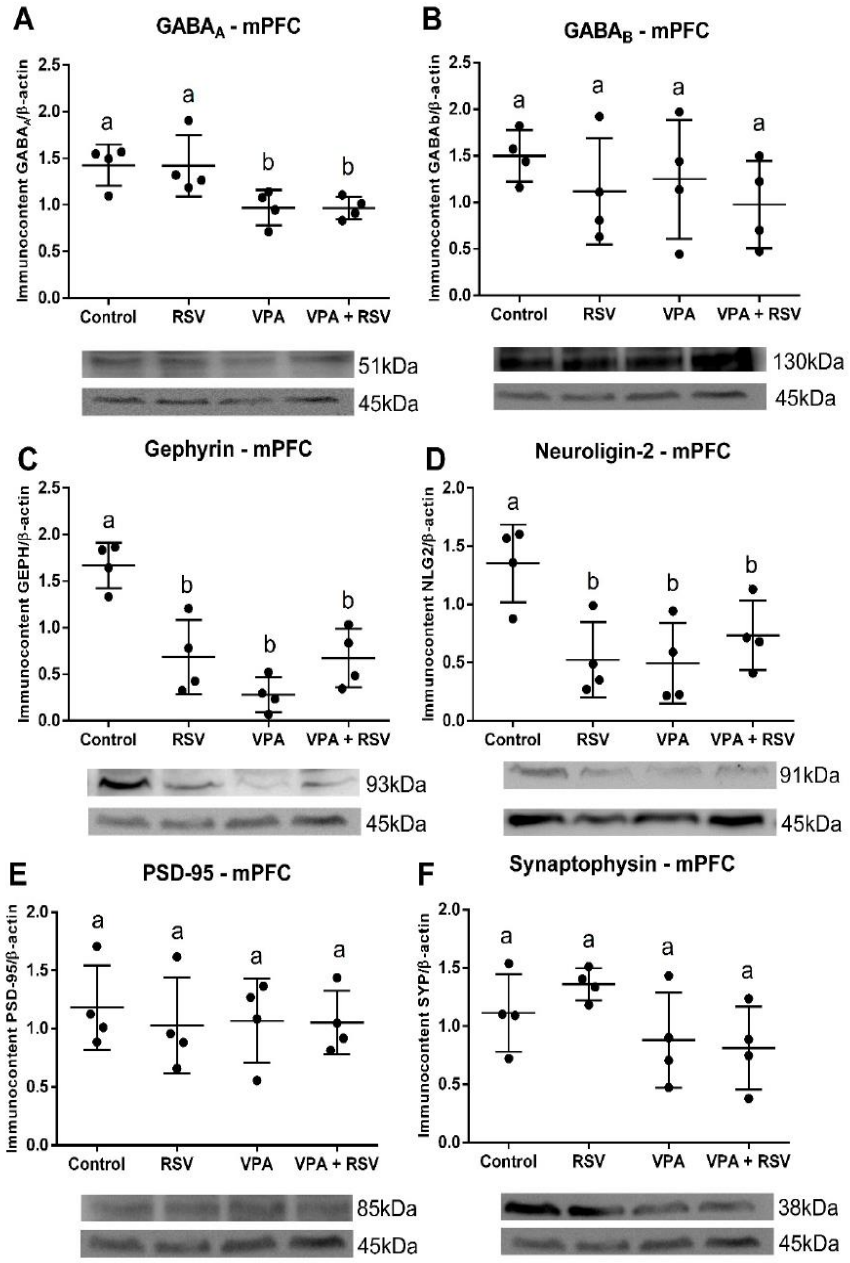

Figure 3. VPA induced a reduction in the immunocontent of GABAA, gephyrin, and neuroligin-2 (the last two also reduced by RSV) in the mPFC. The immunocontent of GABA receptors and synaptic proteins was normalized by the β-actin loading control. Values are shown as mean ± standard deviation. (**A**) $GABA_A$ immunocontent. (**B**) $GABA_B$ immunocontent. (**C**) Gephyrin immunocontent. (**D**) Neuroligin-2 immunocontent. (**E**) PSD-95 immunocontent. (**F**) Synaptophysin immunocontent. Statistical analysis: two-way ANOVA followed by Bonferroni, $p < 0.05$ was considered significant. N_{CON}: 4, N_{RSV}: 4, N_{VPA}: 4, $N_{RSV + VPA}$:4. Different letters indicate significant differences in the post-test when interaction was significant ($p < 0.05$).

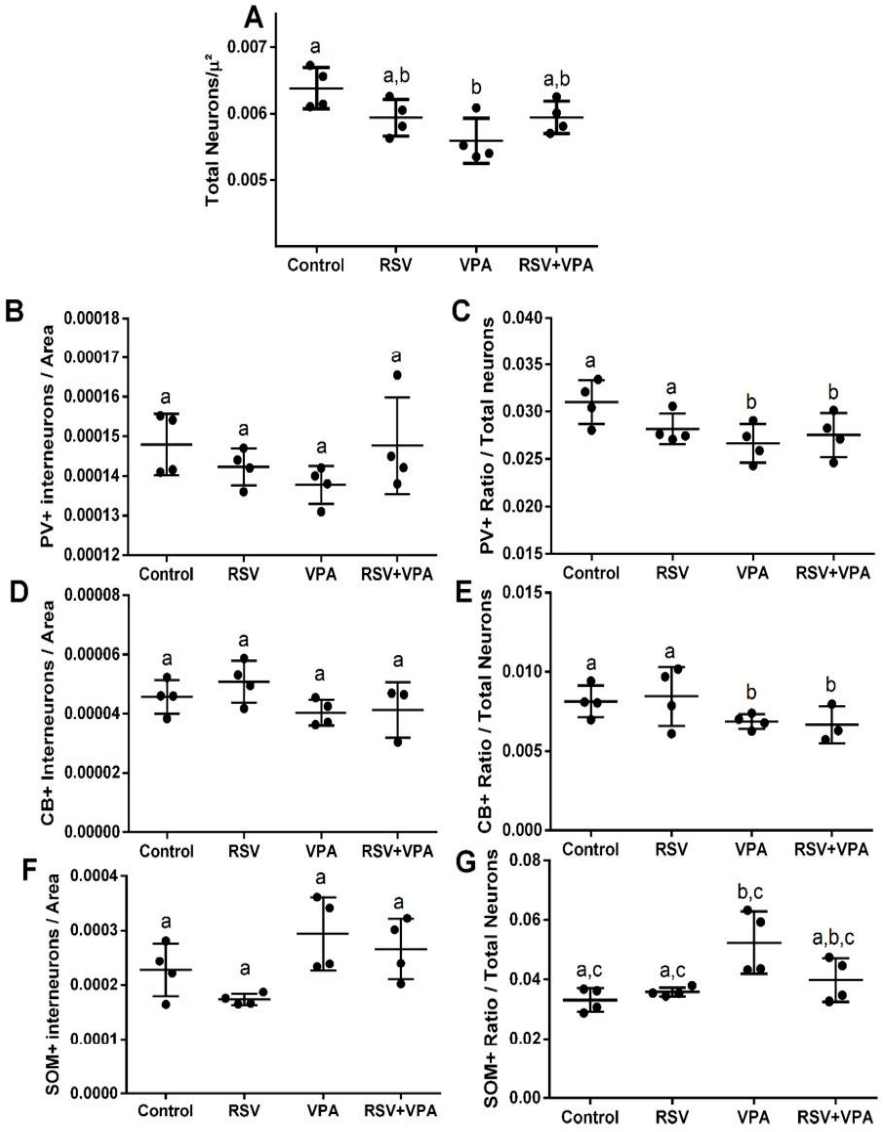

Figure 4. VPA reduced total neurons, CB+ ratio, and PV+ ratio while increasing the SOM+ ratio in the DG without prevention by RSV. (**A**) Quantification of total neurons. (**B**) Quantification of CB+ interneurons. (**C**) Quantification of the ratio of CB+ interneurons/total neurons. (**D**) Quantification of PV+ interneurons. (**E**) Quantification of the ratio of PV+ interneurons/total neurons. (**F**) Quantification of SOM+ interneurons. (**G**) Quantification of the ratio of SOM+ interneurons/total neurons. Values are shown as mean ± standard deviation. Statistical analysis: two-way ANOVA followed by Bonferroni, $p < 0.05$ was considered significant. N_{CON}: 4, N_{RSV}: 4, N_{VPA}: 4, $N_{RSV+VPA}$:4 CB+NeuN+DAPI, and PV+NeuN+DAPI; N_{CON}: 4, N_{RSV}: 4, N_{VPA}: 4, $N_{RSV+VPA}$:3 and SOM+NeuN+DAPI. Different letters indicate significant differences in the post-test when interaction was significant ($p < 0.05$).

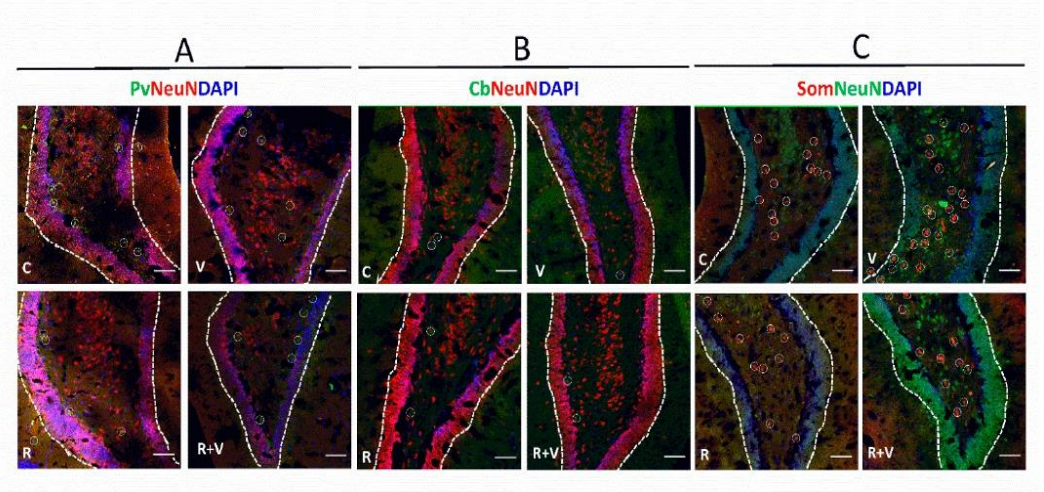

Figure 5. Representative image of total neurons, PV+, CB+, and SOM+ immunofluorescence in the HC. Representative images of the SG, upper layers (II/III). (**A**) Pv, parvalbumin (green); NeuN (red); DAPI (blue). (**B**) Cb, calbindin (green); NeuN (red); DAPI (blue). (**C**) Som, somatostatin (red); NeuN (green); DAPI (blue). Scale bar: 50 µm. The respective interneurons are highlighted within white circles. aCC, anterior cingulate cortex; CB, calbindin-neurons; DG, dentate gyrus; HC, hippocampus; PV, parvalbumin-neurons; SOM, somatostatin-neurons.

2.9. The VPA Altered the Interneuronal Composition in CA1, CA2, CA3, and RSV Presented a per se Effect in CA3

The VPA group decreased the CB+ number in CA1, CA2, and CA3, following a decreased ratio of these neurons in CA2 and CA3 (Supplementary Materials Table S3). The RSV had a per se effect in CA3, decreasing PV+ numbers, but not altering the ratio (Supplementary Materials Table S2). The VPA increased the SOM+ number and ratio in the CA2, while RSV had a per se effect in CA3, increasing the number of SOM+ neurons without affecting the ratio (Supplementary Materials Table S4). For the total neurons, a significant difference was only found between VPA and RSV + VPA groups in CA2 (Supplementary Materials Table S1). No differences were found in other parameters.

2.10. The Immunocontent of the Analyzed Proteins Did Not Differ among Groups in the Hippocampus

In the HC, no significant differences were found for all parameters evaluated. $GABA_A$ (Interaction: F (1, 12) = 0.06436 p = 0.8040. VPA: F (1, 12) = 0.09175 p= 0.7672. RSV: F (1, 12) = 2.034 p = 0.1793) (Figure 6A), $GABA_B$ (Interaction: F (1, 12) = 0.9989 p = 0.3373. VPA: F (1, 12) = 0.7182 p = 0.4133. RSV: F (1, 12) = 0.2652 p = 0.6159) (Figure 6B), gephyrin (Interaction: F $(1, 12) = 8.221 \times 10^{-5}$ p = 0.9929. VPA: F (1, 12) = 2.657 p = 0.1291. RSV: F (1, 12) = 1.099 p = 0.3152) (Figure 6C), neuroligin-2 (Interaction: F (1, 12) = 0.1844 p = 0.6753. VPA: F (1, 12) = 0.8125 p = 0.3851. RSV: F (1, 12) = 0.007832 p = 0.9309) (Figure 6D), PSD-95 (Interaction: F (1, 12) = 0.01751 p = 0.8969. VPA: F (1, 12) = 0.001065 p = 0.9745. RSV: F (1, 12) = 0.5443 p = 0.4748) (Figure 6E), and synaptophysin (Interaction: F (1, 12) = 0.1378 p = 0.7169. VPA: F (1, 12) = 0.3949 p = 0.5415. RSV: F (1, 12) = 3.797 p = 0.0751) (Figure 6F).

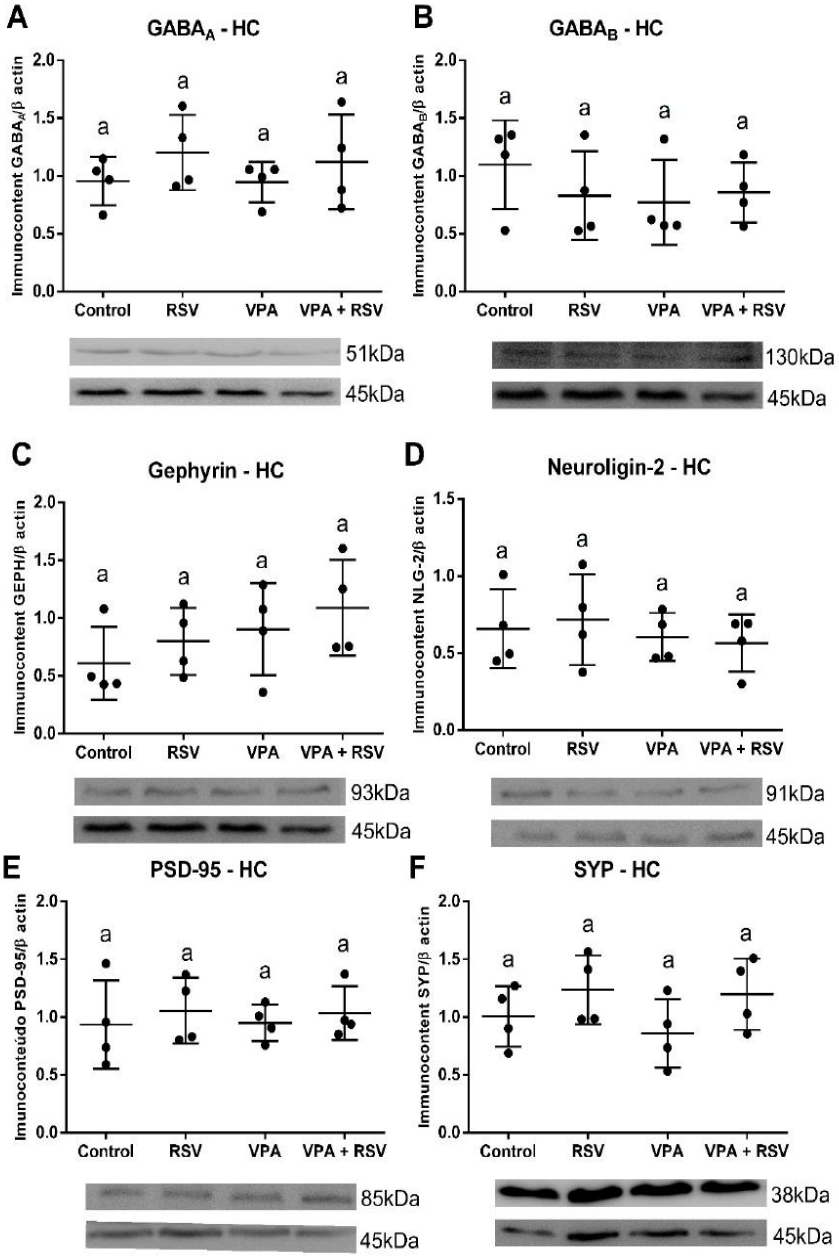

Figure 6. There were no significant differences in the expression of synaptic proteins and GABA receptors in the HC. The immunocontent of GABA receptors and synaptic proteins was normalized by the β-actin loading control. Values are shown as mean ± standard deviation. (**A**) $GABA_A$ immunocontent. (**B**) $GABA_B$ immunocontent. (**C**) Gephyrin immunocontent. (**D**) Neuroligin-2 immunocontent. (**E**) PSD-95 immunocontent. (**F**) Synaptophysin immunocontent. Statistical analysis: two-way ANOVA followed by Bonferroni, $p < 0.05$ was considered significant. N_{CON}: 4, N_{RSV}: 4, N_{VPA}: 4, $N_{RSV + VPA}$:4.

3. Discussion

Changes in the organization of brain cytoarchitecture directly impact not only the local circuits but also the integration among different brain regions. In the autistic brain, cortical disorganization [49,50] and both high local connectivity and low long-range connectivity have already been described [51]. Here, we first studied microarray/RNA-Seq repository datasets of embryos from ASD animal models in order to investigate enriched pathways for the DEGs identified in them.

Firstly, the carbohydrate metabolic imbalance observed in E12.5 in DS2 was also observed in the organoids exposed to VPA (DS3), indicating that this may be the starting point of several subsequent alterations. The proliferation of neuronal progenitors relies mostly on aerobic glycolysis as the energetic source [52]; thus, an alteration in this metabolic pathway may induce early proliferative issues. In the subsequent days (E14.5 and E17.5), the pathways appear to induce a general condition of acceleration of neuronal differentiation, with upregulation of adhesion, neurotransmitter, and synaptic pathways to the detriment of the cell-cycle, gene expression, and protein dynamics regulation. Many of these features are also observed in brain organoids exposed to VPA (DS3), probably impacting the final disposition and organization of the neurons in different brain regions.

VPA has already demonstrated an influence in carbohydrate metabolism and mitochondrial function [53], increasing the production of reactive oxygen species [54]. RSV is a known antioxidant and anti-inflammatory molecule, and, thus, the early treatment (starting in E6.5) may attenuate a possible metabolic alteration induced by VPA. Moreover, VPA is a known inhibitor of histone deacetylases [55,56], while RSV is an activator of sirtuins [57], which may counteract the alterations in gene expression and cell-cycle. Thus, RSV may create a neuroprotective background, preventing alterations caused by VPA and expansion of initial damage throughout embryonic life, resulting in the maintenance of the neuronal composition in the mPFC and HC (to a lesser extent) in postnatal life.

Considering these data and our previous data from adult animals of the VPA animal model (P120) [41], which presented alterations in the neuronal composition of the HC, including disturbances in PV+, CB+, and SOM+, we studied here the same structure and also expanded it for mPFC in young animals (P30). Now, we demonstrate a substantial disorganization in the mPFC and HC neuronal cytoarchitecture in the VPA group, as well as important preventive effects of prenatal treatment with RSV, especially in the mPFC.

The VPA group showed an increased number of total neurons, while the interneurons presented either a reduced ratio or number in the mPFC, depending on the subpopulation. This numerical increase (even not significant in some subregions) is relevant because the ratio of interneurons/total neurons can be influenced by subtle alterations. We demonstrated that the deeper layers of PrL and IL presented the most significant increase in the number of total neurons. Postmortem analysis of ASD patients already demonstrated an increased number of neurons in the mini-columns of the frontal and parietal cortex [49] and patches of disorganization in the cortical layers, especially in the deeper layers [50]; moreover, an increase in the number of total neurons was observed in the dorsolateral cortex, the homologous region to the mPFC [58] in humans.

Next, we explored the gene expression datasets to identify potential mechanisms that could underlie the increased number of neurons in the cortex of VPA mice. The majority of the cortical neurons are excitatory pyramidal cells (about 75–80%) [59]. These neurons are generated in the ventricular zone in the early stages of embryogenesis (around E10 in rodents) [60] and reach the cortex through radial migration from the cortical subplate. VPA animals display an increased number of non-GABAergic neurons and thickness of the cortical layers, concomitant with changes in the expression of cell cycle proteins, suggesting maintenance of the proliferative phase for a longer time [61]. When we observed DS4 gene expression data, we noticed that the cortical subplate, the migrating cells from the subventricular zone, and even the radial glia (directly associated with migration guidance) displayed DEGs associated with cell cycle and gene expression in E14.

Next, we investigated the distribution of specific interneuron subpopulations in the mPFC. Prenatal exposure to VPA reduced the number of GABAergic SOM+ interneurons and the proportion of SOM+ and PV+ interneurons, with no general effect on CB+ (only specific alterations in the subregions). PV+, SOM+, and CB+ are mostly generated in different segments of the GE, developing a migration route that starts around E12.5 in rodents (the same day as the prenatal exposure to VPA) [18].

The SOM+ neurons originate in the medial portion of the GE (MGE) through an initial signaling system based on the increase in SHH expression followed by the expression of the NKX2.1 factor [62]. Since this interneuron population was the only one whose absolute number changed and considering that their migration starts earlier, it is possible that the drastic damage induced by VPA may occur when these cells are still in the proliferative stages. Interestingly, prenatal exposure to VPA at E9.5 reduced the SHH expression in E11.5 embryos [63], which could explain the SOM+ impairments.

On the other hand, the absence of changes in the absolute number (already described in the mPFC of the VPA model [64]) along with the reduction in the ratio of PV+ may suggest a subtle change potentially associated with migration processes, as seen in the anomalous pattern of distribution throughout the subregions. Indeed, while the aCC showed a reduction in number and proportion, the upper layers of PrL showed a completely opposite pattern. Previously, we observed that VPA animals showed an increased proportion of PV+ neurons in the upper layers of the somatosensory area, which was prevented by RSV [36]. CB+ presented a similar pattern to PV+ in relation to the ratio, and these subtle alterations may be associated with the small percentage of this interneuron population.

Interestingly, in DS4, the GE and emerging interneurons at E14 presented major alterations in cell-cycle, gene expression, and protein dynamics, which could result in alterations in the interneuronal proliferation and migration since they are strictly regulated by a sequence of transcription factors, including SHH, NKX2.1, DLX, LHX, SOX.

In addition to the changes in the number and proportion of GABAergic neurons, prenatal exposure to VPA induced a reduction in the immunocontent of the GABAA receptor, a finding already observed in postmortem analysis of ASD patients in the aCC [65] and in the frontal and parietal cortices [26]. Moreover, this alteration possibly contributes to the histological changes observed because this receptor plays an important role in neuronal migration throughout development [66]. Finally, the similar effect of VPA and RSV in reducing the immunocontent of gephyrin and neuroligin-2, two major constituents of inhibitory synapses, may point to an involvement of the Notch pathway, a signaling route highlighted in the DS2 as an altered pathway in late embryonic life, which involved the modulation of synapses [67,68] and is capable of being modulated by both VPA and RSV [69]. However, RSV alone did not cause major histological or behavioral alterations, similar to what was shown in previous studies from our research group [35,36,38].

In the HC, it was possible to observe that prenatal exposure to VPA mainly induced alterations in the DG. The reduction in the total neurons and the alterations in the interneurons, especially SOM+, may induce circuit imbalances with other regions, especially the mPFC, given the important role of SOM+ in integrating the HC and mPFC [70]. VPA is known to reduce neurogenesis in the HC [71] and induce the misplacement of neurons through a pathway mediated by the CXCL12 chemokine and its receptor, CXCR4 [72], which also plays a role in the migration of interneurons. Alterations in CB+ are present in several regions; however, the relatively low abundance of these cells in the HC may hinder accurate quantification. RSV has already demonstrated effects on the modulation of HC interneurons in adults [73]. Thus, prenatal treatment with RSV may cause alterations in the fate of these cells in specific situations. The absence of alterations in the synaptic proteins and GABA receptors in the HC suggests that VPA effects in this region may be restricted to modulation of neuronal populations and organization of brain cytoarchitecture.

Next, we investigated the distribution of specific interneuron subpopulations in the mPFC. Prenatal exposure to VPA reduced the number of GABAergic SOM+ interneurons and the proportion of SOM+ and PV+ interneurons, with no general effect on CB+ (only specific alterations in the subregions). PV+, SOM+, and CB+ are mostly generated in different segments of the GE, developing a migration route that starts around E12.5 in rodents (the same day as the prenatal exposure to VPA) [18].

The SOM+ neurons originate in the medial portion of the GE (MGE) through an initial signaling system based on the increase in SHH expression followed by the expression of the NKX2.1 factor [62]. Since this interneuron population was the only one whose absolute number changed and considering that their migration starts earlier, it is possible that the drastic damage induced by VPA may occur when these cells are still in the proliferative stages. Interestingly, prenatal exposure to VPA at E9.5 reduced the SHH expression in E11.5 embryos [63], which could explain the SOM+ impairments.

On the other hand, the absence of changes in the absolute number (already described in the mPFC of the VPA model [64]) along with the reduction in the ratio of PV+ may suggest a subtle change potentially associated with migration processes, as seen in the anomalous pattern of distribution throughout the subregions. Indeed, while the aCC showed a reduction in number and proportion, the upper layers of PrL showed a completely opposite pattern. Previously, we observed that VPA animals showed an increased proportion of PV+ neurons in the upper layers of the somatosensory area, which was prevented by RSV [36]. CB+ presented a similar pattern to PV+ in relation to the ratio, and these subtle alterations may be associated with the small percentage of this interneuron population.

Interestingly, in DS4, the GE and emerging interneurons at E14 presented major alterations in cell-cycle, gene expression, and protein dynamics, which could result in alterations in the interneuronal proliferation and migration since they are strictly regulated by a sequence of transcription factors, including SHH, NKX2.1, DLX, LHX, SOX.

In addition to the changes in the number and proportion of GABAergic neurons, prenatal exposure to VPA induced a reduction in the immunocontent of the GABAA receptor, a finding already observed in postmortem analysis of ASD patients in the aCC [65] and in the frontal and parietal cortices [26]. Moreover, this alteration possibly contributes to the histological changes observed because this receptor plays an important role in neuronal migration throughout development [66]. Finally, the similar effect of VPA and RSV in reducing the immunocontent of gephyrin and neuroligin-2, two major constituents of inhibitory synapses, may point to an involvement of the Notch pathway, a signaling route highlighted in the DS2 as an altered pathway in late embryonic life, which involved the modulation of synapses [67,68] and is capable of being modulated by both VPA and RSV [69]. However, RSV alone did not cause major histological or behavioral alterations, similar to what was shown in previous studies from our research group [35,36,38].

In the HC, it was possible to observe that prenatal exposure to VPA mainly induced alterations in the DG. The reduction in the total neurons and the alterations in the interneurons, especially SOM+, may induce circuit imbalances with other regions, especially the mPFC, given the important role of SOM+ in integrating the HC and mPFC [70]. VPA is known to reduce neurogenesis in the HC [71] and induce the misplacement of neurons through a pathway mediated by the CXCL12 chemokine and its receptor, CXCR4 [72], which also plays a role in the migration of interneurons. Alterations in CB+ are present in several regions; however, the relatively low abundance of these cells in the HC may hinder accurate quantification. RSV has already demonstrated effects on the modulation of HC interneurons in adults [73]. Thus, prenatal treatment with RSV may cause alterations in the fate of these cells in specific situations. The absence of alterations in the synaptic proteins and GABA receptors in the HC suggests that VPA effects in this region may be restricted to modulation of neuronal populations and organization of brain cytoarchitecture.

software [75]. Quantification was conducted by counting the cells in 8 stacks of at least 2 slices per animal (all stacks were counted individually and with the overlapping image).

The results are shown as the absolute number of total neurons (NeuN+DAPI) and interneurons (CB+NeuN+DAPI, PV+NeuN+DAPI, and SOM+NeuN+DAPI) normalized by area and as the ratio between the number of interneurons and total neurons to obtain a proportion between the inhibitory (interneuron) and excitatory components (the majority of the total neurons) according to the following formula: (CB+, PV+ or SOM+) Interneurons/Total neurons (based on Fontes-Dutra et al. [36]. This ratio was made separately for each interneuron evaluated. The mPFC was subdivided into three subregions, named aCC, PrL, and IL. Each of these regions were subdivided into upper layers (II/III) and deeper layers (IV/V). The total number of neurons, the number of each interneuron (PV+, CB+, and SOM+), and the ratio (interneuron/total neurons) were evaluated in each subfield (i.e., upper layers of aCC, deeper layers of aCC, upper layers of PrL, deeper layers of PrL, upper layers of IL, deeper layers of IL). The amount observed in the deeper + upper layers of a subregion represents the whole subregion (i.e., deeper layers of aCC + upper layers of aCC = whole aCC). The amount observed in whole aCC + whole PrL + whole IL represents the whole mPFC. The HC was subdivided into four subregions: DG, CA1, CA2, and CA3. In each of them, the total number of neurons, the number of each interneuron (PV+, CB+, and SOM+), and the ratio (interneuron/total neurons) were evaluated.

4.4. Western Blotting

Samples from mPFC and HC were homogenized and prepared in a buffer containing 10% SDS, 100 mM EDTA, 500 mM TRIS/HCl buffer (pH 8), and protease inhibitors. The supernatant was collected after centrifugation at 14.000× *g* for 20 min at 4 °C. Total proteins were quantified by the Lowry method [76], and the samples were prepared in a buffer containing glycerol, bromophenol blue, 500 mM TRIS/HCl buffer, and β-mercaptoethanol. Equal amounts of protein (40 µg) were applied to 10% polyacrylamide gels, separated by unidimensional electrophoresis, and transferred to nitrocellulose membranes to detect the immunocontent of $GABA_A$, $GABA_B$, gephyrin, neuroligin-2, PSD-95 and synaptophysin proteins using specific primary antibodies according to the protocol adapted from Deckmann et al., [77]. Technical information and concentrations of the reagents used in the Western Blotting assays are summarized in Supplementary Materials Table S1. After incubation with corresponding secondary peroxidase-associated antibodies (HRP), the chemiluminescent signal was detected using the ImageQuant™ LAS 4000 system (GE HealthCare Life Sciences®, Chicago, IL, USA). The quantification of the relative protein content was performed with the ImageJ® software, and the data were normalized by the endogenous marker β-actin.

4.5. Transcriptomic Analysis

To provide insights into the embryonic processes that could lead to the alterations observed in the postnatal brain of ASD models, we selected five RNA-Seq and microarray datasets [32,78–81] from MIA animal models, VPA-exposed cell cultures, and cortical organoids (Table 1) since databases of VPA-induced animal models are not available yet. The differentially expressed genes (DEGs) of each dataset were analyzed with Cytoscape® [82] using the BiNGO® plug-in [83] to evaluate Gene Ontology (GO) enrichments in a determined set of genes, providing tables with the statistically significant most representative GO terms. We also compared the DEGs observed in each dataset with the Simons Foundation Autism Research Initiative (SFARI) gene database [84] to observe the percentage of DEGs that have an ortholog already described as altered in ASD.

4.6. Statistical Analysis

All the analyses were performed using the GraphPad Prism 6 software (GraphPad Software, La Jolla, CA, USA). Kolmogorov–Smirnov and Shapiro–Wilk tests of normality were applied to determine the data distribution. As the data presented a normal distri-

bution, we chose a parametric test (two-way ANOVA) followed by a Bonferroni post-test. When there was an interaction effect, pairwise comparison was analyzed in the post-hoc; when there was no effect, the effect of exposure to factors (VPA or RSV) was analyzed.

5. Conclusions

The present study demonstrated that the prenatal treatment with RSV was able to prevent important alterations in the neuronal composition of the mPFC induced by prenatal exposure to VPA, probably improving parameters associated with the E/I balance. These findings are in accordance with several other studies that have already demonstrated the neuroprotective effects of RSV in psychiatric disorders, not only in animal models but also in humans, highlighting the translational value of the study. The transcriptomic analysis allowed the establishment of hypotheses to explain the developmental context of these interventions, highlighting the pathways such as WNT, NOTCH, and others in which VPA and RSV may act. Next, we demonstrated that prenatal exposure to VPA alters the neuronal profile in the mPFC and HC, impacting the number and proportion of interneurons, indicating a possible E/I imbalance. Moreover, VPA also induced alterations in the immunocontent of a GABA receptor and synaptic proteins in the mPFC, adding another layer of evidence to comprehend the alterations in the circuitry of this region. In summary, prenatal treatment with RSV was able to prevent neuronal alterations in the mPFC. In addition, our analyses suggest that the investigation of mechanisms involved in the development of interneurons, brain cytoarchitecture, and synaptic content can be a promising strategy to expand the understanding of the pathophysiology of ASD.

Supplementary Materials: The following supporting information can be downloaded at https://www.mdpi.com/article/10.3390/ijms23084075/s1.

Author Contributions: J.S.-T., I.D., G.C.-C., G.D.-F.N., G.B.-N., G.B.S., M.F.-D., R.R. and C.G., experimental design, sample processing, and intellectual contribution. R.R. and C.G., acquisition of financial resources. J.S.-T., I.D., G.C.-C. and M.F.-D., immunofluorescence analyses. J.S.-T., I.D. and GDFN, Western blotting analyses. J.S.-T., I.D., G.C.-C., G.D.-F.N., G.B.-N., G.B.S., M.F.-D. and C.G., data discussion and manuscript preparation. All authors have read and agreed to the published version of the manuscript.

Funding: Conselho Nacional de Desenvolvimento Científico e Tecnológico (CNPq); Coordenação de Aperfeiçoamento de Pessoal de Nível Superior (CAPES); Instituto Nacional de Ciência e Tecnologia em Neuroimunomodulação (INCT-NIM) (Project number 465489/2014-1); Fundo de Incentivo à Pesquisa e Eventos do Hospital de Clínicas de Porto Alegre (FIPE-HCPA).

Institutional Review Board Statement: All procedures were approved by the local Ethics Commission on the Use of Animals (CEUA-UFRGS 35733) and performed according to ethical principles in accordance with the NIH Guide for the Care and Use of Laboratory Animals, as well as Brazilian Arouca Law (11,794, of 8 October 2008).

Informed Consent Statement: Not applicable.

Data Availability Statement: Data is contained within the article or Supplementary Material.

Acknowledgments: We would like to thank all of the funding agencies, including CNPq, CAPES, INCT-NIM, and FIPE-HCPA. We also would like to thank Vitória Cassola de Lemos (Edinburgh, Scotland) for the English writing revision.

Conflicts of Interest: The authors declare no conflict of interest.

References

1. American Psychiatric Association. *Diagnostic and Statistical Manual of Mental Disorders (DSM-5)*; American Psychiatric DSM 5; American Psychiatric Association: Virginia, VA, USA, 2013, ISBN 9780890425541.
2. Maenner, M.J.; Shaw, K.A.; Baio, J.; Washington, A.; Patrick, M.; DiRienzo, M.; Christensen, D.L.; Wiggins, L.D.; Pettygrove, S.; Andrews, J.G.; et al. Prevalence of autism spectrum disorder among children aged 8 Years-Autism and developmental disabilities monitoring network, 11 Sites, United States, 2016. *MMWR Surveill. Summ.* **2020**, *69*, 1–12. [CrossRef]

3. Masi, A.; DeMayo, M.M.; Glozier, N.; Guastella, A.J. An Overview of Autism Spectrum Disorder, Heterogeneity and Treatment Options. *Neurosci. Bull.* **2017**, *33*, 183–193. [CrossRef]
4. Zwaigenbaum, L.; Penner, M. Autism spectrum disorder: Advances in diagnosis and evaluation. *BMJ* **2018**, *361*, k1674. [CrossRef]
5. Shulman, C.; Esler, A.; Morrier, M.J.; Rice, C.E. Diagnosis of Autism Spectrum Disorder Across the Lifespan. *Child Adolesc. Psychiatr. Clin. N. Am.* **2020**, *29*, 253–273. [CrossRef]
6. Baxter, A.J.; Brugha, T.S.; Erskine, H.E.; Scheurer, R.W.; Vos, T.; Scott, J.G. The epidemiology and global burden of autism spectrum disorders. *Psychol. Med.* **2015**, *45*, 601–613. [CrossRef]
7. Spence, S.J.; Schneider, M.T. The Role of Epilepsy and Epileptiform EEGs in Autism Spectrum Disorders. *Pediatr. Res.* **2009**, *65*, 599. [CrossRef] [PubMed]
8. Bolton, P.F.; Carcani-Rathwell, I.; Hutton, J.; Goode, S.; Howlin, P.; Rutter, M. Epilepsy in autism: Features and correlates. *Br. J. Psychiatry* **2011**, *198*, 289–294. [CrossRef] [PubMed]
9. Lukmanji, S.; Manji, S.A.; Kadhim, S.; Sauro, K.M.; Wirrell, E.C.; Kwon, C.S.; Jetté, N. The co-occurrence of epilepsy and autism: A systematic review. *Epilepsy Behav.* **2019**, *98*, 238–248. [CrossRef] [PubMed]
10. Nelson, S.B.; Valakh, V. Excitatory/Inhibitory Balance and Circuit Homeostasis in Autism Spectrum Disorders. *Neuron* **2015**, *87*, 684–698. [CrossRef] [PubMed]
11. Bozzi, Y.; Provenzano, G.; Casarosa, S. Neurobiological bases of autism-epilepsy comorbidity: A focus on excitation/inhibition imbalance. *Eur. J. Neurosci.* **2018**, *47*, 534–548. [CrossRef] [PubMed]
12. Selten, M.; Bokhoven, H.; van Kasri, N.N. Inhibitory control of the excitatory/inhibitory balance in psychiatric disorders. *F1000Research* **2018**, *7*, 23. [CrossRef] [PubMed]
13. Roux, L.; Buzsáki, G. Tasks for inhibitory interneurons in intact brain circuits. *Neuropharmacology* **2015**, *88*, 10–23. [CrossRef] [PubMed]
14. Pelkey, K.A.; Chittajallu, R.; Craig, M.T.; Tricoire, L.; Wester, J.C.; McBain, C.J. Hippocampal GABAergic Inhibitory Interneurons. *Physiol. Rev.* **2017**, *97*, 1619–1647. [CrossRef] [PubMed]
15. Markram, H.; Toledo-Rodriguez, M.; Wang, Y.; Gupta, A.; Silberberg, G.; Wu, C. Interneurons of the neocortical inhibitory system. *Nat. Rev. Neurosci.* **2004**, *5*, 793–807. [CrossRef] [PubMed]
16. Tremblay, R.; Lee, S.; Rudy, B. GABAergic Interneurons in the Neocortex: From Cellular Properties to Circuits. *Neuron* **2016**, *91*, 260–292. [CrossRef]
17. Defelipe, J.; López-Cruz, P.L.; Benavides-Piccione, R.; Bielza, C.; Larrañaga, P.; Anderson, S.; Burkhalter, A.; Cauli, B.; Fairén, A.; Feldmeyer, D.; et al. New insights into the classification and nomenclature of cortical GABAergic interneurons. *Nat. Rev. Neurosci.* **2013**, *14*, 202. [CrossRef] [PubMed]
18. Kelsom, C.; Lu, W. Development and specification of GABAergic cortical interneurons. *Cell Biosci.* **2013**, *3*, 19. [CrossRef]
19. Gentet, L.J.; Kremer, Y.; Taniguchi, H.; Huang, Z.J.; Staiger, J.F.; Petersen, C.C.H. Unique functional properties of somatostatin-expressing GABAergic neurons in mouse barrel cortex. *Nat. Neurosci.* **2012**, *15*, 607–612. [CrossRef]
20. Xia, F.; Richards, B.A.; Tran, M.M.; Josselyn, S.A.; Takehara-Nishiuchi, K.; Frankland, P.W. Parvalbumin-positive interneurons mediate neocortical-hippocampal interactions that are necessary for memory consolidation. *eLife* **2017**, *6*, e27868. [CrossRef]
21. Cho, K.K.A.; Davidson, T.J.; Bouvier, G.; Marshall, J.D.; Schnitzer, M.J.; Sohal, V.S. Cross-hemispheric gamma synchrony between prefrontal parvalbumin interneurons supports behavioral adaptation during rule shift learning. *Nat. Neurosci.* **2020**, *23*, 892–902. [CrossRef]
22. Gibson, J.R.; Bartley, A.F.; Hays, S.A.; Huber, K.M. Imbalance of Neocortical Excitation and Inhibition and Altered UP States Reflect Network Hyperexcitability in the Mouse Model of Fragile X Syndrome. *J. Neurophysiol.* **2008**, *100*, 2615. [CrossRef] [PubMed]
23. Polepalli, J.S.; Wu, H.; Goswami, D.; Halpern, C.H.; Südhof, T.C.; Malenka, R.C. Modulation of excitation on parvalbumin interneurons by neuroligin-3 regulates the hippocampal network. *Nat. Neurosci.* **2017**, *20*, 219–229. [CrossRef]
24. He, L.J.; Liu, N.; Cheng, T.L.; Chen, X.J.; Li, Y.D.; Shu, Y.S.; Qiu, Z.L.; Zhang, X.H. Conditional deletion of Mecp2 in parvalbumin-expressing GABAergic cells results in the absence of critical period plasticity. *Nat. Commun.* **2014**, *5*, 5036. [CrossRef] [PubMed]
25. Yu, F.H.; Mantegazza, M.; Westenbroek, R.E.; Robbins, C.A.; Kalume, F.; Burton, K.A.; Spain, W.J.; McKnight, G.S.; Scheuer, T.; Catterall, W.A. Reduced sodium current in GABAergic interneurons in a mouse model of severe myoclonic epilepsy in infancy. *Nat. Neurosci.* **2006**, *9*, 1142–1149. [CrossRef] [PubMed]
26. Fatemi, S.H.; Reutiman, T.J.; Folsom, T.D.; Thuras, P.D. GABAAreceptor downregulation in brains of subjects with autism. *J. Autism Dev. Disord.* **2009**, *39*, 223–230. [CrossRef] [PubMed]
27. Tang, G.; Gudsnuk, K.; Kuo, S.H.; Cotrina, M.L.; Rosoklija, G.; Sosunov, A.; Sonders, M.S.; Kanter, E.; Castagna, C.; Yamamoto, A.; et al. Loss of mTOR-Dependent Macroautophagy Causes Autistic-like Synaptic Pruning Deficits. *Neuron* **2014**, *83*, 1131–1143. [CrossRef]
28. Parente, D.J.; Garriga, C.; Baskin, B.; Douglas, G.; Cho, M.T.; Araujo, G.C.; Shinawi, M. Neuroligin 2 nonsense variant associated with anxiety, autism, intellectual disability, hyperphagia, and obesity. *Am. J. Med. Genet. A* **2017**, *173*, 213–216. [CrossRef]
29. Guang, S.; Pang, N.; Deng, X.; Yang, L.; He, F.; Wu, L.; Chen, C.; Yin, F.; Peng, J. Synaptopathology involved in autism spectrum disorder. *Front. Cell. Neurosci.* **2018**, *12*, 471. [CrossRef] [PubMed]
30. Glass, R.; Norton, S.; Fox, N.; Kusnecov, A.W. Maternal immune activation with staphylococcal enterotoxin A produces unique behavioral changes in C57BL/6 mouse offspring. *Brain. Behav. Immun.* **2019**, *75*, 12–25. [CrossRef] [PubMed]

31. Boulanger-Bertolus, J.; Pancaro, C.; Mashour, G.A. Increasing role of maternal immune activation in neurodevelopmental disorders. *Front. Behav. Neurosci.* **2018**, *12*, 230. [CrossRef] [PubMed]
32. Oskvig, D.B.; Elkahloun, A.G.; Johnson, K.R.; Phillips, T.M.; Herkenham, M. Maternal immune activation by LPS selectively alters specific gene expression profiles of interneuron migration and oxidative stress in the fetus without triggering a fetal immune response. *Brain. Behav. Immun.* **2012**, *26*, 623–634. [CrossRef] [PubMed]
33. Bergdolt, L.; Dunaevsky, A. Brain changes in a maternal immune activation model of neurodevelopmental brain disorders. *Prog. Neurobiol.* **2019**, *175*, 1–19. [CrossRef]
34. Fontes-Dutra, M.; Rabelo, B.; Santos-Terra, J.; Deckmann, I.; Schwingel, G.B.; Gottfried, C. Maternal Immune Activation and Neuropsychiatric Disorders: The Intricate Puzzle of Autism Spectrum Disorder. In *Perinatal Inflammation and Adult Psychopathology*; Springer: Cham, Switzerland, 2020.
35. Bambini-Junior, V.; Zanatta, G.; Della Flora Nunes, G.; Mueller de Melo, G.; Michels, M.; Fontes-Dutra, M.; Nogueira Freire, V.; Riesgo, R.; Gottfried, C. Resveratrol prevents social deficts in animal model of autism induced by valproic acid. *Neurosci. Lett.* **2014**, *583*, 176–181. [CrossRef]
36. Fontes-Dutra, M.; Santos-Terra, J.; Deckmann, I.; Brum Schwingel, G.; Della-Flora Nunes, G.; Hirsch, M.M.; Bauer-Negrini, G.; Hedin-Pereira, C.; Bambini-Junior, V.; Riesgo, R.S.; et al. Resveratrol prevents cellular and behavioral sensory alterations in the animal model of autism induced by valproic acid. *Front. Synaptic Neurosci.* **2018**, *10*, 9. [CrossRef]
37. Fontes-Dutra, M.; Della-Flora Nunes, G.; Santos-Terra, J.; Souza-Nunes, W.; Bauer-Negrini, G.; Hirsch, M.M.; Green, L.; Riesgo, R.; Gottfried, C.; Bambini-Junior, V. Abnormal empathy-like pro-social behaviour in the valproic acid model of autism spectrum disorder. *Behav. Brain Res.* **2019**, *364*, 11–18. [CrossRef] [PubMed]
38. Hirsch, M.M.; Deckmann, I.; Fontes-Dutra, M.; Bauer-Negrini, G.; Della-Flora Nunes, G.; Nunes, W.; Rabelo, B.; Riesgo, R.; Margis, R.; Bambini-Junior, V.; et al. Behavioral alterations in autism model induced by valproic acid and translational analysis of circulating microRNA. *Food Chem. Toxicol.* **2018**, *115*, 336–343. [CrossRef]
39. Gottfried, C.; Bambini-Junior, V.; Baronio, D.; Zanatta, G.; Bristot, R.; Vaccaro, T.; Riesgo, R. Valproic Acid in Autism Spectrum Disorder: From an Environmental Risk Factor to a Reliable Animal Model. In *Recent Advances in Autism Spectrum Disorders*; IntechOpen: London, UK, 2013; Volume I.
40. Watanabe, Y.; Murakami, T.; Kawashima, M.; Hasegawa-Baba, Y.; Mizukami, S.; Imatanaka, N.; Akahori, Y.; Yoshida, T.; Shibutani, M. Maternal Exposure to Valproic Acid Primarily Targets Interneurons Followed by Late Effects on Neurogenesis in the Hippocampal Dentate Gyrus in Rat Offspring. *Neurotox. Res.* **2017**, *31*, 46–62. [CrossRef]
41. Santos-Terra, J.; Deckmann, I.; Schwingel, G.B.; Paz, A.V.C.; Gama, C.S.; Bambini-Junior, V.; Fontes-Dutra, M.; Gottfried, C. Resveratrol prevents long-term structural hippocampal alterations and modulates interneuron organization in an animal model of ASD. *Brain Res.* **2021**, *1768*, 147593. [CrossRef] [PubMed]
42. Deckmann, I.; Schwingel, G.B.; Fontes-Dutra, M.; Bambini-Junior, V.; Gottfried, C. Neuroimmune Alterations in Autism: A Translational Analysis Focusing on the Animal Model of Autism Induced by Prenatal Exposure to Valproic Acid. *Neuroimmunomodulation* **2018**, *25*, 285–299. [CrossRef] [PubMed]
43. Baronio, D.; Bauer-Negrini, G.; Castro, K.; Della-Flora Nunes, G.; Riesgo, R.; Mendes-Da-Cruz, D.A.; Savino, W.; Gottfried, C.; Bambini-Junior, V. Reduced CD4 T Lymphocytes in Lymph Nodes of the Mouse Model of Autism Induced by Valproic Acid. *Neuroimmunomodulation* **2018**, *25*, 280–284. [CrossRef] [PubMed]
44. Cristiano, C.; Volpicelli, F.; Crispino, M.; Lacivita, E.; Russo, R.; Leopoldo, M.; Calignano, A.; Perrone-Capano, C. Behavioral, Anti-Inflammatory, and Neuroprotective Effects of a Novel FPR2 Agonist in Two Mouse Models of Autism. *Pharmaceuticals* **2022**, *15*, 161. [CrossRef]
45. Magaji, M.G.; Iniaghe, L.O.; Abolarin, M.; Abdullahi, O.I.; Magaji, R.A. Neurobehavioural evaluation of resveratrol in murine models of anxiety and schizophrenia. *Metab. Brain Dis.* **2017**, *32*, 437–442. [CrossRef] [PubMed]
46. Rafeiy-Torghabeh, M.; Ashraf-Ganjouei, A.; Moradi, K.; Bagheri, S.; Mohammadi, M.R.; Akhondzadeh, S. Resveratrol adjunct to methylphenidate improves symptoms of attention-deficit/hyperactivity disorder: A randomized, double-blinded, placebo-controlled clinical trial. *Eur. Child Adolesc. Psychiatry* **2020**, *30*, 799–807. [CrossRef] [PubMed]
47. Quincozes-Santos, A.; Gottfried, C. Resveratrol modulates astroglial functions: Neuroprotective hypothesis. *Ann. N. Y. Acad. Sci.* **2011**, *1215*, 72–78. [CrossRef]
48. Caruso, G.; Torrisi, S.A.; Mogavero, M.P.; Currenti, W.; Castellano, S.; Godos, J.; Ferri, R.; Galvano, F.; Leggio, G.M.; Grosso, G.; et al. Polyphenols and neuroprotection: Therapeutic implications for cognitive decline. *Pharmacol. Ther.* **2022**, *232*, 108013. [CrossRef]
49. Casanova, M.F.; van Kooten, I.A.J.; Switala, A.E.; van Engeland, H.; Heinsen, H.; Steinbusch, H.W.M.; Hof, P.R.; Trippe, J.; Stone, J.; Schmitz, C. Minicolumnar abnormalities in autism. *Acta Neuropathol.* **2006**, *112*, 287–303. [CrossRef] [PubMed]
50. Stoner, R.; Chow, M.L.; Boyle, M.P.; Sunkin, S.M.; Mouton, P.R.; Roy, S.; Wynshaw-Boris, A.; Colamarino, S.A.; Lein, E.S.; Courchesne, E. Patches of Disorganization in the Neocortex of Children with Autism. *N. Engl. J. Med.* **2014**, *370*, 1209–1219. [CrossRef] [PubMed]
51. Belmonte, M.K.; Allen, G.; Beckel-Mitchener, A.; Boulanger, L.M.; Carper, R.A.; Webb, S.J. Autism and abnormal development of brain connectivity. *J. Neurosci.* **2004**, *24*, 9228–9231. [CrossRef] [PubMed]

52. Zheng, X.; Boyer, L.; Jin, M.; Mertens, J.; Kim, Y.; Ma, L.; Ma, L.; Hamm, M.; Gage, F.H.; Hunter, T. Metabolic reprogramming during neuronal differentiation from aerobic glycolysis to neuronal oxidative phosphorylation. *eLife* **2016**, *5*, e13374. [CrossRef] [PubMed]
53. Salsaa, M.; Pereira, B.; Liu, J.; Yu, W.; Jadhav, S.; Hüttemann, M.; Greenberg, M.L. Valproate inhibits mitochondrial bioenergetics and increases glycolysis in Saccharomyces cerevisiae. *Sci. Rep.* **2020**, *10*, 11785. [CrossRef] [PubMed]
54. Tung, E.W.Y.; Winn, L.M. Valproic Acid Increases Formation of Reactive Oxygen Species and Induces Apoptosis in Postimplantation Embryos: A Role for Oxidative Stress in Valproic Acid-Induced Neural Tube Defects. *Mol. Pharmacol.* **2011**, *80*, 979–987. [CrossRef] [PubMed]
55. Göttlicher, M.; Minucci, S.; Zhu, P.; Krämer, O.H.; Schimpf, A.; Giavara, S.; Sleeman, J.P.; Lo Coco, F.; Nervi, C.; Pelicci, P.G.; et al. Valproic acid defines a novel class of HDAC inhibitors inducing differentiation of transformed cells. *EMBO J.* **2001**, *20*, 6969–6978. [CrossRef]
56. Phiel, C.J.; Zhang, F.; Huang, E.Y.; Guenther, M.G.; Lazar, M.A.; Klein, P.S. Histone deacetylase is a direct target of valproic acid, a potent anticonvulsant, mood stabilizer, and teratogen. *J. Biol. Chem.* **2001**, *276*, 36734–36741. [CrossRef] [PubMed]
57. Borra, M.T.; Smith, B.C.; Denu, J.M. Mechanism of human SIRT1 activation by resveratrol. *J. Biol. Chem.* **2005**, *280*, 17187–17195. [CrossRef] [PubMed]
58. Courchesne, E.; Mouton, P.R.; Calhoun, M.E.; Semendeferi, K.; Ahrens-Barbeau, C.; Hallet, M.J.; Barnes, C.C.; Pierce, K. Neuron Number and Size in Prefrontal Cortex of Children With Autism. *JAMA* **2011**, *306*, 2001. [CrossRef]
59. Kanari, L.; Ramaswamy, S.; Shi, Y.; Morand, S.; Meystre, J.; Perin, R.; Abdellah, M.; Wang, Y.; Hess, K.; Markram, H. Objective Morphological Classification of Neocortical Pyramidal Cells. *Cereb. Cortex* **2019**, *29*, 1719–1735. [CrossRef] [PubMed]
60. Wu, Y.K.; Fujishima, K.; Kengaku, M. Differentiation of Apical and Basal Dendrites in Pyramidal Cells and Granule Cells in Dissociated Hippocampal Cultures. *PLoS ONE* **2015**, *10*, e0118482. [CrossRef] [PubMed]
61. Fujimura, K.; Mitsuhashi, T.; Shibata, S.; Shimozato, S.; Takahashi, T. In Utero Exposure to Valproic Acid Induces Neocortical Dysgenesis via Dysregulation of Neural Progenitor Cell Proliferation/Differentiation. *J. Neurosci.* **2016**, *36*, 10908–10919. [CrossRef] [PubMed]
62. Butt, S.J.B.; Fuccillo, M.; Nery, S.; Noctor, S.; Kriegstein, A.; Corbin, J.G.; Fishell, G. The temporal and spatial origins of cortical interneurons predict their physiological subtype. *Neuron* **2005**, *48*, 591–604. [CrossRef] [PubMed]
63. Oyabu, A.; Narita, M.; Tashiro, Y. The effects of prenatal exposure to valproic acid on the initial development of serotonergic neurons. *Int. J. Dev. Neurosci.* **2013**, *31*, 202–208. [CrossRef] [PubMed]
64. Lauber, E.; Filice, F.; Schwaller, B. Prenatal Valproate Exposure Differentially Affects Parvalbumin-Expressing Neurons and Related Circuits in the Cortex and Striatum of Mice. *Front. Mol. Neurosci.* **2016**, *9*, 150. [CrossRef] [PubMed]
65. Oblak, A.; Gibbs, T.T.; Blatt, G.J. Decreased GABA A receptors and benzodiazepine binding sites in the anterior cingulate cortex in autism. *Autism Res.* **2009**, *2*, 205–219. [CrossRef] [PubMed]
66. Bortone, D.; Polleux, F. KCC2 Expression Promotes the Termination of Cortical Interneuron Migration in a Voltage-Sensitive Calcium-Dependent Manner. *Neuron* **2009**, *62*, 53–71. [CrossRef]
67. Giniger, E. Notch signaling and neural connectivity. *Curr. Opin. Genet. Dev.* **2012**, *22*, 339–346. [CrossRef] [PubMed]
68. Salama-Cohen, P.; Arevalo, M.-A.; Grantyn, R.; Rodriguez-Tebar, A. Notch and NGF/p75NTR control dendrite morphology and the balance of excitatory/inhibitory synaptic input to hippocampal neurones through Neurogenin 3. *J. Neurochem.* **2006**, *97*, 1269–1278. [CrossRef]
69. Ji, Y.; Ke, Y.; Gao, S. Intermittent activation of notch signaling promotes bone formation. *Am. J. Transl. Res.* **2017**, *9*, 2933–2944.
70. Abbas, A.I.; Sundiang, M.J.M.; Henoch, B.; Morton, M.P.; Bolkan, S.S.; Park, A.J.; Harris, A.Z.; Kellendonk, C.; Gordon, J.A. Somatostatin Interneurons Facilitate Hippocampal-Prefrontal Synchrony and Prefrontal Spatial Encoding. *Neuron* **2018**, *100*, 926–939.e3. [CrossRef] [PubMed]
71. Juliandi, B.; Tanemura, K.; Igarashi, K.; Tominaga, T.; Furukawa, Y.; Otsuka, M.; Moriyama, N.; Ikegami, D.; Abematsu, M.; Sanosaka, T.; et al. Reduced Adult Hippocampal Neurogenesis and Cognitive Impairments following Prenatal Treatment of the Antiepileptic Drug Valproic Acid. *Stem Cell Rep.* **2015**, *5*, 996–1009. [CrossRef]
72. Danzer, S.C. Valproic Acid Leads New Neurons Down the Wrong Path. *Epilepsy Curr.* **2019**, *19*, 132–133. [CrossRef]
73. Mishra, V.; Shuai, B.; Kodali, M.; Shetty, G.A.; Hattiangady, B.; Rao, X.; Shetty, A.K. Resveratrol Treatment after Status Epilepticus Restrains Neurodegeneration and Abnormal Neurogenesis with Suppression of Oxidative Stress and Inflammation. *Sci. Rep.* **2015**, *5*, 17807. [CrossRef]
74. Paxinos, G.; Watson, C. *The Rat Brain in Stereotaxic Coordinates—The New Coronal Set*, 5th ed.; Academic Press: Cambridge, MA, USA, 2004; Volume 1, ISBN 9780080474120.
75. Schneider, C.A.; Rasband, W.S.; Eliceiri, K.W. NIH Image to ImageJ: 25 years of image analysis. *Nat. Methods* **2012**, *9*, 671–675. [CrossRef]
76. Lowry, O.H.; Rosebrough, N.J.; Farr, A.L.; Randall, R.J. Protein measurement with the Folin phenol reagent. *J. Biol. Chem.* **1951**, *193*, 265–275. [CrossRef]
77. Deckmann, I.; Santos-Terra, J.; Fontes-Dutra, M.; Körbes-Rockenbach, M.; Bauer-Negrini, G.; Schwingel, G.B.; Riesgo, R.; Bambini-Junior, V.; Gottfried, C. Resveratrol prevents brain edema, blood–brain barrier permeability, and altered aquaporin profile in autism animal model. *Int. J. Dev. Neurosci.* **2021**, *81*, 579–604. [CrossRef] [PubMed]

78. Balmer, N.V.; Klima, S.; Rempel, E.; Ivanova, V.N.; Kolde, R.; Weng, M.K.; Meganathan, K.; Henry, M.; Sachinidis, A.; Berthold, M.R.; et al. From transient transcriptome responses to disturbed neurodevelopment: Role of histone acetylation and methylation as epigenetic switch between reversible and irreversible drug effects. *Arch. Toxicol.* **2014**, *88*, 1451–1468. [CrossRef] [PubMed]
79. Cui, K.; Wang, Y.; Zhu, Y.; Tao, T.; Yin, F.; Guo, Y.; Liu, H.; Li, F.; Wang, P.; Chen, Y.; et al. Neurodevelopmental impairment induced by prenatal valproic acid exposure shown with the human cortical organoid-on-a-chip model. *Microsyst. Nanoeng.* **2020**, *6*, 49. [CrossRef] [PubMed]
80. Kalish, B.T.; Kim, E.; Finander, B.; Duffy, E.E.; Kim, H.; Gilman, C.K.; Yim, Y.S.; Tong, L.; Kaufman, R.J.; Griffith, E.C.; et al. Maternal immune activation in mice disrupts proteostasis in the fetal brain. *Nat. Neurosci.* **2020**, *24*, 204–213. [CrossRef] [PubMed]
81. Canales, C.P.; Estes, M.L.; Cichewicz, K.; Angara, K.; Aboubechara, J.P.; Cameron, S.; Prendergast, K.; Su-Feher, L.; Zdilar, I.; Kreun, E.J.; et al. Sequential perturbations to mouse corticogenesis following in utero maternal immune activation. *eLife* **2021**, *10*, e60100. [CrossRef] [PubMed]
82. Shannon, P.; Markiel, A.; Ozier, O.; Baliga, N.S.; Wang, J.T.; Ramage, D.; Amin, N.; Schwikowski, B.; Ideker, T. Cytoscape: A software environment for integrated models of biomolecular interaction networks. *Genome Res.* **2003**, *13*, 2498–2504. [CrossRef] [PubMed]
83. Maere, S.; Heymans, K.; Kuiper, M. BiNGO: A Cytoscape plugin to assess overrepresentation of gene ontology categories in biological networks. *Bioinformatics* **2005**, *21*, 3448–3449. [CrossRef]
84. Banerjee-Basu, S.; Packer, A. SFARI Gene: An evolving database for the autism research community. *Dis. Model. Mech.* **2010**, *3*, 133–135. [CrossRef]

Supplementary Table S1. Total Neurons distribution profile in HC

	Mean ± SD	F (DFn. DFd); p Value	Pairwise comparisons	
Total Neurons/Area CA1	CON: 0.0051±0.00087 RSV:0.0042±0.00052 VPA: 0.0041±0.00048 RSV+VPA:0.0045±0.00047	Interaction:F (1, 12) = 4.036 p =0.0676# VPA: F (1, 12) = 1.210 p =0.2929 RSV: F (1, 12) = 0.6974 p =0.4200	CON vs RSV:	0.4040
			CON vs VPA:	0.2896
			CON vs RSV+VPA:	> 0.9999
			RSV vs VPA:	> 0.9999
			RSV vs RSV+VPA:	> 0.9999
			VPA vs RSV+VPA:	> 0.9999
Total Neurons/Area CA2	CON: 0.0030±0.00013 RSV:0.0027±0.000037 VPA: 0.0026±0.00027 RSV+VPA:0.0031±0.00031	Interaction:F (1, 12) = 12.45 p =0.0042** VPA: F (1, 12) = 0.007008 p =0.9347 RSV: F (1, 12) = 1.116 p =0.3117	CON vs RSV:	0.6355
			CON vs VPA:	0.1516
			CON vs RSV+VPA:	> 0.9999
			RSV vs VPA:	> 0.9999
			RSV vs RSV+VPA:	0.1883
			VPA vs RSV+VPA:	0.0424*
Total Neurons/Area CA3	CON: 0.0029±0.00058 RSV: 0.0027±0.00029 VPA: 0.0028±0.00087 RSV+VPA:0.0032±0.0034	Interaction:F (1, 12) = 1.494 p =0.2450 VPA: F (1, 12) = 0.9729 p =0.3434 RSV: F (1, 12) = 0.6828 p =0.4247	CON vs RSV:	> 0.9999
			CON vs VPA:	> 0.9999
			CON vs RSV+VPA:	> 0.9999
			RSV vs VPA:	> 0.9999
			RSV vs RSV+VPA:	0.8657
			VPA vs RSV+VPA:	> 0.9999

HC: hippocampus; **SD**: standard deviation. p <0.05 was considered significant. *p<0.05. **p<0.01, #trend. Statistical analyses: two-way ANOVA parametric test followed by Bonferroni. N_{CON}: 4. N_{RSV}: 4. N_{VPA}: 4. $N_{RSV+VPA}$: 4.

Supplementary Table S2. Distribution profile of PV neurons in the HC

	Mean ± SD	F (DFn. DFd); p Value	Pairwise comparisons	
PV /Area CA1	CON: 0.00022±0.000023 RSV:0.00021±0.000030 VPA:0.00023±0.000040 RSV+VPA:0.00020±0.000030	Interaction: F (1, 12) = 0.322 p =0.580 VPA: F (1, 12) = 0.03768 p =0.8493 RSV: F (1, 12) = 1.685 p =0.2186	CON vs RSV:	> 0.9999
			CON vs VPA:	> 0.9999
			CON vs RSV+VPA:	> 0.9999
			RSV vs VPA:	> 0.9999
			RSV vs RSV+VPA:	> 0.9999
			VPA vs RSV+VPA:	> 0.9999
PV Ratio CA1	CON: 0.054±0.009 RSV:0.047±0.008 VPA: 0.057±0.005 RSV+VPA:0.050±0.011	Interaction:F (1, 12) = 0.0014 p =0.970 VPA: F (1, 12) = 0.4375 p =0.5208 RSV: F (1, 12) = 3.089 p =0.1043	CON vs RSV:	> 0.9999
			CON vs VPA:	> 0.9999
			CON vs RSV+VPA:	> 0.9999
			RSV vs VPA:	0.6772
			RSV vs RSV+VPA:	> 0.9999
			VPA vs RSV+VPA:	> 0.9999
PV/Area CA2	CON: 0.00016±0.000036 RSV:0.00014±0.000035 VPA: 0.00016±0.000021 RSV+VPA:0.00012±0.000024	Interaction: F (1, 12) = 1.367 p =0.265 VPA: F (1, 12) = 0.7516 p =0.4030 RSV: F (1, 12) = 3.561 p =0.0836#	CON vs RSV:	> 0.9999
			CON vs VPA:	> 0.9999
			CON vs RSV+VPA:	0.4516
			RSV vs VPA:	> 0.9999
			RSV vs RSV+VPA:	> 0.9999
			VPA vs RSV+VPA:	0.3096
PV Ratio CA2	CON: 0.044±0.008 RSV:0.057±0.005 VPA: 0.050±0.013 RSV+VPA: 0.043±0.011	Interaction:F (1, 12) = 4.109 p =0.0655# VPA: F (1, 12) = 0.6387 p =0.4397 RSV: F (1, 12) = 0.3637 p =0.5577	CON vs RSV:	0.05256
			CON vs VPA:	> 0.9999
			CON vs RSV+VPA:	> 0.9999
			RSV vs VPA:	> 0.9999
			RSV vs RSV+VPA:	0.4130
			VPA vs RSV+VPA:	> 0.9999
PV /Area CA3	CON:0.00023±0.000043 RSV:0.00018±0.000017 VPA:0.00023± 0.000040 RSV+VPA: 0.00016±0.000019	Interaction: F (1, 12) = 0.975 p =0.342 VPA: F (1, 12) = 0.6635 p =0.4312 RSV: F (1, 12) = 16.27 p =0.0017**	CON vs RSV:	0.3139
			CON vs VPA:	> 0.9999
			CON vs RSV+VPA:	0.0300*
			RSV vs VPA:	0.2519
			RSV vs RSV+VPA:	> 0.9999
			VPA vs RSV+VPA:	0.0240*
PV Ratio CA3	CON:0.072±0.013 RSV:0.063±0.004 VPA:0.059±0.013 RSV+VPA: 0.052±0.011	Interaction:F (1, 12) = 0.0289 p =0.867 VPA: F (1, 12) = 4.742 p =0.0501# RSV: F (1, 12) = 2.184 p =0.1652	CON vs RSV:	> 0.9999
			CON vs VPA:	0.7366
			CON vs RSV+VPA:	0.1433
			RSV vs VPA:	> 0.9999
			RSV vs RSV+VPA:	> 0.9999
			VPA vs RSV+VPA:	> 0.9999

PV: parvalbumin-positive interneuron; **HC**: hippocampus; **SD**: standard deviation. p <0.05 was considered significant. *p<0.05. **p<0.01, #trend. Statistical analyses: two-way ANOVA parametric test followed by Bonferroni. N_{CON}: 4. N_{RSV}: 4. N_{VPA}: 4. $N_{RSV+VPA}$: 4.

Supplementary Table S3. Distribution profile of CB neurons in the HC

	Mean ± SD	F (DFn. DFd); p Value	Pairwise comparisons	
CB /Area CA1	CON: 0.000072±0.000014 RSV: 0.000097±0.000019 VPA: 0.000044±0.000028 RSV+VPA: 0.000045±0.000015	Interaction:F (1, 11) = 1.151 p =0.3062 VPA: F (1, 11) = 14.32 p =0.0030** RSV: F (1, 11) = 1.421 p =0.2583	CON vs RSV:	0.7420
			CON vs VPA:	0.4284
			CON vs RSV+VPA:	0.6306
			RSV vs VPA:	0.0224*
			RSV vs RSV+VPA:	0.0418*
			VPA vs RSV+VPA:	> 0.9999
CB Ratio CA1	CON: 0.017±0.003 RSV: 0.024±0.003 VPA: 0.015±0.010 RSV+VPA: 0.016±0.008	Interaction:F (1, 12) = 0.782 p =0.3938 VPA: F (1, 12) = 1.679 p =0.2194 RSV: F (1, 12) = 1.258 p =0.2839	CON vs RSV:	0.9263
			CON vs VPA:	> 0.9999
			CON vs RSV+VPA:	> 0.9999
			RSV vs VPA:	0.6471
			RSV vs RSV+VPA:	> 0.9999
			VPA vs RSV+VPA:	> 0.9999
CB /Area CA2	CON: 0.000035±0.0000053 RSV:0.000050±0.000022 VPA:0.000010±0.0000021 RSV+VPA:0.000026±0.000022	Interaction:F (1, 11) = 0.0014 p =0.971 VPA: F (1, 11) = 9.038 p =0.0119* RSV: F (1, 11) = 3.388 p =0.0928#	CON vs RSV:	> 0.9999
			CON vs VPA:	0.2801
			CON vs RSV+VPA:	> 0.9999
			RSV vs VPA:	0.0265*
			RSV vs RSV+VPA:	0.4084
			VPA vs RSV+VPA:	> 0.9999
CB Ratio CA2	CON: 0.015±0.004 RSV:0.018±0.006 VPA: 0.006±0.003 RSV+VPA: 0.009±0.006	Interaction:F (1, 11) = 0.00547 p =0.942 VPA: F (1, 11) = 10.50 p =0.0079** RSV: F (1, 11) = 1.671 p =0.2226	CON vs RSV:	> 0.9999
			CON vs VPA:	0.1972
			CON vs RSV+VPA:	> 0.9999
			RSV vs VPA:	0.0398*
			RSV vs RSV+VPA:	0.3233
			VPA vs RSV+VPA:	> 0.9999
CB /Area CA3	CON:0.000069±0.000021 RSV: 0.000068±0.000014 VPA: 0.000044±0.000019 RSV+VPA: 0.000030±0.000013	Interaction:F (1, 10) = 0.625 p =0.4475 VPA: F (1, 10) = 11.52 p =0.0068** RSV: F (1, 10) = 0.7661 p =0.4020	CON vs RSV:	> 0.9999
			CON vs VPA:	0.5725
			CON vs RSV+VPA:	0.1082
			RSV vs VPA:	0.4995
			RSV vs RSV+VPA:	0.0858#
			VPA vs RSV+VPA:	> 0.9999
CB Ratio CA3	CON: 0.022±0.005 RSV: 0.022±0.006 VPA: 0.013±0.004 RSV+VPA: 0.09±0.003	Interaction: F (1, 10) = 0.679 p =0.429 VPA: F (1, 10) = 19.20 p =0.0014** RSV: F (1, 10) = 0.8092 p =0.3895	CON vs RSV:	> 0.9999
			CON vs VPA:	0.1836
			CON vs RSV+VPA:	0.0347*
			RSV vs VPA:	0.1434
			RSV vs RSV+VPA:	0.0254*
			VPA vs RSV+VPA:	> 0.9999

CB: calbindin-positive interneuron; **HC**: hippocampus; **SD**: standard deviation. p <0.05 was considered significant. *p<0.05. **p<0.01, #trend. Statistical analyses: two-way ANOVA parametric test followed by Bonferroni. N_{CON}: 4. N_{RSV}: 4. N_{VPA}: 4. $N_{RSV+VPA}$: 3.

Supplementary Table S4. Distribution profile of SOM neurons in the HC

	Mean ± SD	F (DFn. DFd); p Value	Pairwise comparisons	
SOM /Area CA1	CON: 0.00017±0.000031 RSV:0.00015±0.000026 VPA: 0.000168±0.000057 RSV+VPA: 0.00021±0.000048	Interaction:F (1, 12) = 2.670 p =0.1282 VPA: F (1, 12) = 2.302 p =0.1551 RSV: F (1, 12) = 0.8441 p =0.3763	CON vs RSV:	> 0.9999
			CON vs VPA:	> 0.9999
			CON vs RSV+VPA:	0.6637
			RSV vs VPA:	> 0.9999
			RSV vs RSV+VPA:	0.2745
			VPA vs RSV+VPA:	0.5772
SOM Ratio CA1	CON: 0.034±0.0098 RSV: 0.039±0.0047 VPA: 0.044±0.0016 RSV+VPA: 0.045±0.0052	Interaction:F (1, 12) = 0.0685 p =0.797 VPA:F (1, 12) = 2.754 p =0.1229 RSV: F (1, 12) = 0.4506 p =0.5148	CON vs RSV:	> 0.9999
			CON vs VPA:	> 0.9999
			CON vs RSV+VPA:	0.7516
			RSV vs VPA:	> 0.9999
			RSV vs RSV+VPA:	> 0.9999
			VPA vs RSV+VPA:	> 0.9999
SOM/Area CA2	CON: 0.00011±0.000017 RSV: 0.00010±0.000018 VPA: 0.000084±0.000013 RSV+VPA:0.000088±0.00001	Interaction:F (1, 12) = 1.030 p =0.3301 VPA: F (1, 12) = 8.942 p =0.0113* RSV: F (1, 12) = 0.2051 p =0.6587	CON vs RSV:	> 0.9999
			CON vs VPA:	0.0907#
			CON vs RSV+VPA:	0.1888
			RSV vs VPA:	0.5879
			RSV vs RSV+VPA:	> 0.9999
			VPA vs RSV+VPA:	> 0.9999
SOM Ratio CA2	CON: 0.038±0.0054 RSV: 0.043±0.0059 VPA: 0.032±0.0066 RSV+VPA:0.031±0.0031	Interaction:F (1, 12) = 1.866 p =0.1970 VPA: F (1, 12) = 11.62 p =0.0052** RSV: F (1, 12) = 0.4153 p =0.531	CON vs RSV:	> 0.9999
			CON vs VPA:	> 0.9999
			CON vs RSV+VPA:	0.4460
			RSV vs VPA:	0.0852#
			RSV vs RSV+VPA:	0.0330*
			VPA vs RSV+VPA:	> 0.9999
SOM /Area CA3	CON: 0.00010±0.000020 RSV: 0.00014±0.000016 VPA: 0.00010±0.000035 RSV+VPA: 0.00014±0.000029	Interaction:F (1, 12) = 0.0885 p =0.771 VPA: F (1, 12) = 0.04458 p =0.8363 RSV: F (1, 12) = 8.007 p =0.0152*	CON vs RSV:	0.5916
			CON vs VPA:	> 0.9999
			CON vs RSV+VPA:	0.3157
			RSV vs VPA:	0.5330
			RSV vs RSV+VPA:	> 0.9999
			VPA vs RSV+VPA:	0.2830
SOM Ratio CA3	CON: 0.037±0.012 RSV: 0.050±0.006 VPA: 0.038±0.008 RSV+VPA: 0.044±0.013	Interaction:F (1, 12) = 0.498 p =0.4935 VPA: F (1, 12) = 0.3335 p =0.5743 RSV: F (1, 12) = 3.713 p =0.0780#	CON vs RSV:	0.5237
			CON vs VPA:	> 0.9999
			CON vs RSV+VPA:	> 0.9999
			RSV vs VPA:	0.6118
			RSV vs RSV+VPA:	> 0.9999
			VPA vs RSV+VPA:	> 0.9999

SOM: somatostatin-positive interneuron; **HC**: hippocampus; **SD**: standard deviation. p <0.05 was considered significant. *p<0.05. **p<0.01, #trend. Statistical analyses: two-way ANOVA parametric test followed by Bonferroni. N_{CON}: 4. N_{RSV}: 4. N_{VPA}: 4. $N_{RSV+VPA}$: 4.

Supplementary Table S5 – Information on key immunofluorescence and western blotting reagents

Immunofluorescence			
Reagent	**Supplier**	**Code**	**Dilution and Time**
Anti-NeuN (Mouse)	Merck	MAB3771	1:500 in PBS-Triton 0.1% overnight at 4ºC
Anti-NeuN	Abcam	Ab177487	1:500 in PBS-Triton 0.1% overnight at 4ºC
Anti-Parvalbumin	Abcam	Ab64555	1:500 in PBS-Triton 0.1% overnight at 4ºC
Anti-Calbindin	Abcam	Ab82812	1:500 in PBS-Triton 0.1% overnight at 4ºC
Anti-Somatostatin	Sigma-Aldrich	SAB4502861	1:500 in PBS-Triton 0.1% overnight at 4ºC
Alexa Fluor 488 Goat Anti-Mouse IgG (H+L)	Molecular Probes	Ab11029	1:2000 in PBS-Triton 0.1% in room temperature for 1h
Alexa Fluor 594 Goat Anti-Rabbit IgG (H+L)	Molecular Probes	Ab150080	1:2000* in PBS-Triton 0.1% in room temperature for 1h
DAPI Nucleic Acid Stain	Invitrogen	MP01306	30 uL per slice
Mounting Medium Fluorshield	Sigma-Aldrich	F6182-20ML	30 uL per slice

* In SOM^+ assay, the concentration was 1:1000

Western blotting			
Reagent	**Supplier**	**Code**	**Dilution**
$GABA_A$ (goat)	Santa Cruz Biotechnology	sc-31405	1:250 in 5% BSA-0.1%TTBS
$GABA_B$ (rabbit)	Santa Cruz Biotechnology	sc-14006	1:500 in 5% BSA-0.1%TTBS
Gephyrin (rabbit)	Abcam	ab32206	1:500 in 5% BSA-0.1%TTBS
Neuroligin-2 (rabbit)	Abcam	ab36602	1:500 in 5% milk -0.1%TTBS
PSD-95 (rabbit)	Abcam	ab18258	1:500 in 5% BSA-0.1%TTBS
Synaptophysin (mouse)	SIGMA Aldrich	S5768	1:1000 in 5% BSA-0.1%TTBS
Anti-β-actin (mouse)	SIGMA Aldrich	A1978	1:3000 in TTBS
IgG-HRP (goat)	Santa Cruz Biotechnology	sc-2354	1:1000 in 5% BSA-0.1%TTBS
IgG-HRP (mouse)	Santa Cruz Biotechnology	sc-2314	1:1000 in 5% milk-0.1%TTBS
IgG-HRP (rabbit)	Santa Cruz Biotechnology	sc-2004	1:1000 in 0.1%TTBS

Common reagents	
PBS	0.1 M pH 7.4 Phosphate-buffered saline
SDS 10%	Sodium dodecyl sulfate
EDTA 100 mM	Ethylenediamine tetraacetic acid
TRIS/HCl buffer 500 mM pH 8	Tris(hydroxymethyl)aminomethane and chloridric acid
TBS	TRIS buffer
TTBS	0.1%Tween20-TBS

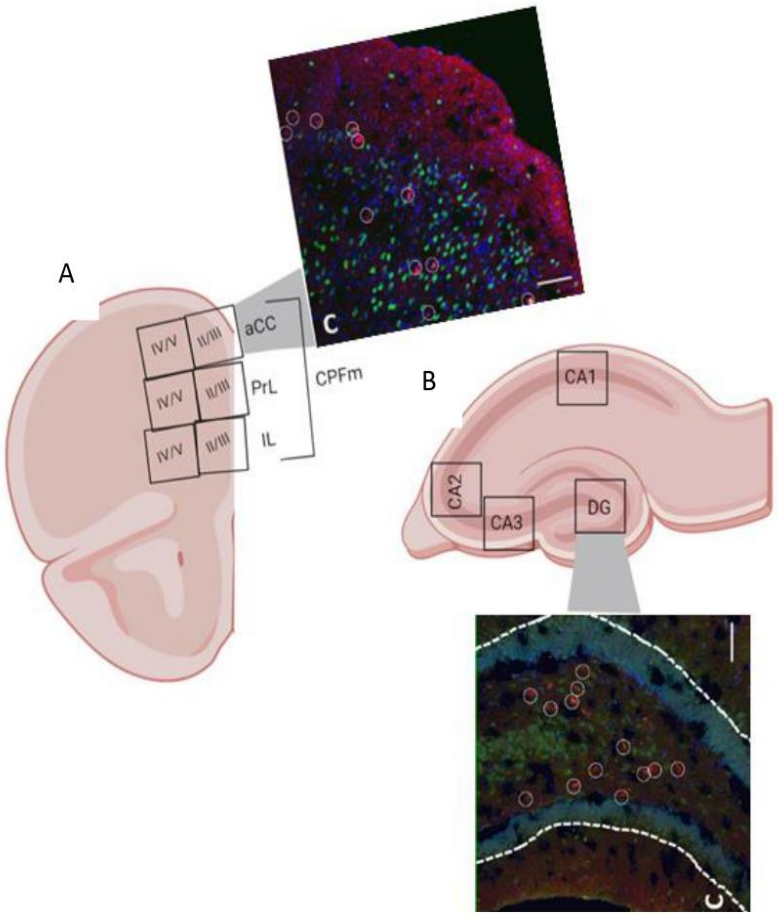

Figure S1. Illustrative scheme of the regions analyzed in this study. **A**) Representation of the mPFC and the three subregions evaluated (aCC, PrL, and IL), each one subdivided according to the cortical layers: upper layers (II/III) and deeper layers (IV/V). The total number of neurons, the number of each interneuron (PV+, CB+, and SOM+), and the ratio (interneuron/total neurons) were evaluated in both subdivisions of cortical layers in the three subregions. The amount observed in the deeper + the upper layers of a subregion was added to calculate the total for the whole subregion. Data for the whole mPFC was calculated as the sum of the amount observed in alle subregions. **B**) Representation of the hippocampus and the four evaluated subregions (DG, CA1, CA2, and CA3). In each of them, the total number of neurons, the number of each interneuron (PV+, CB+, and SOM+), and the ratio (interneuron/total neurons) were evaluated. **C**) Illustrative image. aCC, anterior cingulate cortex; CA, cornu ammonis; CB, calbindin-neurons; DG, dentate gyrus; IL, infralimbic cortex; mPFC, medial frontal cortex; PrL, prelimbic cortex; PV, parvalbumin-neurons; SOM, somatostatin-neurons.

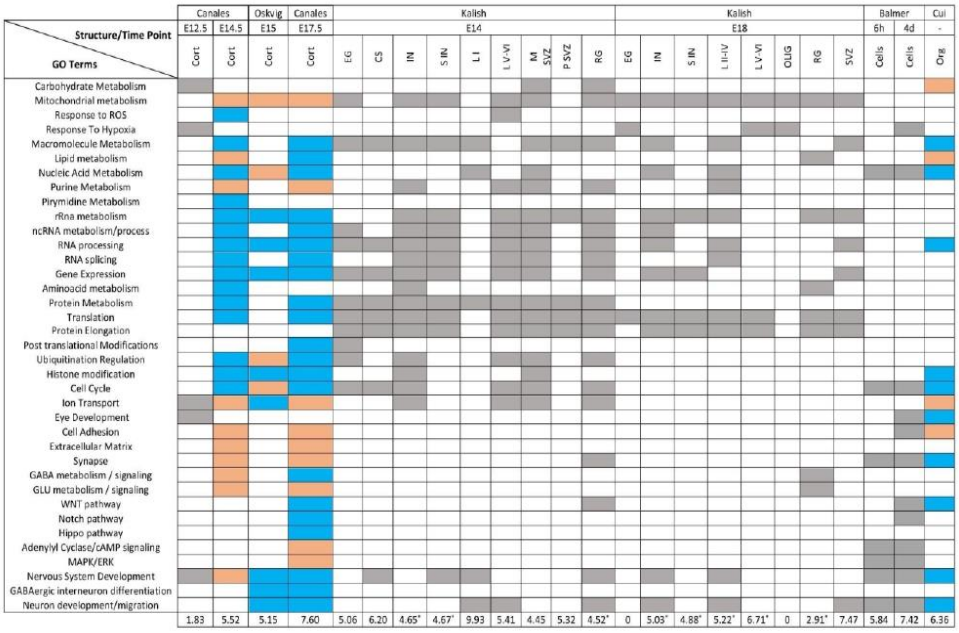

Figure S2. Compilation of the databases from ASD or associated models analyzed in this study. The five databases (described in Table 1) are organized according to the time-point of embryo development (where applicable) with the most relevant pathways listed in the left column. Gray squares represent pathways associated with the DGEs in general; Orange squares represent pathways specifically associated with upregulated DGEs; and blue squares represent pathways specifically associated with downregulated DGEs. The numbers in the bottom line represent the percentage of orthologs identified in the SFARI database, *indicate that a mean was obtained from all of the cells associated with the specific region. Cort.: cortex; CS: cortical subplate; DGE: differentially expressed genes; GE: ganglionic eminence; IN: interneuron; L: layer; OLIG: oligodendrocyte; Org: organoid; RG: radial glia; S IN: striatal interneuron; SVZ: subventricular zone.

Supplementary Figure S3. Ponceau staining of the nitrocellulose membranes – mPFC

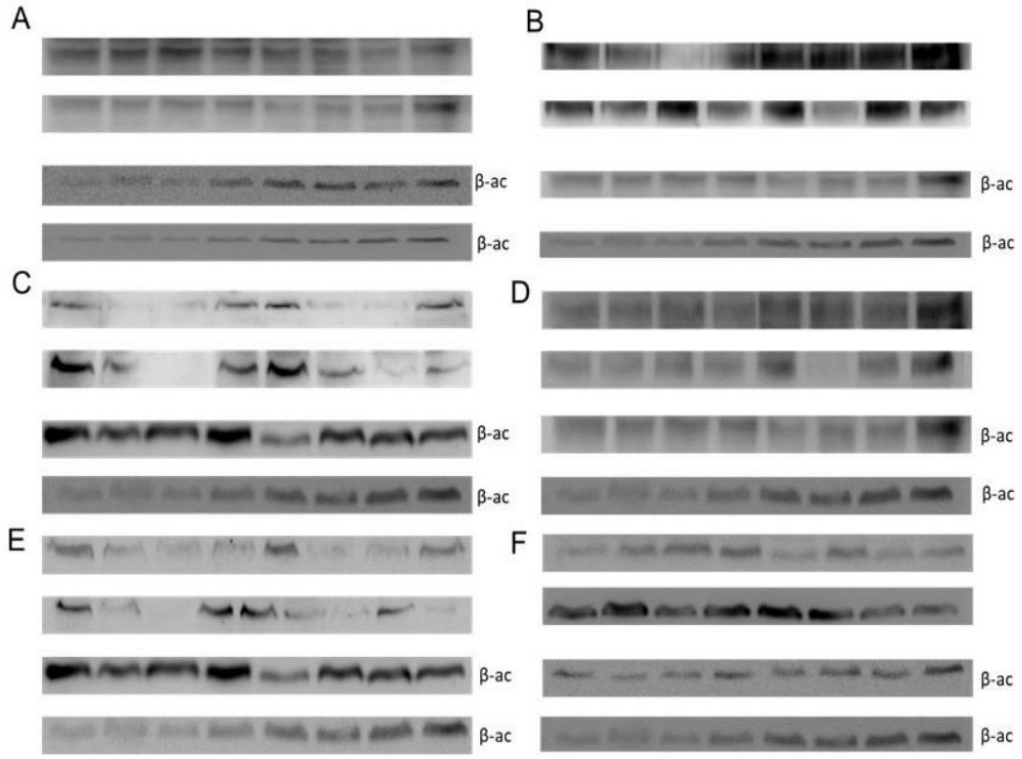

Supplementary Figure S4. **Nitrocellulose membranes mPFC**. A) $GABA_A$; B) $GABA_B$; C) Gephyrin; D) PSD-95; E) Neurolygin-2; F) Synaptophysin. In the image, β-ac stands for β-actin.

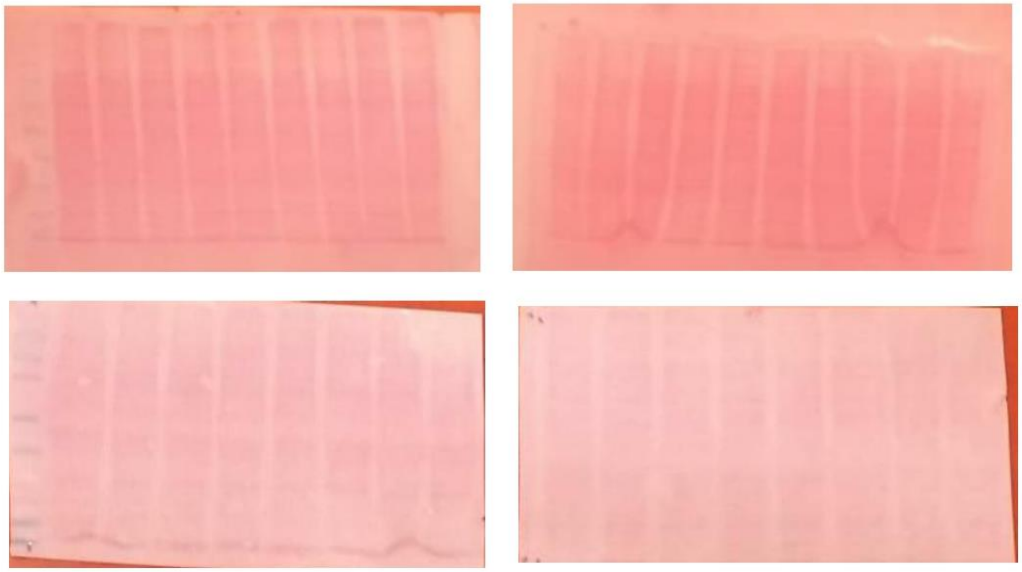

Supplementary Figure S5. Ponceau staining of the nitrocellulose membranes – HC

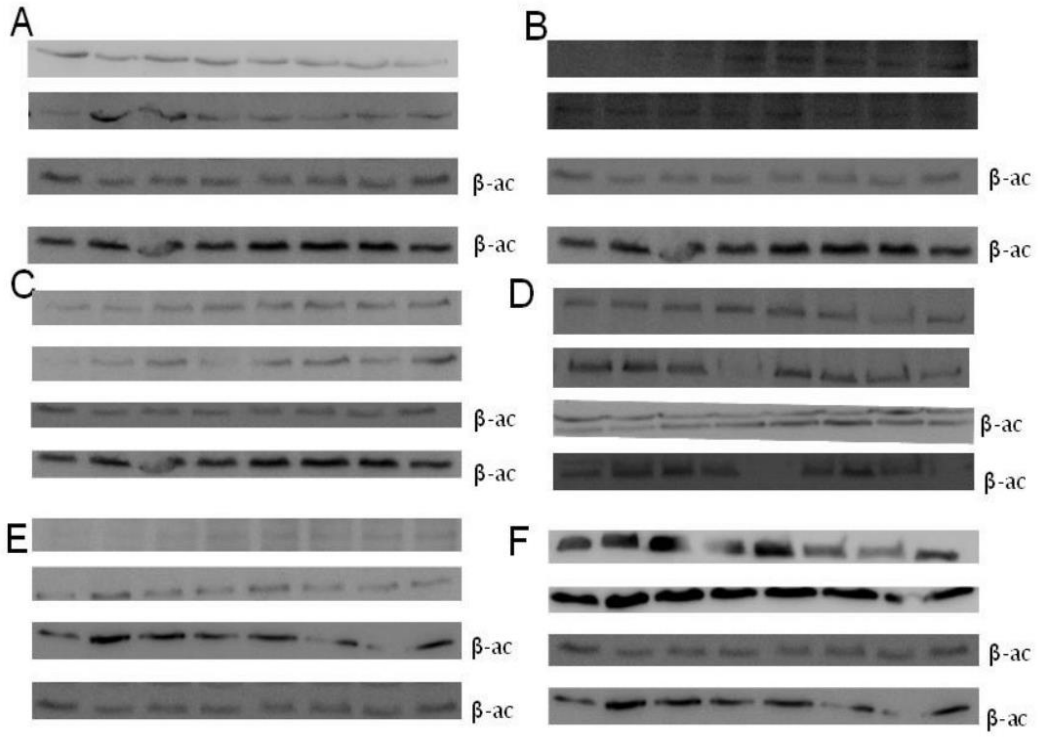

Supplementary Figure S6. **Nitrocellulose membranes HC**. A) $GABA_A$; B) $GABA_B$; C) Gephyrin; D) PSD-95; E) Neurolygin-2; F) Synaptophysin. In the image, β-ac stands for β-actin.

Capítulo III

Artigo publicado:

"*Resveratrol prevents long-term structural hippocampal alterations and modulates interneuron organization in an animal model of ASD*"

Brain Research 2021; 1:1768:147593.
DOI: https://doi.org/10.1016/j.brainres.2021.147593

Resveratrol prevents long-term structural hippocampal alterations and modulates interneuron organization in an animal model of ASD

Júlio Santos-Terra[#1,2,3,4], Iohanna Deckmann[1,2,3,4], Gustavo Brum Schwingel[1,2,3,4], André Vinicius Contri Paz[5], Clarissa S. Gama[3,5,6], Victorio Bambini-Junior[1,3,4,7], Mellanie Fontes-Dutra[1,2,3,4], Carmem Gottfried[#1,2,3,4]

1. Translational Research Group in Autism Spectrum Disorders-GETTEA, Universidade Federal do Rio Grande do Sul (UFRGS), Porto Alegre, RS, Brazil.
2. Department of Biochemistry, Universidade Federal do Rio Grande do Sul (UFRGS), Porto Alegre, RS, Brazil
3. National Institute of Science and Technology on Neuroimmunomodulation (INCT-NIM) - Brazil
4. Autism Wellbeing And Research Development (AWARD) Institute, BR-UK-CA
5. Laboratory of Molecular Psychiatry, National Science and Technology Institute for Translational Medicine, Hospital de Clínicas de Porto Alegre, Universidade Federal do Rio Grande do Sul (UFRGS), Brazil
6. Postgraduate Program in Psychiatry and Behavioral Sciences, Universidade Federal do Rio Grande do Sul (UFRGS), Porto Alegre, Brazil.
7. School of Pharmacology and Biomedical Sciences, University of Central Lancashire, Preston, United Kingdom

#CORRESPONDING AUTHORS:

JS-T (juliosterra@gmail.com) and CG (cgottfried@ufrgs.br)

Departamento de Bioquímica, ICBS, Universidade Federal do Rio Grande do Sul, Ramiro Barcelos 2600 – 21111. CEP: 90035-003 Porto Alegre-RS, Brazil.

E-MAIL ADDRESS OF EACH AUTHOR

JS-T (juliosterra@gmail.com)

ID (iohanna.deckmann@gmail.com)

GBS (brumschwingel@gmail.com)

AVCP (andrecontri@hotmail.com)

CSG (clarissasgama@gmail.com)

VB-J (VBambini-Junior@uclan.ac.uk)

MF-D (dutra.mellanie@gmail.com)

CG (cgottfried@ufrgs.br)

Abbreviations: AKT: AKT serine/threonine kinase 1; ASD: Autism Spectrum Disorder; CA 1-3: cornu ammonis (1-3); CB: calbindin; CK2: casein kinase 2; CNS: central nervous system; DG: dentate gyrus; GSK3β: glycogen synthase kinase 3 beta; HC: hippocampus; KO: knockout; mTOR: mechanistic target of rapamycin kinase; PTEN: phosphatase and tensin homologue; PV: parvalbumin; RSV: resveratrol; SOM: somatostatin; VPA: valproic acid.

ABSTRACT

Autism Spectrum Disorder (ASD) is a neurodevelopmental disorder characterized by impairments in both communication and social interaction, besides repetitive or stereotyped behavior. Although the etiology is unknown, environmental factors such as valproic acid (VPA) increase the risk of ASD onset. Resveratrol (RSV), a neuroprotective molecule, has been shown to counteract the effects of intrauterine exposure to VPA. We aimed to evaluate histological parameters related to hippocampal morphology and to the distribution of parvalbumin- (PV), calbindin- (CB), and somatostatin-positive (SOM) interneurons sub-populations, in addition to evaluate the total/phosphorylation levels of PTEN, AKT, GSK3β and total CK2 in the animal model of autism induced by VPA, as well as addressing the potential protective effect of RSV. On postnatal day 120, histological analysis showed a loss in total neurons in the dentate gyrus (DG) and decreased CB+ neurons in DG and CA1 in VPA animals, both prevented by RSV. In addition, PV+ neurons were diminished in CA1, CA2, and CA3, and SOM^+ were interestingly increased in DG (prevented by RSV) and decreased in CA1 and CA2. A hippocampal lesion similar to sclerosis was also observed in the samples from the VPA group. Besides that, VPA reduced AKT and PTEN immunocontent, and both VPA and RSV increased CK2 immunocontent. Thus, this work demonstrated long-term effects of prenatal exposure to ASD in different sub-populations of interneurons, structural damage of hippocampus, and also alteration in proteins associated with pivotal cell signaling pathways, highlighting the role of RSV as a tool for understanding the pathophysiology of ASD.

Keywords: Autism Spectrum Disorder, resveratrol, animal model, hippocampus, interneuron, long-term alterations.

1. INTRODUCTION

Autism Spectrum Disorder (ASD) is a highly prevalent neurodevelopmental disorder - affecting 1:54 children in the USA, the ratio of 4.3 boys to 1 girl (Maenner et al., 2020) - characterized by impairments in communication and social interaction, as well as repetitive and stereotyped behaviors (American Psychiatric Association, 2013). Despite extensive studies, the etiology of ASD remains unclear; however, it is already known that the final phenotype depends on the interaction between genetic and environmental risk factors (Gottfried et al., 2015). Among the environmental risk factors, the use of the anticonvulsant and mood stabilizer valproic acid (VPA) during pregnancy stands out (Dietert et al., 2011).

In addition to the main characteristics of this disorder, electrophysiological changes are also commonly described, including an imbalance in the delicate excitatory-inhibitory ratio (E/I) in different brain structures (Nelson and Valakh, 2015; Dickinson et al., 2016; Sohal and Rubenstein, 2019; Bruining et al., 2020). The dysfunctional predominance of glutamatergic action over GABAergic is one of the most frequent hypotheses to explain the E/I alterations (Marín and Rubenstein, 2003; Yizhar et al., 2011; Selten et al., 2018) in the central nervous system (CNS).

Interneurons promote the organization of circuits associated with cortical minicolumns and integrate stimuli among different cortical and subcortical regions. Within the subpopulations of these cells, parvalbumin (PV^+) and somatostatin (SOM^+) positive cells stand out as the most predominant (constituting about 70% of interneurons), in addition to other smaller subpopulations such as calbindin positive (CB^+) (Kelsom and Lu, 2013).

In ASD patients, there are descriptions of reduction in PV+ neurons in the prefrontal cortex (Hashemi et al., 2017), while CB^+ neurons have increased density in the dentate gyrus (DG) (Lawrence et al., 2010), but there are no findings describing SOM^+ alterations. Deficits in PV^+ interneurons have already been observed in the cortex of mice with *Mecp2* gene deletion, in the parietal cortex of animals from the VPA model (Gogolla et al., 2009), and in the prefrontal cortex of animals from the maternal immune activation model (Meyer et al., 2008). Regarding SOM^+ interneurons, there are only descriptions of disorders associated with ASD.

The hippocampus (HC), a brain structure closely associated with memory, also contributes to several other behavior components, including sociability, flexible cognition (Rubin et al., 2014), and attention (Goldfarb et al., 2016). Interestingly, interneurons are fundamental to perform these functions: SOM+ interneurons are instrumental in keeping hippocampal synchrony, promoting electrophysiological balance and connectivity (Flossmann et al., 2019)/, while PV^+ interneurons of ventral HC displayed important function

in social memory and social novelty recognition (Deng et al., 2019). Deficits in signaling mechanisms can also contribute to HC dysfunction, for example, the loss of PTEN in neurons of the DG induced increased excitability and connectivity (Santos et al., 2017; Skelton et al., 2019) and the hyperactivity of AKT-mTOR in the HC was associated with ASD-like behaviors (Xing et al., 2019).

Besides that, biological pathways associated with neural plasticity (CHU et al., 2013; WEI; HAN; ZHAO, 2020), such as AKT/GSK3β and CK2/PTEN, likewise can modulate interneurons. Loss of AKT signaling in cortical interneurons was already associated with reduced cell number (Carriere et al., 2020) whereas inhibition of AKT reduced the number of PV^+ cells in the HC (Chang et al., 2016). Studies suggest that GSK3β activity can be modulated by prenatal exposure to VPA (Caracci et al., 2016; Go et al., 2012; Wu et al., 2017) and, interestingly, the inhibition of AKT/GSK3β induced apoptosis of immature interneurons, leading to cell loss (Wei et al., 2020). The phosphatase and tensin homolog (PTEN) conditional knockout (KO) mice present ASD-like behavior and morphological neuronal changes (Cupolillo et al., 2016; Lugo et al., 2014; Shin et al., 2021), besides changes in the composition of interneuronal subpopulations, increasing PV^+ in detriment of SOM^+ (Vogt et al., 2015). Moreover, the specific KO of PTEN in both PV^+ and SOM+ induced ASD-like behavior (Shin et al., 2021). The casein kinase 2 (CK2) is a serine-threonine kinase protein that inactivates PTEN by phosphorylation (Borgo and Ruzzene, 2019). No evidence of a direct CK2 role in interneurons was already described; however, this protein already demonstrated important roles in the HC GABAergic signaling (Kim et al., 2020; Qin et al., 2021).

Recently, neuroimmune aspects have been largely associated with various disorders, including ASD (Gottfried et al., 2015). In this context, arises the resveratrol (RSV), a polyphenol widely studied in different diseases such as cancer, cardiovascular disorders, and diabetes due to its antioxidant and anti-inflammatory effect (Berman et al., 2017). Besides, RSV prevented behavioral and molecular changes in the VPA model, which has marked pro-oxidant and pro-inflammatory characteristics (Bambini-Junior et al., 2014; Fontes-Dutra et al., 2018; Hirsch et al., 2018). Thus, RSV emerges as an important method for assessing neuroimmune changes through its potential neuroprotective effect.

Here, we aimed to evaluate histological parameters related to hippocampal morphology and to the distribution of PV^+, SOM^+, and CB^+ interneurons sub-populations, in addition to evaluate the total/phosphorylation levels of PTEN, AKT, GSK3β, and CK2 in the animal model of autism induced by VPA, as well as assessing the potential protective effect of RSV.

2. RESULTS

2.1. Intrauterine administration of RSV prevented hippocampal long-term structural alterations in the VPA animals.

Prenatal exposure to VPA induced substantial structural alterations in the HC of adult animals (Figure 1B), leading to a discontinuity of the granule cell layer in the DG (Figure 1C) and a loss of neuronal compaction in the CA1 (Figure 1D). RSV entirely prevented the impact of VPA on these parameters.

2.2. Intrauterine administration of RSV prevented the long-term neuronal loss in the dentate gyrus of the VPA group.

RSV treatment prevented the decrease in the number of total neurons in the DG present in animals prenatally exposed to VPA ($F(1, 11) = 11.59$, p interaction = 0.0059, Figure 2A). No significant differences were observed in the CA1 (Figure 2B), CA2 (Figure 2C), and CA3 (Figure 2D) subregions. All neuron counts were normalized by area. Supplementary Table 1 comprises all means, standard deviation, and detailed statistics.

2.3. Intrauterine administration of RSV prevented long-term CB^+ and SOM^+ interneuron alterations in the dentate gyrus induced by prenatal exposure to VPA.

Regarding specific interneuron subpopulations, RSV treatment prevented the decrease in the number of CB^+ Neurons/Area induced by prenatal exposure to VPA ($F(1,10) = 12.43$; p interaction = 0.0055, Figure 3A1). No differences were seen in CB^+ Ratio/Total Neurons (Figure 3A2). In addition, no significant differences were observed in either PV^+ Neurons/Area (Figure 3B1) or PV^+ Ratio/Total Neurons (Figure 3B2).

Interestingly, significant differences were observed in both factors separately ($F(1,11) = 11.03$, p RSV <0.0001; $F(1,11) = 45,52$, p VPA <0.0001) in SOM^+ Neurons/Area (Figure 3C1). RSV prevented the increase in SOM^+ Ratio/Total Neurons induced by prenatal exposure to VPA ($F(1,11) = 8.821$; p interaction= 0.0127, Figure 3C2).

The illustrative Figure 3 shows CB^+ neurons (Figure 3A), PV^+ neurons (Figure 3B), and SOM^+ neurons (Figure 3C) in the DG. All neuron counts were normalized by area. Supplementary Tables 2, 3, and 4 comprise all means, standard deviation, and detailed statistics for CB^+, PV^+, and SOM^+ interneurons, respectively.

2.4. Intrauterine exposure to VPA induced long-term alterations in CB^+, PV^+, and SOM^+ interneurons parameters in the CA1 subregion, whilst RSV prevented CB^+ and PV^+ parameters, as well as demonstrated a *per se* effect in SOM^+.

RSV prenatal treatment prevented both the decrease in CB^+ Neurons/Area ($F(1,10) = 27.50$, p interaction = 0.0004, Figure 4A1) and CB^+ Ratio/Total Neurons induced by prenatal exposure to VPA ($F(1,10) = 11.52$; p interaction = 0.0068, Figure 4A2).

Again, the prenatal exposure to VPA modified interneuron subpopulations in this subregion, decreasing the PV^+ Neurons/Area ($F(1,12) = 8.261$; p interaction = 0.0140, Figure 4B1). Besides, a decrease in PV^+ Ratio/Total Neurons was observed in both groups exposed to VPA with no RSV preventive effects ($F(1, 12) = 7.634$, p VPA = 0.0172, Figure 4B2).

No differences were seen in SOM^+ Neurons/Area (Figure 4C1). Considering SOM^+ Ratio/Total Neurons, significant differences were seen in the factors separately ($F(1,11) = 12.79$, p RSV = 0.0043; $F(1,11) = 7.953$, p VPA = 0.0167): both prenatal exposure to VPA and treatment with RSV (including *per se* effect) decreased SOM^+ Ratio/Total Neurons (Figure 4C2).

The illustrative Figure 4 shows CB^+ neurons (Figure 4A), PV^+ neurons (Figure 4B), and SOM^+ neurons (Figure 4C) in the CA1. All neuron counts were normalized by area. Supplementary Tables 2, 3, and 4 comprise all means, standard deviation, and detailed statistics for CB^+, PV^+, and SOM^+ interneurons, respectively.

2.5. Intrauterine exposure to VPA induced long-term alterations in SOM^+ and PV^+ interneurons parameters in the CA2 subregion, without preventive effect of RSV.

No significant differences were found in either CB^+ Neurons/Area (Figure 5A1) or CB^+ Ratio/Total Neurons (Figure 5A2) among groups, as well as PV^+ Neurons/Area (Figure 5B1). However, the VPA administration during pregnancy decreased PV^+ Ratio/Total Neurons ($F(1,12) = 7.043$; p VPA = 0.0210) without RSV prevention (Figure 5B2).

Regarding SOM^+, there was a significant difference only in the effect of VPA ($F(1,11) = 7.172$, p VPA = 0.0215), decreasing SOM^+ Neurons/Area in comparison to groups not exposed to VPA (Figure 5C1). Besides that, RSV treatment prevented the decrease in SOM^+ Ratio/Total Neurons induced by prenatal exposure to VPA ($F(1,11) = 18.54$; p interaction = 0.0012, Figure 5C2).

The illustrative Figure 5 shows CB^+ neurons (Figure 5A), PV^+ neurons (Figure 5B), and SOM^+ neurons (Figure 5C) in the CA2. All neuron counts were normalized by area. Supplementary Tables 2, 3, and 4 comprise all means, standard deviation, and detailed statistics for CB^+, PV^+, and SOM^+ interneurons, respectively.

2.6. Intrauterine exposure to VPA induced long-term alteration in PV^+ interneurons parameters in the CA3 subregion, without preventive effect of RSV.

No significant differences were found in either CB^+ Neurons/Area (Figure 6A1) or CB^+ Ratio/Total Neurons (Figure 6A2) among groups.

Regarding PV^+, prenatal exposure to VPA decreased both PV^+ Neurons/Area ($F(1,12) = 8.859$, p interaction = 0.0116, Figure 6B1) and PV^+ Ratio ($F(1,12) = 11.56$, p interaction = 0.0012, Figure 6B2).

Lastly, no significant differences were found in either SOM^+ Neurons/Area (Figure 6C1) or SOM^+ Ratio/Total Neurons (Figure 6C2) among groups.

The illustrative Figure 6 shows CB^+ neurons (Figure 6A), PV^+ neurons (Figure 6B), and SOM^+ neurons (Figure 6C) in the CA3. All neuron counts were normalized by area. Supplementary Tables 2, 3, and 4 comprise all means, standard deviation, and detailed statistics for CB^+, PV^+, and SOM^+ interneurons, respectively.

2.7. VPA induced long-term alterations in the hippocampal immunocontents of AKT, PTEN, and CK2 without preventive effect of RSV.

The animals prenatally exposed to VPA (VPA and VPA+RSV) presented decreased levels of PTEN when compared to the other groups (Control and RSV) ($F(1,20) = 21.22$; p VPA = 0.0002) (Supplementary Table 5, Figure 7A).

There were significant differences in RSV factor ($F(1,19) = 4.406$; p RSV = 0.0494) and VPA factor ($F(1,19) = 10.64$, p VPA = 0.0041) in the AKT immunocontent, indicating a decrease in the total AKT levels induced by VPA when compared to the Control group with no preventive effect of RSV treatment (Supplementary Table 5, Figure 7B).

In addition, prenatal exposure to VPA increased the total CK2 immunocontent ($F(1,20) = 6.628$, p = 0.0181) without RSV preventive effect (Supplementary Table 5, Figure 7C).

Finally, no changes were observed in the GSK3β immunocontent (Supplementary Table 4, Figure 7D) and in the phosphorylation levels of the proteins among groups (Supplementary Table 5). Supplementary Figures 1, 2, and 3 represent the nitrocellulose membranes stained with ponceau, as well as images of immunoblottings of the specific primary antibodies, and of the endogenous marker β-actin, respectively.

3. DISCUSSION

Considering that most studies investigate behavioral and morphological alterations in young animals, we set out to evaluate possible changes in the adults of the ASD model induced by prenatal exposure to VPA. Several studies have been focused on the HC due to its plasticity and sensitivity to stressors, in addition to being an area where neurogenesis occurs in adulthood, both in rodents and in humans (Gonçalves et al., 2016). Our research group previously demonstrated age-dependent alterations in the HC of the VPA animal model regarding glutamate metabolism at P15 and P120 (Bristot Silvestrin et al., 2013). At P15, the VPA animals had decreased levels of glutamate transporter GLT1 and increased levels of glutamine synthetase (GS). At P120, the VPA animals had increased glutamate uptake activity, increased levels of GLT1, increased levels of glutathione (GSH), and decreased activity of GS. These data demonstrate important glutamatergic alterations in HC, probably associated with a glutamatergic excitotoxicity pattern already demonstrated in ASD.

In the present study, we demonstrated a significant morphological alteration in hippocampal regions induced by VPA in adult animals at P120. The altered cellular composition in the model of ASD is most prominent in DG, particularly in the granular layer. Moreover, neurons appeared dispersed in CA1. Interestingly, RSV prevented these alterations, indicating some of the preventive behavioral effects observed in previous works (Bambini-Junior et al., 2014; Fontes-Dutra et al., 2018; Hirsch et al., 2018) might be related to direct effects in the HC.

Studies demonstrated the benefits of RSV in restoring hippocampal structure and connectivity in patients with mild cognitive impairments (Köbe et al., 2017) and status epilepticus (Castro et al., 2017), although no significant effects were observed in behavioral tasks of memory performance. These findings might suggest possible similar mechanisms since our previous data revealed no significant effects of RSV in empathy-like prosocial behavior in RSV+VPA rats of similar age (Fontes-Dutra et al., 2019).

The mechanisms of RSV protection are not well established, but some hypotheses grow towards the action of RSV in activating SIRT proteins, especially in view of the HDAC inhibitor action associated with VPA. The hippocampal activity of SIRT1 is fundamental for cognition, memory and synaptic plasticity (Castrol et al., 2017); a study demonstrated that miR-134 mediates these functions through CREB (Gao et al., 2010) and, interestingly, we already demonstrated that RSV normalized the altered levels of mir-134 induced by VPA in our model (Hirsch et al., 2018). Finally, SIRT1 stimulation of mitochondrial biogenesis and activity (mediated by PGC-1α) protected the HC from seizure-induced cell death and reduced oxidative stress (Wang et al., 2015; Chuang et al., 2019), indicating another possible pathway by which RSV plays neuroprotective effects.

Hippocampal excitotoxicity has been associated with neuropsychiatric disorders (Olloquequi et al., 2018), such as ASD (Essa et al., 2013), schizophrenia (Plitman et al., 2014), epilepsy (Thom, 2014), and many others. In schizophrenia, an altered organization in the granular layer from DG is observed in GFAP.HMOX10-12m transgenic model, which astrocytes overexpress the human stress protein heme oxygenase-1 (OX1) (Tavitian et al., 2019), leading to an "immature" DG associated with changes in its molecular profile. In epilepsy, age-dependent patterns of DG are observed, such as neuronal loss in granular cells and CA1 (Pauli et al., 2006; Thom, 2014). These changes in hippocampal structure and shape are relevant to establish the histological hallmarks of hippocampal sclerosis, which involves a neuronal loss in hippocampal subregions, gliosis, or both of them in different levels (Thom, 2014). The present findings suggest possible mechanisms related to this event, opening an interesting issue to be followed up to characterize glial cell alteration in adult VPA rats.

Hippocampal interneurons are a highly diverse population of cells, with functions associated with shape, neurochemical patterns, and location (Maccaferri and Lacaille, 2003). The evaluation of HC subregions CA1, CA2, CA3, and DG at P120 indicated an expansion of the damage induced by prenatal exposure to VPA. In addition to the morphological alteration, also decreased total neurons of DG associated with different natures of alteration among CB^+, PV^+ and SOM^+ interneuronal subpopulations.

In DG, VPA reduced the number and the ratio of CB^+ interneurons, which was prevented by RSV treatment. CB^+ interneurons in DG already demonstrated to be influenced by the electrophysiological status: hippocampal epilepsy in humans induced morphological impairments on CB^+ interneurons both hypertrophy of cell bodies and spiny dendrites (Maglóczky et al., 2000), and loss of general calbindin expression in this region (Bandopadhyay et al., 2014), although, in ASD, a previous study demonstrated increased density of CB^+ interneurons in DG (Lawrence et al., 2010). Interestingly, in a schizophrenia animal model, rats demonstrated an important reduction of CB^+ interneurons in DG (Harte et al., 2007); complementarily, a recent study demonstrated the critical role of DG CCK^+ interneurons (which are mostly CB^+) (Pelkey et al., 2017) in the inhibitory plasticity processes associated with the promotion of enriched early social, sensory and motor experiences (Feng et al., 2020). Furthermore, our group demonstrated that RSV improved early sensory alterations (Fontes-Dutra et al., 2018) and social and stereotypy impairments (Bambini-Junior et al., 2014; Hirsch et al., 2018) possibly due to the protection of early loss of important experiences, preserving this component (CB^+/CCK^+) feature of HC inhibitory circuit.

SOM+ interneurons demonstrated a distinct pattern in DG, not only due to the total neuronal loss (which could increase the SOM^+/total neurons by itself) but also due to increased absolute neuronal numbers. The SOM^+ cells play important roles in DG, promoting contralateral HC connectivity (Eyre and Bartos, 2019), organizing granule cell assemblies associated with memory formation (Yuan et al., 2017) and regulating long term potentiation (Tallent, 2007). Little is known about SOM^+ interneurons in the ASD context. Previous work already demonstrated that the haploinsufficiency of Aridb1 (risk-associated gene for ASD) in SOM^+ cells induces stereotypies and learning/memory issues (Smith et al., 2020). In Dravet syndrome (which is significantly related to ASD behavioral features), SOM^+ cells presented reduced excitability (Chao Tai et al., 2014). Although SOM^+ and CB^+ cells have different embryonic origins (MGE and CGE, respectively) (Kelsom and Lu, 2013), one factor is pivotal to the final interneuron positioning in a specific region: the microenvironment during the moment of arrival. For SOM^+ cells, the present complementary changes in CA1 and CA2 subregions (both in number and ratio, with prevention by RSV only in the CA2 ratio and an including an apparent *per se* effect of RSV towards reduction of SOM ratio in CA1) indicate that VPA may interfere on migration routes, retaining SOM^+ neurons in DG. Impairments in CXCL12 signaling, for example, can misplace the interneurons distribution in HC. Indeed, VPA can interfere with CXCR4 (CXCL12 receptor) (Gul et al., 2009) and induce neuronal accumulation in DG, which replicates the SOM+ neurons pattern (Danzer, 2019). Thus, considering that CA1 and CA2 remain altered at some level in the VPA+RSV group, these changes are probably not related to the core symptoms of ASD.

Differently, RSV may be inducing important effects during pregnancy that prevent DG interneuron alterations, highlighting this subregion as a possible critical component in ASD. However, the *per se* effect of RSV in CA1 highlights the necessity to expand the understanding of the cellular pathways associated with the placement of interneurons in this particular subregion. Moreover, the preventive effect of RSV against VPA-induced total neurons decrease may possibly be related to glutamatergic signaling modulation, such as the AMPA signaling (Manent et al., 2006) and other pathways of signaling (Luhmann et al., 2015), providing important clues to support the correct interneuronal positioning in the RSV+VPA group.

In CA1, we observed important alterations among interneurons subpopulations induced by VPA, including a reduction in PV^+ number and SOM^+ cells. The prenatal administration of RSV was able to prevent CB^+ interneurons-decrease in number and ratio. PV^+ interneurons have been studied in neurodevelopmental context, description of impairments in several animal models includes the presence of ASD-like features in mice

KO for PV ($PV^{-/-}$) (Wöhr et al., 2015), downregulation of PV expression in Angelman Syndrome model (Godavarthi et al., 2014) and altered neuronal layer positioning (increased ratio in superficial layers II-III and reduction in deeper layers IV/V) in somatosensory cortex (Fontes-Dutra et al., 2018). Interestingly, PV^{+} cells in CA1 presents important roles in memory consolidation (Ognjanovski et al., 2017), particularly social memory (Deng et al., 2019) and spatial working memory (Murray et al., 2011), indicating that impairments in this hippocampal subregion may contribute to the empathy-like behavioral alteration that we observed in ASD model. Interestingly, in CA2 and CA3, we also observed a similar pattern for PV^{+} cells, which usually are associated with a complex synaptic organization and the generation of fast-ripples waves (Kohus et al., 2016; Sik et al., 1993), fundamental for memory, planning, and interactions with other regions like the prefrontal cortex (Buzsáki, 2015; Sullivan et al., 2011).

Related to the evaluated signaling pathways, we demonstrated that RSV could not prevent the hippocampal changes of total PTEN, CK2, and AKT. However, considering that no changes were observed in phosphorylation levels and consequently the activity of PTEN, AKT, and GSK3β among groups, it suggests that, at least in HC from P120 animals, these proteins might not play an important role in ASD-like features. PTEN KO mice in PV^{+} and SOM^{+} cells displayed social deficits, repetitive behaviors, and impaired motor coordination/learning similar to ASD. Besides, these animals presented interneuron-dependent behavior alterations: PTEN KO mice in SOM^{+} displayed anxiety-like behaviors, while PTEN KO mice in PV+ presented hyperlocomotion (Shin et al., 2021). Furthermore, one of the proteins that regulate PTEN is CK2, which can inhibit PTEN activity. Here, we observed an increase in the levels of this protein, which confirms the decrease in PTEN also found. Finally, the decrease in AKT may impact mTOR activity which would, in turn, affect synaptic components (Nicolini et al., 2015). Therefore, even if the protein changes demonstrated here cannot fully explain the behavioral and morphological issues of the VPA model, its participation in the autistic phenotype remains to be determined in other brain structures and age.

In summary, the present data shed some light on the ASD pathophysiology at adult age, demonstrating long-term alterations of the gestational VPA-exposure in a key brain region implicated in the many impairments described in ASD, such as sociability and flexible cognition. Furthermore, the most widely available data refer to infant or juvenile ages; few studies focus on bringing insights to the progressive damage of ASD in adult stages, which enhances the translational character of our data as it provides evidence that can improve the understanding of the symptoms associated with ASD in adult patients. Moreover, the

alterations observed in the hippocampal morphology, neuronal composition, and expression of important signaling proteins contribute to the hypothesis of an E/I imbalance in ASD. Especially regarding SOM^+ neurons, this is the first work to our knowledge to demonstrate the involvement of this interneuron in the VPA-ASD animal model, highlighting a new field of study in the disorder. Finally, we demonstrated a long-term preventive effect of prenatal treatment with RSV, being effective in adult ages, particularly related to changes in the neuronal composition of the dentate gyrus and in the morphology of the HC.

4. CONCLUSION

In summary, we demonstrated that prenatal exposure to VPA induced significant hippocampal alterations in morphology, neuronal composition, and protein expression in adult animals with significant preventive effects of RSV. These data highlight the long-term neuroprotection provided by this polyphenol, especially in DG. Considering that the timing of a risk factor exposure during pregnancy is pivotal for ASD triggering and development, with long-term impacts in the nervous system, preventive effects of RSV in HC open new clues in the understanding of ASD pathophysiology. However, the mechanisms behind this pattern are still open to study.

5. METHODOLOGY

5.1. Animals

Wistar rats from the Center for Reproduction and Experimentation of Laboratory Animals (CREAL) were housed in the bioterium of the Department of Biochemistry and maintained under a standard 12/12h light/dark cycle at a constant temperature of 22±2°C. The animals had *ad libitum* access to food and water and were handled following the guidelines established by the National Council for the Control of Animal Experimentation (CONCEA) of Brazil. The ethics committee approved this project of the Federal University of Rio Grande do Sul (CEUA-UFRGS #35733). The animals' euthanasia was performed by anesthetic overdose with ketamine and xilasine, supplied in concentrations three times higher than the concentration required to obtain an anesthetic-surgical plan (300 mg/kg and 40 mg/kg, respectively), following the Euthanasia Practice Guidelines of the National Council for Animal Experimentation Control (Normative Resolution N. 13, 2013).

5.2. Drugs and prenatal treatments

5.2.1. *Drugs*

For inducing the model and experimental treatments, we used resveratrol (RSV - 3.6 mg/Kg; Fluxome, Stenløse, Denmark), dimethyl sulfoxide (DMSO - P.A., equivalent volume of RSV injection; Merck, Germany), valproic acid (VPA - 600 mg/Kg; Acros Organics, NJ, USA).

5.2.2. *Prenatal treatments*

Males and females rats were mated overnight, and pregnancy was verified the next morning through the presence of spermatozoa in the vaginal smear; after pregnancy was confirmed, this day was considered the embryonic day 0.5 (E0.5). Pregnant rats were divided into four groups according to the treatment they received: Control (vehicles), RSV, VPA, or RSV+VPA. From E6.5 to E18.5, the pregnant rats received a daily subcutaneous injection of RSV (Fluxome, Stenløse, Denmark) at 3.6 mg/Kg or dimethyl sulfoxide P.A. (DMSO, equivalent volume of RSV injection) as previously described (Bambini-Junior et al., 2014; Fontes-Dutra et al., 2018). On E12.5, pregnant rats received a single intraperitoneal injection with either VPA at 600 mg/Kg (Acros Organics, NJ, USA) or saline solution 0.9%. Pregnant rats were isolated in E18 until the litter's birth. We consider the day of the birth the postnatal day 0 (P0). The female pups were euthanized at postnatal day (P) P21, and only males were used in this work. After birth and weaning at P21, male offspring were kept until P120. 3-4 animals from different litters per group were used for immunofluorescence assays, and 6 animals from different litters per group were used for western blotting assays. The sample number for the immunofluorescence assay was CON = 4, RSV = 4, VPA = 4 and RSV + VPA = 3; for western blotting, it was 6 for all experimental groups. The animals came from different litters. The total number of animals used in the study was 10 control, 10 RSV, 10 VPA, and 9 RSV+VPA divided randomly in experiments, generated from 6 control dams, 6 RSV, 12 VPA, and 12 RSV+VPA (the excedent offspring was destined to other projects in order to use of biological tissue). Loss rate for the VPA groups was 50% in this protocol.

5.3. Immunofluorescence

The tissues fixed and cryopreserved in OCT® were cut in a Leica® cryostat (-20ºC) and the slices (25 µm) corresponding to the HC were placed on histological slides covered with poly-L-lysine and post-fixed again with 4% paraformaldehyde. We intended to comprise within the following coordinates: bregma: -2.92 mm, interaural: 6.08 mm, Figure 57 in Paxinos Atlas (5th edition) - bregma: -3.24 mm, interaural: 5.76 mm, Figure 60 in Paxinos

Atlas (5th edition). In each histological slide, 3 slices were alternately placed. After that, the staining was performed using specific primary antibodies for PV, SOM, CB, and NeuN, in addition to corresponding secondary antibodies associated with a fluorophore (Alexia® 488 and Alexia® 594) and nuclear DAPI dye according to the protocol described by Fontes-Dutra et al., 2018. The analysis was performed in duplicates. Technical information, including concentrations of the reagents used in immunofluorescence assays, are summarized in Supplementary Table 6. The images were obtained using the Olympus FV1000® confocal microscope at the Center for Microscopy and Microanalysis (CMM-UFRGS) and the Nikon® E600 fluorescence microscope at the Department of Biochemistry (UFRGS). Each coronal section of 25 µm is photographed in stacks by the confocal microscope (on average, 8, dimensions: 635.9 x 635.9 microns). The analyses were performed using the ImageJ® software using the Cell Counter plug-in. The quantification was conducted by counting cells of the 8 stacks of at least 2 slices per animal (all the stacks individually and also with the overlapping image). The counting is done manually by two trained researchers, who are blinded for the experimental groups.

Quantitative evaluation was performed by the absolute number of total neurons (NeuN+) and interneurons (CB^+, PV^+, and SOM^+) - normalized by area - in addition to the ratio between the number of interneurons and total neurons to obtain a ratio between the inhibitory (interneuron) and excitatory components (the majority of the total neurons) according to the following formula: (CB^+, PV^+ or SOM^+) Interneurons/Total neurons (based on Fontes-Dutra et al., 2018). This ratio was made separately for each interneuron evaluated. These assessments were made in the dentate gyrus (DG), CA1, CA2, and CA3.

Due to the magnification used to capture the images (20x), one counting frame was obtained in each subfield (subregion) in each hemi-hippocampus. All images were obtained with a standardized size (635.9x635.9 μm^2) containing a representative portion of each subregion DG, CA1, CA2, and CA3. Considering the anatomical differences intrinsic to biological models, the quantification area of the subregion DG was determined by the contour of the granular layer whilst the contour of CA1/CA2/CA3 was defined as the delimitation of the pyramidal cells layer (Supplementary Figure 4). The averages of the areas in the subfields per animal were DG: 85,104±10,151 μm^2; CA1: 39,638±8,445 μm^2; CA2: 106,168±24,254 μm^2; CA3: 47,478±8,288 μm^2, the average of the total area analyzed per animal was 278,743±33,570 μm^2. All cells present within the delimited region (and the interneurons surrounding the pyramidal/granular layers) were quantified. The averages of the total neurons analyzed in the subfields per animal were DG: 582±64; CA1: 150±18; CA2: 265±42; CA3: 136±15, the average of the total neurons analyzed per animal was 1,113±93.

The averages of CB^+ neurons analyzed in the subfields per animal were DG: 6.5±1.6; CA1: 3.6±1.2; CA2: 6.7±2; CA3: 3.5±1, the average of CB^+ neurons per animal was 20.4±4.5. The averages of PV^+ neurons in the subfields per animal were DG: 12.5±2.3; CA1: 6.7±1.9; CA2: 10.6±1.9; CA3: 5.8±1.4, the average of PV^+ neurons per animal was 35.6±5.1. The averages of SOM^+ neurons in the subfields per animal were DG: 25±12.1; CA1: 5.5±1.79; CA2: 7.75±3.35; CA3: 4.75±1.2, the average of SOM^+ neurons per animal was 43.2±10.

5.4. Protein immunocontent by Western Blotting

The hippocampal samples were homogenized and prepared in a buffer containing 10% SDS, 100mM EDTA, 500mM TRIS, and protease inhibitor, centrifuged at 14000 g for 20 min at 4ºC, and the supernatant was collected. Total proteins were quantified by the Lowry method (LOWRY et al., 1951), samples were prepared in a buffer containing glycerol, bromophenol blue, and 500 mM TRIS, and β-mercaptoethanol. Equal amounts of protein (40µg) were applied to 12% polyacrylamide gels, separated by unidimensional electrophoresis and transferred to nitrocellulose membranes to detect the immunocontent of CK2, PTEN, p-PTEN (Ser380, Thr382/383), AKT, p-AKT (Ser473 and Thr380), GSK3*β* and p-GSK3*β* proteins using specific primary antibodies according to the protocol adapted from (Bristot Silvestrin et al., 2013) The analysis was performed in duplicates. After incubation with corresponding secondary peroxidase-associated antibodies (HRP), the chemiluminescent signal was detected using the ImageQuant™ LAS 4000 system (GE HealthCare Life Sciences®). The quantification of the relative immunocontent was performed with the ImageJ® software, and the data were normalized by the endogenous marker β-actin. Technical information, including concentrations of the reagents used in Western Blotting assays, are summarized in Supplementary Table 7.

5.5. Statistical analysis

The analysis was performed using the GraphPad Prism 6 software (GraphPad Software, La Jolla, California US). Kolmogorov-Smirnov and Shapiro-Wilk tests of normality were applied to determine data distribution. As the data presented a normal distribution, we chose a parametric test (two-way ANOVA) followed by Bonferroni post-test. When there was an interaction effect, pairwise comparison was analyzed in the post hoc; when there was no effect, exposure to factors (VPA or RSV) was analyzed.

6. AUTHOR CONTRIBUTIONS

JS-T, ID, GBS, MF-D, AVCP, CSG, VB-J, and CG: experimental design and intellectual contribution. CSG, VB-J, and CG: acquisition of financial resources. JS-T, ID, and MF-D: immunofluorescence analyses. JS-T, ID, AVCP, and GBS: western blotting analyses. JS-T, ID, MF-D, CSG, VB-J, and CG: data discussion and manuscript preparation.

7. ACKNOWLEDGEMENTS

This work was supported by the Brazilian National Institute of Science and Technology on Neuroimmunomodulation - Instituto Nacional de Ciência e Tecnologia em Neuroimunomodulação (INCT-NIM, Project number 88887.136400/2017-00), Rio de Janeiro, Brazil; National Council of Technological and Scientific Development - Conselho Nacional de Desenvolvimento Científico e Tecnológico (CNPq); Coordination for the Improvement of Higher Education Personnel - Coordenação de Aperfeiçoamento de Pessoal de Nível Superior (CAPES), and Fundo de Incentivo à Pesquisa e Eventos do Hospital de Clínicas de Porto Alegre (FIPE-HCPA #14-0367 and #14-0431). We would also like to thank Fluxome (Stenløse, Denmark) for the generous gift of *trans*-resveratrol and Ms. Vitória Lemos (Edinburgh, Scotland) for the meticulous English writing revision. Graphical abstract generated with BioRender®.

8. CONFLICT OF INTEREST STATEMENT

The authors declare that the research was conducted in the absence of any commercial or financial relationships that could be considered a potential conflict of interest.

9. REFERENCES

American Psychiatric, 2013. DSM 5, American Journal of Psychiatry. https://doi.org/10.1176/appi.books.9780890425596.744053

Bambini-Junior, V., Zanatta, G., Della Flora Nunes, G., Mueller de Melo, G., Michels, M., Fontes-Dutra, M., Nogueira Freire, V., Riesgo, R., Gottfried, C., 2014. Resveratrol prevents social deficts in animal model of autism induced by valproic acid. Neurosci. Lett. 583, 176–181. https://doi.org/10.1016/j.neulet.2014.09.039

Bandopadhyay, R., Liu, J.Y.W., Sisodiya, S.M., Thom, M., 2014. A comparative study of the dentate gyrus in hippocampal sclerosis in epilepsy and dementia. Neuropathol. Appl. 40, 177-190. Neurobiol. https://doi.org/10.1111/nan.12087

Berman, A.Y., Motechin, R.A., Wiesenfeld, M.Y., Holz, M.K., 2017. The therapeutic

potential of resveratrol: a review of clinical trials. NPJ Precis. Oncol. 1. 1, 35. https://doi.org/10.1038/s41698-017-0038-6

Borgo, C., Ruzzene, M., 2019. Role of protein kinase CK2 in antitumor drug resistance. J. Exp. Clin. Cancer Res. 6, 138. https://doi.org/10.1186/s13046-019-1292-y

Bristot Silvestrin, R., Bambini-Junior, V., Galland, F., Daniele Bobermim, L., Quincozes-Santos, A., Torres Abib, R., Zanotto, C., Batassini, C., Brolese, G., Gonçalves, C.-A., Riesgo, R., Gottfried, C., 2013. Animal model of autism induced by prenatal exposure to valproate: Altered glutamate metabolism in the hippocampus. Brain Res. 1495, 52–60. https://doi.org/10.1016/j.brainres.2012.11.048

Bruining, H., Hardstone, R., Juarez-Martinez, E.L., Sprengers, J., Avramiea, A.-E., Simpraga, S., Houtman, S.J., Poil, S.-S., Dallares, E., Palva, S., Oranje, B., Palva, J.M., Mansvelder, H.D., Linkenkaer-Hansen, K., 2020. Measurement of excitation-inhibition ratio in autism spectrum disorder using critical brain dynamics. Sci. Reports 2020 101 10, 1–15. https://doi.org/10.1038/s41598-020-65500-4

Buzsáki, G., 2015. Hippocampal sharp wave-ripple: A cognitive biomarker for episodic memory and planning. Hippocampus 25(10), 1073-1188. https://doi.org/10.1002/hipo.22488

Caracci, M.O., Avila, M.E., De Ferrari, G. V., 2016. Synaptic Wnt/GSK3 β Signaling Hub in Autism. Neural Plast. 2016, 7149527. https://doi.org/10.1155/2016/9603751

Carriere, C.H., Wang, W.X., Sing, A.D., Fekete, A., Jones, B.E., Yee, Y., Ellegood, J., Maganti, H., Awofala, L., Marocha, J., Aziz, A., Wang, L.Y., Lerch, J.P., Lefebvre, J.L., 2020. The γ-protocadherins regulate the survival of GABAergic interneurons during developmental cell death. J. Neurosci. 40, 8652–8668. https://doi.org/10.1523/JNEUROSCI.1636-20.2020

Castro, O.W., Upadhya, D., Kodali, M., Shetty, A.K., 2017. Resveratrol for easing status epilepticus induced brain injury, inflammation, epileptogenesis, and cognitive and memory dysfunction-Are we there yet? Front. Neurol. 8, 603. https://doi.org/10.3389/fneur.2017.00603

Chang, C.Y., Chen, Y.W., Wang, T.W., Lai, W.S., 2016. Akting up in the GABA hypothesis of schizophrenia: Akt1 deficiency modulates GABAergic functions and hippocampus-

dependent functions. Sci. Rep. 6, 33095. https://doi.org/10.1038/srep33095

Chuang, Y.C., Chen, S. Der, Jou, S. Bin, Lin, T.K., Chen, S.F., Chen, N.C., Hsu, C.Y., 2019. Sirtuin 1 regulates mitochondrial biogenesis and provides an endogenous neuroprotective mechanism against seizure-induced neuronal cell death in the hippocampus following status epilepticus. Int. J. Mol. Sci. 20(14), 3588. https://doi.org/10.3390/ijms20143588

Cupolillo, D., Hoxha, E., Faralli, A., De Luca, A., Rossi, F., Tempia, F., Carulli, D., 2016. Autistic-like traits and cerebellar dysfunction in purkinje cell PTEN knock-out mice. Neuropsychopharmacology 41(6), 1457-1466. https://doi.org/10.1038/npp.2015.339

Danzer, S.C., 2019. Valproic Acid Leads New Neurons Down the Wrong Path. Epilepsy Curr. 19(2):132-133. https://doi.org/10.1177/1535759719835366

Deng, X., Gu, L., Sui, N., Guo, J., Liang, J., 2019. Parvalbumin interneuron in the ventral hippocampus functions as a discriminator in social memory. Proc. Natl. Acad. Sci. U. S. A. 116, 16583–16592. https://doi.org/10.1073/pnas.1819133116

Dickinson, A., Jones, M., Milne, E., 2016. Measuring neural excitation and inhibition in autism: Different approaches, different findings and different interpretations. Brain Res. 1648, 277–289. https://doi.org/10.1016/J.BRAINRES.2016.07.011

Dietert, R.R., Dietert, J.M., DeWitt, J.C., 2011. Environmental risk factors for autism. Emerg. Health Threats J. 4, 7111. https://doi.org/10.3402/ehtj.v4i0.7111

Endo, H., Nito, C., Kamada, H., Nishi, T., Chan, P.H., 2006. Activation of the Akt/GSK3β signaling pathway mediates survival of vulnerable hippocampal neurons after transient global cerebral ischemia in rats. J. Cereb. Blood Flow Metab. 26, 1479–1489. https://doi.org/10.1038/sj.jcbfm.9600303

Essa, M.M., Braidy, N., Vijayan, K.R., Subash, S., Guillemin, G.J., 2013. Excitotoxicity in the pathogenesis of autism. Neurotox. Res. 23(4), 393-400. https://doi.org/10.1007/s12640-012-9354-3

Eyre, M.D., Bartos, M., 2019. Somatostatin-Expressing Interneurons Form Axonal Projections to the Contralateral Hippocampus. Front. Neural Circuits. 13, 56. https://doi.org/10.3389/fncir.2019.00056

Feng, T., Alicea, C., Pham, V., Kirk, A., Pieraut, S., 2021. Experience-dependent inhibitory plasticity is mediated by CCK+ basket cells in the developing dentate gyrus. J. Neurosci. . 41(21), 4607-4619. 10.1523/JNEUROSCI.1207-20.2021

Flossmann, T., Kaas, T., Rahmati, V., Kiebel, S.J., Witte, O.W., Holthoff, K., Kirmse, K., 2019. Somatostatin Interneurons Promote Neuronal Synchrony in the Neonatal Hippocampus. Cell Rep. 26(12), 3173-3182.e5. https://doi.org/10.1016/j.celrep.2019.02.061

Fontes-Dutra, M., Della-Flora Nunes, G., Santos-Terra, J., Souza-Nunes, W., Bauer-Negrini, G., Hirsch, M.M., Green, L., Riesgo, R., Gottfried, C., Bambini-Junior, V., 2019. Abnormal empathy-like pro-social behaviour in the valproic acid model of autism spectrum disorder. Behav. Brain Res. 364, 11–18. https://doi.org/10.1016/J.BBR.2019.01.034

Fontes-Dutra, M., Santos-Terra, J., Deckmann, I., Schwingel, G.B., Nunes, G.D.F., Hirsch, M.M., Bauer-Negrini, G., Riesgo, R.S., Bambini-Júnior, V., Hedin-Pereira, C., Gottfried, C., 2018b. Resveratrol prevents cellular and behavioral sensory alterations in the animal model of autism induced by valproic acid. Front. Synaptic Neurosci. 10, 9. https://doi.org/10.3389/fnsyn.2018.00009

Gao, J., Wang, W.Y., Mao, Y.W., Gräff, J., Guan, J.S., Pan, L., Mak, G., Kim, D., Su, S.C., Tsai, L.H., 2010. A novel pathway regulates memory and plasticity via SIRT1 and miR-134. Nature 466, 1105–1109. https://doi.org/10.1038/nature09271

Gao, C., Yuan, X., Jiang, Z., Gan, D., Ding, L., Sun, Y., Zhou, J., Xu, L., Liu, Y., Wang, G., 2019. Regulation of AKT phosphorylation by GSK3β and PTEN to control chemoresistance in breast cancer. Breast Cancer Res. Treat. 176, 291–301. https://doi.org/10.1007/s10549-019-05239-3

Go, H.S., Kim, K.C., Choi, C.S., Jeon, S.J., Kwon, K.J., Han, S.-H., Lee, J., Cheong, J.H., Ryu, J.H., Kim, C.-H., Ko, K.H., Shin, C.Y., 2012. Prenatal exposure to valproic acid increases the neural progenitor cell pool and induces macrocephaly in rat brain via a mechanism involving the GSK-3β/β-catenin pathway. Neuropharmacology 63, 1028–1041. https://doi.org/10.1016/j.neuropharm.2012.07.028

Godavarthi, S.K., Sharma, A., Jana, N.R., 2014. Reversal of reduced parvalbumin neurons in hippocampus and amygdala of Angelman syndrome model mice by chronic

treatment of fluoxetine. J. Neurochem. 130(3), 444-454. https://doi.org/10.1111/jnc.12726

Gogolla, N., LeBlanc, J.J., Quast, K.B., Südhof, T.C., Fagiolini, M., Hensch, T.K., 2009. Common circuit defect of excitatory-inhibitory balance in mouse models of autism. J. Neurodev. Disord. 1(2),172-181. https://doi.org/10.1007/s11689-009-9023-x

Goldfarb, E. V., Chun, M.M., Phelps, E.A., 2016. Memory-Guided Attention: Independent Contributions of the Hippocampus and Striatum. Neuron. 89(2), 317-324. https://doi.org/10.1016/j.neuron.2015.12.014

Gonçalves, J.T., Schafer, S.T., Gage, F.H., 2016. Adult Neurogenesis in the Hippocampus: From Stem Cells to Behavior. Cell. 167(4), 897-914. https://doi.org/10.1016/j.cell.2016.10.021

Gottfried, C., Bambini-Junior, V., Francis, F., Riesgo, R., Savino, W., 2015. The impact of neuroimmune alterations in autism spectrum disorder. Front. Psychiatry 6, 121. https://doi.org/10.3389/fpsyt.2015.00121

Gul, H., Marquez-Curtis, L.A., Jahroudi, N., Lo, J., Turner, A.R., Janowska-Wieczorek, A., 2009. Valproic acid increases CXCR4 expression in hematopoietic stem/progenitor cells by chromatin remodeling. Stem Cells Dev. 18, 831–838. https://doi.org/10.1089/scd.2008.0235

Harte, M.K., Powell, S.B., Swerdlow, N.R., Geyer, M.A., Reynolds, G.P., 2007. Deficits in parvalbumin and calbindin immunoreactive cells in the hippocampus of isolation reared rats. J. Neural Transm. 114(7), 893-898. https://doi.org/10.1007/s00702-007-0627-6

Hashemi, E., Ariza, J., Rogers, H., Noctor, S.C., Martínez-Cerdeño, V., 2017. The Number of Parvalbumin-Expressing Interneurons Is Decreased in the Medial Prefrontal Cortex in Autism. Cereb. Cortex 27, 1931–1943. https://doi.org/10.1093/cercor/bhw021

Hirsch, M.M., Deckmann, I., Fontes-Dutra, M., Bauer-Negrini, G., Della-Flora Nunes, G., Nunes, W., Rabelo, B., Riesgo, R., Margis, R., Bambini-Junior, V., Gottfried, C., 2018. Behavioral alterations in autism model induced by valproic acid and translational analysis of circulating microRNA. Food Chem. Toxicol. 115, 336–343. https://doi.org/10.1016/j.fct.2018.02.061

Kelsom, C., Lu, W., 2013. Development and specification of GABAergic cortical interneurons. Cell Biosci. 3(1), 19. https://doi.org/10.1186/2045-3701-3-19

Kim, J.E., Lee, D.S., Park, H., Kang, T.C., 2020. SRC/CK2/PTEN-mediated glun2b and creb dephosphorylations regulate the responsiveness to AMPA receptor antagonists in chronic epilepsy rats. Int. J. Mol. Sci. 21, 1–23. https://doi.org/10.3390/ijms21249633

Köbe, T., Witte, A.V., Schnelle, A., Tesky, V.A., Pantel, J., Schuchardt, J.P., Hahn, A., Bohlken, J., Grittner, U., Flöel, A., 2017. Impact of resveratrol on glucose control, hippocampal structure and connectivity, and memory performance in patients with mild cognitive impairment. Front. Neurosci. 11, 105. https://doi.org/10.3389/fnins.2017.00105

Kohus, Z., Káli, S., Rovira-Esteban, L., Schlingloff, D., Papp, O., Freund, T.F., Hájos, N., Gulyás, A.I., 2016. Properties and dynamics of inhibitory synaptic communication within the CA3 microcircuits of pyramidal cells and interneurons expressing parvalbumin or cholecystokinin. J. Physiol. 594(13), 3745-3774 https://doi.org/10.1113/JP272231

LaSarge, C.L., Pun, R.Y.K., Gu, Z., Santos, V.R., Danzer, S.C., 2019. Impact of mTOR hyperactive neurons on the morphology and physiology of adjacent neurons: Do PTEN KO cells make bad neighbors? Exp. Neurol. 321, 113029. https://doi.org/10.1016/j.expneurol.2019.113029

Lawrence, Y.A., Kemper, T.L., Bauman, M.L., Blatt, G.J., 2010. Parvalbumin-, calbindin-, and calretinin-immunoreactive hippocampal interneuron density in autism. Acta Neurol. Scand. 121(2), 99-108. https://doi.org/10.1111/j.1600-0404.2009.01234.x

Liu, S., Jia, J., Zhou, H., Zhang, C., Liu, L., Liu, J., Lu, L., Li, X., Kang, Y., Lou, Y., Cai, Z., Ren, Y., Kong, X., Feng, S., 2019. PTEN modulates neurites outgrowth and neuron apoptosis involving the PI3K/Akt/mTOR signaling pathway. Mol. Med. Rep. 20, 4059–4066. https://doi.org/10.3892/mmr.2019.10670

LOWRY, O.H., ROSEBROUGH, N.J., FARR, A.L., RANDALL, R.J., 1951. Protein measurement with the Folin phenol reagent. J. Biol. Chem. 193, 265–75.

Lugo, J.N., Smith, G.D., Arbuckle, E.P., White, J., Holley, A.J., Floruta, C.M., Ahmed, N., Gomez, M.C., Okonkwo, O., 2014. Deletion of PTEN produces autism-like behavioral

deficits and alterations in synaptic proteins. Front. Mol. Neurosci. 7, 27. https://doi.org/10.3389/fnmol.2014.00027

Luhmann, H.J., Fukuda, A., Kilb, W., 2015. Control of cortical neuronal migration by glutamate and GABA. Front. Cell. Neurosci. 9, 4. https://doi.org/10.3389/fncel.2015.00004

Maccaferri, G., Lacaille, J.C., 2003. Interneuron Diversity series: Hippocampal interneuron classifications - Making things as simple as possible, not simpler. Trends Neurosci. 26(10), 564-571. https://doi.org/10.1016/j.tins.2003.08.002

Maenner, M.J., Shaw, K.A., Baio, J., Washington, A., Patrick, M., DiRienzo, M., Christensen, D.L., Wiggins, L.D., Pettygrove, S., Andrews, J.G., Lopez, M., Hudson, A., Baroud, T., Schwenk, Y., White, T., Rosenberg, C.R., Lee, L.C., Harrington, R.A., Huston, M., Hewitt, A., Esler, A., Hall-Lande, J., Poynter, J.N., Hallas-Muchow, L., Constantino, J.N., Fitzgerald, R.T., Zahorodny, W., Shenouda, J., Daniels, J.L., Warren, Z., Vehorn, A., Salinas, A., Durkin, M.S., Dietz, P.M., 2020. Prevalence of autism spectrum disorder among children aged 8 Years-Autism and developmental disabilities monitoring network, 11 Sites, United States, 2016. MMWR Surveill. Summ. 63(2), 1-21. https://doi.org/10.15585/MMWR.SS6904A1

Maglóczky, Z.S., Wittner, L., Borhegyi, Z.S., Halász, P., Vajda, J., Czirják, S., Freund, T.F., 2000. Changes in the distribution and connectivity of interneurons in the epileptic human dentate gyrus. Neuroscience 96(1), 7-25. https://doi.org/10.1016/S0306-4522(99)00474-1

Manent, J.B., Jorquera, I., Ben-Ari, Y., Aniksztejn, L., Represa, A., 2006. Glutamate acting on AMPA but not NMDA receptors modulates the migration of hippocampal interneurons. J. Neurosci. 26(22), 5901-5909. https://doi.org/10.1523/JNEUROSCI.1033-06.2006

Marín, O., Rubenstein, J.L.R., 2003. Cell migration in the forebrain. Annu. Rev. Neurosci. 26, 441–83. https://doi.org/10.1146/annurev.neuro.26.041002.131058

Meyer, U., Nyffeler, M., Yee, B.K., Knuesel, I., Feldon, J., 2008. Adult brain and behavioral pathological markers of prenatal immune challenge during early/middle and late fetal development in mice. Brain. Behav. Immun. 22, 469–486. https://doi.org/10.1016/j.bbi.2007.09.012

Murray, A.J., Sauer, J.F., Riedel, G., McClure, C., Ansel, L., Cheyne, L., Bartos, M., Wisden, W., Wulff, P., 2011. Parvalbumin-positive CA1 interneurons are required for spatial working but not for reference memory. Nat. Neurosci. 14(3), 297-299. https://doi.org/10.1038/nn.2751

Nelson, S.B., Valakh, V., 2015. Excitatory/Inhibitory Balance and Circuit Homeostasis in Autism Spectrum Disorders. Neuron. 87(4), 684-698. https://doi.org/10.1016/j.neuron.2015.07.033

Nicolini, C., Ahn, Y., Michalski, B., Rho, J.M., Fahnestock, M., 2015. Decreased mTOR signaling pathway in human idiopathic autism and in rats exposed to valproic acid. Acta Neuropathol. Commun. 3, 3. https://doi.org/10.1186/s40478-015-0184-4

Ognjanovski, N., Schaeffer, S., Wu, J., Mofakham, S., Maruyama, D., Zochowski, M., Aton, S.J., 2017. Parvalbumin-expressing interneurons coordinate hippocampal network dynamics required for memory consolidation. Nat. Commun. 8, 15039. https://doi.org/10.1038/ncomms15039

Olloquequi, J., Cornejo-Córdova, E., Verdaguer, E., Soriano, F.X., Binvignat, O., Auladell, C., Camins, A., 2018. Excitotoxicity in the pathogenesis of neurological and psychiatric disorders: Therapeutic implications. J. Psychopharmacol. 32(3), 265-275. https://doi.org/10.1177/0269881118754680

Pauli, E., Hildebrandt, M., Romstöck, J., Stefan, H., Blümcke, I., 2006. Deficient memory acquisition in temporal lobe epilepsy is predicted by hippocampal granule cell loss. Neurology 67(8), 1383-1389. https://doi.org/10.1212/01.wnl.0000239828.36651.73

Pelkey, K.A., Chittajallu, R., Craig, M.T., Tricoire, L., Wester, J.C., McBain, C.J., 2017. Hippocampal gabaergic inhibitory interneurons. Physiol. Rev. 97(4), 1619-1747 https://doi.org/10.1152/physrev.00007.2017

Plitman, E., Nakajima, S., de la Fuente-Sandoval, C., Gerretsen, P., Chakravarty, M.M., Kobylianskii, J., Chung, J.K., Caravaggio, F., Iwata, Y., Remington, G., Graff-Guerrero, A., 2014. Glutamate-mediated excitotoxicity in schizophrenia: A review. Eur. Neuropsychopharmacol. 24(10), 1591-1605. https://doi.org/10.1016/j.euroneuro.2014.07.015

Qin, X., Zaki, M.G., Chen, Z., Jakova, E., Ming, Z., Cayabyab, F.S., 2021. Adenosine

Signaling and Clathrin-Mediated Endocytosis of Glutamate AMPA Receptors in Delayed Hypoxic Injury in Rat Hippocampus: Role of Casein Kinase 2. Mol. Neurobiol. 58, 1932–1951. https://doi.org/10.1007/s12035-020-02246-0

Rubin, R.D., Watson, P.D., Duff, M.C., Cohen, N.J., 2014. The role of the hippocampus in flexible cognition and social behavior. Front. Hum. Neurosci. 8, 742. https://doi.org/10.3389/fnhum.2014.00742

Santos, V.R., Pun, R.Y.K., Arafa, S.R., LaSarge, C.L., Rowley, S., Khademi, S., Bouley, T., Holland, K.D., Garcia-Cairasco, N., Danzer, S.C., 2017. PTEN deletion increases hippocampal granule cell excitability in male and female mice. Neurobiol. Dis. 108, 339–351. https://doi.org/10.1016/j.nbd.2017.08.014

Sohal, V.S., Rubenstein, J.L.R., 2019. Excitation-inhibition balance as a framework for investigating mechanisms in neuropsychiatric disorders. Mol. Psychiatry 24, 1248. https://doi.org/10.1038/S41380-019-0426-0

Shin, S., Santi, A., Huang, S., 2021. Conditional Pten knockout in parvalbumin- or somatostatin-positive neurons sufficiently leads to autism-related behavioral phenotypes. Mol. Brain. 14, 24. https://doi.org/10.1186/s13041-021-00731-8

Sik, A., Tamamaki, N., Freund, T.F., 1993. Complete Axon Arborization of a Single CA3 Pyramidal Cell in the Rat Hippocampus, and its Relationship With Postsynaptic Parvalbumin-containing Interneurons. Eur. J. Neurosci. 5(12), 1719-1728. https://doi.org/10.1111/j.1460-9568.1993.tb00239.x

Skelton, P.D., Frazel, P.W., Lee, D., Suh, H., Luikart, B.W., 2019. Pten loss results in inappropriate excitatory connectivity. Mol. Psychiatry 24, 1627–1640. https://doi.org/10.1038/s41380-019-0412-6

Smith, A.L., Jung, E.M., Jeon, B.T., Kim, W.Y., 2020. Arid1b haploinsufficiency in parvalbumin- or somatostatin-expressing interneurons leads to distinct ASD-like and ID-like behavior. Sci. Rep. 10, 7834. https://doi.org/10.1038/s41598-020-64066-5

Sohal, V.S., Rubenstein, J.L.R., 2019. Excitation-inhibition balance as a framework for investigating mechanisms in neuropsychiatric disorders. Mol. Psychiatry 24, 1248. https://doi.org/10.1038/S41380-019-0426-0

Sullivan, D., Csicsvari, J., Mizuseki, K., Montgomery, S., Diba, K., Buzsáki, G., 2011.

Relationships between hippocampal sharp waves, ripples, and fast gamma oscillation: Influence of dentate and entorhinal cortical activity. J. Neurosci. 31(23), 8605-8616 https://doi.org/10.1523/JNEUROSCI.0294-11.2011

Tai, C., Abe, Y., Westenbroek, R.E., Scheuer, T., Catterall, W.A., 2014. Impaired excitability of somatostatin- and parvalbumin-expressing cortical interneurons in a mouse model of Dravet syndrome. Proc. Natl. Acad. Sci. 111, E3139–E3148. https://doi.org/10.1073/pnas.1411131111

Tai, C., Abe, Y., Westenbroek, R.E., Scheuer, T., Catterall, W.A., 2014. Impaired excitability of somatostatin- and parvalbumin-expressing cortical interneurons in a mouse model of Dravet syndrome. Proc. Natl. Acad. Sci. U. S. A. 111(30), E3139-E3148 https://doi.org/10.1073/pnas.1411131111

Tallent, M.K., 2007. Somatostatin in the dentate gyrus. 163, 265-284. Prog. Brain Res. https://doi.org/10.1016/S0079-6123(07)63016-7

Tavitian, A., Song, W., Schipper, H.M., 2019. Dentate Gyrus Immaturity in Schizophrenia. Neuroscientist. 25(6), 528-547. https://doi.org/10.1177/1073858418824072

Thom, M., 2014. Review: Hippocampal sclerosis in epilepsy: A neuropathology review. Neuropathol. Appl. Neurobiol. 40(5), 520-543. https://doi.org/10.1111/nan.12150

Vogt, D., Cho, K.K.A., Lee, A.T., Sohal, V.S., Rubenstein, J.L.R., 2015. The Parvalbumin/Somatostatin Ratio Is Increased in Pten Mutant Mice and by Human PTEN ASD Alleles. Cell Rep. 11, 944–956. https://doi.org/10.1016/j.celrep.2015.04.019

Wang, S.J., Zhao, X.H., Chen, W., Bo, N., Wang, X.J., Chi, Z.F., Wu, W., 2015. Sirtuin 1 activation enhances the PGC-1á/mitochondrial antioxidant system pathway in status epilepticus. Mol. Med. Rep. 11, 521–526. https://doi.org/10.3892/mmr.2014.2724

Wei, Y., Han, X., Zhao, C., 2020. PDK1 regulates the survival of the developing cortical interneurons. Mol. Brain. 13, 65. https://doi.org/10.1186/s13041-020-00604-6

Wöhr, M., Orduz, D., Gregory, P., Moreno, H., Khan, U., Vörckel, K.J., Wolfer, D.P., Welzl, H., Gall, D., Schiffmann, S.N., Schwaller, B., 2015. Lack of parvalbumin in mice leads to behavioral deficits relevant to all human autism core symptoms and related neural morphofunctional abnormalities. Transl. Psychiatry. 5, e525. https://doi.org/10.1038/tp.2015.19

Wu, H.-F., Chen, P.S., Chen, Y.-J., Lee, C.-W., Chen, I.-T., Lin, H.-C., 2017. Alleviation of N-Methyl-d-Aspartate Receptor-Dependent Long-Term Depression via Regulation of the Glycogen Synthase Kinase-3β Pathway in the Amygdala of a Valproic Acid-Induced Animal Model of Autism. Mol. Neurobiol. 54, 5264–5276. https://doi.org/10.1007/s12035-016-0074-1

Xing, X., Zhang, J., Wu, K., Cao, B., Li, X., Jiang, F., Hu, Z., Xia, K., Li, J. Da, 2019. Suppression of Akt-mTOR pathway rescued the social behavior in Cntnap2-deficient mice. Sci. Rep. 9, 3041. https://doi.org/10.1038/s41598-019-39434-5

Yuan, M., Meyer, T., Benkowitz, C., Savanthrapadian, S., Ansel-Bollepalli, L., Foggetti, A., Wulff, P., Alcami, P., Elgueta, C., Bartos, M., 2017. Somatostatin-positive interneurons in the dentate gyrus of mice provide local- and long-range septal synaptic inhibition. Elife. 6, e21105. https://doi.org/10.7554/elife.21105

List of Figures

Figure 1: Prenatal exposure to VPA induced morphological changes in the hippocampus (HC) of P120 animals. A) Illustrative images of HC and subregions. B) Representative images of immunofluorescence of the total HC labelling NeuN (red). C) Representative images of DG, arrows point to the main region where VPA induced neuronal loss (demonstrated with dashed lines in the other groups). D) Representative images of CA1, the arrow points to the loss of compaction observed in the VPA group (the width lines highlight the difference observed in the VPA group). Coordinates: bregma: -2.92 mm, interaural: 6.08 mm, - bregma: -3.24 mm, interaural: 5.76 mm. Scale bar B: 250 µm, Scale Bar C, D: 50 µm. C(Control)=4, R(RSV)=4, V(VPA)=4, R+V(RSV+VPA)=3.

Figure 2: Prenatal exposure to VPA decreased the number of total neurons per area in the dentate gyrus of P120 animals. Values presented as Mean ± SD. Statistical analysis: two-way ANOVA followed by Bonferroni post-test. CON=4, RSV=4, VPA=4, RSV+VPA=3. Symbols indicate significant differences in the post test, when the interaction was significative (#: VPA-CON; *: VPA-RSV, and $: RSV+VPA-VPA $p<0.05$). Complete statistics were summarized in Supplementary Table 1. Factors were applied to avoid decimal numbers in the Y axis.

Figure 3: Representative images of immunofluorescence in the dentate gyrus. A) Cb, calbindin (green); NeuN (red); DAPI (blue), B) Pv, parvalbumin (green); NeuN (red); DAPI

(blue), C) Som, somatostatin (red); NeuN (green); DAPI (blue). A representative interneuron was highlighted in a box in the top corner (scale bar: 10 µm). CON=4, RSV=4, VPA=4, RSV+VPA=3. Scale bar: 50 µm. Arrowheads indicate the respective interneurons. RSV prevented CB^+ reduction induced by VPA in number (A1), no differences were found for ratio (A2). No differences among groups were observed for PV^+ number (B1) and ratio (B2). VPA increased the SOM^+ number (C1) and the preventive effect of RSV was observed in SOM^+ ratio (C2). Symbols indicate significant differences in the post test, when interaction was significative (#: VPA-CON; *: VPA-RSV, and $: RSV+VPA-VPA $p<0.05$). When significant differences appeared only in separated factors, the difference was represented by lines indicating $p<0.05$. Statistical analysis: two-way ANOVA followed by Bonferroni post-test. Data demonstrated as mean ± SD. Complete statistics were summarized in Supplementary Tables 2, 3, and 4. The high density of cellular nuclei (stained blue) and neuronal bodies (especially in the assays where NeuN is marked with red) in some regions result in a violet/purple color. C: Control; R: RSV; V: VPA; R+V: RSV+VPA. Factors were applied to avoid decimal numbers in the Y axis.

Figure 4: Representative images of immunofluorescence in CA1. A) Cb, calbindin (green); NeuN (red); DAPI (blue). B) Pv, parvalbumin (green); NeuN (red); DAPI (blue), C) Som, somatostatin (red); NeuN (green); DAPI (blue). A representative interneuron was highlighted in a box in the top corner (scale bar: 10 µm). CON=4, RSV=4, VPA=4, RSV+VPA=3. Scale bar: 50 µm. Arrowheads indicate the respective interneurons. RSV prevented the reduction in CB^+ number (A1) and ratio (A2) induced by VPA. VPA induced reduction in PV^+ number, not prevented by RSV (B1) and no differences were found for PV^+ ratio (B2). VPA and RSV induced reduction in SOM^+ number (C1) and no differences were found for ratio (C2). Symbols indicate significant differences in the post test, when interaction was significative (#: VPA-CON; *: VPA-RSV, and $: RSV+VPA-VPA $p<0.05$). When significant differences appeared only in separated factors, the difference was represented by lines indicating $p<0.05$. Statistical analysis: two-way ANOVA followed by Bonferroni post-test. Data demonstrated as mean ± SD. Complete statistics were summarized in Supplementary Tables 2, 3, and 4. The high density of cellular nuclei (stained blue) and neuronal bodies (especially in the assays where NeuN is marked with red) in some regions result in a violet/purple color. C: Control; R: RSV; V: VPA; R+V: RSV+VPA. Factors were applied to avoid decimal numbers in the Y axis.

Figure 5: Representative images of immunofluorescence in CA2. A) Cb, calbindin (green); NeuN (red); DAPI (blue). B) Pv, parvalbumin (green); NeuN (red); DAPI (blue), C)

Som, somatostatin (red); NeuN (green); DAPI (blue). A representative interneuron was highlighted in a box in the top corner (scale bar: 10 μm). CON=4, RSV=4, VPA=4, RSV+VPA=3. Scale bar: 50 μm. Arrowheads indicate the respective interneurons. No differences were found in CB^+ number (A1) and ratio (A2). No differences were found in PV^+ number (B1) ratio (B2). VPA induced reduction in SOM^+ number (C1) and RSV prevented reduction in SOM^+ ratio induced by VPA (C2). Symbols indicate significant differences in the post test, when interaction was significative (#: VPA-CON; *: VPA-RSV, and $: RSV+VPA-VPA $p<0.05$). When significant differences appeared only in separated factors, the difference was represented by lines indicating $p<0.05$. Statistical analysis: two-way ANOVA followed by Bonferroni post-test. Data demonstrated as mean ± SD. Complete statistics were summarized in Supplementary Tables 2, 3, and 4. The high density of cellular nuclei (stained blue) and neuronal bodies (especially in the assays where NeuN is marked with red) in some regions result in a violet/purple color. C: Control; R: RSV; V: VPA; R+V: RSV+VPA. Factors were applied to avoid decimal numbers in the Y axis.

Figure 6: Representative images of immunofluorescence in CA3. A) Cb, calbindin (green); NeuN (red); DAPI (blue). B) Pv, parvalbumin (green); NeuN (red); DAPI (blue), C) Som, somatostatin (red); NeuN (green); DAPI (blue). A representative interneuron was highlighted in a box in the top corner (scale bar: 10 μm). CON=4, RSV=4, VPA=4, RSV+VPA=3. Scale bar: 50 μm. Arrowheads indicate the respective interneurons. No differences were found in CB^+ number (A1) and ratio (A2). VPA induced reduction in PV^+ number (B1) and ratio (B2), without RSV prevention. No differences were found in SOM^+ number (C1) and ratio (C2). Symbols indicate significant differences in the post test, when interaction was significative (#: VPA-CON; *: VPA-RSV, and $: RSV+VPA-VPA $p<0.05$). When significant differences appeared only in separated factors, the difference was represented by lines indicating $p<0.05$. Statistical analysis: two-way ANOVA followed by Bonferroni post-test. Data demonstrated as mean ± SD. Complete statistics were summarized in Supplementary Tables 2, 3, and 4. The high density of cellular nuclei (stained blue) and neuronal bodies (especially in the assays where NeuN is marked with red) in some regions result in a violet/purple color. C: Control; R: RSV; V: VPA; R+V: RSV+VPA. Factors were applied to avoid decimal numbers in the Y axis.

Figure 7. Prenatal exposure to VPA induced changes in the immunocontent of Akt, PTEN, and CK2 in the hippocampus of adult animals. Prenatal exposure to VPA decreased the immunocontent of A) PTEN, B) Akt and increased C) CK2, without altering the content of D) GSK3β. No differences were found for phosphorylation levels

(Supplementary Table 5). When significant differences appeared only in separated factors, the difference was represented by lines indicating $p<0.05$. Values presented as Mean ± SD. Statistical analysis: two-way ANOVA followed by Bonferroni post-test. CON=6, RSV=6, VPA=6, RSV+VPA=6. *$p<0.05$. The immunocontent of PTEN (54 kDa), AKT (60 kDa), CK2 (42 kDa) and GSK3β (46 kDa) was normalized by the β-actin (42 kDa) loading control.

Figure 1

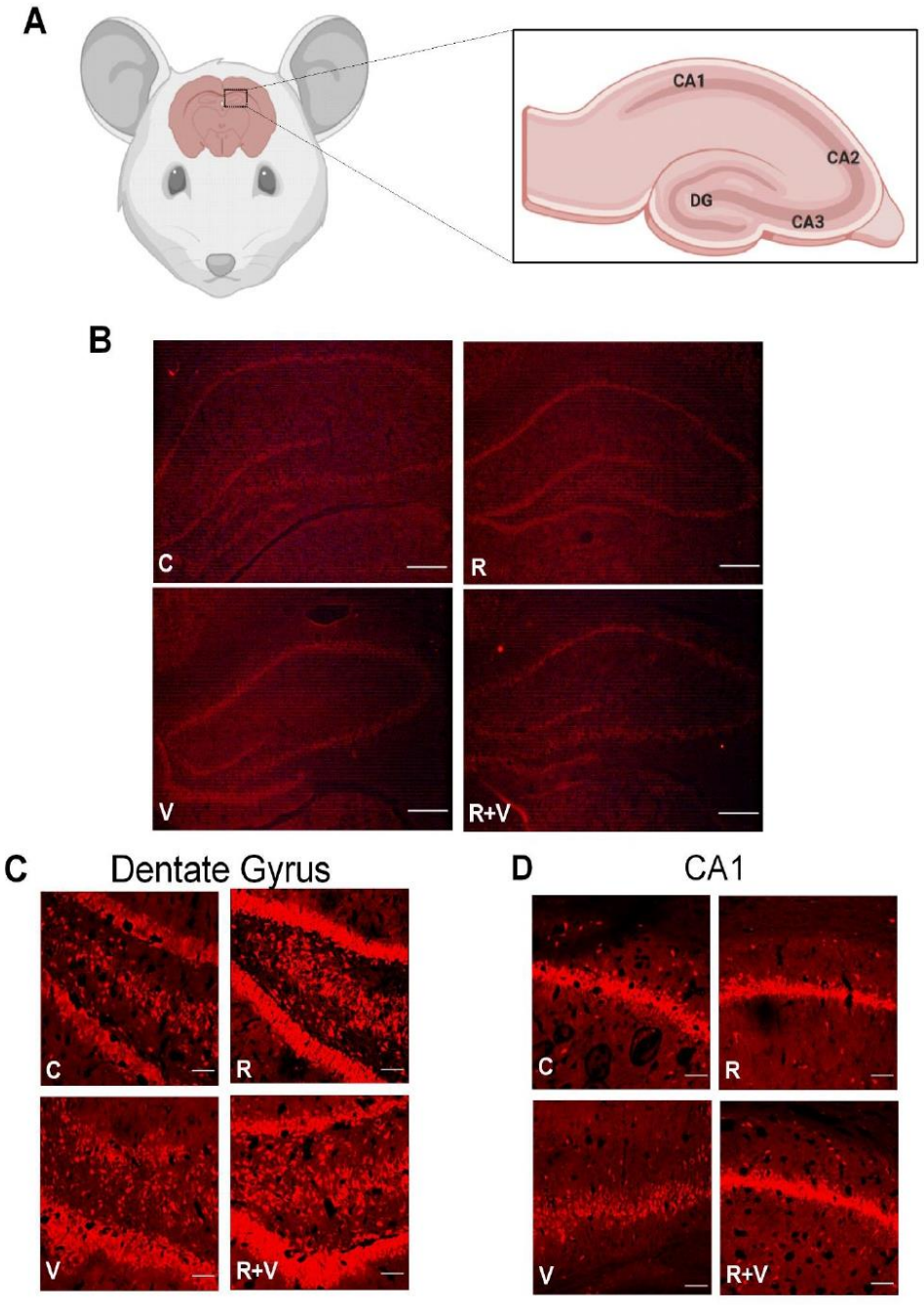

Figure 2

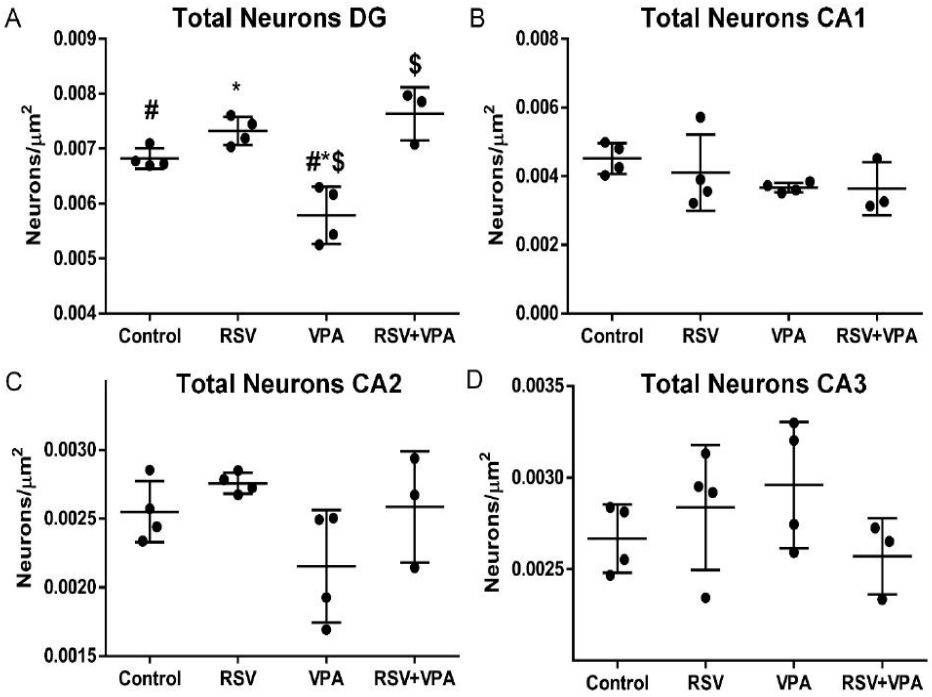
A
Total Neurons DG
Neurons/µm²
0.009
0.008
0.007
0.006
0.005
0.004
#
*
#*$
$
Control
RSV
VPA
RSV+VPA
B
Total Neurons CA1
Neurons/µm²
0.008
0.006
0.004
0.002
0.000
Control
RSV
VPA
RSV+VPA
C
Total Neurons CA2
Neurons/µm²
0.0030
0.0025
0.0020
0.0015
Control
RSV
VPA
RSV+VPA
D
Total Neurons CA3
Neurons/µm²
0.0035
0.0030
0.0025
Control
RSV
VPA
RSV+VPA

Figure 3

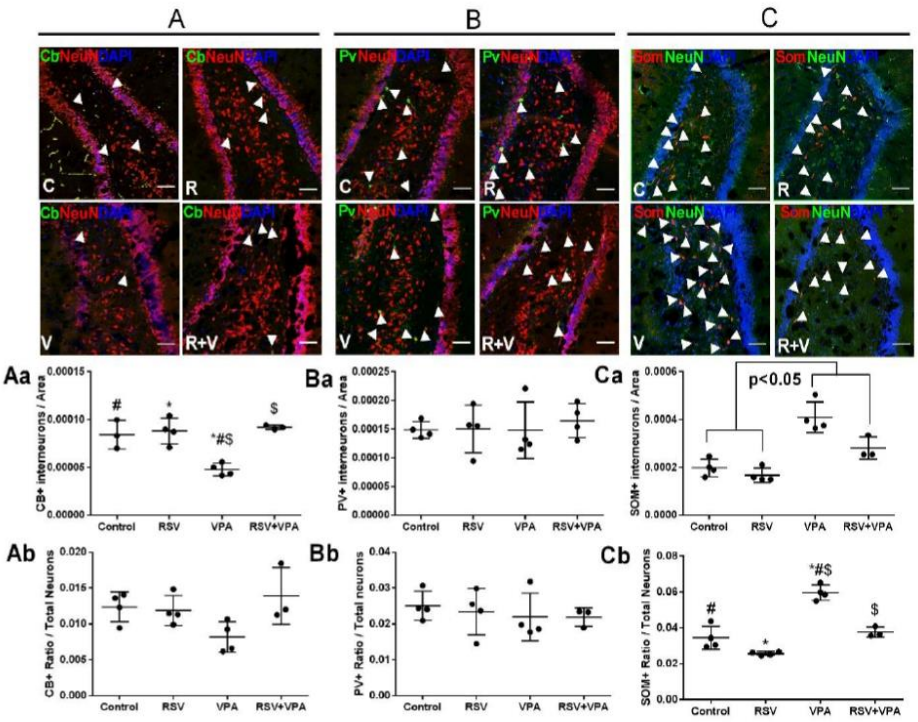
A
B
C
CbNeuNDAPI
PvNeuNDAPI
SomNeuNDAPI
C
R
V
R+V
Aa
Ba
Ca
CB+ interneurons / Area
PV+ interneurons / Area
SOM+ interneurons / Area
p<0.05
Ab
Bb
Cb
CB+ Ratio / Total Neurons
PV+ Ratio / Total neurons
SOM+ Ratio / Total Neurons
Control
RSV
VPA
RSV+VPA

Figure 4

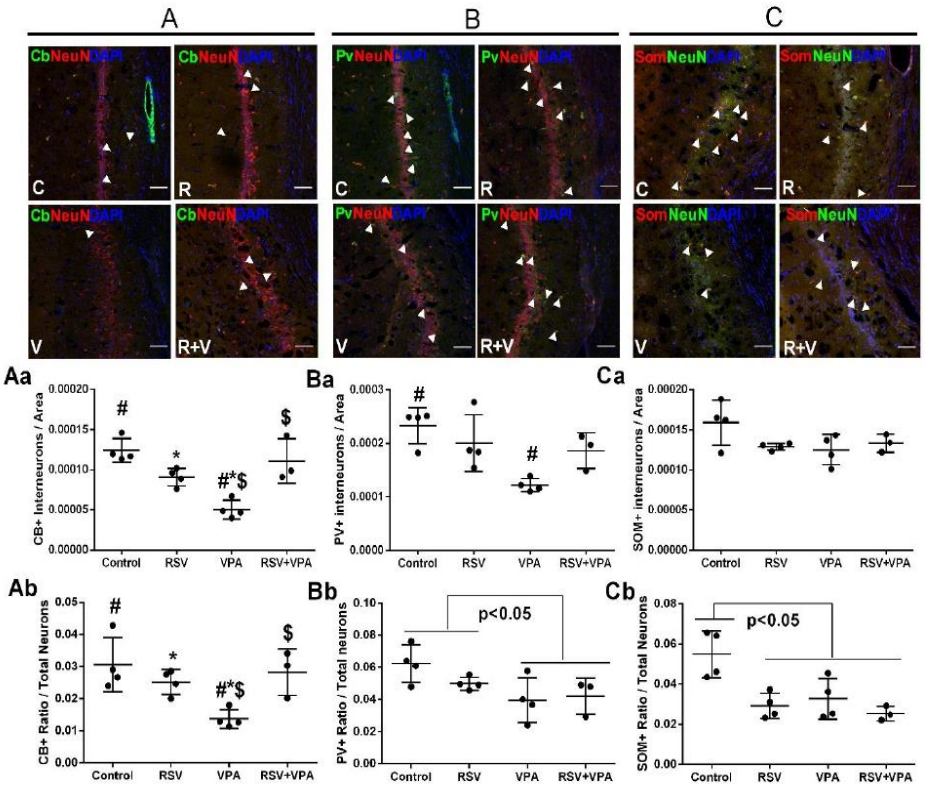
A
B
C
CbNeuNDAPI
PvNeuNDAPI
SomNeuNDAPI
C
R
V
R+V
Aa
Ba
Ca
CB+ interneurons / Area
PV+ interneurons / Area
SOM+ interneurons / Area
Ab
Bb
Cb
CB+ Ratio / Total Neurons
PV+ Ratio / Total neurons
SOM+ Ratio / Total Neurons
p<0.05
Control
RSV
VPA
RSV+VPA

Figure 5

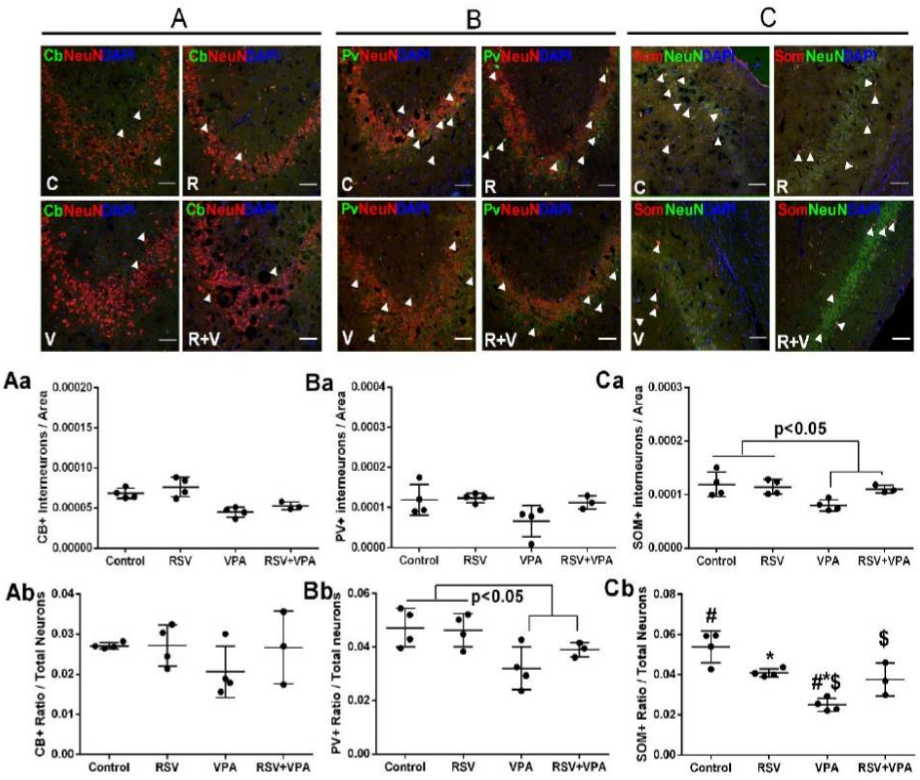
A
B
C
CbNeuNDAPI
PvNeuNDAPI
SomNeuNDAPI
C
R
V
R+V
Aa
Ba
Ca
CB+ interneurons / Area
PV+ interneurons / Area
SOM+ interneurons / Area
p<0.05
Control
RSV
VPA
RSV+VPA
Ab
Bb
Cb
CB+ Ratio / Total Neurons
PV+ Ratio / Total neurons
SOM+ Ratio / Total Neurons
#
*
#*$
$

Figure 6

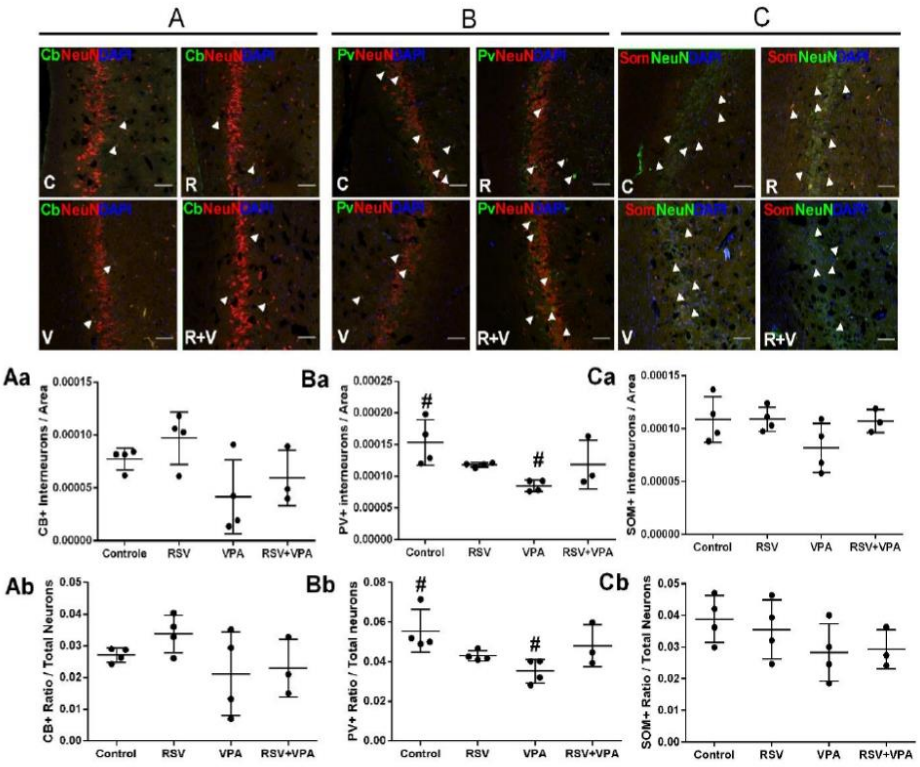
A
B
C
Cb NeuN DAPI
Pv NeuN DAPI
Som NeuN DAPI
C
R
V
R+V
Aa
Ba
Ca
Ab
Bb
Cb
CB+ Interneurons / Area
PV+ interneurons / Area
SOM+ interneurons / Area
CB+ Ratio / Total Neurons
PV+ Ratio / Total neurons
SOM+ Ratio / Total Neurons
Controle
Control
RSV
VPA
RSV+VPA
#

Figure 7

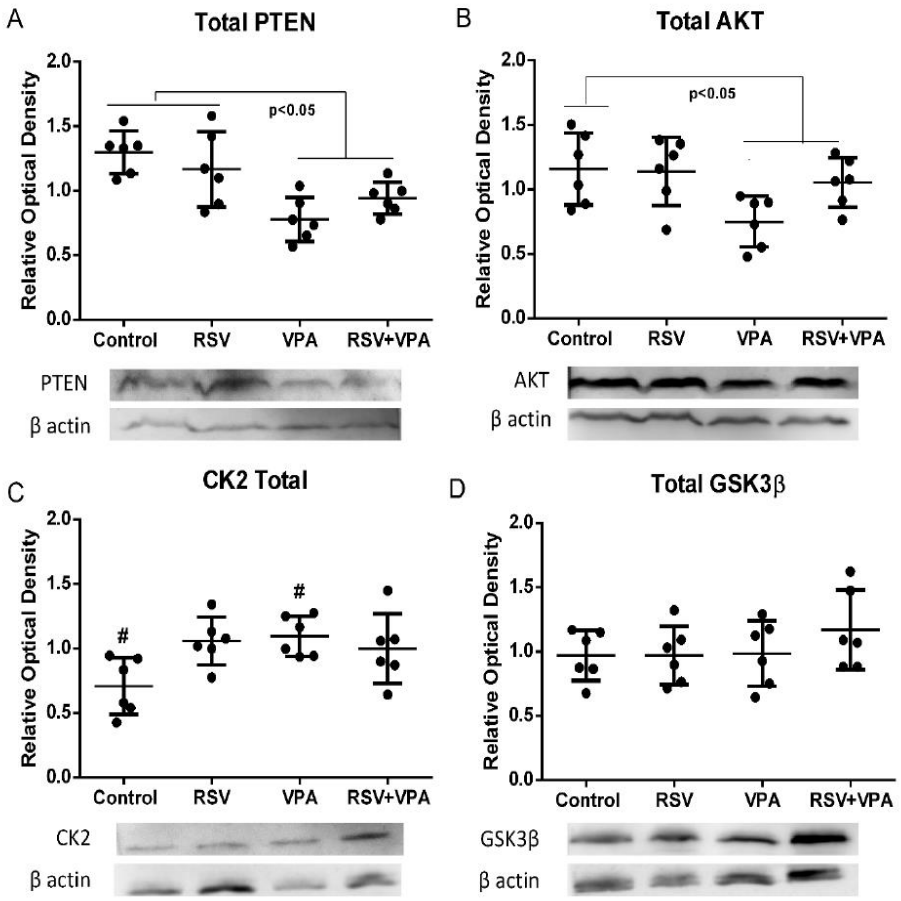
A
Total PTEN
Relative Optical Density
2.0
1.5
1.0
0.5
0.0
p<0.05
Control
RSV
VPA
RSV+VPA
PTEN
β actin
B
Total AKT
Relative Optical Density
p<0.05
Control
RSV
VPA
RSV+VPA
AKT
β actin
C
CK2 Total
Relative Optical Density
#
#
Control
RSV
VPA
RSV+VPA
CK2
β actin
D
Total GSK3β
Relative Optical Density
Control
RSV
VPA
RSV+VPA
GSK3β
β actin

Graphical Abstract

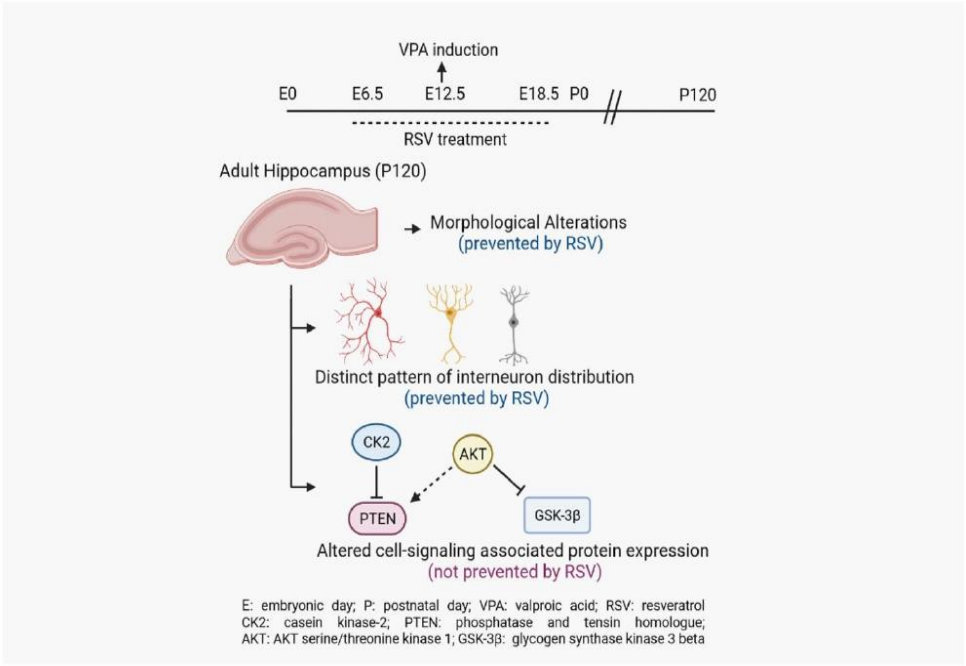

Supplementary Table 1: Immunofluorescence reagents information

Reagent	Supplier	Code	Dilution/Volume
Anti-NeuN (Mouse)	Merck	MAB3771	1:500
Anti-NeuN	Abcam	Ab177487	1:500
Anti-Parvalbumin	Abcam	Ab64555	1:500
Anti-Calbindin	Abcam	Ab82812	1:500
Anti-Somatostatin	Sigma-Aldrich	SAB4502861	1:500
Alexa Fluor 488 Goat Anti-Mouse IgG (H+L)	Molecular Probes	Ab11029	1:2000
Alexa Fluor 594 Goat Anti-Rabbit IgG (H+L)	Molecular Probes	Ab150080	1:2000*
DAPI Nucleic Acid Stain	Invitrogen	MP01306	30 uL per slice
Mounting Medium Fluorshield	Sigma-Aldrich	F6182-20ML	30 uL per slice

* In SOM^+ assay, the concentration was 1:1000

Supplementary Table 2: Western blotting antibodies information

Reagent	Medium	Dilution	Supplier	Time
		Primary Antibodies		
Anti-CK2	5% BSA-TTBS 0,05% buffer	1:1000	CST #2656	Overnight at 4ºC
Anti-PTEN	5% BSA-TTBS 0,05% buffer	1:1000	CST #9559	Overnight at 4ºC
Anti-PTEN (Ser380, Thr382/383)	5% BSA-TTBS 0,05% buffer	1:1000	CST #9549	Overnight at 4ºC
Anti-GSK-3β	5% BSA-TTBS 0,05% buffer	1:1000	CST #9315	Overnight at 4ºC
Anti-GSK-3β (Ser9)	5% BSA-TTBS 0,05% buffer	1:1000	CST #9336	Overnight at 4ºC
Anti-AKT	5% BSA-TTBS 0,05% buffer	1:1000	CST #4691	Overnight at 4ºC
Anti-AKT (Ser473)	5% BSA-TTBS 0,05% buffer	1:1000	CST #9271	Overnight at 4ºC
Anti-AKT (Thr380)	5% BSA-TTBS 0,05% buffer	1:1000	CST #9275	Overnight at 4ºC
β-actin	5% BSA-TTBS 0,05% buffer	1:1000	CST #4967	Overnight at 4ºC
		Secondary Antibody		
Goat anti-rabbit IgG-HRP	5% BSA-TTBS 0,05% buffer	1:2000	BioRad #1706515	Room temperature for 1h

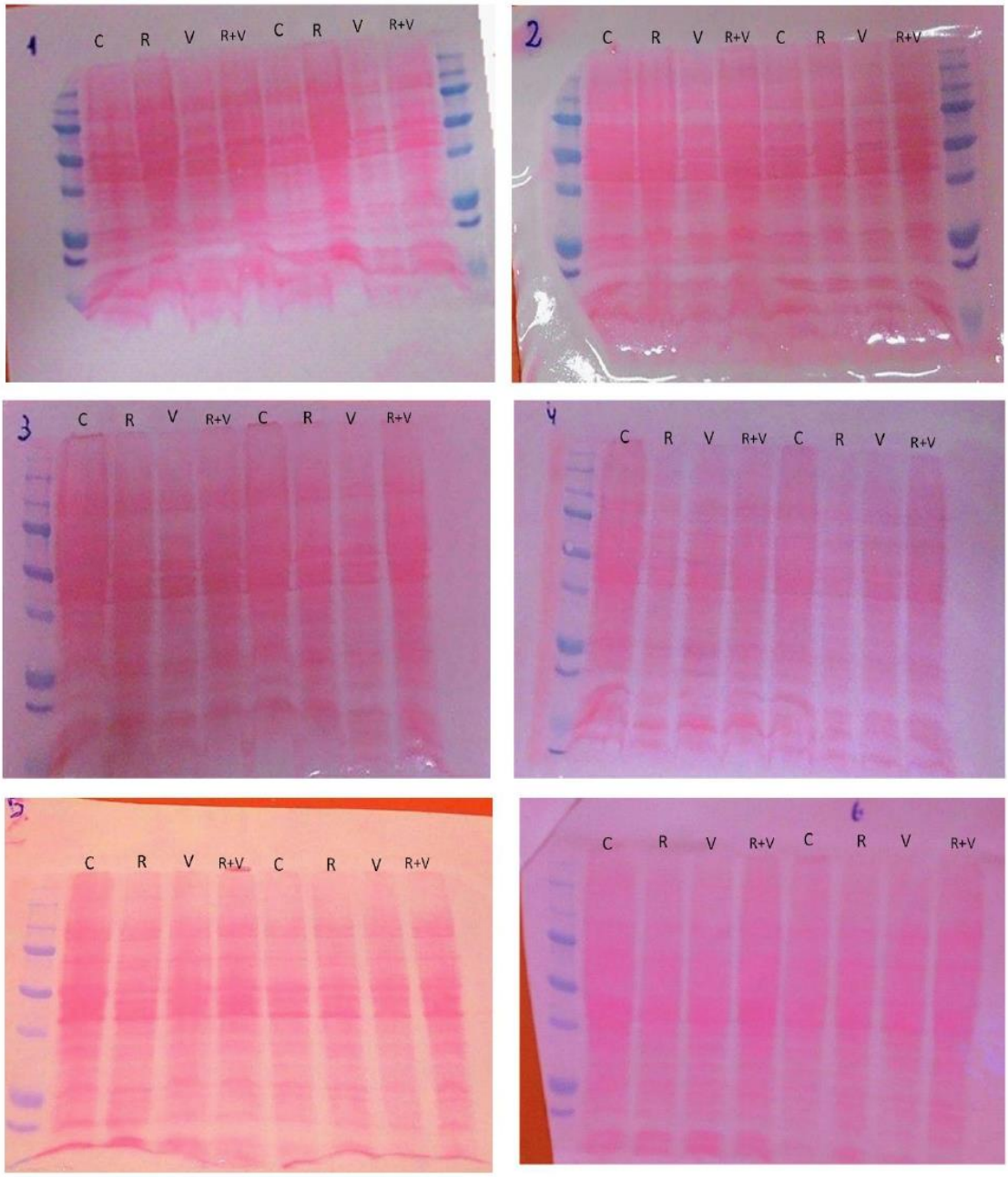

Supplementary Figure 1: ponceau staining of the nitrocellulose membranes. The groups are described as C for control group, R for RSV group, V for VPA group and R+V for RSV+VPA group.

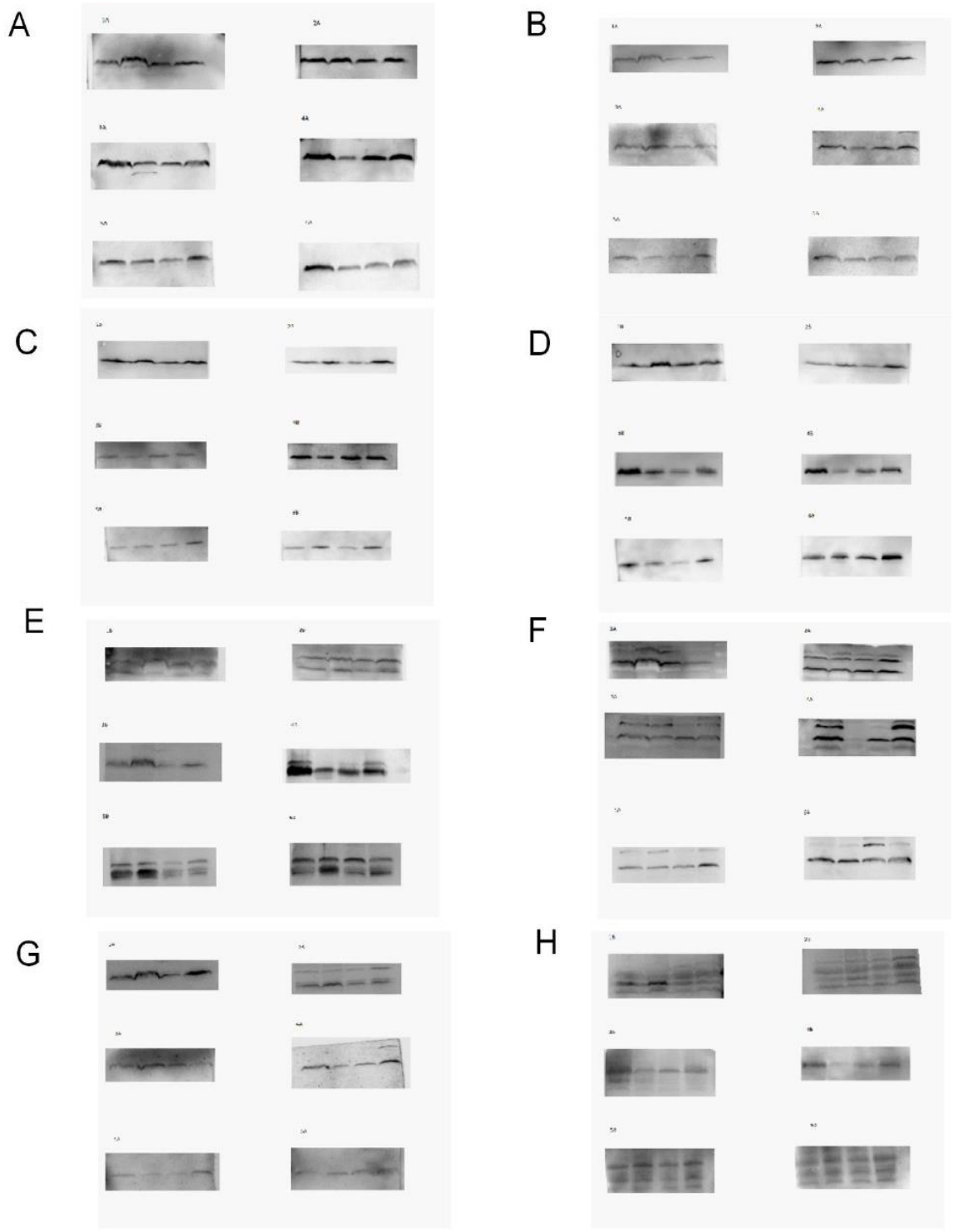

Supplementary Figure 2: nitrocellulose membranes. A) AKT B) PTEN C) CK2 D) GSK3β E) AKT-p308 F) AKT-p473 G) p-PTEN and H) p-GSK3β.

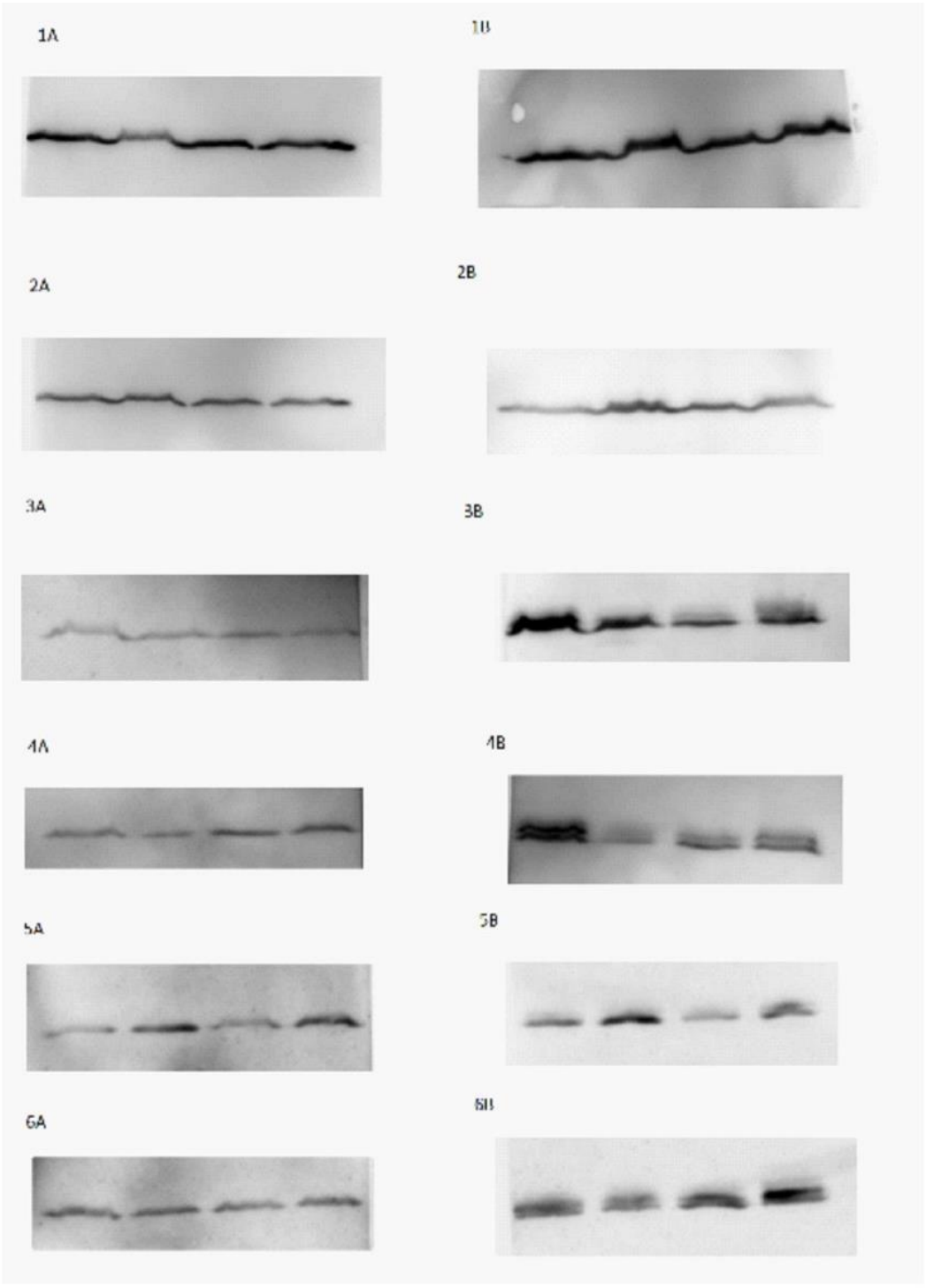

Supplementary Figure 3: nitrocellulose membranes - β-actin

Supplementary Table 3: General description of statistics parameters of total neurons in hippocampal subregions of adult animals. Symbols indicate significant differences in the post test (#: VPA-CON; *: VPA-RSV, and $: RSV+VPA-VPA $p<0.05$, while + indicate significant difference in a separated factor - well described in the respective graph). Values presented as Mean ± SD. CON=4, RSV=4, VPA=4, RSV+VPA=3. Statistical analysis: two-way ANOVA followed by Bonferroni post test. I: factors interaction; V: VPA; R: RSV.

Region	Parameter	Experimental Groups	F value	P value (post test)
Dentate Gyrus	Total Neurons/Area	Control:0.006821±0.0001871 # RSV: 0.007320±0.0002551* VPA:0.005788±0.0005202 *#$ RSV+VPA:0.007634±0.0004870 $	I: F (1, 11) = 11.59 P = 0.0059 V: F (1,11) = 4.981 P = 0.0962 R: F (1, 11) = 35.19 P < 0.0001	#=0.0163 (Cont-VPA) *=0.008 (RSV-VPA) $=0.002(RSV+VPA-VPA)
CA1	Total Neurons/Area	Control: 0.004515±0.0004509 RSV: 0.004101±0.001115 VPA:0.003668±0.0001407 RSV+VPA:0.003636±0.0007657	I: F (1, 11) = 0.2669 P = 0.6156 V: F (1, 11) = 3.140 P = 0.1041 R: F (1, 11) = 0.362 P = 0.5596	No differences
CA2	Total Neurons/Area	Control: 0.002551±0.0002237 RSV: 0.002758±7.605e-005 VPA: 0.002154±0.0004092 RSV+VPA: 0.002585± 0.0004047	I: F (1, 11) = 0.5146 P = 0.4881 V: F (1, 11) = 3.309 P = 0.0962 R: F (1, 11) = 4.148 P = 0.0665	No differences
CA3	Total Neurons/Area	Control: 0.002667±0.0001858 RSV: 0.002836±0.0003415 VPA: 0.002959±0.0003441 RSV+VPA: 0.00257±0.0002077	I: F (1, 11) = 3.530 P = 0.0870 V: F (1, 11) = 0.0081 P = 0.929 R: F (1, 11) = 0.5505 P = 0.4737	No differences

Supplementary Table 4: General description of statistics parameters of total protein and phosphorylated protein levels in the hippocampus of adult animals. Symbols indicate significant differences in the post test (#: VPA-CON; *: VPA-RSV, and $: RSV+VPA-VPA $p<0.05$, while + indicate significant difference in a separated factor - well described in the respective graph). Values presented as Mean ± SD. CON=6, RSV=6, VPA=6, RSV+VPA=6. Statistical analysis: two-way ANOVA followed by Bonferroni post test. I: factors interaction; V: VPA; R: RSV.

Protein	Experimental Groups	F value	p value (post test)
AKT	Control: 1.158 ± 0.2792 RSV: 1.139 ±0.2635 VPA: 0.7497 ± 0.1975 RSV+VPA: 1.054 ± 0.1918	I: F (1, 19) = 1.687 P= 0.2096 V: F (1, 19) = 10.64 P = 0.0041+ R: F (1, 19) = 4.406 P = 0.0494+	No differences
PTEN	Control: 1.298 ± 0.1658 RSV: 1.168 ± 0.2911 VPA: 0.7788 ± 0.1705 RSV+VPA: 0.9422 ± 0.1243	I: F (1, 20) = 3.304 P = 0.0841 V: F (1, 20) = 21.22 P = 0.0002+ R: F (1, 20) = 0.04162 P = 0.8404	No differences
CK2	Control: 0.7075 ± 0.2198 # RSV: 1.057 ± 0.1848 VPA: 1.094 ± 0.1550 # RSV+VPA: 0.9987 ± 0.2702	I: F (1, 20) = 6.628 P = 0.0181 V: F (1, 20) = 3.608 P = 0.0720 R: F (1, 20) = 2.157 P = 0.1575	#=0.0293 (Cont-VPA)
GSK3β	Control: 0.9634 ± 0.07165 RSV: 0.8790 ± 0.1275 VPA: 0.8622 ± 0.1526 RSV+VPA: 0.7144 ± 0.2313	I: F (1, 20) = 0.8127 P = 0.3780 V: F (1, 20) = 1.123 P = 0.3019 R: F (1, 20) = 0.8154 P = 0.3773	No differences
AKT-p308	Control: 0.7722 ± 0.1643 RSV: 0.7932 ± 0.1312 VPA: 0.8595 ± 0.1282 RSV+VPA: 0.7604 ± 0.1498	I: F (1, 18) = 0.3819 P = 0.5443 V: F (1, 18) = 0.007512 P = 0.9319 R: F (1, 18) = 0.4393 P = 0.5159	No differences
AKT-p473	Control:0.8823 ± 0.1911 RSV: 0.7709 ± 0.1410 VPA:0.8549 ± 0.1603 RSV+VPA:0.8938 ± 0.1224	I: F (1, 18) = 1.288 P = 0.2714 V: F (1, 18) = 0.5333 P = 0.4746 R: F (1, 18) = 0.2637 P = 0.6138	No differences
p-PTEN	Control: 0.7768 ± 0.1718 RSV: 0.9135 ± 0.1023 VPA: 0.8584 ± 0.1895 RSV+VPA:0.8584 ± 0.09705	I: F (1, 20) = 1.314 P = 0.2653 V: F (1, 20) = 0.04911 P = 0.8269 R: F (1, 20) = 1.316 P = 0.2648	No differences
p-GSK3β	Control:0.9634 ± 0.07165 RSV:0.8790 ± 0.1275 VPA: 0.8622 ± 0.1526 RSV+VPA: 0.7144 ± 0.2313	I: F (1, 17) = 0.1326 P = 0.7202 V: F (1, 17) = 3.013 P = 0.1007 R: F (1, 17) = 2.277 P = 0.1497	No differences

PARTE III

3. DISCUSSÃO

A caracterização do TEA como uma desordem do neurodesenvolvimento muitas vezes restringe o enfoque dos estudos a idades infantis e juvenis; entretanto, é relevante compreender a desordem a longo prazo, tendo em vista que indivíduos com TEA apresentam redução na expectativa de vida, principalmente devido a alterações congênitas, distúrbios do SNC e suicídio (HIRVIKOSKI *et al.*, 2016). Ainda que complexa, a identificação precoce de aspectos críticos de cada indivíduo aliada a acompanhamentos de longa duração viabiliza expressiva melhora na qualidade de vida (SMITH-DAWALT *et al.*, 2019). Sendo assim, no presente trabalho, buscou-se estabelecer um olhar amplo sobre o TEA, levando em consideração as limitações estabelecidas pela pandemia de COVID-19, a qual demandou adaptações para que o curso inicial do raciocínio fosse mantido.

Iniciando com aspectos críticos que envolvem o desenvolvimento pré e neonatal, optou-se por analisar, na literatura, os FTs em diferentes DNs. Através do Capítulo I foi possível estabelecer uma curadoria dos principais FTs associados a cada desordem, além de demonstrar redes de interação, rotas biológicas potencialmente alteradas e momentos de pico de expressão durante o desenvolvimento, viabilizando uma base de dados essencial para futuros estudos envolvendo idades embrionárias.

Na análise das desordens de cunho genético foi possível observar que mutações pontuais, especialmente quando ocorrem no domínio de ligação ao DNA dos FTs (DAI *et al.*, 2020; TEIXEIRA *et al.*, 2021), são capazes de induzir alterações importantes a longo prazo. Na síndrome de Rett, mutações na proteína MECP2 (SHAHBAZIAN; ZOGHBI, 2001) induzem mudanças de alto impacto, incluindo conteúdo alterado dos neurotransmissores GABA e glutamato e de seus receptores (EL-KHOURY *et al.*, 2014, CALFA *et al.*, 2015), prejuízo na estrutura de IGs (SIGAL *et al.*, 2019), mudanças na estrutura do córtex somatossensorial (LEE; TSYTSAREV; ERZURUMLU, 2017), função prejudicada dos astrócitos (WILLIAMS *et al.*, 2014), dentre outros. A MECP2 possui um pico amplo de expressão pré-natal (CARDOSO-MOREIRA *et al.*, 2019), porém não há especificidade de estrutura encefálica (LAMBERT *et al.*, 2018), indicando expressão ampla nos diferentes tecidos. Além disso, esse FT é particularmente sensível a alterações de metilação, tendo em vista que sua ligação ao DNA - reprimindo a expressão gênica - depende da presença de dinucleotídeos CpG metilados (FUKS *et al.*, 2003). A síndrome de Pitt-Hopkins

(SPTH) também é associada com modificações em um FT de ampla atuação no desenvolvimento, denominado TCF4, e inclui alterações na estrutura cortical e migração neuronal (SCHOOF *et al.*, 2020), além de mudanças na glia radial associadas à via da WNT (WANG *et al.*, 2020) e na função hipocampal (THAXTON *et al.*, 2018). Ressalta-se, ainda, que alterações no TCF4 também são amplamente observadas no TEA e na esquizofrenia (FORREST *et al.*, 2018). O TCF4, entretanto, possui um pico de expressão mais tardio e certa especificidade embrionária de expressão tecidual, fatos que potencialmente explicam as diferenças de severidade em relação à síndrome de Rett, tendo em vista que a MECP2 apresenta ampla expressão nas estruturas encefálicas embrionárias.

As demais desordens genéticas incluem casos raros envolvendo FTs como os da família SOX. Nesses casos, alterações em SOX5, SOX9 e SOX10 estão associadas, respectivamente, com síndrome de Lamb-Shaffer (LAMB *et al.*, 2012), displasia capomélica (KWOK *et al.*, 1995) e síndrome de Waardenburg–Hirschprung (PINGAULT *et al.*, 1998), caracterizadas principalmente por alterações sensoriais e déficits cognitivos. Além disso, alterações em SOX11 estão associadas com microcefalia, déficits cognitivos, alteração na formação dos dedos, características associadas com a síndrome de Coffin-Siris (TSURUSAKI *et al.*, 2014). A diversidade presente nas determinadas “SOXpatias” é explicada pela função de cada FT (ANGELOZZI; LEFEBVRE, 2019): SOX5 possui papel importante na condrogênese e desenvolvimento esqueletal (SMITS *et al.*, 2001) em uma rota dependente de SOX6 e SOX9 (LIU; LEFEBVRE, 2015); SOX9 participa da formação das estruturas vestibulares e no ouvido interno (PARK; SAINT-JEANNET, 2010); SOX10 regula diversas funções associadas com a dinâmica das células da crista neural (WEIDER; WEGNER, 2017) e, finalmente, SOX11 faz parte da rota PAX6-BAF de FTs, essencial para processos de neurogênese (NINKOVIC *et al.*, 2013). Dessa forma, é possível observar que mudanças em FTs com funções mais restritas e/ou específicas são capazes de induzir alterações contundentes durante o neurodesenvolvimento, sendo essencial o aprofundamento dos estudos em desordens de etiologia mais complexa como TEA e esquizofrenia.

Além de potenciais alterações genéticas, os FTs também são extremamente influenciados por aspectos ambientais, especialmente durante o período gestacional (WORKALEMAHU *et al.*, 2018). As adaptações desenvolvidas em resposta a elementos estressores são capazes de induzir alterações profundas na maquinaria

de transcrição (SONG *et al.*, 2016), as quais, dependendo do local, momento e contexto, trazem impactos relevantes nas DNs.

Em estudos avaliando AIM em modelos animais, já foi possível observar uma gama de alterações na expressão de FTs na prole como PAX6, STAT (BEN-REUVEN; REINER, 2019), TBR1 (ZUIKI *et al.*, 2017), REST (CORRADINI *et al.*, 2018), ARX (NAKAMURA *et al.*, 2019), DLX1, DLX2 (OSKVIG *et al.*, 2012) e outros, os quais são fundamentais em processos como laminação cortical (BEDOGNI *et al.*, 2010), desenvolvimento e migração de IGs e regulação do sistema imunológico (BEN-REUVEN; REINER, 2019; OSKVIG *et al.*, 2012). Entretanto, os mecanismos pelos quais uma alteração imunológica induz impactos em FTs no SNC ainda não são completamente compreendidos. Hipotetizamos que uma das possíveis rotas envolvidas nessa sinalização seja a do sistema purinérgico, tendo em vista que esse é um dos principais elos entre o sistema imunológico e o SNC (DI VIRGILIO *et al.*, 2009). Em animais expostos à AIM, a ausência de receptores P2X7 ou o tratamento com um antagonista desse receptor evitou alterações comportamentais, distúrbios na laminação cortical e falhas na formação de sinapses (HORVÁTH *et al.*, 2019). Ainda, a exposição a aumento nos níveis de ATP circulante induziu danos mais severos em animais expostos previamente à MIA (ZOLKIPLI-CUNNINGHAM *et al.*, 2021). Finalmente, existem elos entre mudanças na sinalização purinérgica e expressão alterada de PAX6 (BURNSTOCK; DALE, 2015; MASSÉ *et al.*, 2007) e DLX (GUIBINGA; BARRON; PANDORI, 2014), reforçando um possível ponto de conexão.

A exposição, durante o período gestacional, a compostos como o VPA e o etanol também é capaz de mediar alteração em FTs. A exposição ao VPA modifica a expressão de PAX6 (KIM *et al.*, 2014), NEUROD1 (ZENG *et al.*, 2019) e HES1 (KAWADA *et al.*, 2018), inclusive alterando a linha do tempo de expressão de alguns FTs, o etanol, por sua vez, age sobre PAX6 (ARONNE *et al.*, 2008), POU5F1, SOX2 (SÁNCHEZ-ALVAREZ *et al.*, 2013) e HSF (ISHII *et al.*, 2017). No caso do VPA, é possível que as alterações envolvam pelo menos três aspectos: A) sistema imunológico, visto que a exposição ao VPA é capaz de alterar a expressão de citocinas e a funcionalidade de células imunológicas em modelos animais (DECKMANN *et al.*, 2018); B) capacidade direta do VPA de induzir inibição das HDACs, agindo diretamente na maquinaria de transcrição e modificando o padrão de expressão de FTs (GÖTTLICHER *et al.*, 2001) e C) indução de estresse oxidativo,

condição que já foi associada com alterações em FTs como POU5F1 (PIORCZYNSKI *et al.*, 2022) e SP1 (KAWAI; ARINZE, 2006). Em relação ao etanol, existem diversas descrições da ação nos chamados elementos responsivos ao álcool (do inglês, *alcohol responsive elements* – ARE) (PIGNATARO *et al.*, 2009), alterando a ação de FTs como o HSF1 (CONTET, 2012; UDDIN; SINGH, 2006). Além disso, o etanol também é capaz de induzir alterações nos FTs indiretamente através do estresse oxidativo (LIN *et al.*, 2013). Dessa forma, é possível observar como compostos químicos são capazes de afetar uma miríade de aspectos da transcrição que convergem no contexto das DNs.

Em desordens multifatoriais, a combinação entre os fatores de risco genéticos e ambientais é determinante para os desfechos observados em cada indivíduo (RYLAARSDAM; GUEMEZ-GAMBOA, 2019). No caso do TEA, é possível que uma parte relevante do risco genético esteja relacionado à presença de alelos mutantes em genes codificantes de FTs. Estudos de GWAS já demonstraram esse tipo de associação nos FTs TBR1, ADNP e PAX5 (O'ROAK, B. J. *et al.*, 2014). Além disso, diversos outros estudos ressaltam a relevância de alterações genéticas em outros FTs como SOX5 (ZAWERTON *et al.*, 2020), RARB, FEV (DOAN *et al.*, 2019), PITX3 (THE AUTISM SPECTRUM DISORDERS WORKING GROUP OF THE PSYCHIATRIC GENOMICS CONSORTIUM, 2017), ZNF292 (MIRZAA *et al.*, 2020), SHOX (TROPEANO *et al.*, 2016), MAZ (DE OLIVEIRA *et al.*, 2018), ATF6 (DONG *et al.*, 2018) e outros, demonstrando a diversidade de FTs potencialmente envolvidos nessa desordem. Ainda que existam descrições de redundância nas ações dos FTs (WANG *et al.*, 1996), mínimas alterações já são capazes de estabelecer impactos importantes (STOLT *et al.*, 2004), especialmente tendo em vista as complexas rotas de interação entre os próprios FTs.

Os estudos com modelos animais de TEA auxiliam na elucidação de como componentes ambientais influenciam na desordem. O modelo VPA demonstra os impactos do risco ambiental, tendo em vista as alterações já descritas em FTs como PAX6 e TCF4, os quais são envolvidos em processos centrais do SNC, tais como laminação cortical, geração, desenvolvimento e maturação de neurônios (CHEN, T. *et al.*, 2016; GEORGALA; MANUEL; PRICE, 2011). Nos animais, usualmente utiliza-se uma alta dose única para a indução do modelo, gerando um impacto intenso e pontual (MABUNGA *et al.*, 2015), enquanto em humanos o tratamento usualmente é contínuo e em doses comparativamente menores (CHRISTENSEN *et al.*, 2013).

Apesar disso, essas duas abordagens possivelmente apresentam uma confluência: enquanto nos modelos animais o dano é tão abrupto a ponto de não poder ser revertido pelos mecanismos usuais de reparo, em humanos é possível que as doses menores, porém contínuas, estabeleçam um processo gradual de alteração de transcrição que dificulta reparos ou uso de rotas alternativas. Alterações transcricionais (REPOUSKOU *et al.*, 2020) e epigenéticas (GABRIELE *et al.*, 2018) a longo prazo já são amplamente relacionadas com DNs e, sendo o VPA um importante indutor de mudanças transcricionais, especialmente pela inibição da desacetilação de histonas (KRÄMER *et al.*, 2003), é provável que essa seja uma importante rota de alteração associada com o risco de TEA.

Como mencionado previamente, um aspecto fundamental no contexto do TEA são as alterações no sistema imunológico, já descritas não só em modelos animais como também em humanos (GOTTFRIED *et al.*, 2015; DECKMANN *et al.*, 2018). No modelo animal BTBR, já existem evidências envolvendo alterações imunológicas mediadas por FTs: níveis aumentados de RORγ, T-bet e STAT3 e níveis reduzidos de FOXP3 em células T CD8+, enquanto em células T CD4+ observou-se níveis aumentados de RORγ, T-bet e STAT3 e níveis diminuídos de FOXP3 e HELIOS (AHMAD *et al.*, 2018b, 2018d; ANSARI *et al.*, 2017). Mudanças na expressão gênica de STAT3, RORγ, T-bet e FOXP3 também foram identificadas em tecido encefálico (AHMAD *et al.*, 2018d). Além disso, outras alterações em sinalização por FTs como GATA3 e JAK1 também foram identificadas em múltiplos contextos em animais BTBR (AHMAD *et al.*, 2017, 2018d). O VPA também possui a capacidade de induzir alterações na sinalização de FTs como STAT3 (NI *et al.*, 2017; ZHU, S.; DENMAN; LEE, 2009), FOXP3 (FAYYAD-KAZAN *et al.*, 2010), GATA3 (ROUT; CLAUSEN, 2009), além de induzir, em modelos animais, desbalanço na produção de citocinas como IL-1β, IL-6 e TNF-α (DECKMANN *et al.*, 2018). Dessa forma, é provável que a exposição ao VPA também seja capaz de induzir alterações neuroimunológicas (possivelmente através de regulação de FTs), as quais já são sabidamente fatores de risco para DNs.

De maneira geral, foi possível observar que os FTs estabelecem papéis extremamente relevantes em diferentes DNs, tanto em contextos mais específicos, como no caso das “SOXpatias”, quanto em contextos amplos, como o TCF4, que está envolvido na SPTH, TEA e esquizofrenia. Além disso, os picos de expressão dos FTs no período gestacional aliados às descrições de tecidos e/ou estruturas

onde esses fatores são mais expressos contribuem para demonstrar os potenciais impactos de uma falha na expressão, tanto por questões genéticas quanto ambientais, ressaltando a relevância dos FTs nesse campo de estudos. Finalmente, a presença de diversas rotas biológicas alteradas em comum nas diferentes desordens, especialmente vias do sistema imunológico, vias de ciclo celular, via da WNT e outras, além das descrições de interação entre os próprios FTs, ressaltam a importância de analisar os impactos de forma ampla e integrativa. Alguns dos temas recorrentes no capítulo I foram o envolvimento dos FTs na regulação da organização das estruturas encefálicas, tais como a definição de camadas corticais, além da regulação de processos como a formação de sinapses e posicionamento de neurônios. Tendo em vista esse panorama de informações, a análise pós-natal da organização cortical, tanto no posicionamento quanto no número de células neuronais tornou-se muito relevante no contexto do modelo animal de TEA.

No capítulo II, o principal enfoque foi analisar componentes inibitórios em duas regiões encefálicas em animais jovens com o intuito de verificar potenciais alterações induzidas pelo VPA intraútero, bem como os possíveis efeitos preventivos do RSV. Ao longo desse trabalho, diversas alterações observadas foram associadas com mudanças observadas em bancos de dados de RNA-Seq (do inglês, *RNA sequencing*) e microarranjo de modelos animais de TEA. O intuito desse tipo de abordagem é trazer um embasamento maior para as hipóteses, viabilizando, ainda, um diálogo relevante com as informações obtidas no capítulo I.

Iniciando pelo CPFm, foi possível observar um aumento significativo na quantidade de neurônios totais de forma geral, especialmente representado pelas camadas profundas do CPL e do CI. Aumentos nas dimensões encefálicas no contexto do TEA estão associados, majoritariamente, a dois componentes distintos: A) Acréscimo no volume causado por edema, condição transitória, porém global (AYLWARD *et al.*, 2002), que afeta cerca de 20% dos indivíduos com TEA (SACCO; GABRIELE; PERSICO, 2015) e B) Aumento na celularidade, especialmente em regiões como a amígdala (MARKRAM *et al.*, 2008) e o córtex pré-frontal (COURCHESNE *et al.*, 2011). No nosso grupo, já há indicativos de aumento no volume do CPFm (DECKMANN *et al.*, 2021). No caso do número de neurônios observados no CPFm, há um paralelo com o aumento de 67% em neurônios totais observados em pacientes com TEA (COURCHESNE *et al.*, 2011), demonstrando que ambos os componentes possivelmente contribuem para as mudanças na

citoarquitetura identificadas nessa região. As informações provenientes dos bancos de dados demonstram a presença de genes diferencialmente expressos (GDEs) em regiões e estruturas chave para a migração dos neurônios excitatórios, tais como a subplaca cortical, a zona ventricular e a glia radial, evidenciando a possibilidade de que uma falha de coordenação nessa etapa possa gerar desbalanço na proliferação neuronal. Além disso, o VPA sabidamente atua no ciclo celular de neurônios não-GABAérgicos, os mantendo em etapas proliferativas por mais tempo (FUJIMURA *et al.*, 2016). Interessantemente, FTs como TBR1 e SOX5, já descritos como alterados no contexto do TEA (O'ROAK *et al.*, 2012; PARIKSHAK *et al.*, 2016; ZAWERTON *et al.*, 2020), conforme observado no Capítulo I, são essenciais para a correta proliferação e laminação nos neurônios excitatórios – visto que TBR1 é um dos GDEs observados em organoides expostos ao VPA (CUI *et al.*, 2020), é possível que essa seja uma via envolvida na alteração neuronal observada no Capítulo II.

A alteração em neurônios totais, ainda que não significativa em todas as sub-regiões, implica em um desbalanço na circuitaria a partir do momento em que a razão de IGs para neurônios totais é afetada significativamente. No caso do CPFm como um todo, o principal impacto identificado ocorreu no IGs SOM+, onde tanto número quanto razão apresentaram redução, seguido dos IGs PV+, que apresentaram alteração somente na razão e finalmente os IGs CB+, que não apresentaram qualquer alteração nesse nível. Ao analisarmos as sub-regiões especificamente, foi possível observar alterações significativas em todas as subpopulações de IGs. O tratamento com RSV preveniu diversas alterações.

O impacto disseminado em SOM+ remete a um dano precoce induzido pelo VPA, possivelmente em etapas iniciais do desenvolvimento dessas células. Os SOM+ são originados na porção medial da GE (EGM) através de um sistema de sinalização inicial baseado no aumento da expressão de SHH seguido da expressão do fator NKX2-1 (BUTT *et al.*, 2005), visto que esse IG foi o único cujo número absoluto apresentou alteração e observando que sua trajetória se inicia mais cedo no embrião é possível inferir que a alteração global ocorre quando as células ainda estão etapas proliferativas. Esse resultado corrobora evidências de redução da expressão gênica de SHH em embriões no dia E11,5 quando expostos ao VPA em E9 (MIYAZAKI; NARITA; NARITA, 2005). Além disso, já foi observado um padrão de redução drástica de SOM+ em diferentes regiões encefálicas em modelo animal de AIM, oposto ao identificado em outros IGs como PV+ e CCK+ (BOKSA *et al.*, 2016),

sugerindo uma maior vulnerabilidade dos SOM+, ainda que possíveis mecanismos por trás dessa característica não sejam esclarecidos.

Por outro lado, a ausência de alterações no número absoluto e a redução na proporção de PV+ para neurônios totais indica possivelmente um dano sutil e potencialmente associado a processos de migração, já que a distribuição na análise de subregiões demonstrou um padrão anômalo: enquanto o CCa apresenta redução em número e proporção, as camadas superiores do PL apresentam um padrão de aumento em ambos os parâmetros. Aliado a isso, observou-se no ANEXO 4 que o VPA foi capaz de induzir alteração na expressão do FT LHX6 (ainda que não de SOX6), o qual é fundamental para o correto desenvolvimento e posicionamento dessas células ao longo das camadas corticais (LIODIS *et al.*, 2007). Modificações similares foram observadas nos CB+, remetendo, novamente, a possíveis alterações na migração; entretanto, a baixa quantidade dessa célula na região possivelmente contribui para que os impactos nessa subpopulação sejam mais restritos.

Alterações em IGs no contexto do TEA já foram descritas em múltiplos contextos, majoritariamente através de evidências que demonstram perdas nesse componente inibitório (NOMURA, 2021). No nosso grupo de pesquisa já foi observado um padrão de alteração em neurônios PV+ no córtex somestésico análogo ao CPFm, com o VPA induzindo aumento da razão de PV+ nas camadas superiores e reduzindo nas inferiores, novamente indicando uma alteração na laminação (FONTES-DUTRA *et al.*, 2018). No CPFm, disfunções em PV+ possivelmente estão associadas com as alterações em sociabilidade observadas no modelo VPA (BAMBINI-JUNIOR *et al.*, 2014; HIRSCH *et al.*, 2018), tendo em vista que, nessa região encefálica, os PV+ medeiam processos sociais complexos como novidade social (BROWN *et al.*, 2015), memória de curta duração e flexibilidade cognitiva (MURRAY *et al.*, 2015). Em relação aos CB+, há descrição de redução na densidade em modelo de estresse por separação neonatal, indicando um possível envolvimento desse IG em comportamentos associados com estruturas límbicas como a amígdala (HELMEKE *et al.*, 2008). Os IGs SOM+ também apresentam função importante para o comportamento social no CPFm, sendo relacionados com a capacidade de discriminar estados afetivos (SCHEGGIA *et al.*, 2020) e com a consolidação de memórias aversivas (CUMMINGS; CLEM, 2020) – no contexto do TEA, porém, há escassez de evidências sobre esse IG até o momento.

Nos bancos de dados, evidências de KALISH *et al.*, 2020, corroboram a hipótese de falhas na migração uma vez que tanto a GE quanto os IGs provenientes dessa região apresentam uma série de alterações em diversas vias celulares logo após a indução do referido modelo. É possível que o VPA trace um paralelo nesse aspecto, especialmente tendo em vista a sua capacidade de modificar a expressão de FTs. O aumento na expressão de LHX6 identificado no CPFm é um indicativo de uma mudança na maquinaria transcricional a longo prazo, tendo em vista o papel desse FT no período embrionário.

Em relação aos parâmetros sinápticos e de receptores GABAérgicos no CPFm, a exposição intraútero ao VPA foi capaz de reduzir o imunoconteúdo de $GABA_A$, gefirina e neuroliguina-2, enquanto o tratamento com RSV *per se* teve efeito similar nas referidas proteínas sinápticas. Reduções na expressão de $GABA_A$ já foram observadas no cerebelo, córtex parietal, córtex frontal (FATEMI *et al.*, 2009) e CCa (OBLAK; GIBBS; BLATT, 2009) de indivíduos com TEA. Essa alteração provavelmente tem um reflexo importante em parâmetros comportamentais, uma vez que animais KO seletivo para subunidade 5α do receptor $GABA_A$ apresentam características do tipo TEA (MESBAH-OSKUI *et al.*, 2017). Além disso, em outros modelos como o da síndrome de Jacobs, já se observou prejuízo na sinalização mediada por $GABA_A$ (NAKAMURA *et al.*, 2016). Interessantemente, o tratamento com benzodiazepínicos (agonistas de $GABA_A$) foi capaz de trazer melhorias comportamentais no modelo BTBR (HAN *et al.*, 2014). Finalmente, a dinâmica de expressão de $GABA_A$ durante o desenvolvimento é um fator importante para a migração de IGs (LUHMANN; FUKUDA; KILB, 2015), sendo mais um possível fator que contribui para a alteração vista na distribuição de CB+, PV+ e SOM+ no CPFm.

Em relação às proteínas sinápticas, as alterações observadas tanto pelo VPA quanto para o RSV possivelmente apontam para a via da NOTCH, a qual é sabidamente modulada tanto por RSV quanto por VPA (JI; KE; GAO, 2017). Essa via possui papel importante na regulação do desenvolvimento sináptico (GINIGER, 2012) e, além disso, foi descrita como alterada no banco de dados de CANALES *et al.*, 2020, indicando um papel de relevância no contexto do TEA. Essa via também foi evidenciada no contexto de FTs em alterações genéticas e FTs em interação com fatores de risco ambientais, destacando essa rota de sinalização no contexto de DNs. Apesar do tratamento com RSV ter efeito similar ao do VPA na via da NOTCH, não se observa indicativos de alterações histológicas e comportamentais no grupo

RSV (BAMBINI-JUNIOR *et al.*, 2014; FONTES-DUTRA *et al.*, 2018, 2019; HIRSCH *et al.*, 2018). Entretanto, a análise de gefirina no córtex somestésico demonstrou que o grupo RSV situava-se em níveis intermediários entre controle e VPA, sugerindo que o RSV modula componentes sinápticos (FONTES-DUTRA *et al.*, 2018).

Em relação ao HC, foi possível observar alterações bem mais sutis do que as identificadas no CPFm, indicando que, ao menos nessa idade, o dano se concentra em estruturas corticais como o CPFm e o córtex somestésico (FONTES-DUTRA *et al.*, 2018). O GD foi a principal sub-região afetada, especialmente a composição de IGs SOM+ e quantidade de neurônios totais. Esse tipo de alteração já foi identificada em outro estudo com o modelo VPA, onde a alteração na disposição dos neurônios nessa região foi associada com falhas na sinalização mediada pela quimiocina CXCL12 e seu receptor CXCR4 (DANZER, 2019), os quais também desempenham um papel fundamental também na migração de IGs. Complementarmente, a utilização de VPA em animais de modelo de doença de Alzheimer também foi capaz de promover neurogênese hipocampal através do aumento nos níves de β-catenina e da inibição de GSK-3β (ZENG *et al.*, 2019).

Finalmente, a alteração promovida exclusivamente em SOM+ no HC compõe uma condição que potencialmente altera processos de consolidação de memórias de medo (já descritas no TEA, porém com uma abordagem voltada para o papel da amígdala) (MARKRAM *et al.*, 2008) uma vez que estudos apontam que uma microcircuitaria baseada na inibição lateral dos dendritos das células da camada granular do GD promovida por SOM+ dos dendritos é determinante para esse processo (STEFANELLI *et al.*, 2016). Os SOM+ são fundamentais para a integração e comunicação entre CPFm e HC, pois a inibição de SOM+ hipocampais induz prejuízos na formação de memória de trabalho (ABBAS *et al.*, 2018), de forma que esse tipo de alteração pode contribuir para agravar os prejuízos observados no próprio CPFm. Por fim, em relação às proteínas sinápticas e receptores de GABA, não se observou qualquer alteração no HC, indicando que o dano se restringiu a aspectos histológicos e de citoarquitetura.

O efeito preventivo do RSV se destaca no aspecto de composição de IGs e da manutenção da citoarquitetura do CPFm e de forma parcial no HC. Ao evitar o aumento de neurônios totais, além de equilibrar números e proporções de CB+, PV+ e SOM+, é provável que ocorra uma restauração do equilíbrio E/I, melhorando parâmetros comportamentais, especialmente de sociabilidade, conforme já foi

observado em outros estudos do grupo. Diversas hipóteses surgem para explicar como o RSV pode, de maneira preventiva, dirimir os danos induzidos pelo VPA:

A) O RSV, através de seu papel antioxidante (PINYAEV *et al.*, 2019), estabelece um potencial protetivo ao dano oxidativo induzido pela exposição ao VPA via alteração no metabolismo de carboidratos: essa hipótese é embasada pelos bancos de dados CANALES *et al.*, 2021; CUI *et al.*, 2020 e OSKVIG *et al.*, 2012, que apontam para disfunção no metabolismo de carboidratos e no metabolismo mitocondrial em etapas precoces (E12,5, por exemplo) e que vão progredindo conforme o passar do tempo. A proliferação de progenitores neuronais depende fortemente da glicose aeróbica como forma de obtenção de energia (ZHENG *et al.*, 2016) e, além disso, os mecanismos de geração de ROS operam de maneira refinada como forma de sinalizar a geração de neurônios de camadas profundas e superficiais do córtex (CHUI *et al.*, 2020);

B) A ação anti-inflamatória do RSV ocorre por múltiplas rotas, incluindo a modulação de STAT (COUTINHO *et al.*, 2018), FOXP3 (SINGH *et al.*, 2013), e GATA3 (OKADA *et al.*, 2012), vias já descritas como alteradas no modelo animal de TEA BTBR. Nesse mesmo modelo, o RSV foi capaz de mitigar as alterações nesses FTs, trazendo melhora comportamental (BAKHEET *et al.*, 2017). Tendo em vista que a exposição ao VPA induz uma série de alterações imunológicas (DECKMANN *et al.*, 2018), é possível que essa seja uma via de prevenção do RSV.

C) O RSV, através de seu papel ativador das SIRTs (CHAO *et al.*, 2017) contrapõe a inibição das HDACs promovida pelo VPA (GÖTTLICHER *et al.*, 2001), equilibrando distúrbios na maquinaria transcricional: o VPA já demonstrou papel relevante na modulação de diversos FTs essenciais para o desenvolvimento e migração neuronais, incluindo TCF4, PAX6 e outros, conforme visto no artigo de revisão presente no Capítulo I. Um dos possíveis mecanismos por trás dessa influência provavelmente é a inibição direta de HDACs, as quais possuem ampla descrição de interação com FTs. Vias como a NOTCH e WNT, descritas como alteradas nos bancos de dados, também já foram reportadas como consequências das modificações em FTs no Capítulo I, adicionando mais evidências a essa perspectiva. Dessa forma, ao ativar as SIRTs, que são HDACs, o RSV poderia estabelecer um equilíbrio durante o período de tratamento, evitando o dano brusco da injeção em alta dose do VPA.

D) Estudos *in vitro* apontam o RSV como um importante modulador de CXCR4 e CXCL12 (HAJINEJAD *et al.*, 2018; JANG *et al.*, 2019), rota de sinalização relevante para a composição de neurônios do HC e sabidamente alterada pelo VPA (DANZER, 2019). Essa via específica poderia estar associada aos resultados de prevenção observados no GD.

Figura 2: Principais hipóteses de rotas potencialmente alteradas pelo VPA e moduladas pelo RSV.

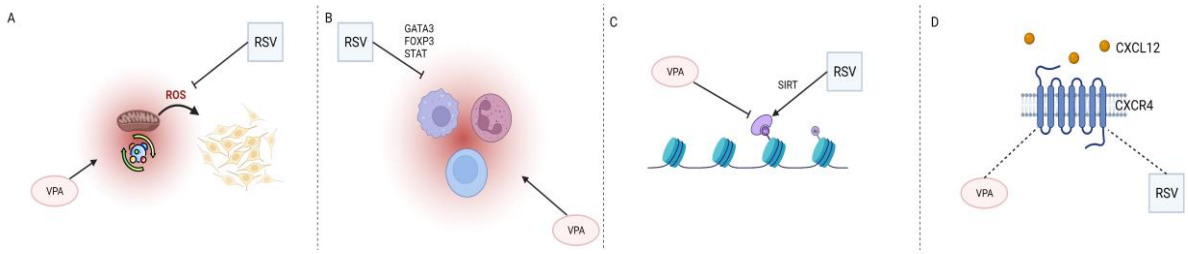

A) O VPA induz aumento nos parâmetros de estresse oxidativo como a geração de espécies reativas de oxigênio. O RSV, através da sua ação antioxidante, evita danos a células altamente suscetíveis como os precursores neurais; B) O VPA induz alterações pró-inflamatórias, alterando parâmetros celulares e de citocinas, enquanto o RSV, através da sua ação anti-inflamatória, previne essas alterações; C) O VPA inibe as HDACs, intensificando processos de transcrição. O RSV é um estimulador de SIRTs, uma classe de HDACs, possivelmente equilibrando o efeito do VPA. D) O VPA modula as vias associadas com o receptor CXCR4 e seu ligante CXCL12, os quais são importantes para manutenção da composição neuronal, especialmente no HC. O RSV também possui ação modulatória nessa via, possivelmente mitigando a ação do VPA.

As análises de bancos de dados demonstram, inicialmente, que uma parcela importante dos GDEs possui uma relevante representação na plataforma SFARI, um dos maiores bancos de dados sobre TEA disponíveis. Além disso, conforme demonstrado ao longo da discussão, foi possível situar diversos dados dentro das alterações observadas, especialmente no CPFm, facilitando a formação de hipóteses mais embasadas.

De forma geral, o desequilíbrio no metabolismo de carboidratos parece ser uma das alterações mais precoces induzidas pelo VPA, conforme observado no dia E12,5 em CANALES *et al*., 2021 e nos organoides em CUI *et al*., 2020. Sabidamente, o VPA é capaz de inibir a ativação da proteína GSK3β (CHEN *et al.*,

1999), situação já associada com um desequilíbrio no metabolismo da glicose (PAL *et al.*, 2014), ressaltando um possível papel dessa via nesse tipo de alteração. Na sequência, diversos bancos apontam para uma regulação positiva de genes associados ao metabolismo mitocondrial CANALES *et al.*, 2021, CUI *et al.*, 2020 e OSKVIG *et al.*, 2012, sugerindo o estabelecimento de uma alteração metabólica potencialmente geradora de EROs (BHATTI; BHATTI; REDDY, 2017). O VPA é capaz de interagir diretamente na mitocôndria através de ação na β-oxidação de ácidos graxos, interferindo na disponibilidade de carnitina e acetilcoenzima-A (SILVA *et al.*, 2008), demonstrando uma possível via que justificaria a alteração observada.

Ao longo do desenvolvimento embrionário, é possível observar uma tendência de aceleração da maturação neuronal, com regulação positiva de componentes como sinapse, adesão celular e metabolismo de purinas, metabolismo de neurotransmissores e outros. Em indivíduos com TEA, já foram descritas alterações de proliferação sináptica desenfreada, seguida de ausência de poda adequada (TANG *et al.*, 2014), além de desbalanço no conteúdo de neurotransmissores como GABA e glutamato (HORDER *et al.*, 2018), enquanto mudanças no perfil de sinalização por purinas já foram amplamente discutidas em modelos animais (NAVIAUX *et al.*, 2014), conforme sumarizado no capítulo em anexo, demonstrando aspectos translacionais importantes. Interessantemente, muitas dessas alterações são observadas nos organoides expostos ao VPA, reafirmando pontos em comum com outros modelos animais e *in vitro* de TEA. Por outro lado, GDEs envolvidos no ciclo celular, expressão gênica e regulação do metabolismo proteico estão negativamente regulados, novamente consolidando indícios de que alteração na maquinaria transcricional, especialmente FTs, podem ser um componente importante na indução dos modelos de TEA.

No intuito de expandir as análises para outras etapas do desenvolvimento, a fim de verificar uma possível progressão dos danos observados na idade jovem, bem como avaliar se as prevenções do RSV se estendem à vida adulta em animais de 120 dias, optou-se por analisar, no HC, IGs e componentes de sinalização celular. A escolha da região se justifica por diversos dados de alterações, inclusive comportamentais. No nosso grupo de pesquisa, observou-se que o VPA induziu alterações comportamentais a longo prazo, prejudicando o comportamento do tipo empático em animais de idades similares à abordada no presente trabalho (FONTES-DUTRA *et al.*, 2019).

Inicialmente, uma das principais alterações hipocampais observadas foi uma impactante alteração morfológica induzida pelo VPA, caracterizada por dois componentes principais: perda neuronal no GD, concedendo a essa região um aspecto “incompleto” e descompactação neuronal em CA1. Esse tipo de alteração remete à esclerose hipocampal (KITAURA *et al.*, 2018), um tipo de lesão progressiva associada a desequilíbrios eletrofisiológicos, especialmente epilepsia (WALKER, 2015). Interessantemente, já foram identificadas (utilizando técnicas de eletrofisiologia *in vitro*) reduções na frequência e no tempo de decaimento de correntes inibitórias, além da presença, *in vivo*, de descargas de ondas lentas durante o ciclo de vigília em 40% na região do córtex sometésico dos animais VPA em idade jovem, sendo todas essas alterações foram prevenidas pelo tratamento pré-natal com RSV (Fontes-Dutra et al., 2022 – *em preparação*). Paralelamente, foi possível observar que o RSV também evitou as alterações morfológicas observadas no HC, sugerindo que, ao evitar alterações eletrofisiológicas desde idades mais precoces, esse composto acaba agindo de forma neuroprotetora.

Diversos estudos já demonstram que o RSV possui capacidades neuroprotetoras em relação a danos hipocampais. Em análise de pacientes com *status epileticus* se observou que o RSV foi capaz de evitar a progressão do dano hipocampal, evitando a progressão de alterações comportamentais (CASTRO *et al.*, 2017), além de melhorar parâmetros de conectividade, metabolismo de glicose e neuroinflamação (KÖBE *et al.*, 2017). Nosso grupo de pesquisa já observou alterações no HC do modelo animal VPA em relação ao metabolismo do glutamato em P120 (BRISTOT SILVESTRIN *et al.*, 2013). Os animais VPA tiveram aumento da atividade de captação de glutamato, níveis aumentados de GLT1, aumento dos níveis de glutationa (GSH) e diminuição da atividade de glutamina sintetase (GS). Esses dados demonstram importantes alterações glutamatérgicas no HC a longo prazo, as quais poderiam contribuir para o dano observado.

Os mecanismos envolvidos no efeito preventivo do RSV ainda não são conhecidos, porém, considerando estudos com outros transtornos psiquiátricos, podemos destacar a modulação de SIRT como uma das hipóteses mais plausíveis. Em modelo animal de esquizofrenia, o RSV foi capaz de inibir o estresse oxidativo no HC através do aumento na expressão de SIRT e BDNF (do inglês, *brain derived neutrophic factor*) (NIU; CAO; JI, 2020), efeito similar foi observado em modelo de declínio cognitivo associado a diabetes (TIAN *et al.*, 2016). As SIRTs também são

responsáveis por equilibrar a dinâmica mitocondrial, regulando, em conjunto com PGC-1α, aspectos de biogênese e mitofagia com o intuito de promover a homeostase metabólica (XU *et al.*, 2018). Esse aspecto é de grande relevância, tendo em vista que na análise de bancos de dados de embriões (abordada no Capítulo II) é possível observar um desbalanço no metabolismo de carboidratos e no metabolismo mitocondrial já em idades precoces no contexto do TEA.

Em relação aos achados quantitativos em cada sub-região para neurônios totais e IGs, houve impacto diferencial da indução com VPA – e, consequentemente do RSV – no GD, CA1, CA2 e CA3. Similarmente ao que já tinha sido observado em animais jovens, o GD se destacou como uma das regiões mais afetadas. A redução quantitativa em neurônios totais foi um dos efeitos mais relevantes do VPA, inclusive explicando a aparência descontínua do GD nas observações em maior aumento, novamente com o RSV proporcionando um efeito preventivo na perda neuronal. Além das hipóteses já elencadas acerca da ação do RSV, outro possível componente é a neurogênese hipocampal. Em modelo de envelhecimento, o tratamento com RSV foi capaz de estimular a neurogênese, prevenir ativação glial e reatividade microglial, além de otimizar a microvasculatura local (KODALI *et al.*, 2015). Efeito similar foi observado em animais expostos a estresse pré-natal, situação em que o RSV promoveu a neurogênese, além de restaurar a expressão de BDNF (MADHYASTHA; SEKHAR; RAO, 2013).

Em relação aos IGs, não foi possível observar alterações significativas em PV+ nessa sub-região, enquanto CB+ demonstrou decréscimo em número e SOM+ representou a alteração mais significativa com aumento em número e razão. Em decorrência do número reduzido em CB+, os resultados podem ser mais voláteis do que os demais IGs. Em relação aos SOM+, foi possível observar que o VPA induziu um aumento no número independente do tratamento com RSV, porém quando se observa a razão de SOM+/neurônios totais é possível observar que o tratamento com RSV é capaz de retomar o equilíbrio nessa proporção.

Alterações em CB+ já foram descritas no contexto do TEA, incluindo um aumento na densidade no GD (LAWRENCE *et al.*, 2010), entretanto as evidências acabam sendo limitadas. Uma questão importante a se destacar é o número reduzido desse tipo de células, o que acaba interferindo diretamente nas quantificações e gerando oscilações que podem ser decorrentes de limitações da técnica. Porém, condições como a exposição a estresse precoce (LI *et al.*, 2017) e

status epileticus induzido por pilocarpina (CARTER *et al.*, 2008) já foram associados com redução a longo prazo na expressão de calbindina, sugerindo que desequilíbrios E/I de fato podem interferir nessa subpopulação, porém se faz necessário ampliar as investigações para outras regiões do HC, como o HC ventral, a fim de obter um panorama mais amplo.

Referente aos SOM+, foi possível observar que o dano visto em P30 se manteve até P120, com o aumento da razão dessa IG no GD. Interessantemente, apesar de não ser capaz de reduzir efetivamente o número de SOM+, o RSV é capaz de estabelecer um equilíbrio na razão, possivelmente através de uma ação parcial no número de SOM+ e de uma ação mais contundente no número de neurônios totais, prevenindo a alteração induzida pelo VPA em P120. No contexto do TEA, há poucas evidências sobre o papel desse IG. Animais KO seletivo para ARIDB1 (gene de risco para o TEA) em IGs SOM+ e PV+ apresentam características do tipo autista (SMITH *et al.*, 2020); similarmente, animais KO para MECP2 nesses mesmos neurônios apresentam características da síndrome de Rett, uma desordem com pontos em comum com o TEA (ITO-ISHIDA *et al.*, 2015).

As demais alterações em SOM+ presentes nas sub-regiões CA1 e CA2 (tanto em número quanto em proporção, com prevenção do RSV na razão de CA2 e efeito *per se* em CA1), remetem a alterações no perfil de migração dos IGs, uma vez que há concentração dessas células no GD em detrimento das sub-regiões. Novamente, a hipótese da rota de sinalização CXCR4-CXCL12 se destaca, tendo em vista a sua influência na composição neuronal do HC (DANZER, 2019). Os IGs SOM+ estão associados com a modulação de memórias, especialmente a regulação das dimensões do engrama (através da inibição lateral, os SOM+ restringem a quantidade de neurônios associada com a formação de determinada memória) (STEFANELLI *et al.*, 2016), além de induzirem plasticidade sináptica de longa duração, modulando toda circuitaria hipocampal (HONORÉ *et al.*, 2021). O fato dos CB+ apresentarem um padrão oposto em relação aos SOM+ nessa região possivelmente ocorre pelo fato das subpopulações serem originadas em locais diferentes, enquanto SOM+ se concentra na EGM, CB+ está mais restrito a CGE (KELSOM; LU, 2013), de forma que o VPA provavelmente atinge essas duas subpopulações de forma diferente.

Em CA1, foi possível observar alterações nas três subpopulações de IGs, ainda que em neurônios totais o número não tenha sido alterado, ainda que o VPA

tenha induzido descompactação da camada granular. O VPA foi capaz de induzir reduções no número PV+ e células SOM+. A administração pré-natal de RSV preveniu diminuições no número e razão de CB+. Os PV+ dessa região já foram associados com processos de consolidação de memórias (OGNJANOVSKI *et al.*, 2017), formação de memória de trabalho espacial (MURRAY *et al.*, 2011) e memórias sociais (DENG *et al.*, 2019). O padrão similar de resultado para PV+ observado em CA2 e CA3 possivelmente contribui para alteração na circuitaria hipocampal, tendo em vista que os PV+ são importantes reguladores das vias que conectam CA1, CA2 e CA3 (NASRALLAH *et al.*, 2019). Esse conjunto de evidências, novamente, remete aos dados observados para comportamento social do tipo empático no modelo VPA: é possível que o RSV seja capaz de mitigar alterações sociais em idades mais avançadas, conforme já indicado em estudos do grupo para outras idades, porém parâmetros associados com memória a aprendizado (essenciais para desempenho do comportamento avaliado, que consiste na abertura de um aparato para liberação de um animal coespecífico) não são totalmente contemplados, mantendo o prejuízo comportamental (FONTES-DUTRA *et al.*, 2019).

Em relação às vias de sinalização avaliadas, observou-se que o RSV não conseguiu prevenir as alterações hipocampais de PTEN total, CK2 e AKT observadas no grupo VPA. No entanto, não ocorreram alterações nos níveis de fosforilação e, possivelmente, na atividade de PTEN, AKT e GSK3β. Camundongos KO específico para PTEN em células PV+ e SOM+ apresentaram déficits sociais, estereotipias e coordenação motora/aprendizagem prejudicada de forma similar ao observado no TEA. Além disso, esses animais apresentaram alterações comportamentais específicas conforme o tipo de neurônio alterado: camundongos KO PTEN em SOM+ exibiram comportamentos semelhantes a ansiedade, enquanto camundongos KO PTEN em PV+ apresentaram hiperlocomoção (SHIN; SANTI; HUANG, 2021). A alteração observada em PTEN pode ter associação com CK2, que está aumentada no grupo VPA, uma vez que a capacidade inibitória de CK2 sobre PTEN (BARATA, 2011) possivelmente também modula seus níveis e/ou atividade. Finalmente, a diminuição de AKT pode impactar a atividade do mTOR que, por sua vez, afeta a regulação da memória hipocampal, tendo em vista que os IGs SOM+ depende do complexo mTORC1 para desempenhar atividades associadas com consolidação de memórias aversivas e memórias espaciais (ARTINIAN *et al.*, 2019), é possível que essa alteração se some às disfunções observadas nessas células.

Ainda que as alterações nas proteínas descritas não possam explicar completamente as questões comportamentais e morfológicas do modelo VPA, a análise da sua participação no contexto do TEA deve ser expandida para outras regiões e idades, tendo em vista o papel relevante em diversas funções dos IGs. Ainda, como já citado, essas proteínas fazem parte de vias que participam de diversos processos envolvendo memória, um aspecto que possivelmente está alterado no modelo VPA em P120, tendo em vista os dados observados no HC.

Análises preliminares de IGs no CPFm (ANEXO 5), demonstram que, ao longo do desenvolvimento, o aumento de celularidade parece ser equilibrado até mesmo no grupo VPA, condizente com as informações de que o aumento no volume encefálico no TEA é um fenômeno transitório (LANGE *et al.*, 2015). Entretanto, as diversas alterações em IGs, não prevenidas pelo RSV, podem ser um reflexo também do desequilíbrio E/I prolongado. Além disso, CPFm e HC apresentam importante conectividade, de forma que alterações nessas regiões possivelmente levam a um impacto recíproco (SIGURDSSON; DUVARCI, 2016). A avaliação de parâmetros de apoptose, bem como do conteúdo de GABA e das enzimas GAD65 e GAD67 em CPFm são alternativas relevantes para verificação da viabilidade e maturação dos IGs a longo prazo nessa região.

Partindo uma perspectiva integrativa, buscou-se identificar, ao longo de três pontos do desenvolvimento, incluindo vida pré-natal, idade jovem (P30) e idade adulta (P120), vias envolvidas em componentes inibitórios, com destaque para os IGs CB+, PV+ e SOM+. As avaliações da literatura e de bancos de dados auxiliaram na formulação de hipóteses concretas, viabilizando diversas opções para análise.

Ao observarmos os picos de expressão dos FTs obtidos em Cardoso-Moreira *et al.,* 2019, é possível visualizar uma concentração em períodos iniciais da gestação, um primeiro indício de que os FTs são possíveis alvos de vulnerabilidade nesse período. Além disso, as rotas enriquecidas para os FTs alterados no TEA ressaltam vias em comum com as observadas na análise de bancos de dados, incluindo regulação da transcrição, via da WNT e vias de metabolismo proteico.

Tendo em vista que o VPA possui ampla ação sobre FTs e sobre a maquinaria de transcrição de forma geral (devido à modulação de HDAC), é possível hipotetizar que uma exposição a alta dose durante um período precoce da gestação possivelmente gera uma cadeia de desequilíbrios na organização da transcrição. Em animais de P30, a observação da severa alteração na citoarquitetura do CPFm pode

ser um indício de que alguma alteração dessa natureza é plausível. Neurônios excitatórios possuem uma rota relativamente mais simplificada de migração (REINER *et al.*, 2016), entretanto IGs demandam rotas de migração complexas que envolvem, além da matriz de expressão de FTs (WONDERS; ANDERSON, 2006), outros elementos de sinalização como semaforinas (CHEN *et al.*, 2008), citocinas (MA *et al.*, 2014), neurotransmissores (HENG; MOONEN; NGUYEN, 2007) e elementos da matriz extracelular (LONG; HUTTNER, 2019). Essa gama de variáveis provavelmente está associada à diversidade de resultados observada nas diferentes subpopulações de IGs, bem como as origens diferentes dessas células na EG.

Diversos componentes também se destacam como possíveis vias envolvidas nas alterações sinápticas observadas em P30. Uma das mais consolidadas é a via da NOTCH, visto que essa via está enriquecida para FTs modificados por fatores ambientais, conforme consta no capítulo I, e se destaca na análise dos bancos de dados. Além disso, as evidências de resultados similares para VPA e RSV reforçam essa possibilidade, dado o padrão similar de expressão em ambos os grupos. Entretanto, outros fatores como o remodelador de cromatina CHD8, um componente alterado em modelos de TEA (KATAYAMA *et al.*, 2016) e sabidamente influenciado pelo VPA (ZOU *et al.*, 2022), também se destaca nesse contexto, tendo em vista que alterações nesse remodelador prejudicam o desenvolvimento das sinapses (JIMÉNEZ *et al.*, 2020) e induzem falhas sinápticas, com desequilíbrio na razão entre sinapses excitatórias e inibitórias (ELLINGFORD *et al.*, 2021). No capítulo I, observou-se que CHD8 também interage com o FT REST (ou RE-1), estabelecendo um possível elo entre mudanças epigenéticas e FTs, já que esse FT também é capaz de modular sinapses, especialmente as inibitórias (PRESTIGIO *et al.*, 2021).

Durante o desenvolvimento, a sinalização por GABA em IGs é fundamental para processos de migração. O influxo de cálcio promovido por esse neurotransmissor induz alterações no citoesqueleto que favorecem a movimentação dos IGs (LUHMANN; FUKUDA; KILB, 2015). De forma complementar, quando há acréscimo na expressão do cotransportador de KCl e consequente troca da característica do GABA de excitatório para inibitório há uma sinalização de parada da migração (INAMURA *et al.*, 2012). Interessantemente, alterações na expressão de REST já foram associadas com redução na expressão do cotransportador de KCl, adiando a troca de característica do GABA de excitatório para inibitório (CORRADINI et al., 2018), conforme visto no capítulo I. Dessa forma, é possível que

a alteração em $GABA_A$ também possa ser um resultado de alterações transcricionais, viabilizando um ambiente de desequilíbrio nas rotas de sinalização durante a vida embrionária que culmina em alterações no equilíbrio E/I durante a vida pós-natal.

Os aspectos hipocampais se destacam principalmente pela observação da progressão do dano entre as idades jovens e adultas. O surgimento de lesões relevantes, bem como as múltiplas alterações na composição de neurônios em diferentes sub-regiões demonstra a relevância de uma intervenção precoce para a preservação da funcionalidade dessa região encefálica. Além disso, o conjunto de dados apresentado sugere que a exposição prolongada a um prejuízo no equilíbrio E/I é capaz de causar danos estruturais no HC. Poucos estudos avaliam adultos com TEA; em relação ao HC nessa idade, especificamente, alguns trabalhos sugerem aumento de volume dessa região (MAIER *et al.*, 2015), além de acúmulo de metabólitos derivados de colina e creatina (SUZUKI *et al.*, 2010), porém há limitações de número amostral e representatividade da amostragem.

De forma geral, foi possível observar pontos importantes e que constituem elos plausíveis dentro da fisiopatologia do TEA ao longo dos capítulos. As alterações na vida intraútero evidenciadas pelo papel dos FTs e pelas análises de bancos de dados sustentam a hipótese de que alterações precoces na transcrição levam a diversos desequilíbrios metabólicos e nas dinâmicas de ciclo celular, aspectos fundamentais para células progenitoras. Além disso, as mudanças na composição neuronal, sinapses, receptores de GABA e proteínas de sinalização possivelmente refletem prejuízos principalmente no componente inibitório, condição que está de acordo com o apontado no TEA por diversas evidências da literatura (BELMONTE *et al.*, 2004; BRUINING *et al.*, 2020; GONÇALVES *et al.*, 2017). Assim, foi possível observar que a intervenção precoce representada pelo tratamento intraútero com RSV foi capaz de prevenir diversas alterações induzidas pela exposição ao VPA inclusive a longo prazo. Essa ação preventiva otimiza o entendimento de aspectos da fisiopatologia do TEA ao longo do desenvolvimento, contribuindo, através de uma perspectiva translacional, para a caracterização de pontos críticos na vida embrionária/fetal, jovem e adulta. Esse tipo de análise expande horizontes sobre intervenções específicas para cada idade, potencialmente embasando novas alternativas terapêuticas voltadas para a melhoria da qualidade de vida de indivíduos com TEA em diferentes faixas etárias.

4. CONSIDERAÇÕES FINAIS E CONCLUSÕES

No presente trabalho, buscou-se analisar, ao longo das etapas do desenvolvimento, diversos aspectos associados aos componentes inibitórios encefálicos no modelo animal de TEA induzido pela exposição pré-natal ao VPA, bem como aferir os potenciais efeitos preventivos do tratamento intraútero com RSV. Além disso, com o intuito de consolidar e fomentar hipóteses, foram utilizadas ferramentas de bioinformática como análises de bancos de dados e avaliação de rotas de interação, além de compilados de dados da literatura.

Através do Capítulo I, foi possível observar a relevância dos FTs no contexto de DNs, demonstrando suas rotas de expressão ao longo da vida intraútero, as principais regiões ou estruturas onde a expressão é mais relevante, bem como as principais rotas envolvidas com cada grupo de FTs. Além disso, a observação de que fatores de risco ambientais, como a exposição ao VPA, são capazes de alterar o padrão de expressão dos FTs, levando a danos teciduais e mudanças comportamentais relevantes, consolidou a análise dos FTs no contexto da fisiopatologia do TEA.

No Capítulo II, observou-se que a exposição pré-natal ao VPA induziu alterações críticas na estrutura do CPFm, modificando a composição neuronal dessa região, afetando não só neurônios totais como também IGs. Além disso, componentes sinápticos e o receptor $GABA_A$ também foram afetados nessa mesma região. No HC, o dano induzido foi proporcionalmente menor, porém, conforme observado posteriormente, já indicava possível prejuízo expandido a longo prazo. O tratamento com RSV foi capaz de prevenir uma ampla gama de alterações, especialmente no CPFm, ainda que nos componentes sinápticos alguns efeitos tenham tido similaridades com o VPA. Através da análise dos bancos de dados, bem como observando as informações compiladas no Capítulo I, foi possível traçar rotas possivelmente alteradas na vida embrionária/fetal, tais como o controle da maquinaria de transcrição, o metabolismo de carboidratos, via da WNT, via da NOTCH e outras possivelmente envolvidas nos danos observados em animais de P30.

No Capítulo III, o dano hipocampal induzido pela exposição pré-natal ao VPA apresenta uma importante expansão, inclusive sob um ponto de vista estrutural, com descontinuidade do GD e descompactação de CA1. Além disso, houve alterações

em IGs ao longo de todas as sub-regiões hipocampais, demonstrando um padrão de dano disseminado, ainda que GD tenha sido a região com maior evidência de prejuízos. Alterações em proteínas de sinalização celular também foram evidenciadas e, ainda que não se possa traçar paralelos diretos com outros resultados, é relevante notar esse outro aspecto de dano na idade adulta. Finalmente, o tratamento pré-natal com RSV foi capaz de trazer diversos benefícios, mitigando os danos estruturais e contribuindo para manutenção do equilíbrio na composição neuronal do HC.

De forma geral, é possível observar o papel protetor do RSV, tendo em vista que o tratamento foi capaz de prevenir diversas alterações induzidas pela exposição ao VPA a curto e longo prazo. Apesar de não ser uma estratégia terapêutica no presente formato, é importante observar o impacto positivo de uma intervenção precoce no contexto do TEA. No grupo de pesquisa, já existem dados demonstrando que a suplementação com RSV em crianças com TEA foi capaz de reverter a irritabilidade e, assim, trazer aumento considerável na qualidade de vida. Sendo assim, o RSV, ao apresentar características antioxidantes, anti-inflamatórias, neuroprotetoras e possivelmente reguladoras da transcrição (com efeito oposto ao VPA) tem um alto potencial no modelo VPA, contribuindo na elucidação de diversos componentes da fisiopatologia do TEA.

Figura 2: Visão geral dos dados obtidos ao longo do trabalho

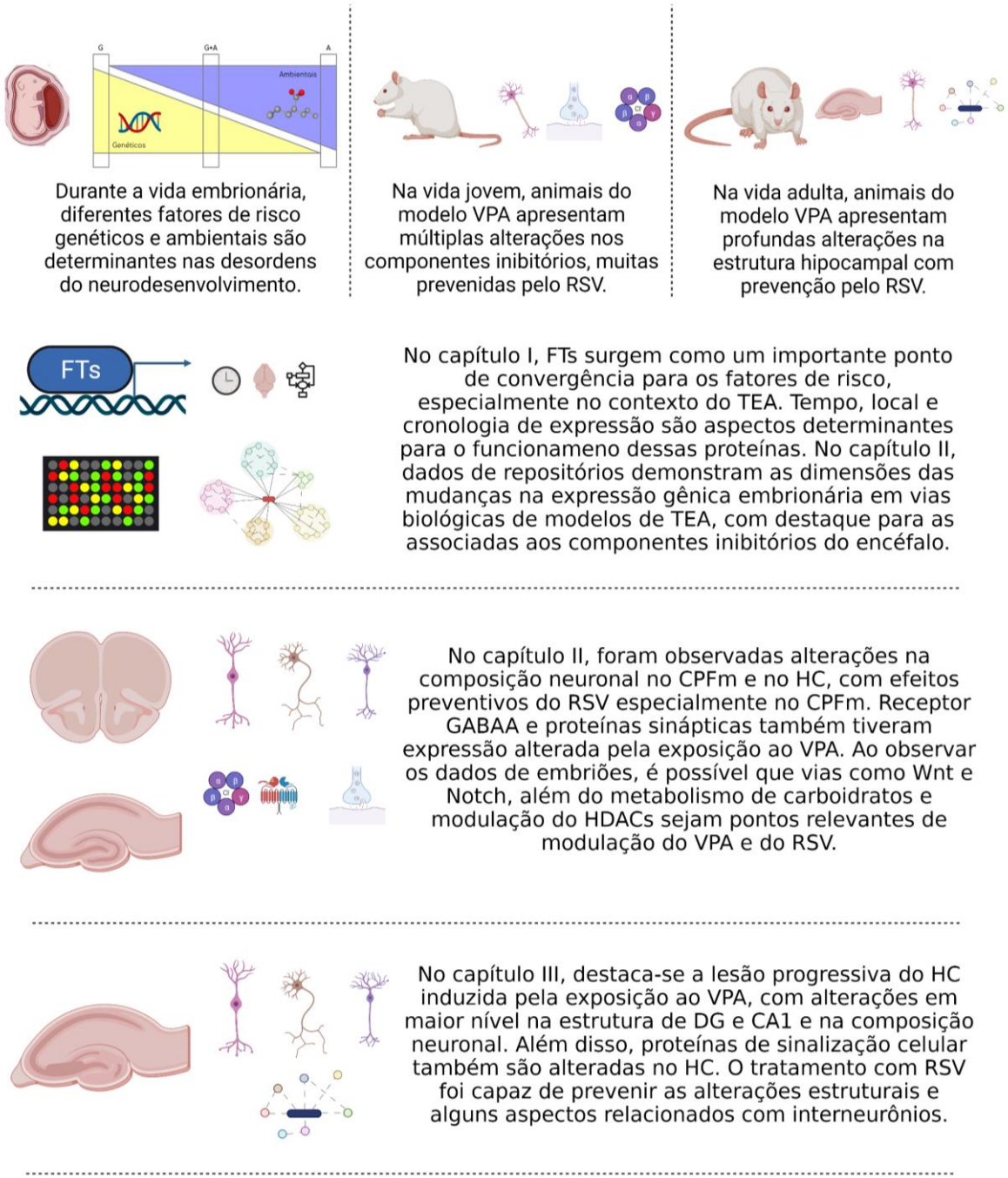

Compilado dos principais achados da presente tese, bem como as associações identificadas entre os diferentes capítulos.

5. PERSPECTIVAS

Em decorrência da pandemia de COVID-19 (do inglês, *coronavírus disease*), diversas etapas que inicialmente seriam contempladas na presente tese precisaram ser adiadas, levando ao surgimento de alternativas, especificamente ferramentas de bioinformática, que pudessem contemplar o desvio de planejamento original.

Observando que a exposição pré-natal ao VPA induz diversas alterações na vida pós-natal e tendo em vista que o tratamento com RSV intraútero é capaz de prevenir uma parte importante dessas alterações, estabelecem-se as seguintes perspectivas em diferentes etapas do desenvolvimento:

- Embriões removidos no dia gestacional 13,5 (E13,5):
    - Analisar, através de RT-qPCR (do inglês, *reverse transcription – quantitative real time polymerase chain reaction*), a expressão de FTs como DLX1, DLX2, DLX 5, DLX6; ARX; SOX6, LHX6 e TCF4;
    - Analisar, através de RT-qPCR a expressão da citocina CXCL12 bem como do receptor CXCR4;
    - Analisar a proliferação e início da migração de IGs através da marcação com BrdU (bromodeoxiuridina) em regiões como a EG.
- Fetos removidos no dia gestacional 19 (E19):
    - Analisar, através de RT-qPCR a expressão de FTs como DLX1, DLX2, DLX 5, DLX6; ARX; SOX6, LHX6 e TCF4;
    - Analisar, através de RT-qPCR a expressão da citocina CXCL12 bem como do receptor CXCR4;
    - Analisar, através de imunofluorescência, a distribuição dos IGs CB+, PV+ e SOM+ ao longo de diferentes regiões encefálicas;
    - Analisar, através de imunofluorescência, a expressão das enzimas GAD65 e GAD67
    - Analisar, através de imunofluorescência, a constituição das camadas corticais, utilizando marcadores específicos para cada camada;
    - Analisar, através de *western blotting*, o conteúdo proteico de proteínas envolvidas nas vias da WNT e da NOTCH em diferentes regiões encefálicas;
    - Analisar, através de HPLC (do inglês, *high-pressure liquid chromatography*), o conteúdo de neurotransmissores GABA e glutamato em diferentes regiões encefálicas.
- Animais com 30 dias (P30):
    - Analisar, através de microinjeção, a morfologia dos IGs CB+, PV+ e SOM+;
    - Analisar, através de imunofluorescência, a distribuição de IGs em outras regiões encefálicas como a região da amígdala e o estriado;

- Analisar, através de ensaios enzimáticos, a atividade das enzimas GAD65 e GAD67;
- Analisar, através de imunofluorescência, a distribuição de sinapses inibitórias e excitatórias em diferentes regiões encefálicas;
- Analisar, através de *western blotting*, a expressão de proteínas envolvidas com as vidas da WNT e NOTCH em diferentes regiões encefálicas.

- Animais com 120 dias (P120)
  - Analisar, através de imunofluorescência, parâmetros de apoptose no HC;
  - Analisar, através de análises eletrofisiológicas *in vitro* e *in vivo*, possíveis alterações no equilíbrio E/I;
  - Analisar, através de testes comportamentais, aspectos de memória espacial, social e de trabalho;
  - Finalizar as análises de IGs no CPFm.

REFERÊNCIAS BIBLIOGRÁFICAS

ABBAS, Atheir I. *et al.* Somatostatin Interneurons Facilitate Hippocampal-Prefrontal Synchrony and Prefrontal Spatial Encoding. **Neuron**, [*s. l.*], v. 100, n. 4, p. 926-939.e3, 2018. Disponível em: https://doi.org/10.1016/j.neuron.2018.09.029. Acesso em: 20 nov. 2019.

ABE, P. *et al.* Intermediate Progenitors Facilitate Intracortical Progression of Thalamocortical Axons and Interneurons through CXCL12 Chemokine Signaling. **Journal of Neuroscience**, [*s. l.*], v. 35, n. 38, p. 13053–13063, 2015. Disponível em: https://doi.org/10.1523/JNEUROSCI.1488-15.2015

AHMAD, Sheikh F. *et al.* Adenosine A2A receptor signaling affects IL-21/IL-22 cytokines and GATA3/T-bet transcription factor expression in CD4+ T cells from a BTBR T+ Itpr3tf/J mouse model of autism. **Journal of Neuroimmunology**, [*s. l.*], v. 311, p. 59–67, 2017. Disponível em: https://doi.org/10.1016/j.jneuroim.2017.08.002. Acesso em: 17 dez. 2020.

AHMAD, Sheikh F. *et al.* Downregulation in Helios transcription factor signaling is associated with immune dysfunction in blood leukocytes of autistic children. **Progress in Neuro-Psychopharmacology and Biological Psychiatry**, [*s. l.*], v. 85, p. 98–104, 2018a. Disponível em: https://doi.org/10.1016/j.pnpbp.2018.04.011. Acesso em: 16 dez. 2020.

AHMAD, Sheikh F. *et al.* Protection by tyrosine kinase inhibitor, tyrphostin AG126, through the suppression of IL-17A, RORγt, and T-bet signaling, in the BTBR mouse model of autism. **Brain Research Bulletin**, [*s. l.*], v. 142, p. 328–337, 2018b. Disponível em: https://doi.org/10.1016/j.brainresbull.2018.08.020. Acesso em: 17 dez. 2020.

AHMAD, Sheikh F. *et al.* Resveratrol attenuates pro-inflammatory cytokines and activation of JAK1-STAT3 in BTBR T+ Itpr3tf/J autistic mice. **European Journal of Pharmacology**, [*s. l.*], v. 829, p. 70–78, 2018c. Disponível em: https://doi.org/10.1016/j.ejphar.2018.04.008. Acesso em: 17 dez. 2020.

AHMAD, Sheikh F. *et al.* Resveratrol attenuates pro-inflammatory cytokines and activation of JAK1-STAT3 in BTBR T + Itpr3 tf/J autistic mice. **European journal of pharmacology**, [*s. l.*], v. 829, p. 70–78, 2018d. Disponível em: https://doi.org/10.1016/J.EJPHAR.2018.04.008. Acesso em: 14 mar. 2022.

AHMAD, Sheikh F. *et al.* S3I-201, a selective Stat3 inhibitor, restores neuroimmune

function through upregulation of Treg signaling in autistic BTBR T+ Itpr3tf/J mice. **Cellular Signalling**, [*s. l.*], v. 52, p. 127–136, 2018e. Disponível em: https://doi.org/10.1016/j.cellsig.2018.09.006. Acesso em: 17 dez. 2020.

AHMAD, Sheikh Fayaz *et al.* Dysregulation of Th1, Th2, Th17, and T regulatory cell-related transcription factor signaling in children with autism. **Molecular Neurobiology**, [*s. l.*], v. 54, n. 6, p. 4390–4400, 2017. Disponível em: https://doi.org/10.1007/s12035-016-9977-0. Acesso em: 16 dez. 2020.

AMERICAN PSYCHIATRIC. **DSM 5**. [*S. l.: s. n.*], 2013. ISSN 2317-1782. Disponível em: https://doi.org/10.1176/appi.books.9780890425596.744053

AMIEL, Jeanne *et al.* Mutations in TCF4, encoding a class I basic helix-loop-helix transcription factor, are responsible for Pitt-Hopkins syndrome, a severe epileptic encephalopathy associated with autonomic dysfunction. **American Journal of Human Genetics**, [*s. l.*], v. 80, n. 5, p. 988–993, 2007. Disponível em: https://doi.org/10.1086/515582. Acesso em: 16 dez. 2020.

ANASTASIADES, Paul G.; CARTER, Adam G. Circuit organization of the rodent medial prefrontal cortex. **Trends in Neurosciences**, [*s. l.*], v. 44, n. 7, p. 550–563, 2021. Disponível em: https://doi.org/10.1016/J.TINS.2021.03.006. Acesso em: 14 mar. 2022.

ANDERSON, S. A. *et al.* Interneuron migration from basal forebrain to neocortex: Dependence on Dlx genes. **Science**, [*s. l.*], v. 278, n. 5337, p. 474–476, 1997. Disponível em: https://doi.org/10.1126/science.278.5337.474

ANGELOZZI, M.; LEFEBVRE, Véronique. SOXopathies: growing family of developmental disorders due to SOX mutations. **Trends in genetics:TIG**, [*s. l.*], v. 35, n. 9, p. 658, 2019. Disponível em: https://doi.org/10.1016/J.TIG.2019.06.003. Acesso em: 14 mar. 2022.

ANSARI, Mushtaq A. *et al.* Adenosine A2A receptor modulates neuroimmune function through Th17/retinoid-related orphan receptor gamma t (RORγt) signaling in a BTBR T+ Itpr3tf/J mouse model of autism. **Cellular Signalling**, [*s. l.*], v. 36, p. 14–24, 2017. Disponível em: https://doi.org/10.1016/j.cellsig.2017.04.014. Acesso em: 17 dez. 2020.

ANTONOUDIOU, Pantelis *et al.* Parvalbumin and Somatostatin Interneurons Contribute to the Generation of Hippocampal Gamma Oscillations. **Journal of Neuroscience**, [*s. l.*], v. 40, n. 40, p. 7668–7687, 2020. Disponível em: https://doi.org/10.1523/JNEUROSCI.0261-20.2020. Acesso em: 14 mar. 2022.

APPS, Matthew A.J.; RUSHWORTH, Matthew F.S.; CHANG, Steve W.C. The Anterior Cingulate Gyrus and Social Cognition: Tracking the Motivation of Others. **Neuron**, [*s. l.*], v. 90, n. 4, p. 692, 2016. Disponível em: https://doi.org/10.1016/J.NEURON.2016.04.018. Acesso em: 14 mar. 2022.

ARDINGER, H. H. *et al.* Verification of the fetal valproate syndrome phenotype. **American Journal of Medical Genetics**, [*s. l.*], v. 29, n. 1, p. 171–185, 1988. Disponível em: https://doi.org/10.1002/AJMG.1320290123. Acesso em: 13 mar. 2022.

ARONNE, María Paula *et al.* Prenatal ethanol exposure reduces the expression of the transcriptional factor Pax6 in the developing rat brain. **Annals of the New York Academy of Sciences**. [*S. l.*]: Blackwell Publishing Inc., 2008. v. 1139, p. 478–498. Disponível em: https://doi.org/10.1196/annals.1432.006. Acesso em: 16 dez. 2020.

ARONOFF, Eyal; HILLYER, Robert; LEON, Michael. Environmental Enrichment Therapy for Autism: Outcomes with Increased Access. **Neural Plasticity**, [*s. l.*], v. 2016, p. e2734915. Disponível em: https://doi.org/10.1155/2016/2734915. Acesso em: 14 mar. 2022.

ARTINIAN, Julien *et al.* Regulation of Hippocampal Memory by mTORC1 in Somatostatin Interneurons. **Journal of Neuroscience**, [*s. l.*], v. 39, n. 43, p. 8439–8456, 2019. Disponível em: https://doi.org/10.1523/JNEUROSCI.0728-19.2019. Acesso em: 14 mar. 2022.

ASCOLI, Giorgio A. *et al.* Petilla terminology: nomenclature of features of GABAergic interneurons of the cerebral cortex. **Nature reviews. Neuroscience**, [*s. l.*], v. 9, n. 7, p. 557–568, 2008. Disponível em: https://doi.org/10.1038/NRN2402. Acesso em: 14 mar. 2022.

ASPERGER, Hans. Die „Autistischen Psychopathen” im Kindesalter. **Archiv für Psychiatrie und Nervenkrankheiten 1944 117:1**, [*s. l.*], v. 117, n. 1, p. 76–136, 1944. Disponível em: https://doi.org/10.1007/BF01837709. Acesso em: 13 mar. 2022.

AYLWARD, E. H. *et al.* Effects of age on brain volume and head circumference in autism. **Neurology**, [*s. l.*], v. 59, n. 2, p. 175–183, 2002. Disponível em: https://doi.org/10.1212/WNL.59.2.175. Acesso em: 14 mar. 2022.

BAKHEET, Saleh A. *et al.* Resveratrol Ameliorates Dysregulation of Th1, Th2, Th17, and T Regulatory Cell-Related Transcription Factor Signaling in a BTBR T + tf/J

Mouse Model of Autism. **Molecular Neurobiology**, [*s. l.*], v. 54, n. 7, p. 5201–5212, 2017. Disponível em: https://doi.org/10.1007/s12035-016-0066-1. Acesso em: 17 dez. 2020.

BAKHEET, Saleh A. *et al.* Resveratrol treatment attenuates chemokine receptor expression in the BTBR T+tf/J mouse model of autism. **Molecular and cellular neurosciences**, [*s. l.*], v. 77, p. 1–10, 2016. Disponível em: https://doi.org/10.1016/J.MCN.2016.09.004. Acesso em: 14 mar. 2022.

BAMBINI-JUNIOR, Victorio *et al.* Animal model of autism induced by prenatal exposure to valproate: Behavioral changes and liver parameters. **Brain Research**, [*s. l.*], v. 1408, p. 8–16, 2011. Disponível em: https://doi.org/10.1016/j.brainres.2011.06.015

BAMBINI-JUNIOR, Victorio *et al.* Resveratrol prevents social deficts in animal model of autism induced by valproic acid. **Neuroscience Letters**, [*s. l.*], v. 583, p. 176–181, 2014. Disponível em: https://doi.org/10.1016/j.neulet.2014.09.039

BANERJEE, Anwesha *et al.* Impairment of cortical GABAergic synaptic transmission in an environmental rat model of autism. **The international journal of neuropsychopharmacology**, [*s. l.*], v. 16, n. 6, p. 1309–1318, 2013. Disponível em: https://doi.org/10.1017/S1461145712001216. Acesso em: 14 mar. 2022.

BANKER, Sarah M. *et al.* Hippocampal contributions to social and cognitive deficits in autism spectrum disorder. **Trends in Neurosciences**, [*s. l.*], v. 44, n. 10, p. 793–807, 2021. Disponível em: https://doi.org/10.1016/J.TINS.2021.08.005. Acesso em: 14 mar. 2022.

BARATA, João T. The impact of PTEN regulation by CK2 on PI3K-dependent signaling and leukemia cell survival. **Advances in enzyme regulation**, [*s. l.*], v. 51, n. 1, p. 37–49, 2011. Disponível em: https://doi.org/10.1016/J.ADVENZREG.2010.09.012. Acesso em: 14 mar. 2022.

BARON-COHEN, Simon. The truth about Hans Asperger's Nazi collusion. **Nature**, [*s. l.*], v. 557, n. 7705, p. 305–306, 2018. Disponível em: https://doi.org/10.1038/D41586-018-05112-1

BARON-COHEN, Simon *et al.* Why Are Autism Spectrum Conditions More Prevalent in Males? **PLOS Biology**, [*s. l.*], v. 9, n. 6, p. e1001081, 2011. Disponível em: https://doi.org/10.1371/JOURNAL.PBIO.1001081. Acesso em: 13 mar. 2022.

BASAVARAJAPPA, Balapal S.; SUBBANNA, Shivakumar. Epigenetic Mechanisms in Developmental Alcohol-Induced Neurobehavioral Deficits. **Brain Sciences**

2016, Vol. 6, Page 12, [*s. l.*], v. 6, n. 2, p. 12, 2016. Disponível em: https://doi.org/10.3390/BRAINSCI6020012. Acesso em: 13 mar. 2022.

BATISTA-BRITO, Renata *et al.* The Cell-Intrinsic Requirement of Sox6 for Cortical Interneuron Development. **Neuron**, [*s. l.*], v. 63, n. 4, p. 466–481, 2009. Disponível em: https://doi.org/10.1016/j.neuron.2009.08.005

BEDOGNI, Francesco *et al.* Tbr1 regulates regional and laminar identity of postmitotic neurons in developing neocortex. **Proceedings of the National Academy of Sciences of the United States of America**, [*s. l.*], v. 107, n. 29, p. 13129–13134, 2010. Disponível em: https://doi.org/10.1073/pnas.1002285107. Acesso em: 16 dez. 2020.

BELMONTE, Matthew K *et al.* Autism and abnormal development of brain connectivity. **The Journal of Neuroscience**, [*s. l.*], v. 24, n. 42, p. 9228–9231, 2004. Disponível em: https://doi.org/10.1523/JNEUROSCI.3340-04.2004

BEN-REUVEN, Lihi; REINER, Orly. Dynamics of cortical progenitors and production of subcerebral neurons are altered in embryos of a maternal inflammation model for autism. **Molecular Psychiatry**, [*s. l.*], v. 26, n. 5, p. 1535-1550, 2019. Disponível em: https://doi.org/10.1038/s41380-019-0594-y. Acesso em: 16 dez. 2020.

BERGER, Brynn E.; NAVAR-BOGGAN, Ann Marie; OMER, Saad B. Congenital rubella syndrome and autism spectrum disorder prevented by rubella vaccination - United States, 2001-2010. **BMC Public Health**, [*s. l.*], v. 11, n. 1, p. 1–5, 2011. Disponível em: https://doi.org/10.1186/1471-2458-11-340/TABLES/3. Acesso em: 13 mar. 2022.

BHATTI, Jasvinder Singh; BHATTI, Gurjit Kaur; REDDY, P. Hemachandra. Mitochondrial dysfunction and oxidative stress in metabolic disorders - A Step towards mitochondria based therapeutic strategies. **Biochimica et biophysica acta**, [*s. l.*], v. 1863, n. 5, p. 1066, 2017. Disponível em: https://doi.org/10.1016/J.BBADIS.2016.11.010. Acesso em: 14 mar. 2022.

BIENVENU, Thomas C.M. *et al.* Cell-Type-Specific Recruitment of Amygdala Interneurons to Hippocampal Theta Rhythm and Noxious Stimuli In Vivo. **Neuron**, [*s. l.*], v. 74, n. 6, p. 1059–1074, 2012. Disponível em: https://doi.org/10.1016/J.NEURON.2012.04.022

BLEULER, M.; BLEULER, R. Dementia praecox oder die Gruppe der Schizophrenien: Eugen Bleuler. **The British journal of psychiatry : the**

journal of mental science, [*s. l.*], v. 149, p. 661–662, 1986. Disponível em: https://doi.org/10.1192/BJP.149.5.661. Acesso em: 13 mar. 2022.

BOKSA, Patricia *et al.* Early Development of Parvalbumin-, Somatostatin-, and Cholecystokinin-Expressing Neurons in Rat Brain following Prenatal Immune Activation and Maternal Iron Deficiency. **Developmental Neuroscience**, [*s. l.*], v. 38, n. 5, p. 342–353, 2016. Disponível em: https://doi.org/10.1159/000454677. Acesso em: 14 mar. 2022.

BONNEFONT-ROUSSELOT, Dominique. Resveratrol and Cardiovascular Diseases. **Nutrients**, [*s. l.*], v. 8, n. 5, p. 250-274, 2016. Disponível em: https://doi.org/10.3390/NU8050250. Acesso em: 14 mar. 2022.

BRIMBERG, L. *et al.* Brain-reactive IgG correlates with autoimmunity in mothers of a child with an autism spectrum disorder. **Molecular Psychiatry 2013 18:11**, [*s. l.*], v. 18, n. 11, p. 1171–1177, 2013. Disponível em: https://doi.org/10.1038/mp.2013.101. Acesso em: 13 mar. 2022.

BRISTOT SILVESTRIN, Roberta *et al.* Animal model of autism induced by prenatal exposure to valproate: Altered glutamate metabolism in the hippocampus. **Brain Research**, [*s. l.*], v. 1495, p. 52–60, 2013b. Disponível em: https://doi.org/10.1016/j.brainres.2012.11.048. Acesso em: 24 maio 2021.

BROCKSCHMIDT, Antje *et al.* Severe mental retardation with breathing abnormalities (Pitt - Hopkins syndrome) is caused by haploinsufficiency of the neuronal bHLH transcription factor TCF4. **Human Molecular Genetics**, [*s. l.*], v. 16, n. 12, p. 1488–1494, 2007. Disponível em: https://doi.org/10.1093/hmg/ddm099. Acesso em: 16 dez. 2020.

BROWN, Alan S.; CONWAY, Fiona. Maternal Immune Activation and Related Factors in the Risk of Offspring Psychiatric Disorders. **Frontiers in Psychiatry**, [*s. l.*], v. 10, n. MAY, p. 430, 2019. Disponível em: https://doi.org/10.3389/FPSYT.2019.00430. Acesso em: 13 mar. 2022.

BROWN, J. A. *et al.* Inhibition of parvalbumin-expressing interneurons results in complex behavioral changes. **Molecular Psychiatry 2015 20:12**, [*s. l.*], v. 20, n. 12, p. 1499–1507, 2015. Disponível em: https://doi.org/10.1038/mp.2014.192. Acesso em: 14 mar. 2022.

BRUINING, Hilgo *et al.* Measurement of excitation-inhibition ratio in autism spectrum disorder using critical brain dynamics. **Scientific Reports 2020 10:1**, [*s. l.*], v. 10, n. 1, p. 1–15, 2020. Disponível em: https://doi.org/10.1038/s41598-020-

65500-4. Acesso em: 9 jul. 2021.

BUCKMASTER, Paul S. *et al.* Heightened seizure severity in somatostatin knockout mice. **Epilepsy Research**, [*s. l.*], v. 48, n. 1–2, p. 43–56, 2002. Disponível em: https://doi.org/10.1016/S0920-1211(01)00318-7

BURNS, Jennifer *et al.* Plant foods and herbal sources of resveratrol. **Journal of agricultural and food chemistry**, [*s. l.*], v. 50, n. 11, p. 3337–3340, 2002. Disponível em: https://doi.org/10.1021/JF0112973. Acesso em: 14 mar. 2022.

BURNSTOCK, Geoffrey; DALE, Nicholas. Purinergic signalling during development and ageing. **Purinergic Signalling**, [*s. l.*], v. 11, n. 3, p. 277, 2015. Disponível em: https://doi.org/10.1007/S11302-015-9452-9. Acesso em: 14 mar. 2022.

BUTT, Simon J B *et al.* The temporal and spatial origins of cortical interneurons predict their physiological subtype. **Neuron**, [*s. l.*], v. 48, n. 4, p. 591–604, 2005. Disponível em: https://doi.org/10.1016/j.neuron.2005.09.034. Acesso em: 29 nov. 2019.

CALFA, Gaston *et al.* Excitation/inhibition imbalance and impaired synaptic inhibition in hippocampal area CA3 of Mecp2 knockout mice. **Hippocampus**, [*s. l.*], v. 25, n. 2, p. 159–168, 2015. Disponível em: https://doi.org/10.1002/hipo.22360. Acesso em: 16 dez. 2020.

CANALES, Cesar P. *et al.* Sequential perturbations to mouse corticogenesis following in utero maternal immune activation. **eLife**, [*s. l.*], v. 10, 2021. Disponível em: https://doi.org/10.7554/ELIFE.60100

CAPUZZO, Giulia; FLORESCO, Stan B. Prelimbic and Infralimbic Prefrontal Regulation of Active and Inhibitory Avoidance and Reward-Seeking. **Journal of Neuroscience**, [*s. l.*], v. 40, n. 24, p. 4773–4787, 2020. Disponível em: https://doi.org/10.1523/JNEUROSCI.0414-20.2020. Acesso em: 14 mar. 2022.

CARDOSO-MOREIRA, Margarida *et al.* Gene expression across mammalian organ development. **Nature**, [*s. l.*], v. 571, n. 7766, p. 505-509, 2019. Disponível em: https://doi.org/10.1038/s41586-019-1338-5

CARRIERE, Candace H. *et al.* The γ-protocadherins regulate the survival of GABAergic interneurons during developmental cell death. **Journal of Neuroscience**, [*s. l.*], v. 40, n. 45, p. 8652–8668, 2020. Disponível em: https://doi.org/10.1523/JNEUROSCI.1636-20.2020. Acesso em: 14 maio 2021.

CARTER, Dawn S. *et al.* Long-term decrease in calbindin-D28K expression in the hippocampus of epileptic rats following pilocarpine-induced status epilepticus.

Epilepsy Research, [*s. l.*], v. 79, n. 2–3, p. 213–223, 2008. Disponível em: https://doi.org/10.1016/J.EPLEPSYRES.2008.02.006

CASTRO, Olagide W. *et al.* Resveratrol for easing status epilepticus induced brain injury, inflammation, epileptogenesis, and cognitive and memory dysfunction-Are we there yet? **Frontiers Media S.A.**, v. 13, n. 8, p. 603-615, 2017. Disponível em: https://doi.org/10.3389/fneur.2017.00603. Acesso em: 14 maio 2021.

CAVALLI, Giacomo; HEARD, Edith. Advances in epigenetics link genetics to the environment and disease. **Nature 2019 571:7766**, [*s. l.*], v. 571, n. 7766, p. 489–499, 2019. Disponível em: https://doi.org/10.1038/s41586-019-1411-0. Acesso em: 13 mar. 2022.

CHADDAD, Ahmad *et al.* Hippocampus and amygdala radiomic biomarkers for the study of autism spectrum disorder. **BMC Neuroscience**, [*s. l.*], v. 18, n. 1, p. 1–12, 2017. Disponível em: https://doi.org/10.1186/S12868-017-0373-0/FIGURES/5. Acesso em: 14 mar. 2022.

CHANG, Chia Yuan *et al.* Akting up in the GABA hypothesis of schizophrenia: Akt1 deficiency modulates GABAergic functions and hippocampus-dependent functions. **Scientific Reports**, [*s. l.*], v. 6, p. e33095, 2016. Disponível em: https://doi.org/10.1038/srep33095. Acesso em: 14 maio 2021.

CHAO, Sung Chuan *et al.* Induction of sirtuin-1 signaling by resveratrol induces human chondrosarcoma cell apoptosis and exhibits antitumor activity. **Scientific Reports 2017**, [*s. l.*], v. 7, n. 1, p. 1–11, 2017. Disponível em: https://doi.org/10.1038/s41598-017-03635-7. Acesso em: 14 mar. 2022.

CHEN, Gang *et al.* Semaphorin-3A guides radial migration of cortical neurons during development. **Nature neuroscience**, [*s. l.*], v. 11, n. 1, p. 36–44, 2008. Disponível em: https://doi.org/10.1038/NN2018. Acesso em: 14 mar. 2022.

CHEN, Guang *et al.* The mood-stabilizing agent valproate inhibits the activity of glycogen synthase kinase-3. **Journal of neurochemistry**, [*s. l.*], v. 72, n. 3, p. 1327–1330, 1999. Disponível em: https://doi.org/10.1046/J.1471-4159.2000.0721327.X. Acesso em: 14 mar. 2022.

CHEN, Tianda *et al.* Tcf4 controls neuronal migration of the cerebral cortex through regulation of Bmp7. **Frontiers in Molecular Neuroscience**, [*s. l.*], v. 9, n. OCT2016, p. 94, 2016. Disponível em: https://doi.org/10.3389/FNMOL.2016.00094/BIBTEX

CHEN, Xiao Fen *et al.* Transcriptional regulation and its misregulation in Alzheimer's disease. **Molecular Brain**, [*s. l.*], v. 6, n. 1, p. 44, 2013. Disponível em: https://doi.org/10.1186/1756-6606-6-44. Acesso em: 14 mar. 2022.

CHEN, Yen Ju *et al.* Genome-wide integrative analysis of circular RNA dysregulation and the corresponding circular RNA-microRNA-mRNA regulatory axes in autism. **Genome Research**, [*s. l.*], v. 30, n. 3, p. gr.255463.119, 2020. Disponível em: https://doi.org/10.1101/GR.255463.119. Acesso em: 13 mar. 2022.

CHESS, Stella. Autism in children with congenital rubella. **Journal of autism and childhood schizophrenia**, [*s. l.*], v. 1, n. 1, p. 33–47, 1971. Disponível em: https://doi.org/10.1007/BF01537741. Acesso em: 13 mar. 2022.

CHRISTENSEN, Jakob *et al.* Prenatal Valproate Exposure and Risk of Autism Spectrum Disorders and Childhood Autism. **JAMA**, [*s. l.*], v. 309, n. 16, p. 1696, 2013. Disponível em: https://doi.org/10.1001/jama.2013.2270

CHRISTIANSON, Arnold L.; CHESTER, Nicole; KROMBERG, Jennifer G.R. Fetal Valproate Syndrome: Clinical and Neuro-developmental Features in Two Sibling Pairs. **Developmental Medicine & Child Neurology**, [*s. l.*], v. 36, n. 4, p. 361–369, 1994. Disponível em: https://doi.org/10.1111/J.1469-8749.1994.TB11858.X. Acesso em: 13 mar. 2022.

CHUI, Angela *et al.* Oxidative stress regulates progenitor behavior and cortical neurogenesis. **Development (Cambridge, England)**, [*s. l.*], v. 147, n. 5, 2020. Disponível em: https://doi.org/10.1242/DEV.184150. Acesso em: 14 mar. 2022.

COGILL, Steven B. *et al.* Co-expression of long non-coding RNAs and autism risk genes in the developing human brain. **BMC Systems Biology**, [*s. l.*], v. 12, n. Suppl 7, 2018. Disponível em: https://doi.org/10.1186/S12918-018-0639-X. Acesso em: 13 mar. 2022.

CONTET, Candice. Gene Expression Under the Influence: Transcriptional Profiling of Ethanol in the Brain. **Current psychopharmacology**, [*s. l.*], v. 1, n. 4, p. 301, 2012. Disponível em: https://doi.org/10.2174/2211556011201040301. Acesso em: 14 mar. 2022.

CONTRERAS, April; HINES, Dustin J.; HINES, Rochelle M. Molecular specialization of GABAergic synapses on the soma and axon in cortical and hippocampal circuit function and dysfunction. **Frontiers in Molecular Neuroscience**, [*s. l.*], v. 12, p. 154, 2019. Disponível em:

https://doi.org/10.3389/FNMOL.2019.00154/BIBTEX

CORNFORD, Eain M.; DIEP, Cynthia P.; PARDRIDGE, William M. Blood–Brain Barrier Transport of Valproic Acid. **Journal of Neurochemistry**, [*s. l.*], v. 44, n. 5, p. 1541–1550, 1985. Disponível em: https://doi.org/10.1111/J.1471-4159.1985.TB08793.X. Acesso em: 13 mar. 2022.

CORRADINI, Irene *et al.* Maternal Immune Activation Delays Excitatory-to-Inhibitory Gamma-Aminobutyric Acid Switch in Offspring. **Biological Psychiatry**, [*s. l.*], v. 83, n. 8, p. 680–691, 2018. Disponível em: https://doi.org/10.1016/j.biopsych.2017.09.030. Acesso em: 16 dez. 2020.

COURCHESNE, Eric *et al.* Neuron number and size in prefrontal cortex of children with autism. **JAMA**, [*s. l.*], v. 306, n. 18, p. 2001–2010, 2011. Disponível em: https://doi.org/10.1001/JAMA.2011.1638. Acesso em: 14 mar. 2022.

CUI, Kangli *et al.* Neurodevelopmental impairment induced by prenatal valproic acid exposure shown with the human cortical organoid-on-a-chip model. **Microsystems & nanoengineering**, [*s. l.*], v. 6, n. 1, 2020. Disponível em: https://doi.org/10.1038/S41378-020-0165-Z. Acesso em: 3 mar. 2022.

CUMMINGS, Kirstie A.; CLEM, Roger L. Prefrontal somatostatin interneurons encode fear memory. **Nature neuroscience**, [*s. l.*], v. 23, n. 1, p. 61–74, 2020. Disponível em: https://doi.org/10.1038/S41593-019-0552-7. Acesso em: 14 mar. 2022.

CUPOLILLO, Dario *et al.* Autistic-like traits and cerebellar dysfunction in purkinje cell PTEN knock-out mice. **Neuropsychopharmacology**, [*s. l.*], 2016. Disponível em: https://doi.org/10.1038/npp.2015.339

CZECH, Herwig. Hans Asperger, National Socialism, and “race hygiene” in Nazi-era Vienna. **Molecular Autism**, [*s. l.*], v. 9, n. 1, p. 1–43, 2018. Disponível em: https://doi.org/10.1186/S13229-018-0208-6/FIGURES/10. Acesso em: 13 mar. 2022.

D’ARGEMBEAU, Arnaud *et al.* Distinct regions of the medial prefrontal cortex are associated with self-referential processing and perspective taking. **Journal of cognitive neuroscience**, [*s. l.*], v. 19, n. 6, p. 935–944, 2007. Disponível em: https://doi.org/10.1162/JOCN.2007.19.6.935. Acesso em: 14 mar. 2022.

DAI, Shuyan *et al.* Structural Basis for DNA Recognition by FOXG1 and the Characterization of Disease-causing FOXG1 Mutations. **Journal of molecular biology**, [*s. l.*], v. 432, n. 23, p. 6146–6156, 2020. Disponível em:

https://doi.org/10.1016/J.JMB.2020.10.007. Acesso em: 14 mar. 2022.

DAMAJ, Lena *et al.* CACNA1A haploinsufficiency causes cognitive impairment, autism and epileptic encephalopathy with mild cerebellar symptoms. **European journal of human genetics : EJHG**, [*s. l.*], v. 23, n. 11, p. 1505–1512, 2015. Disponível em: https://doi.org/10.1038/EJHG.2015.21. Acesso em: 13 mar. 2022.

DANZER, Steve C. Valproic Acid Leads New Neurons Down the Wrong Path. **Epilepsy Currents**, [*s. l.*], v. 19, n.2. p.132, 2019. Disponível em: https://doi.org/10.1177/1535759719835366

DE OLIVEIRA PEREIRA RIBEIRO, Lucas *et al.* Evidence for Association Between OXTR Gene and ASD Clinical Phenotypes. **Journal of Molecular Neuroscience**, [*s. l.*], v. 65, n. 2, p. 213–221, 2018. Disponível em: https://doi.org/10.1007/s12031-018-1088-0. Acesso em: 16 dez. 2020.

DE SÁ COUTINHO, Diego *et al.* Anti-Inflammatory Effects of Resveratrol: Mechanistic Insights. **International journal of molecular sciences**, [*s. l.*], v. 19, n. 6, p. e1812, 2018. Disponível em: https://doi.org/10.3390/IJMS19061812. Acesso em: 14 mar. 2022.

DECKMANN, Iohanna *et al.* Neuroimmune Alterations in Autism: A Translational Analysis Focusing on the Animal Model of Autism Induced by Prenatal Exposure to Valproic Acid. **Neuroimmunomodulation**, [*s. l.*], v. 25, n. 5–6, p. 285–299, 2018. Disponível em: https://doi.org/10.1159/000492113. Acesso em: 16 dez. 2020.

DECKMANN, Iohanna *et al.* Resveratrol prevents brain edema, blood–brain barrier permeability, and altered aquaporin profile in autism animal model. **International Journal of Developmental Neuroscience**, [*s. l.*], v. 81, n. 7, p. 579–604, 2021. Disponível em: https://doi.org/10.1002/JDN.10137. Acesso em: 3 mar. 2022.

DEKKERS, Laura M.S. *et al.* Prevalence of Autism Spectrum Disorders in Ecuador: A Pilot Study in Quito. **Journal of autism and developmental disorders**, [*s. l.*], v. 45, n. 12, p. 4165–4173, 2015. Disponível em: https://doi.org/10.1007/S10803-015-2559-6. Acesso em: 13 mar. 2022.

DEL RÍO, María R.; DEFELIPE, Javier. A light and electron microscopic study of calbindin D-28k immunoreactive double bouquet cells in the human temporal cortex. **Brain research**, [*s. l.*], v. 690, n. 1, p. 133–140, 1995. Disponível em:

https://doi.org/10.1016/0006-8993(95)00641-3. Acesso em: 14 mar. 2022.

DENG, Xiaofei *et al.* Parvalbumin interneuron in the ventral hippocampus functions as a discriminator in social memory. **Proceedings of the National Academy of Sciences of the United States of America**, [*s. l.*], v. 116, n. 33, p.16583-16592, 2019. Disponível em: https://doi.org/10.1073/pnas.1819133116

DESTEFANO, Frank; SHIMABUKURO, Tom T. The MMR Vaccine and Autism. **Annual review of virology**, [*s. l.*], v. 6, n. 1, p. 585, 2019. Disponível em: https://doi.org/10.1146/ANNUREV-VIROLOGY-092818-015515. Acesso em: 13 mar. 2022.

DI VIRGILIO, Francesco *et al.* Purinergic signalling in inflammation of the central nervous system. **Trends in Neurosciences**, [*s. l.*], v. 32, n. 2, p. 79–87, 2009. Disponível em: https://doi.org/10.1016/J.TINS.2008.11.003. Acesso em: 14 mar. 2022.

DICKINSON, R *et al.* Materno-fetal pharmacokinetics and fetal distribution of valproic acid in a pregnant rhesus monkey. | Semantic Scholar. **Pediatric pharmacology**, [*s. l.*], v. 1, n. 1, p. 71–83, 1980. Disponível em: https://www.semanticscholar.org/paper/Materno-fetal-pharmacokinetics-and-fetal-of-acid-in-Dickinson-Lawyer/80d29d539a81e1935dd3b578be30377774a277dd. Acesso em: 13 mar. 2022.

DOAN, Ryan N. *et al.* Recessive gene disruptions in autism spectrum disorder. **Nature Genetics**, [*s. l.*], v. 51, n. 7, p. 1092–1098, 2019. Disponível em: https://doi.org/10.1038/s41588-019-0433-8. Acesso em: 16 dez. 2020.

DONG, Daoyin *et al.* Cellular stress and apoptosis contribute to the pathogenesis of autism spectrum disorder. **Autism Research**, [*s. l.*], v. 11, n. 7, p. 1076–1090, 2018. Disponível em: https://doi.org/10.1002/aur.1966. Acesso em: 16 dez. 2020.

ECKER, Christine; BOOKHEIMER, Susan Y.; MURPHY, Declan G.M. Neuroimaging in autism spectrum disorder: brain structure and function across the lifespan. **The Lancet. Neurology**, [*s. l.*], v. 14, n. 11, p. 1121–1134, 2015. Disponível em: https://doi.org/10.1016/S1474-4422(15)00050-2. Acesso em: 14 mar. 2022.

EGGERTSON, Laura. Lancet retracts 12-year-old article linking autism to MMR vaccines. **CMAJ : Canadian Medical Association Journal**, [*s. l.*], v. 182, n. 4, p. E199, 2010. Disponível em: https://doi.org/10.1503/CMAJ.109-3179. Acesso

em: 13 mar. 2022.

EL-KHOURY, Rita *et al.* GABA and glutamate pathways are spatially and developmentally affected in the brain of Mecp2-deficient mice. **PLoS ONE**, [*s. l.*], v. 9, n. 3, 2014. Disponível em: https://doi.org/10.1371/journal.pone.0092169. Acesso em: 16 dez. 2020.

ELLINGFORD, Robert A. *et al.* Cell-type-specific synaptic imbalance and disrupted homeostatic plasticity in cortical circuits of ASD-associated Chd8 haploinsufficient mice. **Molecular psychiatry**, [*s. l.*], v. 26, n. 7, p. 3614–3624, 2021. Disponível em: https://doi.org/10.1038/S41380-021-01070-9. Acesso em: 14 mar. 2022.

ELSABBAGH, Mayada *et al.* Global Prevalence of Autism and Other Pervasive Developmental Disorders. **Autism Research**, [*s. l.*], v. 5, n. 3, p. 160, 2012. Disponível em: https://doi.org/10.1002/AUR.239. Acesso em: 13 mar. 2022.

ENWRIGHT, John F. *et al.* Reduced Labeling of Parvalbumin Neurons and Perineuronal Nets in the Dorsolateral Prefrontal Cortex of Subjects with Schizophrenia. **Neuropsychopharmacology 2016 41:9**, [*s. l.*], v. 41, n. 9, p. 2206–2214, 2016. Disponível em: https://doi.org/10.1038/npp.2016.24. Acesso em: 14 mar. 2022.

ESHRAGHI, Adrien A. *et al.* Epigenetics and Autism Spectrum Disorder: Is There a Correlation? **Frontiers in Cellular Neuroscience**, [*s. l.*], v. 12, p. 78, 2018. Disponível em: https://doi.org/10.3389/FNCEL.2018.00078. Acesso em: 13 mar. 2022.

EUSTON, David R.; GRUBER, Aaron J.; MCNAUGHTON, Bruce L. The Role of Medial Prefrontal Cortex in Memory and Decision Making. **Neuron**, [*s. l.*], v. 76, n. 6, p. 1057, 2012. Disponível em: https://doi.org/10.1016/J.NEURON.2012.12.002. Acesso em: 14 mar. 2022.

FATEMI, S. Hossein *et al.* GABA(A) receptor downregulation in brains of subjects with autism. **Journal of autism and developmental disorders**, [*s. l.*], v. 39, n. 2, p. 223–230, 2009. Disponível em: https://doi.org/10.1007/S10803-008-0646-7. Acesso em: 2 mar. 2022.

FAUX, Clare *et al.* Neurons on the Move: Migration and Lamination of Cortical Interneurons. **Neurosignals**, [*s. l.*], v. 20, n. 3, p. 168–189, 2012. Disponível em: https://doi.org/10.1159/000334489. Acesso em: 14 mar. 2022.

FAYYAD-KAZAN, Hussein *et al.* Valproate Treatment of Human Cord Blood CD4-

positive Effector T Cells Confers on Them the Molecular Profile (MicroRNA Signature and FOXP3 Expression) of Natural Regulatory CD4-positive Cells through Inhibition of Histone Deacetylase. **The Journal of Biological Chemistry**, [*s. l.*], v. 285, n. 27, p. 20481, 2010. Disponível em: https://doi.org/10.1074/JBC.M110.119628. Acesso em: 14 mar. 2022.

FERRI, Sarah L.; ABEL, Ted; BRODKIN, Edward S. Sex Differences in Autism Spectrum Disorder: A Review. **Current psychiatry reports**, [*s. l.*], v. 20, n. 2, p. 9, 2018. Disponível em: https://doi.org/10.1007/S11920-018-0874-2. Acesso em: 13 mar. 2022.

FOLB, Peter I. *et al.* A Global Perspective on Vaccine Safety and Public Health: The Global Advisory Committee on Vaccine Safety. **American Journal of Public Health**, [*s. l.*], v. 94, n. 11, p. 1926, 2004. Disponível em: https://doi.org/10.2105/AJPH.94.11.1926. Acesso em: 13 mar. 2022.

FOMBONNE, Eric *et al.* Prevalence of Autism Spectrum Disorders in Guanajuato, Mexico: The Leon survey. **Journal of Autism and Developmental Disorders 2016 46:5**, [*s. l.*], v. 46, n. 5, p. 1669–1685, 2016. Disponível em: https://doi.org/10.1007/S10803-016-2696-6. Acesso em: 13 mar. 2022.

FONTES-DUTRA, Mellanie *et al.* Abnormal empathy-like pro-social behaviour in the valproic acid model of autism spectrum disorder. **Behavioural brain research**, [*s. l.*], v. 364, p. 11–18, 2019. Disponível em: https://doi.org/10.1016/J.BBR.2019.01.034. Acesso em: 14 mar. 2022.

FONTES-DUTRA, Mellanie *et al.* Maternal Immune Activation and Neuropsychiatric Disorders: The Intricate Puzzle of Autism Spectrum Disorder. [*s. l.*], p. 167–205, 2020. Disponível em: https://doi.org/10.1007/978-3-030-39335-9_11. Acesso em: 13 mar. 2022.

FONTES-DUTRA, Mellanie *et al.* Resveratrol prevents cellular and behavioral sensory alterations in the animal model of autism induced by valproic acid. **Frontiers in Synaptic Neuroscience**, [*s. l.*], v. 10, p. 9, 2018. Disponível em: https://doi.org/10.3389/FNSYN.2018.00009. Acesso em: 20 maio 2018.

FORREST, Marc P. *et al.* The psychiatric risk gene transcription factor 4 (TCF4) regulates neurodevelopmental pathways associated with schizophrenia, Autism, and intellectual disability. **Schizophrenia Bulletin**, [*s. l.*], v. 44, n. 5, p. 1100–1110, 2018. Disponível em: https://doi.org/10.1093/schbul/sbx164. Acesso em: 16 dez. 2020.

FOWLER, David W; EADIE, Mervyn J; DICKINSON, Ronald G. Transplacental transfer and biotransformation studies of valproic acid and its glucuronide(s) in the perfused human placenta. | Journal of Pharmacology and Experimental Therapeutics. **Journal of Pharmacology and Experimental Therapeutics**, [*s. l.*], v. 249, n. 1, p. 318–323, 1989. Disponível em: https://jpet.aspetjournals.org/content/249/1/318. Acesso em: 13 mar. 2022.

FROMBAUM, Matthieu *et al.* Antioxidant effects of resveratrol and other stilbene derivatives on oxidative stress and *NO bioavailability: Potential benefits to cardiovascular diseases. **Biochimie**, [*s. l.*], v. 94, n. 2, p. 269–276, 2012. Disponível em: https://doi.org/10.1016/J.BIOCHI.2011.11.001. Acesso em: 14 mar. 2022.

FUJIMURA, Kimino *et al.* In Utero Exposure to Valproic Acid Induces Neocortical Dysgenesis via Dysregulation of Neural Progenitor Cell Proliferation/Differentiation. **The Journal of neuroscience : the official journal of the Society for Neuroscience**, [*s. l.*], v. 36, n. 42, p. 10908–10919, 2016. Disponível em: https://doi.org/10.1523/JNEUROSCI.0229-16.2016. Acesso em: 29 nov. 2019.

FUKS, François *et al.* The methyl-CpG-binding protein MeCP2 links DNA methylation to histone methylation. **The Journal of biological chemistry**, [*s. l.*], v. 278, n. 6, p. 4035–4040, 2003. Disponível em: https://doi.org/10.1074/JBC.M210256200. Acesso em: 14 mar. 2022.

GABRIELE, Michele *et al.* The chromatin basis of neurodevelopmental disorders: Rethinking dysfunction along the molecular and temporal axes. **Progress in Neuro-Psychopharmacology and Biological Psychiatry**, [*s. l.*], v. 84, p. 306–327, 2018. Disponível em: https://doi.org/10.1016/J.PNPBP.2017.12.013

GAIL WILLIAMS, P.; HERSH, Joseph H. A male with fetal valproate syndrome and autism. **Developmental medicine and child neurology**, [*s. l.*], v. 39, n. 9, p. 632–634, 1997. Disponível em: https://doi.org/10.1111/J.1469-8749.1997.TB07500.X. Acesso em: 13 mar. 2022.

GALARRETA, Mario; HESTRIN, Shaul. Electrical and chemical synapses among parvalbumin fast-spiking GABAergic interneurons in adult mouse neocortex. **Proceedings of the National Academy of Sciences of the United States of America**, [*s. l.*], v. 99, n. 19, p. 12438, 2002. Disponível em: https://doi.org/10.1073/PNAS.192159599. Acesso em: 14 mar. 2022.

GANGULI, Sourav; CHAVALI, Pavithra L. Intrauterine Viral Infections: Impact of Inflammation on Fetal Neurodevelopment. **Frontiers in Neuroscience**, [*s. l.*], v. 15, p. 1509, 2021. Disponível em: https://doi.org/10.3389/FNINS.2021.771557/BIBTEX

GENTILE, Ivan *et al.* Prevalence of Congenital Cytomegalovirus Infection Assessed Through Viral Genome Detection in Dried Blood Spots in Children with Autism Spectrum Disorders. **In Vivo**, [*s. l.*], v. 31, n. 3, p. 467, 2017. Disponível em: https://doi.org/10.21873/INVIVO.11085. Acesso em: 13 mar. 2022.

GEORGALA, Petrina A.; MANUEL, Martine; PRICE, David J. The Generation of Superficial Cortical Layers Is Regulated by Levels of the Transcription Factor Pax6. **Cerebral Cortex**, [*s. l.*], v. 21, n. 1, p. 81–94, 2011. Disponível em: https://doi.org/10.1093/CERCOR/BHQ061. Acesso em: 14 mar. 2022.

GILBERT, Sam J. *et al.* Atypical recruitment of medial prefrontal cortex in autism spectrum disorders: An fMRI study of two executive function tasks. **Neuropsychologia**, [*s. l.*], v. 46, n. 9, p. 2281–2291, 2008. Disponível em: https://doi.org/10.1016/J.NEUROPSYCHOLOGIA.2008.03.025

GINIGER, Edward. Notch signaling and neural connectivity. **Current opinion in genetics & development**, [*s. l.*], v. 22, n. 4, p. 339–346, 2012. Disponível em: https://doi.org/10.1016/j.gde.2012.04.003. Acesso em: 29 nov. 2019.

GOLDBERG, Melissa C. *et al.* Children with high functioning autism show increased prefrontal and temporal cortex activity during error monitoring. **Developmental Cognitive Neuroscience**, [*s. l.*], v. 1, n. 1, p. 47–56, 2011. Disponível em: https://doi.org/10.1016/J.DCN.2010.07.002

GONÇALVES, Joana *et al.* Testing the excitation/inhibition imbalance hypothesis in a mouse model of the autism spectrum disorder: in vivo neurospectroscopy and molecular evidence for regional phenotypes. **Molecular Autism**, [*s. l.*], v. 8, n. 1, p. 8-47, 2017. Disponível em: https://doi.org/10.1186/S13229-017-0166-4. Acesso em: 14 mar. 2022.

GONÇALVES, J. Tiago; SCHAFER, Simon T.; GAGE, Fred H. Adult Neurogenesis in the Hippocampus: From Stem Cells to Behavior. **Cell**, v. 167, n. 4, p. 897-914, 2016. Disponível em: https://doi.org/10.1016/j.cell.2016.10.021

GOTTFRIED, Carmem *et al.* The impact of neuroimmune alterations in autism spectrum disorder. **Frontiers in Psychiatry**, [*s. l.*], v. 6, n. SEP, p. 121, 2015. Disponível em: https://doi.org/10.3389/FPSYT.2015.00121/BIBTEX

GÖTTLICHER, Martin *et al.* Valproic acid defines a novel class of HDAC inhibitors inducing differentiation of transformed cells. **The EMBO Journal**, [*s. l.*], v. 20, n. 24, p. 6969, 2001. Disponível em: https://doi.org/10.1093/EMBOJ/20.24.6969. Acesso em: 14 mar. 2022.

GROSSMANN, Tobias. The role of medial prefrontal cortex in early social cognition. **Frontiers in Human Neuroscience**, [*s. l.*], v. 1, n. JUL, p. 340, 2013. Disponível em: https://doi.org/10.3389/FNHUM.2013.00340/BIBTEX

GUANG, Shiqi *et al.* Synaptopathology Involved in Autism Spectrum Disorder. **Frontiers in cellular neuroscience**, [*s. l.*], v. 12, p. 470, 2018. Disponível em: https://doi.org/10.3389/FNCEL.2018.00470. Acesso em: 3 mar. 2022.

GUGLER, Roland; VON UNRUH, Gerd E. Clinical Pharmacokinetics of Valproic Acid. **Clinical Pharmacokinetics 1980 5:1**, [*s. l.*], v. 5, n. 1, p. 67–83, 2012. Disponível em: https://doi.org/10.2165/00003088-198005010-00002. Acesso em: 13 mar. 2022.

GUIBINGA, Ghiabe Henri; BARRON, Nikki; PANDORI, William. Striatal Neurodevelopment Is Dysregulated in Purine Metabolism Deficiency and Impacts DARPP-32, BDNF/TrkB Expression and Signaling: New Insights on the Molecular and Cellular Basis of Lesch-Nyhan Syndrome. **PLOS ONE**, [*s. l.*], v. 9, n. 5, p. e96575, 2014. Disponível em: https://doi.org/10.1371/JOURNAL.PONE.0096575. Acesso em: 14 mar. 2022.

GUO, Baolin *et al.* Anterior cingulate cortex dysfunction underlies social deficits in Shank3 mutant mice. **Nature Neuroscience**, [*s. l.*], v. 22, n. 8, p. 1223–1234, 2019. Disponível em: https://doi.org/10.1038/s41593-019-0445-9. Acesso em: 14 mar. 2022.

GUO, Jiami; ANTON, E. S. Decision Making During Interneuron Migration in the Developing Cerebral Cortex. **Trends in cell biology**, [*s. l.*], v. 24, n. 6, p. 342, 2014. Disponível em: https://doi.org/10.1016/J.TCB.2013.12.001. Acesso em: 14 mar. 2022.

GUO, Yan Jie *et al.* Resveratrol alleviates MPTP-induced motor impairments and pathological changes by autophagic degradation of α-synuclein via SIRT1-deacetylated LC3. **Molecular nutrition & food research**, [*s. l.*], v. 60, n. 10, p. 2161–2175, 2016. Disponível em: https://doi.org/10.1002/MNFR.201600111. Acesso em: 14 mar. 2022.

GURVICH, Nadia *et al.* Association of valproate-induced teratogenesis with histone

deacetylase inhibition in vivo. **FASEB journal : official publication of the Federation of American Societies for Experimental Biology**, [*s. l.*], v. 19, n. 9, p. 1166–1168, 2005. Disponível em: https://doi.org/10.1096/FJ.04-3425FJE. Acesso em: 14 mar. 2022.

HAJINEJAD, Mehrdad *et al.* Resveratrol pretreatment enhanced homing of SDF-1α-preconditioned bone marrow-derived mesenchymal stem cells in a rat model of liver cirrhosis. **Journal of cellular biochemistry**, [*s. l.*], v. 119, n. 3, p. 2939–2950, 2018. Disponível em: https://doi.org/10.1002/JCB.26500. Acesso em: 14 mar. 2022.

HAN, Sung *et al.* Enhancement of inhibitory neurotransmission by GABAA receptors having α2,3-subunits ameliorates behavioral deficits in a mouse model of autism. **Neuron**, [*s. l.*], v. 81, n. 6, p. 1282–1289, 2014. Disponível em: https://doi.org/10.1016/J.NEURON.2014.01.016. Acesso em: 14 mar. 2022.

HAN, Velda X. *et al.* Maternal immune activation and neuroinflammation in human neurodevelopmental disorders. **Nature Reviews Neurology 2021 17:9**, [*s. l.*], v. 17, n. 9, p. 564–579, 2021. Disponível em: https://doi.org/10.1038/s41582-021-00530-8. Acesso em: 13 mar. 2022.

HANSEN, Stefan N.; SCHENDEL, Diana E.; PARNER, Erik T. Explaining the Increase in the Prevalence of Autism Spectrum Disorders: The Proportion Attributable to Changes in Reporting Practices. **JAMA Pediatrics**, [*s. l.*], v. 169, n. 1, p. 56–62, 2015. Disponível em: https://doi.org/10.1001/JAMAPEDIATRICS.2014.1893. Acesso em: 13 mar. 2022.

HASAN, Md Mohidul; BAE, Hanhong. An Overview of Stress-Induced Resveratrol Synthesis in Grapes: Perspectives for Resveratrol-Enriched Grape Products. **Molecules : A Journal of Synthetic Chemistry and Natural Product Chemistry**, [*s. l.*], v. 22, n. 2, p. 294, 2017. Disponível em: https://doi.org/10.3390/MOLECULES22020294. Acesso em: 14 mar. 2022.

HELMEKE, C. *et al.* Imbalance of immunohistochemically characterized interneuron populations in the adolescent and adult rodent medial prefrontal cortex after repeated exposure to neonatal separation stress. **Neuroscience**, [*s. l.*], v. 152, n. 1, p. 18–28, 2008. Disponível em: https://doi.org/10.1016/J.NEUROSCIENCE.2007.12.023

HELSMOORTEL, Céline *et al.* A SWI/SNF-related autism syndrome caused by de

novo mutations in ADNP. **Nature Genetics**, [*s. l.*], v. 46, n. 4, p. 380–384, 2014. Disponível em: https://doi.org/10.1038/ng.2899. Acesso em: 16 dez. 2020.

HENDOUEI, Fatemeh *et al.* Resveratrol as adjunctive therapy in treatment of irritability in children with autism: A double-blind and placebo-controlled randomized trial. **Journal of clinical pharmacy and therapeutics**, [*s. l.*], v. 45, n. 2, p. 324–334, 2020. Disponível em: https://doi.org/10.1111/JCPT.13076. Acesso em: 14 mar. 2022.

HENG, Julian Ik Tsen; MOONEN, Gustave; NGUYEN, Laurent. REVIEW ARTICLE: Neurotransmitters regulate cell migration in the telencephalon. **European Journal of Neuroscience**, [*s. l.*], v. 26, n. 3, p. 537–546, 2007. Disponível em: https://doi.org/10.1111/J.1460-9568.2007.05694.X. Acesso em: 14 mar. 2022.

HIRSCH, Mauro Mozael *et al.* Behavioral alterations in autism model induced by valproic acid and translational analysis of circulating microRNA. **Food and Chemical Toxicology**, [*s. l.*], v. 115, p. 336–343, 2018. Disponível em: https://doi.org/10.1016/j.fct.2018.02.061. Acesso em: 15 mar. 2021.

HIRVIKOSKI, Tatja *et al.* Premature mortality in autism spectrum disorder. **The British journal of psychiatry : the journal of mental science**, [*s. l.*], v. 208, n. 3, p. 232–238, 2016. Disponível em: https://doi.org/10.1192/BJP.BP.114.160192. Acesso em: 14 mar. 2022.

HOFMANN, Gabrielle *et al.* Hilar somatostatin interneuron loss reduces dentate gyrus inhibition in a mouse model of temporal lobe epilepsy. **Epilepsia**, [*s. l.*], v. 57, n. 6, p. 977–983, 2016. Disponível em: https://doi.org/10.1111/EPI.13376. Acesso em: 14 mar. 2022.

HONORÉ, Eve *et al.* Hippocampal Somatostatin Interneurons, Long-Term Synaptic Plasticity and Memory. **Frontiers in Neural Circuits**, [*s. l.*], v. 15, p. e687558, 2021. Disponível em: https://doi.org/10.3389/FNCIR.2021.687558. Acesso em: 14 mar. 2022.

HORDER, Jamie *et al.* Glutamate and GABA in autism spectrum disorder—a translational magnetic resonance spectroscopy study in man and rodent models. **Translational Psychiatry 2018**, [*s. l.*], v. 8, n. 1, p. 1–11, 2018. Disponível em: https://doi.org/10.1038/s41398-018-0155-1. Acesso em: 14 mar. 2022.

HORVÁTH, Gergely *et al.* P2X7 Receptors Drive Poly(I:C) Induced Autism-like Behavior in Mice. **The Journal of neuroscience : the official journal of the**

Society for Neuroscience, [*s. l.*], v. 39, n. 13, p. 2542–2561, 2019. Disponível em: https://doi.org/10.1523/JNEUROSCI.1895-18.2019. Acesso em: 14 mar. 2022.

HSIEH, Jenny *et al.* Histone deacetylase inhibition-mediated neuronal differentiation of multipotent adult neural progenitor cells. **Proceedings of the National Academy of Sciences of the United States of America**, [*s. l.*], v. 101, n. 47, p. 16659–16664, 2004. Disponível em: https://doi.org/10.1073/pnas.0407643101. Acesso em: 16 dez. 2020.

INAMURA, Naoko *et al.* Intrinsic and extrinsic mechanisms control the termination of cortical interneuron migration. **The Journal of neuroscience : the official journal of the Society for Neuroscience**, [*s. l.*], v. 32, n. 17, p. 6032–6042, 2012. Disponível em: https://doi.org/10.1523/JNEUROSCI.3446-11.2012. Acesso em: 14 mar. 2022.

INGRAM, Jennifer L. *et al.* Prenatal exposure of rats to valproic acid reproduces the cerebellar anomalies associated with autism. **Neurotoxicology and Teratology**, [*s. l.*], v. 22, n. 3, p. 319–324, 2000. Disponível em: https://doi.org/10.1016/S0892-0362(99)00083-5

IP, Jacque P.K.; MELLIOS, Nikolaos; SUR, Mriganka. Rett syndrome: Insights into genetic, molecular and circuit mechanisms. **Nature Reviews Neuroscience**, [*s. l.*], v. 19, n. 6, p. 368-382, 2018. Disponível em: https://doi.org/10.1038/s41583-018-0006-3

ISHII, Seiji *et al.* Variations in brain defects result from cellular mosaicism in the activation of heat shock signalling. **Nature Communications**, [*s. l.*], v. 8, n. 1, p. 1–15, 2017. Disponível em: https://doi.org/10.1038/ncomms15157. Acesso em: 16 dez. 2020.

ITO-ISHIDA, Aya *et al.* Loss of MeCP2 in Parvalbumin-and Somatostatin-Expressing Neurons in Mice Leads to Distinct Rett Syndrome-like Phenotypes. **Neuron**, [*s. l.*], v. 88, n. 4, p. 651–658, 2015. Disponível em: https://doi.org/10.1016/J.NEURON.2015.10.029

JACOT-DESCOMBES, Sarah *et al.* Altered synaptic ultrastructure in the prefrontal cortex of Shank3-deficient rats. **Molecular Autism**, [*s. l.*], v. 11, n. 1, p. 1–17, 2020. Disponível em: https://doi.org/10.1186/S13229-020-00393-8/TABLES/2. Acesso em: 14 mar. 2022.

JANG, Yin Gi *et al.* Resveratrol inhibits DHT-induced progression of prostate cancer

cell line through interfering with the AR and CXCR4 pathway. **The Journal of steroid biochemistry and molecular biology**, [*s. l.*], v. 192, e105406, 2019. Disponível em: https://doi.org/10.1016/J.JSBMB.2019.105406. Acesso em: 14 mar. 2022.

JI, Yaoting; KE, Yongxin; GAO, Song. Intermittent activation of notch signaling promotes bone formation. **American journal of translational research**, [*s. l.*], v. 9, n. 6, p. 2933–2944, 2017. Disponível em: http://www.ncbi.nlm.nih.gov/pubmed/28670381. Acesso em: 29 nov. 2019.

JIMÉNEZ, Jessica A. *et al.* Chd8 haploinsufficiency impairs early brain development and protein homeostasis later in life. **Molecular autism**, [*s. l.*], v. 11, n. 1, p. 74, 2020. Disponível em: https://doi.org/10.1186/S13229-020-00369-8. Acesso em: 14 mar. 2022.

KAAR, Stephen J. *et al.* Pre-frontal parvalbumin interneurons in schizophrenia: a meta-analysis of post-mortem studies. **Journal of neural transmission (Vienna, Austria : 1996)**, [*s. l.*], v. 126, n. 12, p. 1637–1651, 2019. Disponível em: https://doi.org/10.1007/S00702-019-02080-2. Acesso em: 14 mar. 2022.

KALISH, Brian T. *et al.* Maternal immune activation in mice disrupts proteostasis in the fetal brain. **Nature Neuroscience 2020 24:2**, [*s. l.*], v. 24, n. 2, p. 204–213, 2020. Disponível em: https://doi.org/10.1038/s41593-020-00762-9. Acesso em: 3 mar. 2022.

KALLIORA, Charikleia *et al.* Dual PPARα/γ activation inhibits SIRT1-PGC1α axis and causes cardiac dysfunction. **JCI Insight**, [*s. l.*], v. 4, n. 17, p. e129556, 2019. Disponível em: https://doi.org/10.1172/JCI.INSIGHT.129556. Acesso em: 14 mar. 2022.

KANNER, Leo. Autistic disturbances of affective contact. **Nervous Child**, [*s. l.*], v. 2, p. 217–250, 1943. Disponível em: https://simonsfoundation.s3.amazonaws.com/share/071207-leo-kanner-autistic-affective-contact.pdf. Acesso em: 13 mar. 2022.

KANNER, LEO. PROBLEMS OF NOSOLOGY AND PSYCHODYNAMICS OF EARLY INFANTILE AUTISM*. **American Journal of Orthopsychiatry**, [*s. l.*], v. 19, n. 3, p. 416–426, 1949. Disponível em: https://doi.org/10.1111/J.1939-0025.1949.TB05441.X. Acesso em: 13 mar. 2022.

KATAYAMA, Yuta *et al.* CHD8 haploinsufficiency results in autistic-like phenotypes in mice. **Nature**, [*s. l.*], v. 537, n. 7622, p. 675-679, 2016. Disponível em:

https://doi.org/10.1038/nature19357

KAUFFMAN, Stuart. Gene regulation networks: a theory for their global structure and behaviors. **Current topics in developmental biology**, [*s. l.*], v. 6, n. 6, p. 145–182, 1971. Disponível em: https://doi.org/10.1016/S0070-2153(08)60640-7. Acesso em: 14 mar. 2022.

KAUFMAN, T. C.; LEWIS, R.; WAKIMOTO, B. Cytogenetic analysis of chromosome 3 in Drosophila melanogaster: The homoeotic gene complex in polytene chromosome interval 84A-B. **Genetics**, [*s. l.*], v. 94, n. 1, p. 115-33, 1980.

KAWADA, Koichi *et al.* Involvement of endoplasmic reticulum stress and neurite outgrowth in the model mice of autism spectrum disorder. **Neurochemistry International**, [*s. l.*], v. 119, p. 115–119, 2018. Disponível em: https://doi.org/10.1016/j.neuint.2017.07.004. Acesso em: 16 dez. 2020.

KAWAGUCHI, Yasuo; KUBOTA, Yoshiyuki. GABAergic cell subtypes and their synaptic connections in rat frontal cortex. **Cerebral cortex (New York, N.Y. : 1991)**, [*s. l.*], v. 7, n. 6, p. 476–486, 1997. Disponível em: https://doi.org/10.1093/CERCOR/7.6.476. Acesso em: 14 mar. 2022.

KAWAGUCHI, Yasuo; SHINDOU, Tomomi. Noradrenergic excitation and inhibition of GABAergic cell types in rat frontal cortex. **The Journal of neuroscience : the official journal of the Society for Neuroscience**, [*s. l.*], v. 18, n. 17, p. 6963–6976, 1998. Disponível em: https://doi.org/10.1523/JNEUROSCI.18-17-06963.1998. Acesso em: 14 mar. 2022.

KAWAI, Yumiko; ARINZE, Ifeanyi J. Valproic Acid–Induced Gene Expression through Production of Reactive Oxygen Species. **Cancer Research**, [*s. l.*], v. 66, n. 13, p. 6563–6569, 2006. Disponível em: https://doi.org/10.1158/0008-5472.CAN-06-0814. Acesso em: 14 mar. 2022.

KELSOM, Corey; LU, Wange. Development and specification of GABAergic cortical interneurons. **Cell & Bioscience 2013 3:1**, [*s. l.*], v. 3, n. 1, p. 1–19, 2013b. Disponível em: https://doi.org/10.1186/2045-3701-3-19. Acesso em: 2 mar. 2022.

KIM, Ji Eun *et al.* SRC/CK2/PTEN-mediated glun2b and creb dephosphorylations regulate the responsiveness to AMPA receptor antagonists in chronic epilepsy rats. **International Journal of Molecular Sciences**, [*s. l.*], v. 21, n. 24, p. 1–23, 2020. Disponível em: https://doi.org/10.3390/ijms21249633. Acesso em: 14 maio 2021.

KIM, Ji Woon *et al.* Pharmacological modulation of AMPA receptor rescues social impairments in animal models of autism. **Neuropsychopharmacology : official publication of the American College of Neuropsychopharmacology**, [*s. l.*], v. 44, n. 2, p. 314–323, 2019. Disponível em: https://doi.org/10.1038/S41386-018-0098-5. Acesso em: 14 mar. 2022.

KIM, Ki Chan *et al.* Male-specific alteration in excitatory post-synaptic development and social interaction in pre-natal valproic acid exposure model of autism spectrum disorder. **Journal of neurochemistry**, [*s. l.*], v. 124, n. 6, p. 832–843, 2013. Disponível em: https://doi.org/10.1111/JNC.12147. Acesso em: 14 mar. 2022.

KIM, Ki Chan *et al.* MeCP2 Modulates Sex Differences in the Postsynaptic Development of the Valproate Animal Model of Autism. **Molecular neurobiology**, [*s. l.*], v. 53, n. 1, p. 40–56, 2016. Disponível em: https://doi.org/10.1007/S12035-014-8987-Z. Acesso em: 14 mar. 2022.

KIM, Ki Chan *et al.* Pax6-dependent cortical glutamatergic neuronal differentiation regulates autism-like behavior in prenatally valproic acid-exposed rat offspring. **Molecular neurobiology**, [*s. l.*], v. 49, n. 1, p. 512-28, 2014. Disponível em: https://doi.org/10.1007/s12035-013-8535-2. Acesso em: 16 dez. 2020.

KITAURA, Hiroki *et al.* Pathophysiological Characteristics Associated With Epileptogenesis in Human Hippocampal Sclerosis. **EBioMedicine**, [*s. l.*], v. 29, p. 38–46, 2018. Disponível em: https://doi.org/10.1016/J.EBIOM.2018.02.013/ATTACHMENT/B59B0BA6-2D16-4E33-89B6-0AEFADE27DF7/MMC1.PDF. Acesso em: 14 mar. 2022.

KÖBE, Theresa *et al.* Impact of resveratrol on glucose control, hippocampal structure and connectivity, and memory performance in patients with mild cognitive impairment. **Frontiers in Neuroscience**, [*s. l.*], v. 11, p. 105, 2017. Disponível em: https://doi.org/10.3389/fnins.2017.00105

KODALI, Maheedhar *et al.* Resveratrol Prevents Age-Related Memory and Mood Dysfunction with Increased Hippocampal Neurogenesis and Microvasculature and Reduced Glial Activation. **Scientific Reports 2015 5:1**, [*s. l.*], v. 5, n. 1, p. 1–16, 2015. Disponível em: https://doi.org/10.1038/srep08075. Acesso em: 14 mar. 2022.

KONRADI, Christine *et al.* Hippocampal interneurons are abnormal in schizophrenia. **Schizophrenia Research**, [*s. l.*], v. 131, n. 1–3, p. 165–173, 2011. Disponível

em: https://doi.org/10.1016/J.SCHRES.2011.06.007

KOREN, Gideon *et al.* Major malformations with valproic acid. **Canadian Family Physician**, [*s. l.*], v. 52, n. 4, p. 441, 2006. Disponível em: /pmc/articles/PMC1481679/. Acesso em: 13 mar. 2022.

KOSHO, Tomoki; MIYAKE, Noriko; CAREY, John C. Coffin-Siris syndrome and related disorders involving components of the BAF (mSWI/SNF) complex: Historical review and recent advances using next generation sequencing. **American Journal of Medical Genetics Part C: Seminars in Medical Genetics**, [*s. l.*], v. 166, n. 3, p. 241–251, 2014. Disponível em: https://doi.org/10.1002/ajmg.c.31415. Acesso em: 16 dez. 2020.

KRÄMER, Oliver H. *et al.* The histone deacetylase inhibitor valproic acid selectively induces proteasomal degradation of HDAC2. **The EMBO Journal**, [*s. l.*], v. 22, n. 13, p. 3411, 2003. Disponível em: https://doi.org/10.1093/EMBOJ/CDG315. Acesso em: 14 mar. 2022.

KVITSIANI, D. *et al.* Distinct behavioural and network correlates of two interneuron types in prefrontal cortex. **Nature 2013 498:7454**, [*s. l.*], v. 498, n. 7454, p. 363–366, 2013. Disponível em: https://doi.org/10.1038/nature12176. Acesso em: 14 mar. 2022.

KWOK, C. *et al.* Mutations in SOX9, the gene responsible for campomelic dysplasia and autosomal sex reversal. **American Journal of Human Genetics**, [*s. l.*], v. 57, n. 5, p. 1028–1036, 1995. Disponível em: /pmc/articles/PMC1801368/?report=abstract. Acesso em: 16 dez. 2020.

LAMB, Allen N. *et al.* Haploinsufficiency of SOX5 at 12p12.1 is associated with developmental delays with prominent language delay, behavior problems, and mild dysmorphic features. **Human Mutation**, [*s. l.*], v. 33, n. 4, p. 728–740, 2012. Disponível em: https://doi.org/10.1002/humu.22037. Acesso em: 16 dez. 2020.

LAMBERT, Samuel A. *et al.* The Human Transcription Factors. **Cell**, [*s. l.*], v. 172, n. 4, p. 650–665, 2018. Disponível em: https://doi.org/10.1016/J.CELL.2018.01.029/ATTACHMENT/EDE37821-FD6F-41B7-9A0E-9D5410855AE6/MMC2.XLSX. Acesso em: 14 mar. 2022.

LANGE, Nicholas *et al.* Longitudinal Volumetric Brain Changes in Autism Spectrum Disorder Ages 6–35 Years. **Autism research : official journal of the International Society for Autism Research**, [*s. l.*], v. 8, n. 1, p. 82, 2015.

Disponível em: https://doi.org/10.1002/AUR.1427. Acesso em: 14 mar. 2022.

LAUBACH, Mark *et al.* What, If Anything, Is Rodent Prefrontal Cortex? **eNeuro**, [*s. l.*], v. 5, n. 5, p. ENEURO.0315-18.2018, 2018. Disponível em: https://doi.org/10.1523/ENEURO.0315-18.2018. Acesso em: 14 mar. 2022.

LAUBER, Emanuel; FILICE, Federica; SCHWALLER, Beat. Prenatal Valproate Exposure Differentially Affects Parvalbumin-Expressing Neurons and Related Circuits in the Cortex and Striatum of Mice. **Frontiers in molecular neuroscience**, [*s. l.*], v. 9, n. DEC2016, p. 150, 2016. Disponível em: https://doi.org/10.3389/FNMOL.2016.00150. Acesso em: 14 mar. 2022.

LAVIN, Claudio *et al.* The anterior cingulate cortex: an integrative hub for human socially-driven interactions. **Frontiers in Neuroscience**, [*s. l.*], v. 0, p. 64, 2013. Disponível em: https://doi.org/10.3389/FNINS.2013.00064

LAWRENCE, Y. A. *et al.* Parvalbumin-, calbindin-, and calretinin-immunoreactive hippocampal interneuron density in autism. **Acta neurologica Scandinavica**, [*s. l.*], v. 121, n. 2, p. 99–108, 2010. Disponível em: https://doi.org/10.1111/J.1600-0404.2009.01234.X. Acesso em: 14 mar. 2022.

LE, Trung N. *et al.* Dlx homeobox genes promote cortical interneuron migration from the basal forebrain by direct repression of the semaphorin receptor neuropilin-2. **Journal of Biological Chemistry**, [*s. l.*], v. 282, n. 26, p. 19071–19081, 2007. Disponível em: https://doi.org/10.1074/jbc.M607486200

LE, Trung N. *et al.* GABAergic Interneuron Differentiation in the Basal Forebrain Is Mediated through Direct Regulation of Glutamic Acid Decarboxylase Isoforms by *Dlx* Homeobox Transcription Factors. **The Journal of Neuroscience**, [*s. l.*], v. 37, n. 36, p. 8816–8829, 2017. Disponível em: https://doi.org/10.1523/JNEUROSCI.2125-16.2017

LEE, Li Jen; TSYTSAREV, Vassiliy; ERZURUMLU, Reha S. Structural and functional differences in the barrel cortex of Mecp2 null mice. **Journal of Comparative Neurology**, [*s. l.*], v. 525, n. 18, p. 3951–3961, 2017. Disponível em: https://doi.org/10.1002/cne.24315. Acesso em: 16 dez. 2020.

LEE, Tong Ihn; YOUNG, Richard A. Transcriptional Regulation and its Misregulation in Disease. **Cell**, [*s. l.*], v. 152, n. 6, p. 1237, 2013. Disponível em: https://doi.org/10.1016/J.CELL.2013.02.014. Acesso em: 14 mar. 2022.

LEJARRAGA, Horacio *et al.* Screening for developmental problems at primary care level: a field programme in San Isidro, Argentina. **Paediatric and perinatal**

epidemiology, [*s. l.*], v. 22, n. 2, p. 180–187, 2008. Disponível em: https://doi.org/10.1111/J.1365-3016.2007.00897.X. Acesso em: 13 mar. 2022.

LENART, Jacek *et al.* Altered expression of glutamatergic and GABAergic genes in the valproic acid-induced rat model of autism: A screening test. **Toxicology**, [*s. l.*], v. 440, p. 152500, 2020. Disponível em: https://doi.org/10.1016/J.TOX.2020.152500

LI, G. *et al.* Regional Distribution of Cortical Interneurons and Development of Inhibitory Tone Are Regulated by Cxcl12/Cxcr4 Signaling. **Journal of Neuroscience**, [*s. l.*], v. 28, n. 5, p. 1085–1098, 2008. Disponível em: https://doi.org/10.1523/JNEUROSCI.4602-07.2008

LI, Ji Tao *et al.* Suppressed Calbindin Levels in Hippocampal Excitatory Neurons Mediate Stress-Induced Memory Loss. **Cell reports**, [*s. l.*], v. 21, n. 4, p. 891–900, 2017. Disponível em: https://doi.org/10.1016/J.CELREP.2017.10.006. Acesso em: 14 mar. 2022.

LI, Yixin *et al.* Reduced protein expressions of cytomembrane GABA A Rβ3 at different postnatal developmental stages of rats exposed prenatally to valproic acid. **Brain research**, [*s. l.*], v. 1671, p. 33–42, 2017. Disponível em: https://doi.org/10.1016/J.BRAINRES.2017.06.018. Acesso em: 14 mar. 2022.

LIGUZ-LECZNAR, Monika; URBAN-CIECKO, Joanna; KOSSUT, Malgorzata. Somatostatin and Somatostatin-Containing Neurons in Shaping Neuronal Activity and Plasticity. **Frontiers in Neural Circuits**, [*s. l.*], v. 10, n. JUNE, p. 48, 2016. Disponível em: https://doi.org/10.3389/FNCIR.2016.00048. Acesso em: 14 mar. 2022.

LIN, Xinghua *et al.* A Novel Transcription Mechanism Activated by Ethanol: Induction of slc7a11 gene expression via inhibition of the dna-binding activity of transcriptional repressor octamer-binding transcription factor 1 (OCT-1) *. **Journal of Biological Chemistry**, [*s. l.*], v. 288, n. 21, p. 14815–14823, 2013. Disponível em: https://doi.org/10.1074/JBC.M113.466565. Acesso em: 14 mar. 2022.

LIODIS, Petros *et al.* Lhx6 Activity Is Required for the Normal Migration and Specification of Cortical Interneuron Subtypes. **Journal of Neuroscience**, [*s. l.*], v. 27, n. 12, p. 3078–3089, 2007. Disponível em: https://doi.org/10.1523/JNEUROSCI.3055-06.2007. Acesso em: 14 mar. 2022.

LIU, Chia Feng; LEFEBVRE, Véronique. The transcription factors SOX9 and

SOX5/SOX6 cooperate genome-wide through super-enhancers to drive chondrogenesis. **Nucleic acids research**, [*s. l.*], v. 43, n. 17, p. 8183–8203, 2015. Disponível em: https://doi.org/10.1093/NAR/GKV688. Acesso em: 14 mar. 2022.

LIU, Chun xue *et al.* Developmental profiling of ASD-related shank3 transcripts and their differential regulation by valproic acid in zebrafish. **Development genes and evolution**, [*s. l.*], v. 226, n. 6, p. 389–400, 2016. Disponível em: https://doi.org/10.1007/S00427-016-0561-4. Acesso em: 14 mar. 2022.

LLOYD, Katie Alexandra; SILLS, Graeme. A scientific review: mechanisms of valproate-mediated teratogenesis. **Bioscience Horizons: The International Journal of Student Research**, [*s. l.*], v. 6, p. 2013, 2013. Disponível em: https://doi.org/10.1093/BIOHORIZONS/HZT003. Acesso em: 14 mar. 2022.

LONG, Katherine R.; HUTTNER, Wieland B. How the extracellular matrix shapes neural development. **Royal Society Open Biology**, [*s. l.*], v. 9, n. 1, 2019. Disponível em: https://doi.org/10.1098/RSOB.180216. Acesso em: 14 mar. 2022.

LOPARO, D.; WALDMAN, I. D. The oxytocin receptor gene (OXTR) is associated with autism spectrum disorder: a meta-analysis. **Molecular psychiatry**, [*s. l.*], v. 20, n. 5, p. 640–646, 2015. Disponível em: https://doi.org/10.1038/MP.2014.77. Acesso em: 13 mar. 2022.

LOVETT-BARRON, Matthew *et al.* Dendritic inhibition in the hippocampus supports fear learning. **Science (New York, N.Y.)**, [*s. l.*], v. 343, n. 6173, p. 857–863, 2014. Disponível em: https://doi.org/10.1126/SCIENCE.1247485. Acesso em: 14 mar. 2022.

LUGO, Joaquin N. *et al.* Deletion of PTEN produces autism-like behavioral deficits and alterations in synaptic proteins. **Frontiers in Molecular Neuroscience**, [*s. l.*], v. 16, p. 7-27, 2014. Disponível em: https://doi.org/10.3389/fnmol.2014.00027

LUHMANN, Heiko J.; FUKUDA, A.; KILB, W. Control of cortical neuronal migration by glutamate and GABA. **Frontiers in Cellular Neuroscience**, [*s. l.*], v. 9, n. JAN, p. 4, 2015. Disponível em: https://doi.org/10.3389/FNCEL.2015.00004/BIBTEX

MA, Lei *et al.* Interleukin-1 beta guides the migration of cortical neurons. **Journal of neuroinflammation**, [*s. l.*], v. 11, p. 114, 2014. Disponível em: https://doi.org/10.1186/1742-2094-11-114. Acesso em: 14 mar. 2022.

MABUNGA, Darine Froy N *et al.* Exploring the Validity of Valproic Acid Animal Model of Autism. **Experimental neurobiology**, [*s. l.*], v. 24, n. 4, p. 285–300, 2015. Disponível em: https://doi.org/10.5607/en.2015.24.4.285

MADHYASTHA, Sampath; SEKHAR, Sudhanshu; RAO, Gayathri. Resveratrol improves postnatal hippocampal neurogenesis and brain derived neurotrophic factor in prenatally stressed rats. **International Journal of Developmental Neuroscience**, [*s. l.*], v. 31, n. 7, p. 580–585, 2013. Disponível em: https://doi.org/10.1016/J.IJDEVNEU.2013.06.010

MAENNER, Matthew J. *et al.* Prevalence and Characteristics of Autism Spectrum Disorder Among Children Aged 8 Years — Autism and Developmental Disabilities Monitoring Network, 11 Sites, United States, 2018. **MMWR. Surveillance Summaries**, [*s. l.*], v. 70, n. 11, p. 1–16, 2021. Disponível em: https://doi.org/10.15585/MMWR.SS7011A1. Acesso em: 13 mar. 2022.

MAIER, Simon *et al.* Increased hippocampal volumes in adults with high functioning autism spectrum disorder and an IQ>100: A manual morphometric study. **Psychiatry research**, [*s. l.*], v. 234, n. 1, p. 152–155, 2015. Disponível em: https://doi.org/10.1016/J.PSCYCHRESNS.2015.08.002. Acesso em: 14 mar. 2022.

MAIN, Stacey L.; KULESZA, Randy J. Repeated prenatal exposure to valproic acid results in cerebellar hypoplasia and ataxia. **Neuroscience**, [*s. l.*], v. 340, p. 34–47, 2017. Disponível em: https://doi.org/10.1016/J.NEUROSCIENCE.2016.10.052

MARKRAM, Kamila *et al.* Abnormal Fear Conditioning and Amygdala Processing in an Animal Model of Autism. **Neuropsychopharmacology**, [*s. l.*], v. 33, n. 4, p. 901–912, 2008. Disponível em: https://doi.org/10.1038/sj.npp.1301453. Acesso em: 29 nov. 2019.

MARKRAM, Kamila; MARKRAM, Henry. The Intense World Theory – A Unifying Theory of the Neurobiology of Autism. **Frontiers in Human Neuroscience**, [*s. l.*], v. 4, n. 1, p. 224, 2010. Disponível em: https://doi.org/10.3389/FNHUM.2010.00224. Acesso em: 13 mar. 2022.

MARSH, Eric D. *et al.* Developmental interneuron subtype deficits after targeted loss of Arx. **BMC Neuroscience**, [*s. l.*], v. 17, n. 1, p. 35, 2016. Disponível em: https://doi.org/10.1186/s12868-016-0265-8

MASSÉ, Karine *et al.* Purine-mediated signalling triggers eye development. **Nature**

2007 449:7165, [*s. l.*], v. 449, n. 7165, p. 1058–1062, 2007. Disponível em: https://doi.org/10.1038/nature06189. Acesso em: 14 mar. 2022.

MESBAH-OSKUI, Lia *et al.* Reduced expression of α5GABAA receptors elicits autism-like alterations in EEG patterns and sleep-wake behavior. **Neurotoxicology and Teratology**, [*s. l.*], v. 61, p. 115–122, 2017. Disponível em: https://doi.org/10.1016/J.NTT.2016.10.009

MIHALJEVIĆ, Bojan *et al.* Classification of GABAergic interneurons by leading neuroscientists. **Scientific Data 2019 6:1**, [*s. l.*], v. 6, n. 1, p. 1–6, 2019. Disponível em: https://doi.org/10.1038/s41597-019-0246-8. Acesso em: 14 mar. 2022.

MINAKOVA, Elena; WARNER, Barbara B. Maternal immune activation, central nervous system development and behavioral phenotypes. **Birth defects research**, [*s. l.*], v. 110, n. 20, p. 1539–1550, 2018. Disponível em: https://doi.org/10.1002/BDR2.1416. Acesso em: 13 mar. 2022.

MIRY, Omid; LI, Jie; CHEN, Lu. The Quest for the Hippocampal Memory Engram: From Theories to Experimental Evidence. **Frontiers in Behavioral Neuroscience**, [*s. l.*], v. 14, p. 270, 2021. Disponível em: https://doi.org/10.3389/FNBEH.2020.632019/BIBTEX

MIRZAA, Ghayda M. *et al.* De novo and inherited variants in ZNF292 underlie a neurodevelopmental disorder with features of autism spectrum disorder. **Genetics in Medicine**, [*s. l.*], v. 22, n. 3, p. 538-546, 2020. Disponível em: https://doi.org/10.1038/s41436-019-0693-9

MIYAZAKI, Kaoru; NARITA, Naoko; NARITA, Masaaki. Maternal administration of thalidomide or valproic acid causes abnormal serotonergic neurons in the offspring: implication for pathogenesis of autism. **International Journal of Developmental Neuroscience**, [*s. l.*], v. 23, n. 2–3, p. 287–297, 2005. Disponível em: https://doi.org/10.1016/J.IJDEVNEU.2004.05.004. Acesso em: 29 nov. 2019.

MOLLINEDO, Pilar *et al.* Cellular and animal models of skin alterations in the autism-related ADNP syndrome. **Scientific Reports**, [*s. l.*], v. 9, n. 1, p. 736, 2019. Disponível em: https://doi.org/10.1038/s41598-018-36859-2. Acesso em: 16 dez. 2020.

MONTIEL-NAVA, Cecilia; PEÑA, Joaquín A. Epidemiological findings of pervasive developmental disorders in a Venezuelan study. **Autism : the international**

journal of research and practice, [*s. l.*], v. 12, n. 2, p. 191–202, 2008. Disponível em: https://doi.org/10.1177/1362361307086663. Acesso em: 8 mar. 2022.

MORRIS, Colleen A. Williams Syndrome. [*s. l.*], 2017. Disponível em: https://www.ncbi.nlm.nih.gov/books/NBK1249/. Acesso em: 16 dez. 2020.

MURRAY, Andrew J. *et al.* Parvalbumin-positive CA1 interneurons are required for spatial working but not for reference memory. **Nature Neuroscience**, [*s. l.*], v. 14, p. 297-299, 2011. Disponível em: https://doi.org/10.1038/nn.2751

MURRAY, Andrew J. *et al.* Parvalbumin-positive interneurons of the prefrontal cortex support working memory and cognitive flexibility. **Scientific Reports 2015 5:1**, [*s. l.*], v. 5, n. 1, p. 1–14, 2015. Disponível em: https://doi.org/10.1038/srep16778. Acesso em: 14 mar. 2022.

NAKAMURA, Jay P. *et al.* Maternal immune activation targeted to a window of parvalbumin interneuron development improves spatial working memory: Implications for autism. **Brain, behavior, and immunity**, [*s. l.*], v. 91, p. 339–349, 2021. Disponível em: https://doi.org/10.1016/J.BBI.2020.10.012. Acesso em: 14 mar. 2022.

NAKAMURA, Jay P. *et al.* The maternal immune activation model uncovers a role for the Arx gene in GABAergic dysfunction in schizophrenia. **Brain, Behavior, and Immunity**, [*s. l.*], v. 81, p. 161–171, 2019. Disponível em: https://doi.org/10.1016/j.bbi.2019.06.009. Acesso em: 16 dez. 2020.

NAKAMURA, Tsutomu *et al.* PX-RICS-deficient mice mimic autism spectrum disorder in Jacobsen syndrome through impaired GABAA receptor trafficking. **Nature Communications 2016 7:1**, [*s. l.*], v. 7, n. 1, p. 1–16, 2016. Disponível em: https://doi.org/10.1038/ncomms10861. Acesso em: 14 mar. 2022.

NASRALLAH, Kaoutsar *et al.* Routing Hippocampal Information Flow through Parvalbumin Interneuron Plasticity in Area CA2. **Cell reports**, [*s. l.*], v. 27, n. 1, p. 86-98.e3, 2019. Disponível em: https://doi.org/10.1016/J.CELREP.2019.03.014. Acesso em: 14 mar. 2022.

NAVIAUX, J. C. *et al.* Reversal of autism-like behaviors and metabolism in adult mice with single-dose antipurinergic therapy. **Translational psychiatry**, [*s. l.*], v. 4, p. 6, 2014. Disponível em: https://doi.org/10.1038/TP.2014.33. Acesso em: 14 mar. 2022.

NI, Lulu *et al.* The histone deacetylase inhibitor valproic acid inhibits NKG2D

expression in natural killer cells through suppression of STAT3 and HDAC3. **Scientific reports**, [*s. l.*], v. 7, p. e45266, 2017. Disponível em: https://doi.org/10.1038/SREP45266. Acesso em: 14 mar. 2022.

NINKOVIC, Jovica *et al.* The BAF complex interacts with Pax6 in adult neural progenitors to establish a neurogenic cross-regulatory transcriptional network. **Cell stem cell**, [*s. l.*], v. 13, n. 4, p. 403–418, 2013. Disponível em: https://doi.org/10.1016/J.STEM.2013.07.002. Acesso em: 14 mar. 2022.

NIU, Juan; CAO, Yuquan; JI, Yongjuan. Resveratrol, a SIRT1 Activator, Ameliorates MK-801-Induced Cognitive and Motor Impairments in a Neonatal Rat Model of Schizophrenia. **Frontiers in psychiatry**, [*s. l.*], v. 11, p. 716, 2020. Disponível em: https://doi.org/10.3389/FPSYT.2020.00716. Acesso em: 14 mar. 2022.

NOMURA, Toshihiro. Interneuron Dysfunction and Inhibitory Deficits in Autism and Fragile X Syndrome. **Cells**, [*s. l.*], v. 10, p. 10, 2021. Disponível em: https://doi.org/10.3390/CELLS10102610. Acesso em: 14 mar. 2022.

O'ROAK, B. J. *et al.* Recurrent de novo mutations implicate novel genes underlying simplex autism risk. **Nature Communications**, [*s. l.*], v. 5, p. 5595, 2014. Disponível em: https://doi.org/10.1038/ncomms6595. Acesso em: 16 dez. 2020.

O'ROAK, Brian J. *et al.* Multiplex targeted sequencing identifies recurrently mutated genes in autism spectrum disorders. **Science**, [*s. l.*], v. 338, n. 6114, p. 1619–1622, 2012. Disponível em: https://doi.org/10.1126/science.1227764. Acesso em: 16 dez. 2020.

OBLAK, Adrian; GIBBS, T. T.; BLATT, G. J. Decreased GABAA receptors and benzodiazepine binding sites in the anterior cingulate cortex in autism. **Autism Research**, [*s. l.*], v. 2, n. 4, p. 205–219, 2009. Disponível em: https://doi.org/10.1002/AUR.88. Acesso em: 14 mar. 2022.

OGNJANOVSKI, Nicolette *et al.* Parvalbumin-expressing interneurons coordinate hippocampal network dynamics required for memory consolidation. **Nature Communications**, [*s. l.*], v. 8, p. e15039, 2017. Disponível em: https://doi.org/10.1038/ncomms15039

OHTSUKA, Nobuhisa *et al.* GABAergic neurons regulate lateral ventricular development via transcription factor Pax5. **Genesis**, [*s. l.*], v. 51, n. 4, p. 234–245, 2013. Disponível em: https://doi.org/10.1002/dvg.22370. Acesso em: 16 dez. 2020.

OKADA, Akinobu *et al.* Identification of early-responsive genes correlated to valproic

acid-induced neural tube defects in mice. **Birth Defects Research Part A - Clinical and Molecular Teratology**, [*s. l.*], v. 73, n. 4, p. 229–238, 2005. Disponível em: https://doi.org/10.1002/bdra.20131. Acesso em: 16 dez. 2020.

OKADA, Yui *et al.* Dietary Resveratrol Prevents the Development of Food Allergy in Mice. **PLOS ONE**, [*s. l.*], v. 7, n. 9, p. e44338, 2012. Disponível em: https://doi.org/10.1371/JOURNAL.PONE.0044338. Acesso em: 14 mar. 2022.

ÖNGÜR, D.; PRICE, Joseph L. The Organization of Networks within the Orbital and Medial Prefrontal Cortex of Rats, Monkeys and Humans. **Cerebral Cortex**, [*s. l.*], v. 10, n. 3, p. 206–219, 2000. Disponível em: https://doi.org/10.1093/CERCOR/10.3.206. Acesso em: 14 mar. 2022.

OSKVIG, Devon B. *et al.* Maternal immune activation by LPS selectively alters specific gene expression profiles of interneuron migration and oxidative stress in the fetus without triggering a fetal immune response. **Brain, Behavior, and Immunity**, [*s. l.*], v. 26, n. 4, p. 623, 2012. Disponível em: https://doi.org/10.1016/J.BBI.2012.01.015. Acesso em: 3 mar. 2022.

PACKER, Adam M; YUSTE, Rafael. Dense, unspecific connectivity of neocortical parvalbumin-positive interneurons: a canonical microcircuit for inhibition? **The Journal of neuroscience : the official journal of the Society for Neuroscience**, [*s. l.*], v. 31, n. 37, p. 13260–13271, 2011. Disponível em: https://doi.org/10.1523/JNEUROSCI.3131-11.2011. Acesso em: 29 nov. 2019.

PAGANI, Marco *et al.* Deletion of Autism Risk Gene Shank3 Disrupts Prefrontal Connectivity. **Journal of Neuroscience**, [*s. l.*], v. 39, n. 27, p. 5299–5310, 2019. Disponível em: https://doi.org/10.1523/JNEUROSCI.2529-18.2019. Acesso em: 14 mar. 2022.

PAL, Krishnendu *et al.* Inhibition of gsk-3 induces differentiation and impaired glucose metabolism in renal cancer. **Molecular Cancer Therapeutics**, [*s. l.*], v. 13, n. 2, p. 285–296, 2014. Disponível em: https://doi.org/10.1158/1535-7163.MCT-13-0681/85875/AM/INHIBITION-OF-GSK-3-INDUCES-DIFFERENTIATION-AND. Acesso em: 14 mar. 2022.

PANTAZOPOULOS, Harry *et al.* Decreased Numbers of Somatostatin-Expressing Neurons in the Amygdala of Subjects With Bipolar Disorder or Schizophrenia: Relationship to Circadian Rhythms. **Biological psychiatry**, [*s. l.*], v. 81, n. 6, p. 536–547, 2017. Disponível em: https://doi.org/10.1016/J.BIOPSYCH.2016.04.006. Acesso em: 14 mar. 2022.

PARIKSHAK, Neelroop N. *et al.* Genome-wide changes in lncRNA, splicing, and regional gene expression patterns in autism. **Nature**, [*s. l.*], v. 540, n. 7633, p. 423–427, 2016. Disponível em: https://doi.org/10.1038/nature20612. Acesso em: 16 dez. 2020.

PARK, Byung Yong; SAINT-JEANNET, Jean Pierre. Long-term consequences of Sox9 depletion on inner ear development. **Developmental dynamics : an official publication of the American Association of Anatomists**, [*s. l.*], v. 239, n. 4, p. 1102, 2010. Disponível em: https://doi.org/10.1002/DVDY.22259. Acesso em: 14 mar. 2022.

PARKER, Elaine L. *et al.* Viral-Immune Cell Interactions at the Maternal-Fetal Interface in Human Pregnancy. **Frontiers in Immunology**, [*s. l.*], v. 11, p. 2561, 2020. Disponível em: https://doi.org/10.3389/FIMMU.2020.522047/BIBTEX

PATERNO, Rosalia *et al.* Hippocampal gamma and sharp-wave ripple oscillations are altered in a Cntnap2 mouse model of autism spectrum disorder. **Cell reports**, [*s. l.*], v. 37, p. 6, 2021. Disponível em: https://doi.org/10.1016/J.CELREP.2021.109970. Acesso em: 14 mar. 2022.

PATTERSON, Paul H. Modeling Autistic Features in Animals. **Pediatric research**, [*s. l.*], v. 69, n. 5 Pt 2, p. 34R, 2011. Disponível em: https://doi.org/10.1203/PDR.0B013E318212B80F. Acesso em: 13 mar. 2022.

PAULA, Cristiane S. *et al.* Brief report: prevalence of pervasive developmental disorder in Brazil: a pilot study. **Journal of autism and developmental disorders**, [*s. l.*], v. 41, n. 12, p. 1738–1742, 2011. Disponível em: https://doi.org/10.1007/S10803-011-1200-6. Acesso em: 13 mar. 2022.

PAXINOS, George; WATSON, Charles. **The Rat Brain in Stereotaxic Coordinates - The New Coronal Set**. 5th editioned. [*S. l.: s. n.*], 2004. v. 1

PELKEY, Kenneth A. *et al.* Hippocampal GABAergic Inhibitory Interneurons. **Physiological Reviews**, [*s. l.*], v. 97, n. 4, p. 1619, 2017. Disponível em: https://doi.org/10.1152/PHYSREV.00007.2017. Acesso em: 2 mar. 2022.

PI, Hyun Jae *et al.* Cortical interneurons that specialize in disinhibitory control. **Nature**, [*s. l.*], v. 503, n. 7477, p. 521–524, 2013. Disponível em: https://doi.org/10.1038/NATURE12676. Acesso em: 14 mar. 2022.

PIGNATARO, Leonardo *et al.* The regulation of neuronal gene expression by alcohol. **Pharmacology & therapeutics**, [*s. l.*], v. 124, n. 3, p. 324, 2009. Disponível em: https://doi.org/10.1016/J.PHARMTHERA.2009.09.002. Acesso em: 14 mar.

2022.

PINGAULT, Véronique *et al.* SOX10 mutations in patients with Waardenburg-Hirschsprung disease. **Nature Genetics**, [*s. l.*], v. 18, n. 2, p. 171–173, 1998. Disponível em: https://doi.org/10.1038/ng0298-171. Acesso em: 16 dez. 2020.

PINYAEV, S. I. *et al.* Influence of Resveratrol on Oxidation Processes and Lipid Phase Characteristics in Damaged Somatic Nerves. **BioMed Research International**, [*s. l.*], v. 2019, p. e2381907, 2019. Disponível em: https://doi.org/10.1155/2019/2381907. Acesso em: 14 mar. 2022.

PIORCZYNSKI, Ted B. *et al.* NRF2 activation protects against valproic acid-induced disruption of neurogenesis in P19 cells. **Differentiation**, [*s. l.*], v. 123, p. 18–29, 2022. Disponível em: https://doi.org/10.1016/J.DIFF.2021.12.002

POWELL, Elizabeth M. *et al.* Genetic disruption of cortical interneuron development causes region- and GABA cell type-specific deficits, epilepsy, and behavioral dysfunction. **The Journal of neuroscience : the official journal of the Society for Neuroscience**, [*s. l.*], v. 23, n. 2, p. 622–631, 2003. Disponível em: https://doi.org/10.1523/JNEUROSCI.23-02-00622.2003. Acesso em: 14 mar. 2022.

PRESTIGIO, Cosimo *et al.* Rest/nrsf drives homeostatic plasticity of inhibitory synapses in a target-dependent fashion. **eLife**, [*s. l.*], v. 10, p. e69058, 2021. Disponível em: https://doi.org/10.7554/ELIFE.69058

PROVENZANO, Giovanni *et al.* Altered Expression of GABAergic Markers in the Forebrain of Young and Adult Engrailed-2 Knockout Mice. **Genes**, [*s. l.*], v. 11, p. 4, 2020. Disponível em: https://doi.org/10.3390/GENES11040384. Acesso em: 14 mar. 2022.

PROVENZANO, Giovanni *et al.* Comparative gene expression analysis of two mouse models of autism: Transcriptome profiling of the BTBR and En2-/- Hippocampus. **Frontiers in Neuroscience**, [*s. l.*], v. 10, n. AUG, p. 396, 2016. Disponível em: https://doi.org/10.3389/FNINS.2016.00396/BIBTEX

QIN, Xin *et al.* Adenosine Signaling and Clathrin-Mediated Endocytosis of Glutamate AMPA Receptors in Delayed Hypoxic Injury in Rat Hippocampus: Role of Casein Kinase 2. **Molecular Neurobiology**, [*s. l.*], v. 58, n. 5, p. 1932–1951, 2021. Disponível em: https://doi.org/10.1007/s12035-020-02246-0. Acesso em: 14 maio 2021.

RAHMAN, Masum; NGUYEN, Hoang. **Valproic Acid**. 1. ed. Treasure Island:

StatPearls [Internet], 2022. v. 1*E-book*.

REINER, Orly *et al.* Regulation of neuronal migration, an emerging topic in autism spectrum disorders. **Journal of Neurochemistry**, [*s. l.*], v. 136, n. 3, p. 440–456, 2016. Disponível em: https://doi.org/10.1111/jnc.13403

REPOUSKOU, Anastasia *et al.* Long term transcriptional and behavioral effects in mice developmentally exposed to a mixture of endocrine disruptors associated with delayed human neurodevelopment. **Scientific Reports 2020 10:1**, [*s. l.*], v. 10, n. 1, p. 1–16, 2020. Disponível em: https://doi.org/10.1038/s41598-020-66379-x. Acesso em: 14 mar. 2022.

RIAZ, Sadia *et al.* Prelimbic and infralimbic cortical inactivations attenuate contextually driven discriminative responding for reward. **Scientific Reports 2019 9:1**, [*s. l.*], v. 9, n. 1, p. 1–13, 2019. Disponível em: https://doi.org/10.1038/s41598-019-40532-7. Acesso em: 14 mar. 2022.

RICE, Catherine. Prevalence of Autism Spectrum Disorders - Autism and Developmental Disabilities Monitoring Network, Six Sites, United States, 2000. **Surveill Summ.**, [*s. l.*], v. 56, n. 1, p. 1–11, 2007. Disponível em: https://www.cdc.gov/mmwr/preview/mmwrhtml/ss5601a1.htm. Acesso em: 13 mar. 2022.

RICHARDS, Rose *et al.* Increased hippocampal shape asymmetry and volumetric ventricular asymmetry in autism spectrum disorder. **NeuroImage: Clinical**, [*s. l.*], v. 26, p. 102207, 2020. Disponível em: https://doi.org/10.1016/j.nicl.2020.102207

RIEDEMANN, Therese. Diversity and Function of Somatostatin-Expressing Interneurons in the Cerebral Cortex. **International journal of molecular sciences**, [*s. l.*], v. 20, p. 12, 2019. Disponível em: https://doi.org/10.3390/IJMS20122952. Acesso em: 14 mar. 2022.

RINALDI, Tania; PERRODIN, Catherine; MARKRAM, Henry. Hyper-connectivity and hyper-plasticity in the medial prefrontal cortex in the valproic Acid animal model of autism. **Frontiers in neural circuits**, [*s. l.*], v. 2, n. OCT, 2008. Disponível em: https://doi.org/10.3389/NEURO.04.004.2008. Acesso em: 14 mar. 2022.

ROBBINS, Richard J. *et al.* A selective loss of somatostatin in the hippocampus of patients with temporal lobe epilepsy. **Annals of Neurology**, [*s. l.*], v. 29, n. 3, p. 325–332, 1991. Disponível em: https://doi.org/10.1002/ANA.410290316. Acesso em: 14 mar. 2022.

ROBERTSON, Susan E. *et al.* Rubella and congenital rubella syndrome: global update. **Revista panamericana de salud publica = Pan American journal of public health**, [*s. l.*], v. 14, n. 5, p. 306–315, 2003. Disponível em: https://doi.org/10.1590/S1020-49892003001000005. Acesso em: 13 mar. 2022.

RODIER, Patricia M. *et al.* Embryological origin for autism: Developmental anomalies of the cranial nerve motor nuclei. **Journal of Comparative Neurology**, [*s. l.*], v. 370, n. 2, p. 247–261, 1996. Disponível em: https://doi.org/10.1002/(SICI)1096-9861(19960624)370:2<247::AID-CNE8>3.0.CO;2-2

ROSENBERG, Rebecca E. *et al.* Characteristics and concordance of autism spectrum disorders among 277 twin pairs. **Archives of pediatrics & adolescent medicine**, [*s. l.*], v. 163, n. 10, p. 907–914, 2009. Disponível em: https://doi.org/10.1001/ARCHPEDIATRICS.2009.98. Acesso em: 13 mar. 2022.

ROSENBERG, Roger N.; PASCUAL, Juan M. **Rosenberg's Molecular and Genetic Basis of Neurological and Psychiatric Disease: Fifth Edition**. [*S. l.: s. n.*], 2014.

ROTZOLL, M. *et al.* [Nazi action T4 euthanasia programme: historical research, individual life stories and the culture of remembrance]. **Der Nervenarzt**, [*s. l.*], v. 81, n. 11, p. 1326–1332, 2010. Disponível em: https://doi.org/10.1007/S00115-010-3054-0. Acesso em: 13 mar. 2022.

ROUT, Ujjwal K.; CLAUSEN, Pete. Common increase of GATA-3 level in PC-12 cells by three teratogens causing autism spectrum disorders. **Neuroscience research**, [*s. l.*], v. 64, n. 2, p. 162–169, 2009. Disponível em: https://doi.org/10.1016/J.NEURES.2009.02.009. Acesso em: 14 mar. 2022.

RUBENSTEIN, J. L.R.; MERZENICH, M. M. Model of autism: increased ratio of excitation/inhibition in key neural systems. **Genes, brain, and behavior**, [*s. l.*], v. 2, n. 5, p. 255, 2003. Disponível em: https://doi.org/10.1034/j.1601-183X.2003.00037.x. Acesso em: 14 mar. 2022.

RUBIN, Rachael D. *et al.* The role of the hippocampus in flexible cognition and social behavior. **Frontiers in Human Neuroscience**, [*s. l.*], v. 8, p. 742, 2014. Disponível em: https://doi.org/10.3389/fnhum.2014.00742

RYLAARSDAM, Lauren; GUEMEZ-GAMBOA, Alicia. Genetic Causes and Modifiers of Autism Spectrum Disorder. **Frontiers in Cellular Neuroscience**, [*s. l.*], v. 13, p. 385, 2019. Disponível em: https://doi.org/10.3389/FNCEL.2019.00385/BIBTEX

SACCO, Roberto; GABRIELE, Stefano; PERSICO, Antonio M. Head circumference and brain size in autism spectrum disorder: A systematic review and meta-analysis. **Psychiatry research**, [*s. l.*], v. 234, n. 2, p. 239–251, 2015. Disponível em: https://doi.org/10.1016/J.PSCYCHRESNS.2015.08.016. Acesso em: 14 mar. 2022.

SAILER, L. *et al.* Consequences of prenatal exposure to valproic acid in the socially monogamous prairie voles. **Scientific Reports 2019 9:1**, [*s. l.*], v. 9, n. 1, p. 1–14, 2019. Disponível em: https://doi.org/10.1038/s41598-019-39014-7. Acesso em: 14 mar. 2022.

SALLOUM-ASFAR, Salam *et al.* Circulating non-coding rnas as a signature of autism spectrum disorder symptomatology. **International Journal of Molecular Sciences**, [*s. l.*], v. 22, p. 12, 2021. Disponível em: https://doi.org/10.3390/IJMS22126549/S1. Acesso em: 13 mar. 2022.

SAMAEI, Areoo *et al.* Resveratrol Adjunct Therapy for Negative Symptoms in Patients With Stable Schizophrenia: A Double-Blind, Randomized Placebo-Controlled Trial. **The international journal of neuropsychopharmacology**, [*s. l.*], v. 23, n. 12, p. 775–782, 2020. Disponível em: https://doi.org/10.1093/IJNP/PYAA006. Acesso em: 14 mar. 2022.

SÁNCHEZ-ALVAREZ, Rosa *et al.* Ethanol Diverts Early Neuronal Differentiation Trajectory of Embryonic Stem Cells by Disrupting the Balance of Lineage Specifiers. **PLoS ONE**, [*s. l.*], v. 8, n. 5, p. e63794, 2013. Disponível em: https://doi.org/10.1371/journal.pone.0063794. Acesso em: 16 dez. 2020.

SANDIN, Sven *et al.* The Heritability of Autism Spectrum Disorder. **JAMA**, [*s. l.*], v. 318, n. 12, p. 1182, 2017. Disponível em: https://doi.org/10.1001/JAMA.2017.12141. Acesso em: 13 mar. 2022.

SARMAH, Swapnalee *et al.* Embryonic ethanol exposure alters expression of sox2 and other early transcripts in zebrafish, producing gastrulation defects. **Scientific Reports**, [*s. l.*], v. 10, n. 1, p. e3591 2020. Disponível em: https://doi.org/10.1038/s41598-020-59043-x. Acesso em: 16 dez. 2020.

SATTERSTROM, F Kyle *et al.* Large-Scale Exome Sequencing Study Implicates Both Developmental and Functional Changes in the Neurobiology of Autism. **Cell**, [*s. l.*], v. 180, n. 3, p. 568-584, 2020. Disponível em: https://doi.org/10.1016/j.cell.2019.12.036. Acesso em: 13 mar. 2022.

SAWADA, Kazuhiko; KAMIYA, Shiori; AOKI, Ichio. Neonatal valproic acid exposure

produces altered gyrification related to increased parvalbumin-immunopositive neuron density with thickened sulcal floors. **PloS one**, [*s. l.*], v. 16, p. 4, 2021. Disponível em: https://doi.org/10.1371/JOURNAL.PONE.0250262. Acesso em: 14 mar. 2022.

SCHEGGIA, Diego *et al.* Somatostatin interneurons in the prefrontal cortex control affective state discrimination in mice. **Nature neuroscience**, [*s. l.*], v. 23, n. 1, p. 47–60, 2020. Disponível em: https://doi.org/10.1038/S41593-019-0551-8. Acesso em: 14 mar. 2022.

SCHEPICI, Giovanni *et al.* Autism Spectrum Disorder and miRNA: An Overview of Experimental Models. **Brain Sciences**, [*s. l.*], v. 9, p. 10, 2019. Disponível em: https://doi.org/10.3390/BRAINSCI9100265. Acesso em: 13 mar. 2022.

SCHNEIDER, Tomasz *et al.* Gender-specific behavioral and immunological alterations in an animal model of autism induced by prenatal exposure to valproic acid. **Psychoneuroendocrinology**, [*s. l.*], v. 33, n. 6, p. 728–740, 2008. Disponível em: https://doi.org/10.1016/j.psyneuen.2008.02.011. Acesso em: 24 maio 2021.

SCHNEIDER, Tomasz; PRZEWŁOCKI, Ryszard. Behavioral Alterations in Rats Prenatally Exposed to Valproic Acid: Animal Model of Autism. **Neuropsychopharmacology**, [*s. l.*], v. 30, n. 1, p. 80–89, 2005. Disponível em: https://doi.org/10.1038/sj.npp.1300518

SCHNEIDER, Tomasz; TURCZAK, Joanna; PRZEWŁOCKI, Ryszard. Environmental enrichment reverses behavioral alterations in rats prenatally exposed to valproic acid: issues for a therapeutic approach in autism. **Neuropsychopharmacology : official publication of the American College of Neuropsychopharmacology**, [*s. l.*], v. 31, n. 1, p. 36–46, 2006. Disponível em: https://doi.org/10.1038/SJ.NPP.1300767. Acesso em: 14 mar. 2022.

SCHOOF, Melanie *et al.* The basic helix-loop-helix transcription factor TCF4 impacts brain architecture as well as neuronal morphology and differentiation. **European Journal of Neuroscience**, [*s. l.*], v. 51, n. 11, p. 2219–2235, 2020. Disponível em: https://doi.org/10.1111/ejn.14674. Acesso em: 16 dez. 2020.

SCHUMANN, Cynthia Mills *et al.* The Amygdala Is Enlarged in Children But Not Adolescents with Autism; the Hippocampus Is Enlarged at All Ages. **Journal of Neuroscience**, [*s. l.*], v. 24, n. 28, p. 6392–6401, 2004. Disponível em: https://doi.org/10.1523/JNEUROSCI.1297-04.2004. Acesso em: 14 mar. 2022.

SHAHBAZIAN, Mona D.; ZOGHBI, Huda Y. Molecular genetics of Rett syndrome and clinical spectrum of MECP2 mutations. **Curr Opin Neurol**, v. 4, n. 2. p. 171-6, 2001. Disponível em: https://doi.org/10.1097/00019052-200104000-00006. Acesso em: 16 dez. 2020.

SHARMA, Kedarlal *et al.* Involvement of MeCP2 in Regulation of Myelin-Related Gene Expression in Cultured Rat Oligodendrocytes. **Journal of Molecular Neuroscience**, [*s. l.*], v. 57, n. 2, p. 176–184, 2015. Disponível em: https://doi.org/10.1007/s12031-015-0597-3. Acesso em: 16 dez. 2020.

SHERR, Elliott H. The ARX story (epilepsy, mental retardation, autism, and cerebral malformations): one gene leads to many phenotypes. **Current opinion in pediatrics**, [*s. l.*], v. 15, n. 6, p. 567–571, 2003. Disponível em: https://doi.org/10.1097/00008480-200312000-00004. Acesso em: 13 mar. 2022.

SHIN, Sangyep; SANTI, Andrea; HUANG, Shiyong. Conditional Pten knockout in parvalbumin- or somatostatin-positive neurons sufficiently leads to autism-related behavioral phenotypes. **Molecular Brain**, [*s. l.*], v. 14, n. 1, p. 24, 2021. Disponível em: https://doi.org/10.1186/s13041-021-00731-8

SIGAL, Yaron M. *et al.* Structural maturation of cortical perineuronal nets and their perforating synapses revealed by superresolution imaging. **Proceedings of the National Academy of Sciences of the United States of America**, [*s. l.*], v. 116, n. 14, p. 7071–7076, 2019. Disponível em: https://doi.org/10.1073/pnas.1817222116. Acesso em: 16 dez. 2020.

SIGURDSSON, Torfi; DUVARCI, Sevil. Hippocampal-prefrontal interactions in cognition, behavior and psychiatric disease. **Frontiers in Systems Neuroscience**, [*s. l.*], v. 9, n. JAN2016, p. 190, 2016. Disponível em: https://doi.org/10.3389/FNSYS.2015.00190/BIBTEX

SILVA, Guilherme Testa *et al.* Enhanced long-term microcircuit plasticity in the valproic Acid animal model of autism. **Frontiers in synaptic neuroscience**, [*s. l.*], v. 1, n. 1, p. 1–9, 2009. Disponível em: https://doi.org/10.3389/NEURO.19.001.2009. Acesso em: 14 mar. 2022.

SILVA, M. F.B. *et al.* Valproic acid metabolism and its effects on mitochondrial fatty acid oxidation: a review. **Journal of inherited metabolic disease**, [*s. l.*], v. 31, n. 2, p. 205–216, 2008. Disponível em: https://doi.org/10.1007/S10545-008-0841-X. Acesso em: 14 mar. 2022.

SINGH, Narendra *et al.* Resveratrol ameliorates lupus by epigenetic modulation of

Foxp3 and IL-17 genes resulting in differential regulation of regulatory T cells and Th17 cells via activation of aryl hydrocarbon receptor (P5129). **The Journal of Immunology**, [*s. l.*], v. 190, n. 137 Supplement, 2013.

SMITH, Amanda L. *et al.* Arid1b haploinsufficiency in parvalbumin- or somatostatin-expressing interneurons leads to distinct ASD-like and ID-like behavior. **Scientific Reports**, [*s. l.*], v. 10, n. 1, p. e7834, 2020. Disponível em: https://doi.org/10.1038/s41598-020-64066-5

SMITH DAWALT, Leann *et al.* Mortality in Individuals with Autism Spectrum Disorder: Predictors over a 20-Year Period. **Autism : the international journal of research and practice**, [*s. l.*], v. 23, n. 7, p. 1732, 2019. Disponível em: https://doi.org/10.1177/1362361319827412. Acesso em: 14 mar. 2022.

SMITS, Patrick *et al.* The transcription factors L-Sox5 and Sox6 are essential for cartilage formation. **Developmental cell**, [*s. l.*], v. 1, n. 2, p. 277–290, 2001. Disponível em: https://doi.org/10.1016/S1534-5807(01)00003-X. Acesso em: 14 mar. 2022.

SOMERVILLE, Leah H.; HEATHERTON, Todd F.; KELLEY, William M. Anterior cingulate cortex responds differentially to expectancy violation and social rejection. **Nature Neuroscience 2006 9:8**, [*s. l.*], v. 9, n. 8, p. 1007–1008, 2006. Disponível em: https://doi.org/10.1038/nn1728. Acesso em: 14 mar. 2022.

SONG, Liang *et al.* A transcription factor hierarchy defines an environmental stress response network. **Science (New York, N.Y.)**, [*s. l.*], v. 354, p. e6312, 2016. Disponível em: https://doi.org/10.1126/SCIENCE.AAG1550. Acesso em: 14 mar. 2022.

SOUTO, Andreh A *et al.* Determination of trans-Resveratrol Concentrations in Brazilian Red Wines by HPLC. **JOURNAL OF FOOD COMPOSITION AND ANALYSIS**, [*s. l.*], v. 14, p. 441–445, 2001. Disponível em: https://doi.org/10.1006/jfca.2000.0970. Acesso em: 14 mar. 2022.

SPENCE, Sarah J; SCHNEIDER, Mark T. The Role of Epilepsy and Epileptiform EEGs in Autism Spectrum Disorders. **Pediatric research**, [*s. l.*], v. 65, n. 6, p. 599, 2009. Disponível em: https://doi.org/10.1203/01.PDR.0000352115.41382.65. Acesso em: 2 mar. 2022.

SRAGOVICH, Shlomo; MERENLENDER-WAGNER, Avia; GOZES, Illana. ADNP Plays a Key Role in Autophagy: From Autism to Schizophrenia and Alzheimer’s

Disease. **John Wiley and Sons Inc.**, [*s. l.*], v. 39, n. 11, p. e2017, 2017. Disponível em: https://doi.org/10.1002/bies.201700054. Acesso em: 16 dez. 2020.

SSUCHAREWA, G. E. Die schizoiden Psychopathien im Kindesalter. (Part 1 of 2). **European Neurology**, [*s. l.*], v. 60, n. 3–4, p. 235–247, 1926. Disponível em: https://doi.org/10.1159/000190478. Acesso em: 13 mar. 2022.

STAGNO, S. *et al.* Auditory and Visual Defects Resulting from Symptomatic and Subclinical Congenital Cytomegaloviral and Toxoplasma Infections. **Pediatrics**, [*s. l.*], v. 59, n. 5, p. 669–678, 1977. Disponível em: https://doi.org/10.1542/PEDS.59.5.669. Acesso em: 13 mar. 2022.

STAIGER, Jochen F. *et al.* Calbindin-containing interneurons are a target for VIP-immunoreactive synapses in rat primary somatosensory cortex. **The Journal of comparative neurology**, [*s. l.*], v. 468, n. 2, p. 179–189, 2004. Disponível em: https://doi.org/10.1002/CNE.10953. Acesso em: 14 mar. 2022.

STEFANELLI, Thomas *et al.* Hippocampal Somatostatin Interneurons Control the Size of Neuronal Memory Ensembles. **Neuron**, [*s. l.*], v. 89, n. 5, p. 1074–1085, 2016. Disponível em: https://doi.org/10.1016/j.neuron.2016.01.024. Acesso em: 29 nov. 2019.

STEINMAN, Gary. COVID-19 and autism. **Medical Hypotheses**, [*s. l.*], v. 1, n. 42, p. 109797, 2020. Disponível em: https://doi.org/10.1016/j.mehy.2020.109797. Acesso em: 13 mar. 2022.

STEVENS, Sara A. *et al.* Autism characteristics in children with fetal alcohol spectrum disorders. **Child Neuropsychology**, [*s. l.*], v. 19, n. 6, p. 579–587, 2013. Disponível em: https://doi.org/10.1080/09297049.2012.727791. Acesso em: 13 mar. 2022.

STODGELL, Christopher J. *et al.* Induction of the homeotic gene Hoxa1 through valproic acid's teratogenic mechanism of action. **Neurotoxicology and teratology**, [*s. l.*], v. 28, n. 5, p. 617–624, 2006. Disponível em: https://doi.org/10.1016/J.NTT.2006.08.004. Acesso em: 14 mar. 2022.

STOLT, C. Claus *et al.* Transcription factors Sox8 and Sox10 perform non-equivalent roles during oligodendrocyte development despite functional redundancy. **Development**, [*s. l.*], v. 131, n. 10, p. 2349–2358, 2004. Disponível em: https://doi.org/10.1242/DEV.01114. Acesso em: 14 mar. 2022.

SUGATHAN, Aarathi *et al.* CHD8 regulates neurodevelopmental pathways

associated with autism spectrum disorder in neural progenitors. **Proceedings of the National Academy of Sciences of the United States of America**, [*s. l.*], v. 111, n. 42, p. E4468–E4477, 2014. Disponível em: https://doi.org/10.1073/PNAS.1405266111. Acesso em: 13 mar. 2022.

SUI, Li; CHEN, Meng. Prenatal exposure to valproic acid enhances synaptic plasticity in the medial prefrontal cortex and fear memories. **Brain Research Bulletin**, [*s. l.*], v. 87, n. 6, p. 556–563, 2012. Disponível em: https://doi.org/10.1016/J.BRAINRESBULL.2012.01.011

SUN, Gerald J. *et al.* Tangential migration of neuronal precursors of glutamatergic neurons in the adult mammalian brain. **Proceedings of the National Academy of Sciences of the United States of America**, [*s. l.*], v. 112, n. 30, p. 9484–9489, 2015. Disponível em: https://doi.org/10.1073/PNAS.1508545112/SUPPL_FILE/PNAS.1508545112.SM04.MP4. Acesso em: 14 mar. 2022.

SUZUKI, Katsuaki *et al.* Metabolite alterations in the hippocampus of high-functioning adult subjects with autism. **International Journal of Neuropsychopharmacology**, [*s. l.*], v. 13, n. 4, p. 529–534, 2010. Disponível em: https://doi.org/10.1017/S1461145709990952. Acesso em: 14 mar. 2022.

TAI, C. *et al.* Impaired excitability of somatostatin- and parvalbumin-expressing cortical interneurons in a mouse model of Dravet syndrome. **Proceedings of the National Academy of Sciences**, [*s. l.*], v. 111, n. 30, p. E3139–E3148, 2014. Disponível em: https://doi.org/10.1073/pnas.1411131111

TANG, Guomei *et al.* Loss of mTOR-dependent macroautophagy causes autistic-like synaptic pruning deficits. **Neuron**, [*s. l.*], v. 83, n. 5, p. 1131–1143, 2014. Disponível em: https://doi.org/10.1016/J.NEURON.2014.07.040. Acesso em: 3 mar. 2022.

TEIXEIRA, José R. *et al.* Transcription factor 4 and its association with psychiatric disorders. **Translational Psychiatry 2021 11:1**, [*s. l.*], v. 11, n. 1, p. 1–12, 2021. Disponível em: https://doi.org/10.1038/s41398-020-01138-0. Acesso em: 14 mar. 2022.

THAXTON, X Courtney *et al.* Common Pathophysiology in Multiple Mouse Models of Pitt-Hopkins Syndrome. **The Journal Of Neuroscience**, [*s. l.*], v. 38, n. 4, p. 918-936, 2018. Disponível em: https://doi.org/10.1523/JNEUROSCI.1305-17.2017

THE AUTISM SPECTRUM DISORDERS WORKING GROUP OF THE PSYCHIATRIC GENOMICS CONSORTIUM. Meta-analysis of GWAS of over 16,000 individuals with autism spectrum disorder highlights a novel locus at 10q24.32 and a significant overlap with schizophrenia. **Molecular autism**, [*s. l.*], v. 8, p. 21, 2017. Disponível em: https://doi.org/10.1186/s13229-017-0137-9

THOMPSON, Jeremy M.; NEUGEBAUER, Volker. Cortico-limbic pain mechanisms. **Neuroscience letters**, [*s. l.*], v. 702, p. 15, 2019. Disponível em: https://doi.org/10.1016/J.NEULET.2018.11.037. Acesso em: 14 mar. 2022.

TIAN, Xia *et al.* Resveratrol limits diabetes-associated cognitive decline in rats by preventing oxidative stress and inflammation and modulating hippocampal structural synaptic plasticity. **Brain Research**, [*s. l.*], v. 1650, p. 1–9, 2016. Disponível em: https://doi.org/10.1016/J.BRAINRES.2016.08.032

TRAKOSHIS, Stavros *et al.* Intrinsic excitation-inhibition imbalance affects medial prefrontal cortex differently in autistic men versus women. **eLife**, [*s. l.*], v. 9, p. 1–31, 2020. Disponível em: https://doi.org/10.7554/ELIFE.55684

TREFFERT, Darold A. Epidemiology of Infantile Autism. **Archives of General Psychiatry**, [*s. l.*], v. 22, n. 5, p. 431–438, 1970. Disponível em: https://doi.org/10.1001/ARCHPSYC.1970.01740290047006. Acesso em: 13 mar. 2022.

TROPEANO, Maria *et al.* Microduplications at the pseudoautosomal SHOX locus in autism spectrum disorders and related neurodevelopmental conditions. **Journal of Medical Genetics**, [*s. l.*], v. 53, n. 8, p. 536–547, 2016. Disponível em: https://doi.org/10.1136/jmedgenet-2015-103621. Acesso em: 16 dez. 2020.

TSURUSAKI, Yoshinori *et al.* De novo SOX11 mutations cause Coffin–Siris syndrome. **Nature Communications 2014**, [*s. l.*], v. 5, n. 1, p. 1–7, 2014. Disponível em: https://doi.org/10.1038/ncomms5011. Acesso em: 14 mar. 2022.

TURUNEN, Joni A. *et al.* Mitochondrial aspartate/glutamate carrier SLC25A12 gene is associated with autism. **Autism research : official journal of the International Society for Autism Research**, [*s. l.*], v. 1, n. 3, p. 189–192, 2008. Disponível em: https://doi.org/10.1002/AUR.25. Acesso em: 13 mar. 2022.

TZAKIS, Nikolaos; HOLAHAN, Matthew R. Social Memory and the Role of the Hippocampal CA2 Region. **Frontiers in Behavioral Neuroscience**, [*s. l.*], v. 13, p. 233, 2019. Disponível em:

https://doi.org/10.3389/FNBEH.2019.00233/BIBTEX

UDDIN, R. K.; SINGH, S. M. Ethanol-responsive genes: identification of transcription factors and their role in metabolomics. **The Pharmacogenomics Journal 2007 7:1**, [*s. l.*], v. 7, n. 1, p. 38–47, 2006. Disponível em: https://doi.org/10.1038/sj.tpj.6500394. Acesso em: 14 mar. 2022.

URBAN-CIECKO, Joanna; BARTH, Alison L. Somatostatin-expressing neurons in cortical networks. **Nature Reviews Neuroscience**, [*s. l.*], v. 17, n. 7, p. 401–409, 2016. Disponível em: https://doi.org/10.1038/nrn.2016.53. Acesso em: 14 mar. 2022.

UZUNOVA, Genoveva; PALLANTI, Stefano; HOLLANDER, Eric. Excitatory/inhibitory imbalance in autism spectrum disorders: Implications for interventions and therapeutics. **The world journal of biological psychiatry : the official journal of the World Federation of Societies of Biological Psychiatry**, [*s. l.*], v. 17, n. 3, p. 174–186, 2016. Disponível em: https://doi.org/10.3109/15622975.2015.1085597. Acesso em: 13 mar. 2022.

VEENSTRA-VANDERWEELE, Jeremy; BLAKELY, Randy D. Networking in Autism: Leveraging Genetic, Biomarker and Model System Findings in the Search for New Treatments. **Neuropsychopharmacology 2011 37:1**, [*s. l.*], v. 37, n. 1, p. 196–212, 2011. Disponível em: https://doi.org/10.1038/npp.2011.185. Acesso em: 13 mar. 2022.

VEGAS, Nancy *et al.* Mutations in TBR1 gene leads to cortical malformations and intellectual disability. **European Journal of Medical Genetics**, [*s. l.*], v. 61, n. 12, p. 759–764, 2018. Disponível em: https://doi.org/10.1016/j.ejmg.2018.09.012. Acesso em: 16 dez. 2020.

VERONICA WITTE, A. *et al.* Effects of resveratrol on memory performance, hippocampal functional connectivity, and glucose metabolism in healthy older adults. **The Journal of neuroscience : the official journal of the Society for Neuroscience**, [*s. l.*], v. 34, n. 23, p. 7862–7870, 2014. Disponível em: https://doi.org/10.1523/JNEUROSCI.0385-14.2014. Acesso em: 14 mar. 2022.

VOGELGESANG, Steffen *et al.* Persistent expression of serotonin receptor 5b alters breathing behavior in male MeCP2 knockout mice. **Frontiers in Molecular Neuroscience**, [*s. l.*], v. 11, p. 28, 2018. Disponível em: https://doi.org/10.3389/fnmol.2018.00028. Acesso em: 16 dez. 2020.

VOJTECHOVA, Iveta *et al.* Behavioral Alterations and Decreased Number of

Parvalbumin-Positive Interneurons in Wistar Rats after Maternal Immune Activation by Lipopolysaccharide: Sex Matters. **International journal of molecular sciences**, [*s. l.*], v. 22, p. 6, 2021. Disponível em: https://doi.org/10.3390/IJMS22063274. Acesso em: 14 mar. 2022.

VOLK, David W. *et al.* Deficits in transcriptional regulators of cortical parvalbumin neurons in schizophrenia. **American Journal of Psychiatry**, [*s. l.*], v. 169, n. 10, p. 1082–1091, 2012. Disponível em: https://doi.org/10.1176/appi.ajp.2012.12030305. Acesso em: 17 dez. 2020.

VOLK, David W.; EDELSON, Jessica R.; LEWIS, David A. Altered expression of developmental regulators of parvalbumin and somatostatin neurons in the prefrontal cortex in schizophrenia. **Schizophrenia Research**, [*s. l.*], v. 177, n. 1–3, p. 3–9, 2016. Disponível em: https://doi.org/10.1016/j.schres.2016.03.001. Acesso em: 17 dez. 2020.

VOLK, David W.; EDELSON, Jessica R.; LEWIS, David A. Cortical inhibitory neuron disturbances in schizophrenia: Role of the ontogenetic transcription factor Lhx6. **Schizophrenia Bulletin**, [*s. l.*], v. 40, n. 5, p. 1053–1061, 2014. Disponível em: https://doi.org/10.1093/schbul/sbu068. Acesso em: 17 dez. 2020.

VORGIAS, Demetrios; BERNSTEIN, Bettina. **Fetal Alcohol Syndrome**. 1. ed. Treasure Island: StatPearls [Internet], 2022. v. 1*E-book*.

WALKER, Matthew Charles. Hippocampal Sclerosis: Causes and Prevention. **Seminars in neurology**, [*s. l.*], v. 35, n. 3, p. 193–200, 2015. Disponível em: https://doi.org/10.1055/S-0035-1552618. Acesso em: 14 mar. 2022.

WANG, Jingyi; JOHN, Yohan; BARBAS, Helen. Pathways for Contextual Memory: The Primate Hippocampal Pathway to Anterior Cingulate Cortex. **Cerebral Cortex**, [*s. l.*], v. 31, n. 3, p. 1807–1826, 2021. Disponível em: https://doi.org/10.1093/CERCOR/BHAA333. Acesso em: 14 mar. 2022.

WANG, Ruixiang *et al.* Potentiation of glutamatergic synaptic transmission onto dorsal raphe serotonergic neurons in the valproic acid model of autism. **Frontiers in Pharmacology**, [*s. l.*], v. 9, n. OCT, p. 1185, 2018. Disponível em: https://doi.org/10.3389/FPHAR.2018.01185/BIBTEX

WANG, Y. *et al.* Dlx5 and Dlx6 Regulate the Development of Parvalbumin-Expressing Cortical Interneurons. **Journal of Neuroscience**, [*s. l.*], v. 30, n. 15, p. 5334–5345, 2010. Disponível em: https://doi.org/10.1523/JNEUROSCI.5963-09.2010

WANG, Yafei *et al.* Transcription Factor 4 Safeguards Hippocampal Dentate Gyrus Development by Regulating Neural Progenitor Migration. **Cerebral Cortex**, [*s. l.*], v. 30, n. 5, p. 3102–3115, 2020. Disponível em: https://doi.org/10.1093/cercor/bhz297. Acesso em: 16 dez. 2020.

WANG, Yukang *et al.* Functional redundancy of the muscle-specific transcription factors Myf5 and myogenin. **Nature,** [*s. l.*], v. 379, n. 6568, p. 823–825, 1996. Disponível em: https://doi.org/10.1038/379823a0. Acesso em: 14 mar. 2022.

WEATHERBEE, Scott D. *et al.* Ultrabithorax regulates genes at several levels of the wing-patterning hierarchy to shape the development of the Drosophila haltere. **Genes and Development**, [*s. l.*], v. 12, n. 10, p. 1474-1482, 1998. Disponível em: https://doi.org/10.1101/gad.12.10.1474

WEI, Ran *et al.* A single low dose of valproic acid in late prenatal life alters postnatal behavior and glutamic acid decarboxylase levels in the mouse. **Behavioural brain research**, [*s. l.*], v. 314, p. 190–198, 2016. Disponível em: https://doi.org/10.1016/J.BBR.2016.08.006. Acesso em: 14 mar. 2022.

WEI, Yongjie; HAN, Xiaoning; ZHAO, Chunjie. PDK1 regulates the survival of the developing cortical interneurons. **Molecular Brain**, [*s. l.*], v. 13, p. 65, 2020. Disponível em: https://doi.org/10.1186/s13041-020-00604-6

WEIDER, Matthias; WEGNER, Michael. SoxE factors: Transcriptional regulators of neural differentiation and nervous system development. **Seminars in cell & developmental biology**, [*s. l.*], v. 63, p. 35–42, 2017. Disponível em: https://doi.org/10.1016/J.SEMCDB.2016.08.013. Acesso em: 14 mar. 2022.

WEINTRAUB, Karen. The prevalence puzzle: Autism counts. **Nature**, [*s. l.*], v. 479, n. 7371, p. 22–24, 2011. Disponível em: https://doi.org/10.1038/479022A. Acesso em: 13 mar. 2022.

WELLS, Peter G. *et al.* Receptor- and reactive intermediate-mediated mechanisms of teratogenesis. **Handbook of experimental pharmacology**, [*s. l.*], v. 196, n. 196, p. 131–162, 2010. Disponível em: https://doi.org/10.1007/978-3-642-00663-0_6. Acesso em: 14 mar. 2022.

WEN, Zhu *et al.* Identification of autism-related MECP2 mutations by whole-exome sequencing and functional validation. **Molecular Autism**, [*s. l.*], v. 8, n. 1, p. 1–10, 2017. Disponível em: https://doi.org/10.1186/S13229-017-0157-5/FIGURES/3. Acesso em: 13 mar. 2022.

WERLING, Donna M.; GESCHWIND, Daniel H. Recurrence rates provide evidence

for sex-differential, familial genetic liability for autism spectrum disorders in multiplex families and twins. **Molecular autism**, [*s. l.*], v. 6, n. 1, p. 27, 2015. Disponível em: https://doi.org/10.1186/S13229-015-0004-5. Acesso em: 13 mar. 2022.

WHITNEY, Elizabeth R. *et al.* Cerebellar Purkinje cells are reduced in a subpopulation of autistic brains: a stereological experiment using calbindin-D28k. **Cerebellum (London, England)**, [*s. l.*], v. 7, n. 3, p. 406–416, 2008. Disponível em: https://doi.org/10.1007/S12311-008-0043-Y. Acesso em: 14 mar. 2022.

WILLIAMS, Emily Cunningham *et al.* Mutant astrocytes differentiated from Rett syndrome patients-specific iPSCs have adverse effects on wildtype neurons. **Human Molecular Genetics**, [*s. l.*], v. 23, n. 11, p. 2968–2980, 2014. Disponível em: https://doi.org/10.1093/hmg/ddu008. Acesso em: 16 dez. 2020.

WILLNER, Paul. Validation criteria for animal models of human mental disorders: learned helplessness as a paradigm case. **Progress in neuro-psychopharmacology & biological psychiatry**, [*s. l.*], v. 10, n. 6, p. 677–690, 1986. Disponível em: https://doi.org/10.1016/0278-5846(86)90051-5. Acesso em: 14 mar. 2022.

WILTSE, Jeanette. Mode of action: inhibition of histone deacetylase, altering WNT-dependent gene expression, and regulation of beta-catenin--developmental effects of valproic acid. **Critical reviews in toxicology**, [*s. l.*], v. 35, n. 8–9, p. 727–738, 2005. Disponível em: https://doi.org/10.1080/10408440591007403. Acesso em: 14 mar. 2022.

WIN-SHWE, Tin Tin *et al.* Social behavior, neuroimmune markers and glutamic acid decarboxylase levels in a rat model of valproic acid-induced autism. **The Journal of toxicological sciences**, [*s. l.*], v. 43, n. 11, p. 631–643, 2018. Disponível em: https://doi.org/10.2131/JTS.43.631. Acesso em: 14 mar. 2022.

WINGENDER, Edgar *et al.* TFClass: A classification of human transcription factors and their rodent orthologs. **Nucleic Acids Research**, [*s. l.*], v. 43, p. 97-102, 2015. Disponível em: https://doi.org/10.1093/nar/gku1064

WONDERS, Carl P.; ANDERSON, Stewart A. The origin and specification of cortical interneurons. **Nature reviews. Neuroscience**, [*s. l.*], v. 7, n. 9, p. 687–696, 2006. Disponível em: https://doi.org/10.1038/NRN1954. Acesso em: 14 mar. 2022.

WORKALEMAHU, Tsegaselassie *et al.* Genetic and Environmental Influences on Fetal Growth Vary during Sensitive Periods in Pregnancy. **Scientific Reports 2018 8:1**, [*s. l.*], v. 8, n. 1, p. 1–8, 2018. Disponível em: https://doi.org/10.1038/s41598-018-25706-z. Acesso em: 14 mar. 2022.

XU, Jing *et al.* Brain SIRT1 mediates metabolic homeostasis and neuroprotection. **Frontiers in Endocrinology**, [*s. l.*], v. 9, p. 702, 2018. Disponível em: https://doi.org/10.3389/FENDO.2018.00702/BIBTEX

YANG, Alex J.T.; BAGIT, Ahmed; MACPHERSON, Rebecca E.K. Resveratrol, Metabolic Dysregulation, and Alzheimer's Disease: Considerations for Neurogenerative Disease. **International Journal of Molecular Sciences**, [*s. l.*], v. 22, p. 9, 2021. Disponível em: https://doi.org/10.3390/IJMS22094628. Acesso em: 14 mar. 2022.

YANG, Jian Quan; YANG, Chao Hua; YIN, Bao Qi. Combined the GABA-A and GABA-B receptor agonists attenuates autistic behaviors in a prenatal valproic acid-induced mouse model of autism. **Behavioural brain research**, [*s. l.*], v. 403, p. e113094, 2021. Disponível em: https://doi.org/10.1016/J.BBR.2020.113094. Acesso em: 14 mar. 2022.

YERI, Ashish *et al.* Total Extracellular Small RNA Profiles from Plasma, Saliva, and Urine of Healthy Subjects. **Scientific reports**, [*s. l.*], v. 7, p. 44061, 2017. Disponível em: https://doi.org/10.1038/SREP44061. Acesso em: 13 mar. 2022.

ZAWERTON, Ash *et al.* Widening of the genetic and clinical spectrum of Lamb–Shaffer syndrome, a neurodevelopmental disorder due to SOX5 haploinsufficiency. **Genetics in Medicine**, [*s. l.*], v. 22, n. 3, p. 524–537, 2020. Disponível em: https://doi.org/10.1038/s41436-019-0657-0. Acesso em: 16 dez. 2020.

ZENG, Qinghua *et al.* Valproic Acid Stimulates Hippocampal Neurogenesis via Activating the Wnt/β-Catenin Signaling Pathway in the APP/PS1/Nestin-GFP Triple Transgenic Mouse Model of Alzheimer's Disease. **Frontiers in aging neuroscience**, [*s. l.*], v. 11, p. 62, 2019. Disponível em: https://doi.org/10.3389/fnagi.2019.00062. Acesso em: 29 nov. 2019.

ZHENG, Xinde *et al.* Metabolic reprogramming during neuronal differentiation from aerobic glycolysis to neuronal oxidative phosphorylation. **eLife**, [*s. l.*], v. 5, n. JUN2016, p. e13374, 2016. Disponível em: https://doi.org/10.7554/ELIFE.13374. Acesso em: 14 mar. 2022.

ZHU, Shiguo; DENMAN, Cecele J; LEE, Dean A. Valproic Acid Selectively Inhibits STAT3 Phosphorylation. **Blood**, [*s. l.*], v. 114, n. 22, p. 1720–1720, 2009. Disponível em: https://doi.org/10.1182/BLOOD.V114.22.1720.1720. Acesso em: 14 mar. 2022.

ZHU, Xiaoxia *et al.* Activation of Sirt1 by resveratrol inhibits TNF-α induced inflammation in fibroblasts. **PloS one**, [*s. l.*], v. 6, p. 11, 2011. Disponível em: https://doi.org/10.1371/JOURNAL.PONE.0027081. Acesso em: 14 mar. 2022.

ZIEMINSKA, Elzbieta *et al.* Glutamate, glutamine and GABA levels in rat brain measured using MRS, HPLC and NMR methods in study of two models of autism. **Frontiers in Molecular Neuroscience**, [*s. l.*], v. 11, p. 418, 2018. Disponível em: https://doi.org/10.3389/FNMOL.2018.00418/BIBTEX

ZOLKIPLI-CUNNINGHAM, Zarazuela *et al.* Metabolic and behavioral features of acute hyperpurinergia and the maternal immune activation mouse model of autism spectrum disorder. **PLOS ONE**, [*s. l.*], v. 16, n. 3, p. e0248771, 2021. Disponível em: https://doi.org/10.1371/JOURNAL.PONE.0248771. Acesso em: 14 mar. 2022.

ZOU, Zhaonan *et al.* Epigenetic landscape of drug responses revealed through large-scale ChIP-seq data analyses. **BMC Bioinformatics**, [*s. l.*], v. 23, n. 1, p. 1–20, 2022. Disponível em: https://doi.org/10.1186/S12859-022-04571-8/TABLES/1. Acesso em: 14 mar. 2022.

ZUIKI, Masashi *et al.* Luteolin attenuates interleukin-6-mediated astrogliosis in human iPSC-derived neural aggregates: A candidate preventive substance for maternal immune activation-induced abnormalities. **Neuroscience Letters**, [*s. l.*], v. 653, p. 296–301, 2017. Disponível em: https://doi.org/10.1016/j.neulet.2017.06.004. Acesso em: 16 dez. 2020.

ZWEIER, Christiane *et al.* Haploinsufficiency of TCF4 causes syndromal mental retardation with intermittent hyperventilation (Pitt-Hopkins syndrome). **American Journal of Human Genetics**, [*s. l.*], v. 80, n. 5, p. 994–1001, 2007. Disponível em: https://doi.org/10.1086/515583. Acesso em: 16 dez. 2020.

ANEXOS

ANEXO 1 – Carta de aprovação da comissão de ética no uso de animais (projeto 35733)

U F R G S
UNIVERSIDADE FEDERAL DO RIO GRANDE DO SUL

PRÓ-REITORIA DE PESQUISA

Comissão De Ética No Uso De Animais

CEUA UFRGS

CARTA DE APROVAÇÃO

Comissão De Ética No Uso De Animais analisou o projeto:

Número: 35733
Título: ANÁLISE HISTOLÓGICA, MOLECULAR E FUNCIONAL DE INTERNEURÔNIOS INIBITÓRIOS PARVALBUMINA E SOMATOSTATINA POSITIVOS AO LONGO DO DESENVOLVIMENTO EM MODELO ANIMAL DE AUTISMO

Vigência: 13/08/2018 à 10/03/2022

Pesquisadores:

Equipe UFRGS:

CARMEM JURACY SILVEIRA GOTTFRIED - coordenador desde 13/08/2018
MATHEUS COSTA SCHIAFFINO - Aluno de Mestrado desde 13/08/2018
MELLANIE FONTES DUTRA DA SILVA - Aluno de Doutorado desde 13/08/2018
IOHANNA DECKMANN - Aluno de Doutorado desde 13/08/2018
GUILHERME BAUER NEGRINI - Aluno de Doutorado desde 13/08/2018
JÚLIO SANTOS TERRA MACHADO - Aluno de Doutorado desde 13/08/2018
Gustavo Brum Schwingel - Aluno de Doutorado desde 13/08/2018
Bruna Frizzo Rabelo - Aluno de Mestrado desde 13/08/2018

Comissão De Ética No Uso De Animais aprovou o mesmo , em reunião realizada em 25/02/2019 - Plenarinho - andar térreo do Prédio da Reitoria - Campus Centro Farroupilha PORTO ALEGRE, em seus aspectos éticos e metodológicos, para a utilização de 400 ratos Wistar, sendo 224 fêmeas e 76 machos, de idades que variam de E-13,5 dias (E=embrião/fetos) a 120 dias, provenientes do Depto de Bioquímica; de acordo com os preceitos das Diretrizes e Normas Nacionais e Internacionais, especialmente a Lei 11.794 de 08 de novembro de 2008, o Decreto 6899 de 15 de julho de 2009, e as normas editadas pelo Conselho Nacional de Controle da Experimentação Animal (CONCEA), que disciplinam a produção, manutenção e/ou utilização de animais do filo Chordata, subfilo Vertebrata (exceto o homem) em atividade de ensino ou pesquisa.

Porto Alegre, Sexta-Feira, 15 de Março de 2019

MARCELO MELLER ALIEVI
Coordenador da comissão de ética

ANEXO 2 – Parecer favorável comissão de pesquisa (COMPESQ)

PPG-Ciências Biológicas Bioquímica

UNIVERSIDADE FEDERAL DO RIO GRANDE DO SUL
INSTITUTO DE CIÊNCIAS BÁSICAS DA SAÚDE

Parecer de Projeto de Doutorado

O projeto do aluno **Júlio Santos Terra Machado**, intitulado: **"Análise histológica, molecular e funcional de interneurônios inibitórios parvalbumina e somatostatina positivos ao longo do desenvolvimento em modelo animal de autismo"**, orientado pela Profa. Dra. Carmem Juracy Silveira Gottfried, encaminhado para avaliação pelo PPG - Bioquímica teve a seguinte análise e parecer:

ANÁLISE DO PROJETO

1. **Mérito científico**

[X] Relevante

[ ] Sugestões de alterações:

2. **Fundamentação**

[X] Adequada

[ ] Sugestões de alterações:

3. **Objetivos**

[X] Bem definidos

[ ] Sugestões de alterações:

4. **Metodologia**

[X] Adequada

[ ] Sugestões de alterações:

5. **Cálculo do número amostral**

[X] Realizado

[ ] Não aplicável

[ ] Não realizado:

6. Considerações Éticas

[ ] Descritas

[ ] Não aplicável

[X] Sugestões de alterações: Os aspectos éticos estão bem descritos no projeto, apenas sugiro acrescentar o grau de severidade em cada técnica envolvendo o uso de animais. Essa informação pode ser obtida no site da UFRGS > PROPESQ > Comissões e Comitês > CEUA > Grau de Severidade dos Procedimentos.

7. Descarte dos Resíduos Químicos e Biológicos

[X] Descritos

[ ] Não aplicável

[ ] Sugestões de alterações:

8. Cronograma de Execução

[X] Apresentado

[ ] Não apresentado

9. Referências Bibliográficas

[ ] Pertinentes

[X] Sugestões de alterações: As referências bibliográficas usadas no projeto são pertinentes e atualizadas em relação ao tema proposto, apenas sugiro a padronização das mesmas. Em apenas algumas referências consta a informação "disponível em" seguida do link para acesso.

PARECER FINAL:

[X] Aprovado

[ ] Diligência

Porto Alegre, 21 de maio de 2018.

Atenciosamente,

Juliana Bender Hoppe

JULIANA BENDER HOPPE
CPF 004278730-56
PÓS-DOUTORANDA DO PPG BIOQUÍMICA

Prof. Dr. Diogo Onofre Gomes de Souza
Coordenador do PPG em C.B.:
Bioquímica-ICBS/UFRGS

ANEXO 3 – Capítulo de livro aceito para publicação (editora Springer Nature)

Purinergic signaling in autism spectrum disorder

Iohanna Deckmann[a,b,c,#], Júlio Santos-Terra[a,b,c,#],Carmem Gottfried [a,b,c]

a Translational Research Group in Autism Spectrum Disorder - GETTEA, Universidade Federal do Rio Grande do Sul (UFRGS), Porto Alegre, Brazil.
b National Institute of Science and Technology in Neuroimmunomodulation - INCT-NIM, Brazil.
c Autism Wellbeing and Research Development - AWARD - Initiative BR-UK-CA
# ID (iohanna.deckmann@gmail.com) and JS-T (juliosterra@gmail.com) authors contributed equally.

Corresponding authors: ID and CG (cgottfried@ufrgs.br)
Departamento de Bioquímica, ICBS, Universidade Federal do Rio Grande do Sul, Ramiro Barcelos 2600 – 21111. CEP: 90035-003 Porto Alegre-RS, Brazil.

Abstract

Autism spectrum disorder (ASD) is a highly prevalent neurodevelopmental disorder estimated to affect 1:54 individuals, characterized by impairments in the social approach and stereotyped behavior patterns. The etiology of this disorder is still unclear; however, disturbances in the regulation of purinergic signaling contribute to establishing the ASD phenotype. Purinergic signaling is a system that involves second extracellular messengers able to triggers responses in several biological processes, activating the immune system, modulating bioenergetics, and promoting neuromodulation, by activation of specific receptors subtypes: metabotropic P1, ionotropic P2X, and metabotropic P2Y. In addition, several psychiatric disorders, including epilepsy, schizophrenia, Alzheimer and, in recent years, ASD, present altered components associated with the purinergic system, such as mitochondrial dysfunction, polymorphisms in genes that encode purinergic receptors, abnormalities in intermediaries of purine metabolism, among others. This chapter summarizes the contribution of purinergic signaling in ASD phenotype and hypothesizes how this intricate puzzle involves extracellular messengers and ASD pathophysiology, focusing on pathways associated with metabolism, neuroimmune modulation, and neurodevelopment. **Keywords:** autism spectrum disorder; purinergic signaling;

immunomodulation; neurodevelopment; microRNA; second messengers; metabolism; cell signaling.

1. Introduction

Autism spectrum disorder (ASD) is one of the neuropsychiatric disorders with the highest incidence nowadays. As it is a condition that originates during early neurodevelopment, involving epigenetic changes, several experimental approaches shed light on possible mechanisms involved in the ASD triggering. In this context, the purinergic system emerges as a strong candidate for its phenotype modulation.

2. ASD

ASD is a neurodevelopmental disorder characterized by two sets of characteristic behavioral alterations: communication/social interaction impairments and stereotyped/repetitive behaviors (American Psychiatric Association, 2013). Although the ASD etiology remains unclear, it is already known that both genetic and environmental risk factors can contribute to the onset (Gottfried et al., 2015). Furthermore, the most recent prevalence data of ASD from the USA shows that 1:54 8-years-old children are affected and that the ratio of males/females is 4:1 (Maenner et al., 2020), demonstrating a high prevalence that has been rising in the last decades. Besides that, the absence of biomarkers and the heterogeneity of the disorder challenge the diagnosis and, consequently, the implementation of adequate therapeutic strategies (Masi et al., 2017).

Beyond the core behavioral dyad, ASD individuals may also experience a series of comorbidities, including epilepsy, anxiety, perception alterations, gastrointestinal disturbance, sleep impairments, and many others (Doshi-Velez et al., 2014). The high incidences of electrophysiological (8%-30% of the individuals with ASD) (Spence and Schneider, 2009; Bolton et al., 2011; Lukmanji et al., 2019) and sensory alterations (more than 90% of the individuals) (Chang et al., 2014) support the connectivity theory in ASD: the brain, in this case, presents an excitatory/inhibitory imbalance added to impaired connectivity of different brain regions, leading to local hyper processing, resulting in the impaired interpretation of the different stimuli.

Several pathways have already been described as altered in ASD, both in the brain and in peripheral tissues. Immune system alterations stand out in ASD, including descriptions of increased content of pro-inflammatory cytokines, altered lymphocyte profile, and high levels of autoimmune diseases (Deckmann et al., 2018). In the brain, the highlights are for routes associated with glutamate and GABA neurotransmission (Horder et al., 2018), as well as pathways involved in synaptic plasticity (Bourgeron, 2015) and the activation and reactivity of glial cells such as astrocytes and microglia (Petrelli et al., 2016).

Purinergic signaling studies in ASD are emerging in recent years, demonstrating several roles that will be discussed in this chapter. In an overview, this system can be the link that unites immune and brain dysfunctions, helping to understand the pathophysiology of autism.

3. Purinergic System and autism-like features

As reviewed by Ulrich *et al*., (2012) and Fumagalli *et al*., (2017), brain development in embryonic life is finely regulated by a range of biological processes. It has been demonstrated that purinergic signaling plays an essential role in organizing embryonic and fetal development and organogenesis in a time-dependent manner, controlling purinergic signaling molecules, such as adenosine (ADO) triphosphate (ATP), the Ca^{2+} release from radial glia, differential receptor subtypes expression, among others (Ulrich et al., 2012; Fumagalli et al., 2017). Here, we present an overview of the contribution of the dysfunction of purines and pyrimidines metabolism in ASD. A summary of the main findings can be seen in Figure 1.

3.1 Humans

The neurobiological bases of ASD-like features (social impairments and stereotyped behavior) are still a challenge for science due to the dynamics and crosslinking of distinct biological pathways, including purinergic signaling throughout development. Single nucleotide polymorphisms (SNP) in the ADO A2A receptor gene (*ADORA2A*) were already associated with ASD (rs2236624-CC and rs2298383) and phenotypic variability, including impaired scores in behavioral assessments (rs3761422, rs5751876 and, rs35320474) (Freitag et al., 2009). Interestingly, ASD patients also

demonstrated mutations in the ADO A3 receptor gene (*ADORA3*), identified as rs77883500 and rs139935750, and, in an *in-vitro* assay; the presence of the first SNP induced enhanced levels of cGMP, resulting in increased activity of the serotonin transporter (Campbell et al., 2013).

A *postmortem* analysis of cerebellum from idiopathic ASD patients demonstrated that the cluster of genes associated with impaired social behavior had gene ontology enrichment for purinergic-signaling genes, demonstrating an important overlap (Ginsberg et al., 2012). In a recent study, gene set enrichment analysis of a polygenic risk score in ASD individuals demonstrated an association ($R2=0.064$; β, −5.30; SE 1.30; $P < .001$) of adenylyl cyclase activity and cyclic ADO monophosphate (cAMP) concentration with ASD traits (Takahashi et al., 2020). cAMP pathways were also associated with variants identified in ASD in an *in-silico* study (Luo et al., 2018). Finally, a differential presence of metabolites derived from purine metabolism was found in ASD subjects' urine, indicating the general impact of purinergic metabolism in this disorder (Gevi et al., 2016).

According to the region evaluated in a *postmortem* analysis of ASD individuals, the expression of phosphodiesterases (PDE) demonstrated differential results: reduced expression of PDE4A5, PDE4B1, PDE4B3, PDE4B4, and PDE4B2 in the cerebellum and enhanced expression of PDE4AX, PDE4A1, and PDE4B2 in the encephalic region BA9. These alterations are relevant in this context because these enzymes regulate the levels of cAMP, a second messenger in purinergic signaling (Braun et al., 2007). The fragile X syndrome is a genetic disorder with an important overlap of symptoms with ASD, including poor eye contact, difficulties with peer relationships, social withdrawal, repetitive behaviors (Kaufmann et al., 2017). A study using three different fragile X syndrome model systems containing a non-functional *FMR1* gene (human neural progenitor cells, mice, and drosophila), pointed to a general lowered cAMP production in human neural progenitor cells and mice brain, even suggesting that cAMP metabolism can be used as a biomarker in fragile X syndrome (Kelley et al., 2007).

Overall, the data present important roles of purinergic signaling in ASD, especially regarding ADO metabolism and associated pathways. In the next section, the discussion of animal models will clarify these pathways, demonstrating how a purinergic imbalance could influence the severity of ASD traits.

3.2 Animal Models

Several animal models are used in the study of ASD, including a) knockout (KO) for specific ASD-associated genes; b) maternal immune activation (MIA), especially induced by prenatal exposure to polyinosinic:polycytidylic acid (poly(I:C)) or lipopolysaccharides (LPS); and c) prenatal exposure to valproic acid, among others. In this section, we will discuss the evidence of purinergic involvement in the pathophysiology of ASD models and models of associated psychiatric disorders.

In the offspring from the MIA model induced by prenatal exposure to LPS, purinergic signaling disturbance probably contributed to the impaired astrocyte function due to microglial activation. In two articles, the increased opening of Cx43 and Panx1 channels in hippocampal astrocytes was associated with the release of ATP and glutamate (GLU), which enhanced Ca^{2+} levels after interacting with their receptors (ATP: P2X7 and P2Y1; GLU: mGLUR5), leading to an activated profile in astrocytes and cell death in neurons (Avendaño et al., 2015; Chávez et al., 2019).

Injection of intraperitoneal ATP in postnatal life induces a broad spectrum of alterations, including global reduction of mitochondrial function, altered profile of metabolites, increased levels of corticosterone and cytokines (IL-10, IL-6, and CXCL10), and impaired behavioral performances in exploratory and locomotor features (ASD-like traits). Moreover, when this approach is performed in the offspring of the poly(I:C) model, the alteration in body temperature lasted much longer when compared to controls. This evidence demonstrates the general issues of a hyperpurinerigic condition and highlights that animals exposed to MIA are more susceptible to postnatal dysregulation of purinergic signaling (which can be induced by several environmental factors) (Zolkipli-Cunningham et al., 2021).

Interestingly, purinergic receptors are pivotal for the ASD features derived from the MIA model induced by poly(I:C): the offspring originated from a) dams heterozygous or KO for P2X7 and b) females treated with a specific P2X7 antagonist (JNJ47965567) did not present any ASD-associated characteristics, while wild-types (WT) submitted to MIA had several alterations including impaired sociability, increased stereotyped behavior, increased IL-6, CXCL1, and TNF-α brain content, synapse malformation, disruption of cortical lamination and others. Postnatal administration of JNJ47965567 attenuated the altered parameters in WT exposed to MIA, while administration of ATP elicited ASD traits in animals that were not

submitted to any prenatal intervention (Horváth et al., 2019). Inhibition of P2X7 also improved social deficits, dendritic spine dynamics, and other parameters in a model of Rett Syndrome (Garré et al., 2020). Conversely, the P2X4 receptor demonstrated a completely different association: heterozygous or KO animals displayed reduced social interaction and maternal separation-induced ultrasonic vocalizations. Moreover, only KO animals had sensory impairments, anxiety-like behavior, and altered expression of GLU receptors (prefrontal cortex: reduced GluN2A and Glu2B; hippocampus: reduced GluN1 and enhanced GluA1 and GluA2) (Wyatt et al., 2013).

The distinctive effects of P2X7 and P2X4 are intriguing, while lack of P2X7 protected against MIA-derived impairments, the loss of P2X4 induced ASD-like symptoms. We hypothesize that this difference occurs because P2X7 is a significant inductor of Ca^{2+} release when activated, which could cause excitotoxicity. Activation of P2X7 was already associated with apoptosis/necrosis in neural progenitor cells in the hippocampus (Khan et al., 2018). On the other hand, P2X4 is pivotal for microglial function, especially brain-derived neurotrophic factor (BDNF) release and regulation of synaptic formation and plasticity, processes already associated with ASD pathophysiology (Trang et al., 2009; Montilla et al., 2020). Strikingly, animals KO for A2A, another purinergic receptor, demonstrated enhanced sociability and increased anxiety, implying the broad behavioral factors associated with each receptor (López-Cruz et al., 2017).

Regarding other animal models, the inbred BTBR T+tf/J (BTBR) mouse strain, a genetic model that replicates repetitive behaviors and social deficits seen in ASD individuals, has decreased striatal function of A2A receptor, probably contributing to impairments of dopaminergic neurons (Squillace et al., 2014). The deletion of a PDE4 regulator, named CC2D1A, considered an ASD model, induced spatial memory deficits associated with PDE4 hyperactivity and cAMP reduced levels in the hippocampus (Zamarbide et al., 2019). In the valproic acid embryological exposure model, zebrafish presented increased AMP hydrolysis, A2R1 mRNA expression, and ATP/ADP catabolism in the brain (Zimmermann et al., 2017). In murine, valproic acid increased the AMP/ATP ratio in the midbrain and reduced it in the cortex, possibly inducing a purinergic signaling imbalance (Hegazy et al., 2015), as well as hippocampal upregulation of P2X4 and P2Y2 receptor expressions, and P2X4 receptor expression in the medial prefrontal cortex (Hirsch et al., 2020).

In this section, we discussed how elements from the purinergic signaling universe are associated with ASD or ASD-like features. The major highlight is the important roles of receptors A, P2X, and P2Y, which will lead the discussion in the section “7. Therapeutic Approaches and Purinergic System in ASD”.

4. Purinergic System and Metabolism in ASD

4.1 ADO

Purines and pyrimidines metabolism intermediates are essential signaling molecules for various biological processes, such as providing energy for cell functions by the Na^+/K^+-ATPase activity, a membrane-active pump that requires a huge amount of ATP produced in central nervous system (CNS) (Fumagalli et al., 2017). ADO is a product of ATP hydrolysis and a key molecule involved in purinergic signaling, energetic metabolism, folate metabolism, and other pathways. Studies already demonstrated that ADO might mediate the beneficial effects of the ketogenic diet (Masino et al., 2009), improving electrophysiological impairments (which are common in ASD) (Masino et al., 2013). Besides that, indirect stimulation of ADO production improved behavioral alterations in ASD children (Masino et al., 2011).

The modulation of oligodendrocytes development is one of the major functions of ADO. Shen et al., (2018) postulate that this molecule interacts with oligodendrocyte progenitor cells in different times, stimulating proliferation, differentiation, and myelination (Shen et al., 2018). Interestingly, it was demonstrated in the Lesch-Nyan syndrome, characterized by a deficiency in the hypoxanthine-guanine phosphoribosyltransferase enzyme (HPRT) - which leads to impairments in purine biosynthesis - altered patterns of ADO receptors (ADORA1A and ADORA2A) (Bertelli et al., 2006), besides altered expression of oligodendrocyte transcription factor 2 and myelin basic protein, important oligodendrocyte markers (Kang et al., 2013), which may be associated with the ADO roles in the development of oligodendrocytes. HPRT deficiency also resulted in reduced mRNA expression of P2X3, P2X5, P2Y2, P2Y4, P2Y12, P2Y13, and P2Y14 receptors, which was associated with impaired Ca^{2+} signaling in neuroblastoma cells (Erdorf et al., 2011). In addition, another study demonstrated that HPRT silencing reduced P2Y1 mRNA expression and induced other relevant alterations like reduced pCREB expression,

altered activation of ERK1/2 MAP kinases, and decreased phosphorylation of β-catenin (Mastrangelo et al., 2012). This disorder is marked by self-injury behavior (among other behavioral features), a characteristic that is also found in 42% of ASD individuals (Steenfeldt-Kristensen et al., 2020).

The ADO deaminase enzyme (ADA), which is necessary for ADO conversion to inosine and further excretion in the form of uric acid, has been studied in the context of ASD for decades. The first work demonstrated that ASD individuals presented lower levels of ADA activity in the blood (Stubbs et al., 1982). Following that, several studies clarified this difference: the presence of ADA2 alleles, which cause 15-20% reduction in the catalytic reduction, was significantly more frequent in ASD subjects (Persico et al., 2000). The polymorphism named Asp8As induced a reduction of 35% in ADA activity and was associated with ASD in an Italian study (Bottini et al., 2001); however, the same association was not found in a North American study (Hettinger et al., 2008). As hypothesized by Cheffer et al., (2018), this conflict may occur because ADA reduction probably overstimulates A1 receptors, which was described as beneficial in ASD (Cheffer et al., 2018).

Throughout this chapter, ADO will be discussed in specific sections, especially in “7. Therapeutic Approaches and Purinergic System in ASD”. Here, we can already observe that ADO metabolism is an integrative topic, mediating the ketogenic diet’s effects and modulating important cells like the oligodendrocytes. The alterations described in ADA in humans add relevance to investigate possible pharmacological approaches.

4.2 Mitochondria

The neural signaling requires high mitochondrial energy demand due to ion transport by pumps such as Na^+/K^+-ATPase, and the mitochondria are key organelles for energy support through ATP synthesis. Here, we discuss how dysfunctions, even subtle, in mitochondrial energy production are involved in the pathophysiology of disorders such as ASD.

4.2.1 Data from Humans

Altered mitochondrial metabolism has been studied in ASD since the 1980s, when lactic and pyruvic acidosis with additional structural mitochondrial alterations were reported in Rett syndrome patients (a condition with a huge overlap of symptoms with ASD) (Philippart, 1986). From there, several articles reported issues in this context and, in this section, we will focus on alterations that most likely impair the content of ADO-associated mediators (ATP, ADP, AMP, and others), possibly disturbing the purinergic signaling.

An analysis of maternal serum from women exposed to high levels of pollution during pregnancy demonstrated an important relation with ASD increased risks in their children. The primary enriched metabolites were associated with mitochondrial dysfunction (MD), especially tricarboxylic acid cycle, carnitine shuttle, and others, suggesting a possible involvement in the onset of ASD (Kim et al., 2021). A meta-analysis of ASD studies highlighted 5% of MD prevalence in the ASD population, much higher than the general average of MD (0.01%). Moreover, these alterations were associated with impaired behavioral parameters and increased presence of developmental regression and motor delay (Rossignol and Frye, 2012). Interestingly, a recent study clarified mitochondrial damage in DR: mitochondria derived from peripheral blood mononuclear cells had increased respiration rates, lower reserve capacity (associated with more susceptibility to reactive species), and more damage in the mtDNA compared to ASD-no DR subjects (Singh et al., 2020).

Serum microRNA (miR) interfered in the MT respiration in peripheral blood mononuclear cells from different ASD subpopulations (defined by the IL-1β/IL-10 ratio) (Jyonouchi et al., 2019); complementary, the mitochondria from platelets and neutrophils presented impaired respiration and decreased reactive oxygen species (ROS) production (only in neutrophils, indicating the reduced function of these cells) (Abdel-Rahman et al., 2020). Finally, fibroblasts derived from ASD individuals demonstrated increased mitochondrial respiratory profile, altered mitochondrial dynamics (biogenesis, fusion, and fission), aberrant anti-inflammatory defenses, , and morphological alterations (Pecorelli et al., 2020).

Metabolomic analysis of urine from ASD individuals demonstrated increased levels of 3-hydroxy-3-methylglutaric acid, 3-methylglutaconic acid, and ethylmalonic acid, indicating impairments in oxidative phosphorylation (Stathopoulos et al., 2020). Using a similar approach, several groups of altered mitochondria-associated metabolites were identified in ASD patients, suggesting that the differential clusters

observed can be used not only as biomarkers but also as indicators for personalized therapeutic approaches (Smith et al., 2020).

Postmortem analysis of the cerebral cortex from ASD subjects showed downregulation of gene clusters related to mitochondrial function and synaptic plasticity (Schwede et al., 2018). In the temporal lobe of ASD patients, altered protein levels and decreased activity of respiratory chain protein complexes were observed, in addition to a disturbance in the biogenesis, dynamics, and antioxidant defense. In this work, the authors highlight that mitochondrial issues may be associated with the huge synaptic impairments in this brain region (Tang et al., 2013). Besides, a decreased expression of electron transport chain complexes in the cerebellum and the frontal and temporal regions were observed in the brain from autistic children (Chauhan et al., 2011). mitochondria plays important roles in synaptic Ca^{2+} buffering and ATP supply necessary to synaptic plasticity (Rossi and Pekkurnaz, 2019); interestingly, proteins that stimulate synaptic increase, like Bcl-xL, also stimulate mitochondrial proliferation, demonstrating an important connection between these structures (Eltokhi et al., 2021).

This evidence indicates a prominent role of mitochondrial impairments in the pathophysiology of ASD. The disturbances in MT can induce oxidative stress, leading to cell damage and apoptosis, impairment of synaptic plasticity, ATP production decrease, and many other effects. In all of these contexts, purinergic signaling may also be involved, suggesting an important field in further studies.

4.2.2 Data from Animal Models

Fragile X syndrome animal models provide an interesting approach for ASD studies due to several points in common between these disorders, including behavioral traits. In *Fmr1* KO mice, mitochondrial transcription factor NRF1; ATP synthase subunits ATP5A and ATPB, and mitochondrial anion channel VDAC1 (a component of the outer membrane) were reduced in extracellular vesicles in the cortex and astrocytes (Ha et al., 2021), inducing several mitochondrial disturbances. In another study, astrocytes from *Fmr1* KO mice demonstrated enhanced ROS production with no change in respiration rates (Vandenberg et al., 2021). Disturbances in astrocyte function, as already discussed in section 3, are extremely deleterious, especially when metabolic features are altered due to the direct

impairment of neurons. In neurons of *Fmr1* KO, the presence of “leak” in the c subunit of ATP-synthase was associated with dendritic and synaptic impairments (Licznerski et al., 2020).

MIA has been linked to a higher risk for the child to develop autism or schizophrenia-related symptoms. The pathogen-free poly(I:C) has been used to induce an important MIA model for the study of neurodevelopmental disorders, which shows relatively high construct and face validity. This ASD animal model decreased ATP production, associated with lower activity of complex I in leukocytes, suggesting a long-term immune dysfunction associated with mitochondrial impairments (Giulivi et al., 2013). In BTBR animals, mitochondria isolated from the brain demonstrated decreased oxidative phosphorylation (probably associated with reduced complex I activity), increased fragmentation, and activation of fission proteins, which were attenuated by ketogenic diet (Ahn et al., 2020). These two consolidated ASD models illustrate that mitochondria can contribute to both immune and brain alterations, key factors in the pathophysiology of the disorder.

More recently, studies demonstrated that loss or altered expression of parvalbumin (PV) induces MT alterations. PV is an important marker of a specific type of GABAergic interneurons, with several alterations already described in ASD (Fontes-Dutra et al., 2018; Filice et al., 2020). Besides, PV comprises a family of proteins with calcium-binding properties, influencing biological properties, such as neural function (Antonoudiou et al., 2020) and immune response (Beers et al., 2001). In the first study with PV KO mice, the loss of PV resulted in an increased number and length of MT and increased dendritic branching in the neocortex (Janickova et al., 2020). In the second study, the same group observed that, according to age, the absence of PV enhanced the generation of ROS and increased mitochondrial length (Janickova and Schwaller, 2020). Interestingly, purinergic signaling impairments during pregnancy were able to induce interneuron alterations: exposure to caffeine delayed the migration of somatostatin-positive interneurons (Silva et al., 2013), indicating that PV, which originates from the same area (ganglionic eminence), may also be affected.

Most of all, this data demonstrates that mitochondria are a pivotal piece in the intricate ASD puzzle. In animal models, we can observe the direct impact of MT dysfunction in synaptic plasticity, immune cell function, neuronal survival, and other features. Although not described directly, the purinergic signaling alterations already

observed in these conditions are likely associated, at least in part, with mitochondrial impairments.

5. Purinergic System and Neuroimmune Aspects in ASD

A component intimately involved with the pathophysiology of ASD is the immune system, associated with a pro-inflammatory condition. Neuroinflammation has a key role in a wide plethora of CNS diseases, whose pathophysiology can be studied by the modulation of the neuroimmune processes by molecules such as ADO. ADO is capable of modulating A1AR and A2AAR receptors, which can negatively modulate the excitatory transmission and promote synaptic plasticity, respectively (Martí Navia et al., 2020). This is particularly important in the ASD context, considering the excitatory/inhibitory imbalance in brain cortical structures. KO mice to A1AR have increased neuroinflammation and microglial activity (Synowitz et al., 2006). The A2AR, on the other hand, has an anti-inflammatory role and can be negatively regulated by the miR-214, which promotes the release of inflammatory cytokines TNF-α and IL-6. The anti-inflammatory effect was exacerbated upon the combination of miR-214 antagomiR and A2AR agonist (Zhao et al., 2015).

Owing to their role in both releasing pro-inflammatory mediators and responding to immunological signaling released from other cells, microglia and astrocytes are the brain cells that react to the alterations in the neural environment, migrating to the site of the damage, phagocytosing, and secreting inflammatory mediators (Fumagalli et al., 2011). The microglia perform a crucial role in neuroinflammation. On the one hand, it performs the necessary surveillance to maintain the CNS homeostasis; on the other, when activated, it further spreads inflammation. Besides, the neuroinflammation facilitates the loosening of the blood-brain barrier, allowing inflammatory infiltrate from the periphery towards the CNS. Anyway, it is a cell susceptible to the modulation of purinergic signaling (Fumagalli et al., 2011). During injury events, such as cerebral ischemia, the injury site receives a large amount of ATP, which activates resident microglia via purinergic receptors (Melani et al., 2005). In this case, the P2X7 receptor has a double-edged role: both increasing generalized inflammatory responses, mainly by the IL-1β release (Ferrari et al., 1997; Grahames et al., 1999), and promotes a neurotrophic factors release counteracting the neuronal death (Suzuki et al., 2004). P2Y receptors are also recruited, especially, the

involvement of P2Y12 in microglial chemotaxis was already described (Ohsawa et al., 2007). In a complementary way, the astrocytes also perform an important role in the neuroinflammation, becoming hypertrophic and acquiring a reactive profile to form the glial scar. The astrogliosis can be triggered by a set of factors, including the ATP released by stressed cells, which activates the P2X7 receptor, mediating the signaling for the synthesis of pro-inflammatory cytokines (Solle et al., 2001) and neurotransmitters such as glutamate (Duan et al., 2003), diminishing their uptake and reducing the glutamine synthetase activity (Lo et al., 2008). Moreover, P2Y2 stimulation modulates the astrocyte migration (Wang et al., 2005) whilst P2Y1 receptors signaling astrogliosis via the PI3-K/Akt signaling pathway (Franke et al., 2009).

In the context of autism, few studies describe the inflammatory modulation mediated by purinergic signaling. The treatment of BTBR mouse strain with SCH 5826 (SCH, an A2AR antagonist) showed increased levels of $CD4^+IL\text{-}21^+$, $CD4^+IL\text{-}22^+$, $CD4^+GATA3^+$, and $CD4^+T\text{-}bet^+$ and decreased $CD4^+CTLA\text{-}4^+$ expression in splenic cells, besides increased mRNA and protein expression levels of IL-21, IL-22, GATA3, and T-bet in brain tissue (Ahmad et al., 2017b). Regarding toll-like receptors (TLRs), the same treatment increased the percentage of splenic $CD14^+TLR2^+$ cells, $CD14^+TLR3^+$ cells, $CD14^+TLR4^+$ cells, and decreased the percentage of $CD14^+IL\text{-}27^+$ cells, in addition to TLR2, TLR3, TLR4, and NF-κB p65 mRNA and protein expression increased in brain tissue, and decreased IL-27 and IκBα expression (Ahmad et al., 2017a). In addition, the treatment of BTBR mouse strain with SCH promoted, in the brain, (a) increased mRNA of $CCR3^+$, $CCR4^+$, $CCR5^+$, $CCR6^+$, $CCR7^+$, $CXCR3^+$, $CXCR4^+$, and $CXCR5^+$ (Ahmad et al., 2018), (b) increased the Th1 response, (c) decreased Th2 response, and (d) increased protein levels of IL-2+, IL-6+, IL-9+, IFN-γ+, and TNF-α+ and decreased $TGF\text{-}\beta^+$ (Ansari et al., 2017a). Another study in the same model demonstrated, in $CD4^+$ cells, increased positive cells of $IL\text{-}17A^+$ and $ROR\gamma t^+$ and decreased of $Foxp3^+$ and $IL\text{-}10^+$ (Ansari et al., 2017b). These data demonstrate the important anti-inflammatory role of the A2A receptor since the inhibition of ADO binding via SCH-mediated antagonism was able to replicate deficits commonly described in ASD. More details on the role of this receptor can be read in the section "7. Therapeutic Approaches and Purinergic System in ASD" in the subtopic related to the A2AR agonist CGS 21680.

6. Purinergic System and Molecular Modulation in ASD

The purinergic system either can modulate or be modulated by molecular changes. For example, several SNPs have been identified in the P2X7 receptor, generating many complex outcomes (Di Virgilio et al., 2017). In addition, P2X7 can be regulated by DNA methylation (Liu et al., 2017), transcriptions factors, such as Specificity protein 1 (Sp1) (whose affinity to the P2X7 promoter increases during *status epilepticus*) (Engel et al., 2017), alternative splicing and post-translational regulation, such as phosphorylation as reviewed by Jimenez-Mateos (Jimenez-Mateos et al., 2019).

In the context of ASD, since the diagnostic criterion is purely clinical, there is a growing interest in blood-altered molecules, with potential to be used as molecular markers to anticipate diagnosis, such as miR. These molecules are small non-coding RNAs that regulate the translation of messenger RNAs into their corresponding proteins, essential in controlling several cellular processes during development and in adulthood. As expected, the purinergic signaling can also be modulated by miR; these molecules influence purinergic receptors, ectonucleotidases, and the expression of other molecular components of the purinergic signaling network (Ferrari et al., 2016; Jimenez-Mateos et al., 2019).

Considering that epilepsy is present in 8%-30% of individuals with ASD (Spence and Schneider, 2009; Bolton et al., 2011; Lukmanji et al., 2019), studies with animal models of epilepsy are essential in understanding the pathophysiological mechanisms of ASD (in the absence of studies on this disorder). Important electrophysiological alterations were demonstrated in a unilateral mouse model of *status epilepticus*, with suppression of P2X7 receptor-gated inward currents in the contralateral hippocampus. Besides, the inhibition of miR-22 increased P2X7 receptor expression and cytokine levels in the contralateral hippocampus, causing spontaneous seizures more frequently in these mice. In addition, P2rx7$^{-/-}$ mice do not exhibit the effects of miR-22 inhibition, however, had transiently suppressed spontaneous seizures when microRNA-22 was injected. These data support the role of miR-22 in targeting P2X7 receptors, preventing both seizures and neuroinflammation (Jimenez-Mateos et al., 2015).

In a complementary way, transcription factors are also able to modulate both miR and purinergic receptors expression. *In-vitro* studies demonstrated that Sp1, a

transcription factor highly expressed in the brain, induces the transcription of the P2X7 receptor (García-Huerta et al., 2012). Moreover, it was demonstrated, both in neuronal activity induce *in-vitro* and in a mouse model of *status epilepticus*, that Sp1 can induce the transcription of both miR-22 and P2X7 receptor, as well as induces the transcription of miR-22 in a calcium-sensitive way, shedding some light on neuronal activity-dependent P2X7 receptor expression (Engel et al., 2017). Besides miR-22, other miR are associated with the P2X7 receptor in hippocampi from WT and P2X7 receptor KO mice following *status epilepticus*. Wild-type mice presented up-regulation of 50 miR and down-regulation of 35 miR after lack of the P2X7 receptor (involved in signaling pathways and inflammation), whereas in *status epilepticus* mice, the P2X7 receptor deficiency led to the up-regulation of 44 miR while 13 miR were down-regulated (associated with cell death), emphasizing the impact of P2X7 receptor alterations in the maintenance of normal cellular homeostasis and pathological processes via distinct patterns of miR expression (Conte et al., 2020).

Lastly, due to their importance as regulatory molecules, new molecules with miR-mimicking or miR antagonist (antagomiR) activity have been received increasing attention. For example, traumatic spinal cord injury is worsened by a massive release of glutamate and ATP, which could be generated by an over-expression and activation of purinergic receptors, especially P2X7, producing excitotoxicity in neurodegenerative diseases. In that regard, the miR-135a-5p was identified to be a post-transcriptional modulator of P2X7, over-expressing the P2X7 receptor when in decreased levels. Besides, the antagomiR-135a increased the P2X7 expression whereas the miR-135a-mimicked reduced the P2X7 expression protecting cells from excitotoxic death (Reigada et al., 2019). Therapeutic approaches involving purinergic signaling will be discussed in more detail in the following topic. Thus, the interplay between purinergic signaling and miR modulation in ASD should be elucidated in future investigations. An overview of metabolism, neuroimmune aspects and molecular modulation can be seen in Figure 2.

7. Therapeutic Approaches and Purinergic System in ASD

Regarding therapeutic approaches, several human disorders still do not have a specific treatment, as in the case of ASD, whose treatment involves medications that help with the associated symptoms. However, several studies bring new therapeutic

opportunities for the treatment of different pathologies: for example, the stimulation or inhibition of specific purinergic receptors P1 or P2 to improve issues related to the dysregulation of purinergic signaling. An overview can be seen in Table 1 and Figure 3.

7.1. ADO and P1 receptors modulators

7.1.1. CGS 21680

The CGS-21680 (CGS) is a drug agonist selective of ADO A2A subtype receptor. The treatment of BTBR mouse strain with CGS changes gene and protein expression levels of several molecules in spleen and brain: a) in splenic cells, decreased production of positive cells to $CD4^+IL\text{-}21^+$, $CD4^+IL\text{-}22^+$, $CD4^+GATA3^+$, and $CD4^+T\text{-}bet^+$, and increased $CD4^+CTLA\text{-}4$ (Ahmad et al., 2017b); b) in splenic cells and brain tissue, decreased $CD14^+TLR2^+$ cells, $CD14^+TLR3^+$ cells, $CD14^+TLR4^+$ cells and TLR2, TLR3, TLR4, and NF-κB mRNA and protein expression, respectively (Ahmad et al., 2017a); c) in splenic $CD8^+$ T cells, decreased positive cells of $CCR3^+$, $CCR4^+$, $CCR5^+$, $CCR6^+$, $CCR7^+$, $CXCR3^+$, $CXCR4^+$, and $CXCR5^+$, and decreased mRNA of C-C and C-X-C chemokine receptors in the brain tissue (Ahmad et al., 2018); d) in total spleen and splenic $CD4^+$ T cells, diminished positive cells of $IL\text{-}2^+$, $IL\text{-}6^+$, $IL\text{-}9^+$, $IFN\text{-}\gamma^+$, and $TNF\text{-}\alpha^+$ and increased $TGF\text{-}\beta^+$, and improvement in respective mRNA and protein expression in brain tissue of BTBR mouse strain (Ansari et al., 2017a); e) in $CD4^+$ cells, diminished the IL-17A, RORγt, Stat3, and pStat3 levels and elevates the $Foxp3^+$ and $IL\text{-}10^+$ protein and expression levels (Ansari et al., 2017b). In addition to the molecular improvements, CGS also ameliorated the learning deficits, attenuated the self-grooming behavior and the response to the hot plate test in BTBR mice (Ansari et al., 2017b; Amodeo et al., 2018).

In C58 mice, a lineage that exhibits a robust repetitive behavior phenotype (one of the diagnostic criteria for ASD), a combination of three drugs (CGS, L-741,626 (a dopamine D2 receptor antagonist), and glutamate mGlu5 positive allosteric modulator) reduced repetitive motor behavior in C58 mice and four-fold increase in BDNF mRNA expression (Muehlmann et al., 2020). The combination of two ADO A1 (N6-cyclopentyladenosine - CPA) and A2A (CGS) receptor agonists also reduced repetitive behavior in both male and female C58 mice (in a dose-dependent manner),

and increased the number of Fos transcripts and Fos positive cells in the dorsal striatum (Lewis et al., 2019). This same drug combination (CPA and CGS) also attenuated stereotypy behavior in a dose-dependent manner in deer mice, animals with elevated rates of spontaneous stereotypy (Tanimura et al., 2010).

7.1.2. Propentofylline

Propentofylline is a xanthine phosphodiesterase inhibitor and ADO reuptake blocker. A double-blind and placebo-controlled clinical trial demonstrated that the association with propentofylline (initiating at 300 mg/d) and risperidone (initiating at 0.5 mg/d) was able to diminish the irritability in ASD patients evaluated by Childhood Autism Rating Scale, demonstrating the propentofylline as a promising adjunctive treatment probably due to their anti-inflammatory and anti-excitatory properties (Behmanesh et al., 2019).

Taken together, these data suggest the important contribution of the A2AR modulation in the improvement of neuroimmune and behavioral dysfunction observed in animal models.

7.2. P2 receptors modulators

7.2.1. Suramin

Suramin is a P2 non-selective purinergic antagonist. A pilot study double-blind, placebo-controlled, translational in male subjects with ASD showed, in a preliminary way, that a single dose of 20 mg/kg of suramin improved the language and social interaction, as well as decrease the repetitive behaviors (Naviaux et al., 2017). Indeed, the same dose in the valproic acid animal model of ASD restored sociability and decreased anxiety-like behavior, as well as normalized the increase of IL-6 expression in the medial prefrontal cortex in juvenile rats (Hirsch et al., 2020).

In the ASD-mouse by gestational exposure to poly(I:C), a single dose of suramin again restored, in a transitory manner, the social behavior and the novelty preference, beyond normalize metabolic pathways disturbed in the mouse model, related mainly to purine metabolism (Naviaux et al., 2014). The weekly injection of suramin (10 or 20 mg/kg) reverted the social behavior and sensorimotor coordination

deficits, rescued the mitochondrial respiratory chain hyperactivity abnormalities (decreasing the enzymatic activity of respiratory chain Complex I activity and Complex IV activity), corrected the reduction in the phosphorylation of ERK1 and 2, and in the phosphorylation of calcium/calmodulin-dependent protein kinase II, as well prevented Purkinje cell loss and restores the diminished levels of P2X7 and P2Y2 immunocontent (Naviaux et al., 2013).

Another study in fragile X syndrome model induced by *Fmr1* KO mice demonstrated that a purinergic antagonist strategy improved the animal performance in novelty preference, marble burying, and social behavior, normalizing abnormal synaptosomes and metabolomics alteration, particularly related to purine metabolism (Naviaux et al., 2015).

7.2.2. Brilliant Blue G

Brilliant Blue G is a specific P2X7 receptor (P2X7R) antagonist. Pregnant mice received 45 mg/kg of this molecule on gestation day 17 (E17) before administration of lipopolysaccharide (LPS), an inductor of maternal immune activation. The inhibition of P2X7R reduced the preterm birth rate, improved the performance on neuromotor tests of the offspring, and rescued the density of cortical neurons (Tsimis et al., 2017).

7.2.3. JNJ-47965567, A438079, OxATP, and A740003

Owing to the presence of convulsive episodes in a considerable percentage of ASD patients, data obtained in epilepsy studies are a great contribution in this sense.

The JNJ-47965567, a specific P2X7 receptor antagonist, reduced spontaneous seizures during continuous video-EEG monitoring, microgliosis, and astrogliosis in a 30 mg/kg dose (Jimenez-Pacheco et al., 2016). Another P2X7R antagonist with a promising therapeutic approach is A438079, able to reduce both the seizure duration and the neuronal death after intracerebroventricular microinjection of 1.75 nmol (Engel et al., 2012).

On the other hand, P2X7R antagonists can increase seizure susceptibility induced by pilocarpine. Both OxATP (a nonselective P2X7R antagonist) and A438079 and

A740003 (selective P2X7R antagonists) infusion increased pilocarpine-induced seizure susceptibility (Kim and Kang, 2011).

7.3. Adenylate cyclase modulators

Adenylate cyclase (EC 4.6.1.1) is an enzyme that catalyzes the ATP into cyclic ADO monophosphate (cAMP) and its modulation can direct the level of secondary messengers.

7.3.1. NB001

NB001 is an experimental compound that suppresses type 1 adenylate cyclase (ADCY1) protein activity. The Fmr1 knockout neurons have increased Adcy1 mRNA translation and, consequently, excessive ADCY1 protein. The administration of NB001 in Fmr1 KO mice attenuated the ASD-like behaviors, such as social interaction deficits and stereotyped behaviors (Sethna et al., 2017).

7.3.2. Diterpenoid Forskolin

The diterpenoid forskolin (FSK EC 266-410-9) is an adenylate cyclase activator that increases intracellular cAMP. The administration of FSK during 15 days rescued the memory dysfunction, decreased muscle coordination and gait imbalance, improved the changes in enzyme activity in neuronal mitochondrial electron transport chain complexes, as well as decreased pro-inflammatory cytokines, oxidative stress, and lipid biomarkers in a dose-dependent manner in an ASD-animal model induced by intracerebroventricular injection of propionic acid (Mehan et al., 2020).

7.4. Other types of therapeutic molecules

7.4.1. 5-aminolevulinic acid

The 5-aminolevulinic acid is an endogenous non-protein amino acid precursor of the heme group. This treatment improved the ASD-like behaviors such as learning and memory, ameliorated oxidative stress and mitochondrial dysfunction in the

hippocampus, and rescue the reduced number of PV interneurons of valproic acid-exposed rats (Matsuo et al., 2020).

7.4.2. Exogenous ATP and UTP

In primary astrocyte cultures derived from the Fmr1 KO mouse model, the presence of exogenous ATP and UTP triggered an elevation in intracellular calcium responses and in synaptogenic protein TSP-1 expression, which be modulated by P2Y receptors (Reynolds et al., 2021). The modulatory role of ATP is evidenced in a study using human primary skin fibroblasts from ASD patients, demonstrating that Ca^{2+} release in response to activation of exogenous ATP is decreased in ASD subjects and opening the way for new therapeutic targets (Schmunk et al., 2017).

7.4.2. Exogenous UMP and CMP

A group of four patients that presented developmental delay (especially language), seizure, ataxia, motor impairments, and other autistic-associated characteristics was treated with pyrimidines UMP and CMP, demonstrating improvement in several of these features. The treatment interruption resulted in the recurrence of the symptoms, indicating that the supplement with pyrimidines may counteract a continuous catabolic status in these patients (Page et al., 1997).

8. Concluding remarks

Neurodevelopmental disorders, including ASD, are a set of conditions that affect typical brain development. The embryonic period is especially susceptible to micro and macro-environmental changes. This includes, for example, immune changes via maternal immune activation, which can onset a plethora of dysregulations in the prenatal brain that persists through life: synaptic activity alterations, mitochondrial dysfunctions, aberrant behaviors, among others. Noteworthy, purinergic signaling plays a key regulatory role in all these processes. Beyond that, considering the purinergic system contribution in several outcomes, novel therapeutic approaches have been proposed mainly by the regulation of receptors, but also by enzymatic modulation and mitochondrial intermediates.

Undoubtedly, more needs to be learned regarding how purinergic intermediates contribute both to the onset and the maintaining of neuropsychiatric disorders such as ASD; however, taken together, this overview of data highlights the purinergic signaling involvement both in typical and pathological brain development, as well as a target for novel therapeutic approaches.

Funding statement: This work was supported by Instituto Nacional de Ciência e Tecnologia em Neuroimunomodulação (INCT-NIM #465489/2014-1), Rio de Janeiro, Brazil; Conselho Nacional de Desenvolvimento Científico e Tecnológico (CNPq), Coordenação de Aperfeiçoamento de Pessoal de Nível Superior (CAPES).

Conflict of Interest: The authors declare that they have no conflict of interest.

Acknowledgments: We would like to thank Dr. Mauro Hirsch on behalf of the authors for their important intellectual contribution in the publication “Effects of single-dose antipurinergic therapy on behavioral and molecular alterations in the valproic acid-induced animal model of autism”, by Hirsch et al., 2020. Figures created with <BioRender.com>.

References

Abdel-Rahman EA, Zaky EA, Aboulsaoud M, Elhossiny RM, Youssef WY, Mahmoud AM, Ali SS (2020) Autism spectrum disorder (ASD)-associated mitochondrial deficits are revealed in children’s platelets but unimproved by hyperbaric oxygen therapy. Free Radic Res Available at: https://www.tandfonline.com/doi/abs/10.1080/10715762.2020.1856376 [Accessed June 21, 2021].

Ahmad SF, Ansari MA, Nadeem A, Bakheet SA, AL-Ayadhi LY, Attia SM (2017a) Toll-like receptors, NF-κB, and IL-27 mediate adenosine A2A receptor signaling in BTBR T+ Itpr3tf/J mice. Prog Neuro-Psychopharmacology Biol Psychiatry 79:184–191 Available at: https://pubmed.ncbi.nlm.nih.gov/28668513/ [Accessed June 22, 2021].

Ahmad SF, Ansari MA, Nadeem A, Bakheet SA, Almutairi MM, Attia SM (2017b)

Adenosine A2A receptor signaling affects IL-21/IL-22 cytokines and GATA3/T-bet transcription factor expression in CD4+ T cells from a BTBR T+ Itpr3tf/J mouse model of autism. J Neuroimmunol 311:59–67 Available at: https://pubmed.ncbi.nlm.nih.gov/28807491/ [Accessed June 22, 2021].

Ahmad SF, Ansari MA, Nadeem A, Bakheet SA, Mohammad R, Attia SM (2018) Immune Alterations in CD8+ T Cells Are Associated with Neuronal C-C and C-X-C Chemokine Receptor Regulation Through Adenosine A2A Receptor Signaling in a BTBR T+ Itpr3tf/J Autistic Mouse Model. Mol Neurobiol 55:2603–2616 Available at: https://pubmed.ncbi.nlm.nih.gov/28421534/ [Accessed June 22, 2021].

Ahn Y, Sabouny R, Villa BR, Yee NC, Mychasiuk R, Uddin GM, Rho JM, Shutt TE (2020) Aberrant mitochondrial morphology and function in the btbr mouse model of autism is improved by two weeks of ketogenic diet. Int J Mol Sci 21 Available at: https://pubmed.ncbi.nlm.nih.gov/32380723/ [Accessed June 21, 2021].

American Psychiatric Association (2013) Diagnostic and Statistical Manual of Mental Disorders, 5th Edition (DSM-5).

Amodeo DA, Cuevas L, Dunn JT, Sweeney JA, Ragozzino ME (2018) The adenosine A2A receptor agonist, CGS 21680, attenuates a probabilistic reversal learning deficit and elevated grooming behavior in BTBR mice. Autism Res 11:223–233 Available at: https://pubmed.ncbi.nlm.nih.gov/29193861/ [Accessed June 22, 2021].

Ansari MA, Attia SM, Nadeem A, Bakheet SA, Raish M, Khan TH, Al-Shabanah OA, Ahmad SF (2017a) Activation of adenosine A2A receptor signaling regulates the expression of cytokines associated with immunologic dysfunction in BTBR T+ Itpr3tf/J mice. Mol Cell Neurosci 82:76–87 Available at: https://pubmed.ncbi.nlm.nih.gov/28465254/ [Accessed June 22, 2021].

Ansari MA, Nadeem A, Attia SM, Bakheet SA, Raish M, Ahmad SF (2017b) Adenosine A2A receptor modulates neuroimmune function through Th17/retinoid-related orphan receptor gamma t (RORγt) signaling in a BTBR T+ Itpr3tf/J mouse model of autism. Cell Signal 36:14–24 Available at: https://pubmed.ncbi.nlm.nih.gov/28438638/ [Accessed June 22, 2021].

Antonoudiou P, Tan YL, Kontou G, Louise Upton A, Mann EO (2020) Parvalbumin and somatostatin interneurons contribute to the generation of hippocampal gamma oscillations. J Neurosci 40:7668–7687 Available at: https://doi.org/10.1523/JNEUROSCI.0261-20.2020 [Accessed June 21, 2021].

Avendaño BC, Montero TD, Chávez CE, von Bernhardi R, Orellana JA (2015) Prenatal exposure to inflammatory conditions increases Cx43 and Panx1 unopposed channel opening and activation of astrocytes in the offspring effect on neuronal survival. Glia 63:2058–2072 Available at: https://onlinelibrary.wiley.com/doi/full/10.1002/glia.22877 [Accessed June 21, 2021].

Beers DR, Ho BK, Siklós L, Alexianu ME, Mosier DR, Habib Mohamed A, Otsuka Y, Kozovska ME, McAlhany RE, Glenn Smith R, Appel SH (2001) Parvalbumin overexpression alters immune-mediated increases in intracellular calcium, and delays disease onset in a transgenic model of familial amyotrophic lateral sclerosis. J Neurochem 79:499–509 Available at: https://onlinelibrary.wiley.com/doi/full/10.1046/j.1471-4159.2001.00582.x [Accessed June 21, 2021].

Behmanesh H, Moghaddam HS, Mohammadi MR, Akhondzadeh S (2019) Risperidone Combination Therapy with Propentofylline for Treatment of Irritability in Autism Spectrum Disorders: A Randomized, Double-Blind, Placebo-Controlled Clinical Trial. Clin Neuropharmacol 42:189–196 Available at: https://pubmed.ncbi.nlm.nih.gov/31725473/ [Accessed June 22, 2021].

Bertelli M, Cecchin S, Lapucci C, Jacomelli G, Jinnah HA, Pandolfo M, Micheli V (2006) Study of the adenosinergic system in the brain of HPRT knockout mouse (Lesch-Nyhan disease). Clin Chim Acta 373:104–107 Available at: https://pubmed.ncbi.nlm.nih.gov/16793031/ [Accessed June 21, 2021].

Bolton PF, Carcani-Rathwell I, Hutton J, Goode S, Howlin P, Rutter M (2011) Epilepsy in autism: Features and correlates. Br J Psychiatry 198:289–294 Available at: /pmc/articles/PMC3065774/ [Accessed June 21, 2021].

Bottini N, De Luca D, Saccucci P, Fiumara A, Elia M, Porfirio MC, Lucarelli P, Curatolo P (2001) Autism: Evidence of association with adenosine deaminase

genetic polymorphism. Neurogenetics 3:111–113 Available at: https://pubmed.ncbi.nlm.nih.gov/11354825/ [Accessed June 21, 2021].

Bourgeron T (2015) From the genetic architecture to synaptic plasticity in autism spectrum disorder. Nat Rev Neurosci 16:551–563 Available at: www.nature.com/reviews/neuro [Accessed June 21, 2021].

Braun NN, Reutiman TJ, Lee S, Folsom TD, Fatemi SH (2007) Expression of phosphodiesterase 4 is altered in the brains of subjects with autism. Neuroreport 18:1841–1844 Available at: https://pubmed.ncbi.nlm.nih.gov/18090323/ [Accessed June 21, 2021].

Campbell NG, Zhu C-B, Lindler KM, Yaspan BL, Kistner-Griffin E, Hewlett WA, Tate CG, Blakely RD, Sutcliffe JS (2013) Rare coding variants of the adenosine A3 receptor are increased in autism: on the trail of the serotonin transporter regulome. Mol Autism 4:28 Available at: /pmc/articles/PMC3882891/ [Accessed June 21, 2021].

Chang YS, Owen JP, Desai SS, Hill SS, Arnett AB, Harris J, Marco EJ, Mukherjee P (2014) Autism and sensory processing disorders: Shared white matter disruption in sensory pathways but divergent connectivity in social-emotional pathways. PLoS One 9:103038 Available at: /pmc/articles/PMC4116166/ [Accessed June 21, 2021].

Chauhan A, Gu F, Essa MM, Wegiel J, Kaur K, Brown WT, Chauhan V (2011) Brain region-specific deficit in mitochondrial electron transport chain complexes in children with autism. J Neurochem 117:209–220 Available at: /pmc/articles/PMC4839269/ [Accessed June 21, 2021].

Chávez CE, Oyarzún JE, Avendaño BC, Mellado LA, Inostroza CA, Alvear TF, Orellana JA (2019) The Opening of Connexin 43 Hemichannels Alters Hippocampal Astrocyte Function and Neuronal Survival in Prenatally LPS-Exposed Adult Offspring. Front Cell Neurosci 13.

Cheffer A, Castillo ARG, Corrêa-Velloso J, Gonçalves MCB, Naaldijk Y, Nascimento IC, Burnstock G, Ulrich H (2018) Purinergic system in psychiatric diseases. Mol Psychiatry 23:94–106 Available at:

http://www.ncbi.nlm.nih.gov/pubmed/28948971 [Accessed June 3, 2019].

Conte G, Nguyen NT, Alves M, de Diego-Garcia L, Kenny A, Nicke A, Henshall DC, Jimenez-Mateos EM, Engel T (2020) P2X7 Receptor-Dependent microRNA Expression Profile in the Brain Following Status Epilepticus in Mice. Front Mol Neurosci 13 Available at: /pmc/articles/PMC7485385/ [Accessed June 22, 2021].

Deckmann I, Schwingel GB, Fontes-Dutra M, Bambini-Junior V, Gottfried C (2018) Neuroimmune Alterations in Autism: A Translational Analysis Focusing on the Animal Model of Autism Induced by Prenatal Exposure to Valproic Acid. Neuroimmunomodulation 25:285–299 Available at: http://www.ncbi.nlm.nih.gov/pubmed/30157484 [Accessed May 10, 2019].

Di Virgilio F, Dal Ben D, Sarti AC, Giuliani AL, Falzoni S (2017) The P2X7 Receptor in Infection and Inflammation. Immunity 47:15–31 Available at: https://pubmed.ncbi.nlm.nih.gov/28723547/ [Accessed June 22, 2021].

Doshi-Velez F, Ge Y, Kohane I (2014) Comorbidity clusters in autism spectrum disorders: An electronic health record time-series analysis. Pediatrics 133:e54 Available at: /pmc/articles/PMC3876178/ [Accessed June 21, 2021].

Duan S, Anderson CM, Keung EC, Chen Y, Chen Y, Swanson RA (2003) P2X7 receptor-mediated release of excitatory amino acids from astrocytes. J Neurosci 23:1320–1328 Available at: https://pubmed.ncbi.nlm.nih.gov/12598620/ [Accessed June 22, 2021].

Eltokhi A, Santuy A, Merchan-Perez A, Sprengel R (2021) Glutamatergic dysfunction and synaptic ultrastructural alterations in schizophrenia and autism spectrum disorder: Evidence from human and rodent studies. Int J Mol Sci 22:1–26 Available at: https://pubmed.ncbi.nlm.nih.gov/33374598/ [Accessed June 21, 2021].

Engel T, Brennan GP, Sanz-Rodriguez A, Alves M, Beamer E, Watters O, Henshall DC, Jimenez-Mateos EM (2017) A calcium-sensitive feed-forward loop regulating the expression of the ATP-gated purinergic P2X7 receptor via specificity protein 1 and microRNA-22. Biochim Biophys Acta - Mol Cell Res 1864:255–266.

Engel T, Gomez-Villafuertes R, Tanaka K, Mesuret G, Sanz-Rodriguez A, Garcia-Huerta P, Miras-Portugal MT, Henshall DC, Diaz-Hernandez M (2012) Seizure suppression and neuroprotection by targeting the purinergic P2X7 receptor during status epilepticus in mice. FASEB J 26:1616–1628 Available at: https://pubmed.ncbi.nlm.nih.gov/22198387/ [Accessed June 22, 2021].

Erdorf M, von der Ohe J, Seifert R (2011) Impaired P2X and P2Y receptor-mediated signaling in HPRT-deficient B103 neuroblastoma cells. Neurosci Lett 504:311–315 Available at: https://pubmed.ncbi.nlm.nih.gov/21982803/ [Accessed June 21, 2021].

Ferrari D, Bianchi N, Eltzschig HK, Gambari R (2016) MicroRNAs Modulate the Purinergic Signaling Network. Trends Mol Med:905–918.

Ferrari D, Chiozzi P, Falzoni S, Hanau S, Di Virgilio F (1997) Purinergic modulation of interleukin-1β release from microglial cells stimulated with bacterial endotoxin. J Exp Med 185:579–582 Available at: http://rupress.org/jem/article-pdf/185/3/579/1110644/5402.pdf [Accessed June 22, 2021].

Filice F, Janickova L, Henzi T, Bilella A, Schwaller B (2020) The Parvalbumin Hypothesis of Autism Spectrum Disorder. Front Cell Neurosci 14:577525 Available at: www.frontiersin.org [Accessed June 21, 2021].

Fontes-Dutra M, Santos-Terra J, Deckmann I, Schwingel GB, Nunes GD-F, Hirsch MM, Bauer-Negrini G, Riesgo RSRSRS, Bambini-Júnior V, Hedin-Pereira C, Gottfried C, Brum Schwingel G, Della-Flora Nunes G, Hirsch MMMM, Bauer-Negrini G, Hedin-Pereira C, Bambini-Junior V, Riesgo RSRSRS, Gottfried C (2018) Resveratrol prevents cellular and behavioral sensory alterations in the animal model of autism induced by valproic acid. Front Synaptic Neurosci 10:9.

Franke H, Sauer C, Rudolph C, Krügel U, Hengstler JG, Illes P (2009) P2 receptor-mediated stimulation of the PI3-K/Akt-pathway in vivo. Glia 57:1031–1045 Available at: https://pubmed.ncbi.nlm.nih.gov/19115395/ [Accessed June 22, 2021].

Freitag CM, Agelopoulos K, Huy E, Rothermundt M, Krakowitzky P, Meyer J, Deckert J, Gontard A, Hohoff C, Freitag AE Konstantin Agelopoulos AE Ellen Huy AE

Matthias Rothermundt AE Petra Krakowitzky AE Jobst Meyer AE Jü rgen Deckert AE Alexander von Gontard AE Christa Hohoff CM (2009) Adenosine A receptor gene () variants may increase autistic symptoms and anxiety in autism spectrum disorder Adenosine A 2A receptor gene (ADORA2A) variants may increase autistic symptoms and anxiety in autism spectrum disorder. Eur Child Adolesc Psychiatry 19 Available at: http://www.hapmap.org [Accessed June 21, 2021].

Fumagalli M, Lecca D, Abbracchio MP (2011) Role of purinergic signalling in neuro-immune cells and adult neural progenitors. Front Biosci 16:2326–2341 Available at: https://pubmed.ncbi.nlm.nih.gov/21622179/ [Accessed June 22, 2021].

Fumagalli M, Lecca D, Abbracchio MP, Ceruti S (2017) Pathophysiological role of purines and pyrimidines in neurodevelopment: Unveiling new pharmacological approaches to congenital brain diseases. Front Pharmacol 8 Available at: https://pubmed.ncbi.nlm.nih.gov/29375373/ [Accessed June 21, 2021].

García-Huerta P, Diáz-Hernandez M, Delicado EG, Pimentel-Santillana M, Miras-Portugals MT, Gońez-Villafuertes R (2012) The specificity protein factor Sp1 mediates transcriptional regulation of P2X7 receptors in the nervous system. J Biol Chem 287:44628–44644.

Garré JM, Silva HM, Lafaille JJ, Yang G (2020) P2X7 receptor inhibition ameliorates dendritic spine pathology and social behavioral deficits in Rett syndrome mice. Nat Commun 11:1–13 Available at: https://doi.org/10.1038/s41467-020-15590-5 [Accessed June 21, 2021].

Gevi F, Zolla L, Gabriele S, Persico AM (2016) Urinary metabolomics of young Italian autistic children supports abnormal tryptophan and purine metabolism. Mol Autism 7:47 Available at: https://pubmed.ncbi.nlm.nih.gov/27904735/ [Accessed June 21, 2021].

Ginsberg MR, Rubin RA, Falcone T, Ting AH, Natowicz MR (2012) Brain Transcriptional and Epigenetic Associations with Autism. PLoS One 7 Available at: https://pubmed.ncbi.nlm.nih.gov/22984548/ [Accessed June 21, 2021].

Giulivi C, Napoli E, Schwartzer J, Careaga M, Ashwood P (2013) Gestational

exposure to a viral mimetic poly(I:C) Results in long-lasting changes in mitochondrial function by leucocytes in the adult offspring. Mediators Inflamm 2013 Available at: https://pubmed.ncbi.nlm.nih.gov/24174710/ [Accessed June 21, 2021].

Gottfried C, Bambini-Junior V, Francis F, Riesgo R, Savino W (2015) The Impact of Neuroimmune Alterations in Autism Spectrum Disorder. Front psychiatry 6:121 Available at: http://journal.frontiersin.org/Article/10.3389/fpsyt.2015.00121/abstract [Accessed February 1, 2018].

Grahames CBA, Michel AD, Chessell IP, Humphrey PPA (1999) Pharmacological characterization of ATP- and LPS-induced IL-1β release in human monocytes. Br J Pharmacol 127:1915–1921 Available at: http://www.stockton-press.co.uk/bjp [Accessed June 22, 2021].

Ha BG, Heo JY, Jang YJ, Park TS, Choi JY, Jang WY, Jeong SJ (2021) Depletion of mitochondrial components from extracellular vesicles secreted from astrocytes in a mouse model of fragile x syndrome. Int J Mol Sci 22:1–14 Available at: https://pubmed.ncbi.nlm.nih.gov/33401721/ [Accessed June 21, 2021].

Hegazy HG, Ali EHA, Elgoly AHM (2015) Interplay between pro-inflammatory cytokines and brain oxidative stress biomarkers: Evidence of parallels between butyl paraben intoxication and the valproic acid brain physiopathology in autism rat model. Cytokine 71:173–180 Available at: http://dx.doi.org/10.1016/j.cyto.2014.10.027.

Hettinger JA, Liu X, Holden JJA (2008) The G22A polymorphism of the ADA gene and susceptibility to autism spectrum disorders. J Autism Dev Disord 38:14–19 Available at: https://pubmed.ncbi.nlm.nih.gov/17340203/ [Accessed June 21, 2021].

Hirsch MM, Deckmann I, Santos-Terra J, Staevie GZ, Fontes-Dutra M, Carello-Collar G, Körbes-Rockenbach M, Brum Schwingel G, Bauer-Negrini G, Rabelo B, Gonçalves MCB, Corrêa-Velloso J, Naaldijk Y, Castillo AR, Schneider T, Bambini-Junior V, Ulrich H, Gottfried C (2020) Effects of single-dose antipurinergic therapy on behavioral and molecular alterations in the valproic

acid-induced animal model of autism. Neuropharmacology:107930 Available at: https://linkinghub.elsevier.com/retrieve/pii/S0028390819305015 [Accessed January 15, 2020].

Horder J, Petrinovic MM, Mendez MA, Bruns A, Takumi T, Spooren W, Barker GJ, Künnecke B, Murphy DG (2018) Glutamate and GABA in autism spectrum disorder—a translational magnetic resonance spectroscopy study in man and rodent models. Transl Psychiatry 8:106 Available at: http://www.nature.com/articles/s41398-018-0155-1 [Accessed June 3, 2019].

Horváth G, Otrokocsi L, Beko K, Baranyi M, Kittel Á, Fritz-Ruenes PA, Sperlágh B (2019) P2X7 receptors drive poly(I:C) induced autism-like behavior in mice. J Neurosci 39:2542–2561 Available at: /pmc/articles/PMC6435822/ [Accessed June 21, 2021].

Janickova L, Rechberger KF, Wey L, Schwaller B (2020) Absence of parvalbumin increases mitochondria volume and branching of dendrites in inhibitory Pvalb neurons in vivo: A point of convergence of autism spectrum disorder (ASD) risk gene phenotypes. Mol Autism 11 Available at: https://pubmed.ncbi.nlm.nih.gov/32517751/ [Accessed June 21, 2021].

Janickova L, Schwaller B (2020) Parvalbumin-Deficiency Accelerates the Age-Dependent ROS Production in Pvalb Neurons in vivo: Link to Neurodevelopmental Disorders. Front Cell Neurosci 14 Available at: https://pubmed.ncbi.nlm.nih.gov/33132847/ [Accessed June 21, 2021].

Jimenez-Mateos EM et al. (2015) MicroRNA targeting of the P2X7 purinoceptor opposes a contralateral epileptogenic focus in the hippocampus. Sci Rep 5 Available at: /pmc/articles/PMC4668358/ [Accessed June 22, 2021].

Jimenez-Mateos EM, Smith J, Nicke A, Engel T (2019) Regulation of P2X7 receptor expression and function in the brain. Brain Res Bull 151:153–163 Available at: https://pubmed.ncbi.nlm.nih.gov/30593878/ [Accessed June 22, 2021].

Jimenez-Pacheco A, Diaz-Hernandez M, Arribas-Blázquez M, Sanz-Rodriguez A, Olivos-Oré LA, Artalejo AR, Alves M, Letavic M, Teresa Miras-Portugal M, Conroy RM, Delanty N, Farrell MA, O'Brien DF, Bhattacharya A, Engel T,

Henshall DC (2016) Transient P2X7 receptor antagonism produces lasting reductions in spontaneous seizures and gliosis in experimental temporal lobe epilepsy. J Neurosci 36:5920–5932 Available at: /pmc/articles/PMC6601816/ [Accessed June 22, 2021].

Jyonouchi H, Geng L, Toruner GA, Rose S, Bennuri SC, Frye RE (2019) Serum microrna s in ASD: Association with monocyte cytokine profiles and mitochondriarespiration. Front Psychiatry 10 Available at: https://pubmed.ncbi.nlm.nih.gov/31551826/ [Accessed June 21, 2021].

Kang TH, Park Y, Bader JS, Friedmann T (2013) The Housekeeping Gene Hypoxanthine Guanine Phosphoribosyltransferase (HPRT) Regulates Multiple Developmental and Metabolic Pathways of Murine Embryonic Stem Cell Neuronal Differentiation. PLoS One 8:74967 Available at: /pmc/articles/PMC3794013/ [Accessed June 21, 2021].

Kaufmann WE, Kidd SA, Andrews HF, Budimirovic DB, Esler A, Haas-Givler B, Stackhouse T, Riley C, Peacock G, Sherman SL, Brown WT, Berry-Kravis E (2017) Autism spectrum disorder in fragile X syndrome: Cooccurring conditions and current treatment. Pediatrics 139:S194–S206 Available at: www.aappublications.org/news [Accessed June 21, 2021].

Kelley DJ, Davidson RJ, Elliott JL, Lahvis GP, Yin JCP, Bhattacharyya A (2007) The cyclic AMP cascade is altered in the fragile X nervous system. PLoS One 2 Available at: https://pubmed.ncbi.nlm.nih.gov/17895972/ [Accessed June 21, 2021].

Khan MT, Liu J, Nerlich J, Tang Y, Franke H, Illes P (2018) Regulation of P2X7 receptor function of neural progenitor cells in the hippocampal subgranular zone by neuronal activity in the dentate gyrus. Neuropharmacology 140:139–149 Available at: https://pubmed.ncbi.nlm.nih.gov/30092245/ [Accessed June 21, 2021].

Kim JE, Kang TC (2011) The P2X7 receptor-pannexin-1 complex decreases muscarinic acetylcholine receptor-mediated seizure susceptibility in mice. J Clin Invest 121:2037–2047 Available at: /pmc/articles/PMC3083785/ [Accessed June 22, 2021].

Kim JH, Yan Q, Uppal K, Cui X, Ling C, Walker DI, Heck JE, von Ehrenstein OS, Jones DP, Ritz B (2021) Metabolomics analysis of maternal serum exposed to high air pollution during pregnancy and risk of autism spectrum disorder in offspring. Environ Res 196:110823.

Lewis MH, Rajpal H, Muehlmann AM (2019) Reduction of repetitive behavior by co-administration of adenosine receptor agonists in C58 mice. Pharmacol Biochem Behav 181:110–116 Available at: /pmc/articles/PMC6629027/ [Accessed June 22, 2021].

Licznerski P et al. (2020) ATP Synthase c-Subunit Leak Causes Aberrant Cellular Metabolism in Fragile X Syndrome. Cell 182:1170-1185.e9 Available at: https://pubmed.ncbi.nlm.nih.gov/32795412/ [Accessed June 21, 2021].

Liu J, Li N, Sheng R, Wang R, Xu Z, Mao Y, Wang Y, Liu Y (2017) Hypermethylation downregulates P2X7 receptor expression in astrocytoma. Oncol Lett 14:7699–7704 Available at: http://www.spandidos-publications.com/10.3892/ol.2017.7241/abstract [Accessed June 22, 2021].

Lo JC, Huang WC, Chou YC, Tseng CH, Lee WL, Sun SH (2008) Activation of P2X7 receptors decreases glutamate uptake and glutamine synthetase activity in RBA-2 astrocytes via distinct mechanisms. J Neurochem 105:151–164 Available at: https://onlinelibrary.wiley.com/doi/full/10.1111/j.1471-4159.2007.05119.x [Accessed June 22, 2021].

López-Cruz L, Carbó-Gas M, Pardo M, Bayarri P, Valverde O, Ledent C, Salamone JD, Correa M (2017) Adenosine A2A receptor deletion affects social behaviors and anxiety in mice: Involvement of anterior cingulate cortex and amygdala. Behav Brain Res 321:8–17 Available at: https://pubmed.ncbi.nlm.nih.gov/28007538/ [Accessed June 21, 2021].

Lukmanji S, Manji SA, Kadhim S, Sauro KM, Wirrell EC, Kwon CS, Jetté N (2019) The co-occurrence of epilepsy and autism: A systematic review. Epilepsy Behav 98:238–248 Available at: https://pubmed.ncbi.nlm.nih.gov/31398688/ [Accessed June 21, 2021].

Luo W, Zhang C, Jiang YH, Brouwer CR (2018) Systematic reconstruction of autism

biology from massive genetic mutation profiles. Sci Adv 4:1701799 Available at: /pmc/articles/PMC5895441/ [Accessed June 21, 2021].

Maenner MJ et al. (2020) Prevalence of Autism Spectrum Disorder Among Children Aged 8 Years — Autism and Developmental Disabilities Monitoring Network, 11 Sites, United States, 2016. MMWR Surveill Summ 69:1–12 Available at: http://www.cdc.gov/mmwr/volumes/69/ss/ss6904a1.htm?s_cid=ss6904a1_w [Accessed May 13, 2020].

Martí Navia A, Dal Ben D, Lambertucci C, Spinaci A, Volpini R, Marques-Morgado I, Coelho JE, Lopes L V., Marucci G, Buccioni M (2020) Adenosine Receptors as Neuroinflammation Modulators: Role of A1 Agonists and A2A Antagonists. Cells 9 Available at: https://pubmed.ncbi.nlm.nih.gov/32708189/ [Accessed June 21, 2021].

Masi A, DeMayo MM, Glozier N, Guastella AJ (2017) An Overview of Autism Spectrum Disorder, Heterogeneity and Treatment Options. Neurosci Bull 33:183–193.

Masino S, Kawamura Jr. M, Wasser C, Pomeroy L, Ruskin D (2009) Adenosine, Ketogenic Diet and Epilepsy: The Emerging Therapeutic Relationship Between Metabolism and Brain Activity. Curr Neuropharmacol 7:257–268 Available at: /pmc/articles/PMC2769009/ [Accessed June 21, 2021].

Masino SA, Kawamura M, Cote JL, Williams RB, Ruskin DN (2013) Adenosine and autism: A spectrum of opportunities. Neuropharmacology 68:116–121 Available at: https://pubmed.ncbi.nlm.nih.gov/22940000/ [Accessed June 21, 2021].

Masino SA, Kawamura M, Plotkin LM, Svedova J, DiMario FJ, Eigsti IM (2011) The relationship between the neuromodulator adenosine and behavioral symptoms of autism. Neurosci Lett 500:1–5 Available at: /pmc/articles/PMC3745825/ [Accessed June 21, 2021].

Mastrangelo L, Kim JE, Miyanohara A, Kang TH, Friedmann T (2012) Purinergic signaling in human pluripotent stem cells is regulated by the housekeeping gene encoding hypoxanthine guanine phosphoribosyltransferase. Proc Natl Acad Sci U S A 109:3377–3382 Available at: https://pubmed.ncbi.nlm.nih.gov/22331909/

[Accessed June 21, 2021].

Matsuo K, Yabuki Y, Fukunaga K (2020) 5-aminolevulinic acid inhibits oxidative stress and ameliorates autistic-like behaviors in prenatal valproic acid-exposed rats. Neuropharmacology 168 Available at: https://pubmed.ncbi.nlm.nih.gov/31991146/ [Accessed June 22, 2021].

Mehan S, Rahi S, Tiwari A, Kapoor T, Rajdev K, Sharma R, Khera H, Kosey S, Kukkar U, Dudi R (2020) Adenylate cyclase activator forskolin alleviates intracerebroventricular propionic acid-induced mitochondrial dysfunction of autistic rats. Neural Regen Res 15:1140–1149 Available at: /pmc/articles/PMC7034277/ [Accessed June 22, 2021].

Melani A, Turchi D, Vannucchi MG, Cipriani S, Gianfriddo M, Pedata F (2005) ATP extracellular concentrations are increased in the rat striatum during in vivo ischemia. Neurochem Int 47:442–448.

Montilla A, Mata GP, Matute C, Domercq M (2020) Contribution of p2x4 receptors to cns function and pathophysiology. Int J Mol Sci 21:1–16 Available at: https://pubmed.ncbi.nlm.nih.gov/32756482/ [Accessed June 21, 2021].

Muehlmann AM, Maletz S, King MA, Lewis MH (2020) Pharmacological targeting of striatal indirect pathway neurons improves subthalamic nucleus dysfunction and reduces repetitive behaviors in C58 mice. Behav Brain Res 391 Available at: https://pubmed.ncbi.nlm.nih.gov/32461129/ [Accessed June 22, 2021].

Naviaux J, Schuchbauer M, Li K, Wang L, Risbrough V, Powell S, Naviaux R (2014) Reversal of autism-like behaviors and metabolism in adult mice with single-dose antipurinergic therapy. Transl Psychiatry 4.

Naviaux JC, Wang L, Li K, Bright A, Alaynick WA, Williams KR, Powell SB, Naviaux RK (2015) Antipurinergic therapy corrects the autism-like features in the Fragile X (Fmr1 knockout) mouse model. Mol Autism 6:1 Available at: http://www.molecularautism.com/content/6/1/1 [Accessed June 22, 2021].

Naviaux RK et al. (2017) Low-dose suramin in autism spectrum disorder: a small, phase I/II, randomized clinical trial. Ann Clin Transl Neurol 4:491–505.

Naviaux RK, Zolkipli Z, Wang L, Nakayama T, Naviaux JC, Le TP, Schuchbauer MA, Rogac M, Tang Q, Dugan LL, Powell SB (2013) Antipurinergic Therapy Corrects the Autism-Like Features in the Poly(IC) Mouse Model Lakshmana MK, ed. PLoS One 8:e57380 Available at: https://dx.plos.org/10.1371/journal.pone.0057380 [Accessed May 10, 2019].

Ohsawa K, Irino Y, Nakamura Y, Akazawa C, Inoue K, Kohsaka S (2007) Involvement of P2X4 and P2Y12 receptors in ATP-induced microglial chemotaxis. Glia 55:604–616 Available at: https://pubmed.ncbi.nlm.nih.gov/17299767/ [Accessed June 22, 2021].

Page T, Yu A, Fontanesi J, Nyhan WL (1997) Developmental disorder associated with increased cellular nucleotidase activity. Proc Natl Acad Sci U S A 94:11601–11606 Available at: www.pnas.org. [Accessed June 22, 2021].

Pecorelli A, Ferrara F, Messano N, Cordone V, Schiavone ML, Cervellati F, Woodby B, Cervellati C, Hayek J, Valacchi G (2020) Alterations of mitochondrial bioenergetics, dynamics, and morphology support the theory of oxidative damage involvement in autism spectrum disorder. FASEB J 34:6521–6538 Available at: https://faseb.onlinelibrary.wiley.com/doi/full/10.1096/fj.201902677R [Accessed June 21, 2021].

Persico AM, Militerni R, Bravaccio C, Schneider C, Melmed R, Trillo S, Montecchi F, Palermo MT, Pascucci T, Puglisi-Allegra S, Reichelt K-L, Conciatori M, Baldi A, Keller F (2000) Adenosine deaminase alleles and autistic disorder: Case-control and family-based association studies. Am J Med Genet 96:784–790 Available at: https://pubmed.ncbi.nlm.nih.gov/11121182/ [Accessed June 21, 2021].

Petrelli F, Pucci L, Bezzi P (2016) Astrocytes and Microglia and Their Potential Link with Autism Spectrum Disorders. Front Cell Neurosci 10:21.

Philippart M (1986) Clinical recognition of Rett syndrome. Am J Med Genet 24:111–118 Available at: https://pubmed.ncbi.nlm.nih.gov/3087171/ [Accessed June 21, 2021].

Reigada D, Calderón-García AÁ, Soto-Catalán M, Nieto-Díaz M, Muñoz-Galdeano T, del Águila Á, Maza RM (2019) MicroRNA-135a-5p reduces P2X7-dependent rise

in intracellular calcium and protects against excitotoxicity. J Neurochem 151:116–130 Available at: http://www.targe [Accessed June 22, 2021].

Reynolds KE, Wong CR, Scott AL (2021) Astrocyte-mediated purinergic signaling is upregulated in a mouse model of Fragile X syndrome. Glia 69:1816–1832 Available at: https://pubmed.ncbi.nlm.nih.gov/33754385/ [Accessed June 22, 2021].

Rossi MJ, Pekkurnaz G (2019) Powerhouse of the mind: mitochondrial plasticity at the synapse. Curr Opin Neurobiol 57:149–155.

Rossignol DA, Frye RE (2012) Mitochondrial dysfunction in autism spectrum disorders: A systematic review and meta-analysis. Mol Psychiatry 17:290–314 Available at: https://pubmed.ncbi.nlm.nih.gov/21263444/ [Accessed June 21, 2021].

Schmunk G, Nguyen RL, Ferguson DL, Kumar K, Parker I, Gargus JJ (2017) High-Throughput screen detects calcium signaling dysfunction in typical sporadic autism spectrum disorder. Sci Rep 7 Available at: https://pubmed.ncbi.nlm.nih.gov/28145469/ [Accessed June 22, 2021].

Schwede M, Nagpal S, Gandal MJ, Parikshak NN, Mirnics K, Geschwind DH, Morrow EM (2018) Strong correlation of downregulated genes related to synaptic transmission and mitochondria in post-mortem autism cerebral cortex. J Neurodev Disord 10 Available at: https://pubmed.ncbi.nlm.nih.gov/29859039/ [Accessed June 21, 2021].

Sethna F, Feng W, Ding Q, Robison AJ, Feng Y, Wang H (2017) Enhanced expression of ADCY1 underlies aberrant neuronal signalling and behaviour in a syndromic autism model. Nat Commun 8 Available at: /pmc/articles/PMC5321753/ [Accessed June 22, 2021].

Shen HY, Huang N, Reemmer J, Xiao L (2018) Adenosine actions on oligodendroglia and myelination in autism spectrum disorder. Front Cell Neurosci 12 Available at: https://pubmed.ncbi.nlm.nih.gov/30581380/ [Accessed June 21, 2021].

Silva CG, Métin C, Fazeli W, Machado NJ, Darmopil S, Launay PS, Ghestem A, Nesa MP, Bassot E, Szabó E, Baqi Y, Müller CE, Tomé AR, Ivanov A, Isbrandt

D, Zilberter Y, Cunha RA, Esclapez M, Bernard C (2013) Adenosine receptor antagonists including caffeine alter fetal brain development in mice. Sci Transl Med 5:197ra104-197ra104 Available at: https://stm.sciencemag.org/content/5/197/197ra104 [Accessed June 21, 2021].

Singh K, Singh IN, Diggins E, Connors SL, Karim MA, Lee D, Zimmerman AW, Frye RE (2020) Developmental regression and mitochondrial function in children with autism. Ann Clin Transl Neurol 7:683–694 Available at: https://pubmed.ncbi.nlm.nih.gov/32343046/ [Accessed June 21, 2021].

Smith AM, Natowicz MR, Braas D, Ludwig MA, Ney DM, Donley ELR, Burrier RE, Amaral DG (2020) A Metabolomics Approach to Screening for Autism Risk in the Children's Autism Metabolome Project. Autism Res 13:1270–1285 Available at: https://pubmed.ncbi.nlm.nih.gov/32558271/ [Accessed June 21, 2021].

Solle M, Labasi J, Perregaux DG, Stam E, Petrushova N, Koller BH, Griffiths RJ, Gabel CA (2001) Altered cytokine production in mice lacking P2X7 receptors. J Biol Chem 276:125–132 Available at: https://pubmed.ncbi.nlm.nih.gov/11016935/ [Accessed June 22, 2021].

Spence SJ, Schneider MT (2009) The role of epilepsy and epileptiform EEGs in autism spectrum disorders. Pediatr Res 65:599–606 Available at: http://www.ncbi.nlm.nih.gov/pubmed/19454962 [Accessed November 26, 2019].

Squillace M, Dodero L, Federici M, Migliarini S, Errico F, Napolitano F, Krashia P, Di Maio A, Galbusera A, Bifone A, Scattoni ML, Pasqualetti M, Mercuri NB, Usiello A, Gozzi A (2014) Dysfunctional dopaminergic neurotransmission in asocial BTBR mice. Transl Psychiatry 4 Available at: https://pubmed.ncbi.nlm.nih.gov/25136890/ [Accessed June 21, 2021].

Stathopoulos S, Gaujoux R, Lindeque Z, Mahony C, Van Der Colff R, Van Der Westhuizen F, O'Ryan C (2020) DNA Methylation Associated with Mitochondrial Dysfunction in a South African Autism Spectrum Disorder Cohort. Autism Res 13:1079–1093 Available at: https://pubmed.ncbi.nlm.nih.gov/32490597/ [Accessed June 21, 2021].

Steenfeldt-Kristensen C, Jones CA, Richards C (2020) The Prevalence of Self-

injurious Behaviour in Autism: A Meta-analytic Study. J Autism Dev Disord 50:3857–3873 Available at: https://doi.org/10.1007/s10803-020-04443-1 [Accessed June 21, 2021].

Stubbs G, Litt M, Lis E, Jackson R, Voth W, Lindberg A, Litt R (1982) Adenosine Deaminase Activity Decreased in Autism. J Am Acad Child Psychiatry 21:71–74.

Suzuki T, Hide I, Ido K, Kohsaka S, Inoue K, Nakata Y (2004) Production and Release of Neuroprotective Tumor Necrosis Factor by P2X 7 Receptor-Activated Microglia. J Neurosci 24:1–7 Available at: https://www.jneurosci.org/content/24/1/1 [Accessed June 22, 2021].

Synowitz M, Glass R, Färber K, Markovic D, Kronenberg G, Herrmann K, Schnermann J, Nolte C, Van Rooijen N, Kiwit J, Kettenmann H (2006) A1 adenosine receptors in microglia control glioblastoma-host interaction. Cancer Res 66:8550–8557 Available at: https://pubmed.ncbi.nlm.nih.gov/16951167/ [Accessed June 21, 2021].

Takahashi N, Harada T, Nishimura T, Okumura A, Choi D, Iwabuchi T, Kuwabara H, Takagai S, Nomura Y, Takei N, Tsuchiya KJ (2020) Association of Genetic Risks with Autism Spectrum Disorder and Early Neurodevelopmental Delays among Children without Intellectual Disability. JAMA Netw Open 3:1921644 Available at: https://jamanetwork.com/ [Accessed June 21, 2021].

Tang G, Gutierrez Rios P, Kuo SH, Akman HO, Rosoklija G, Tanji K, Dwork A, Schon EA, DiMauro S, Goldman J, Sulzer D (2013) Mitochondrial abnormalities in temporal lobe of autistic brain. Neurobiol Dis 54:349–361.

Tanimura Y, Vaziri S, Lewis MH (2010) Indirect basal ganglia pathway mediation of repetitive behavior: Attenuation by adenosine receptor agonists. Behav Brain Res 210:116–122 Available at: https://pubmed.ncbi.nlm.nih.gov/20178817/ [Accessed June 22, 2021].

Trang T, Beggs S, Wan X, Salter MW (2009) P2X4-receptor-mediated synthesis and release of brain-derived neurotrophic factor in microglia is dependent on calcium and p38-mitogen-activated protein kinase activation. J Neurosci 29:3518–3528 Available at: /pmc/articles/PMC3589565/ [Accessed June 21, 2021].

Tsimis ME, Lei J, Rosenzweig JM, Arif H, Shabi Y, Alshehri W, Talbot CC, Baig-Ward KM, Segars J, Graham EM, Burd I (2017) P2X7 receptor blockade prevents preterm birth and perinatal brain injury in a mouse model of intrauterine inflammation. Biol Reprod 97:230–239 Available at: https://pubmed.ncbi.nlm.nih.gov/29044426/ [Accessed June 22, 2021].

Ulrich H, Abbracchio MP, Burnstock G (2012) Extrinsic Purinergic Regulation of Neural Stem/Progenitor Cells: Implications for CNS Development and Repair. Stem Cell Rev Reports 8:755–767.

Vandenberg GG, Dawson NJ, Head A, Scott GR, Scott AL (2021) Astrocyte-mediated disruption of ROS homeostasis in Fragile X mouse model. Neurochem Int 146 Available at: https://pubmed.ncbi.nlm.nih.gov/33785420/ [Accessed June 21, 2021].

Wang M, Kong Q, Gonzalez FA, Sun G, Erb L, Seye C, Weisman GA (2005) P2Y2 nucleotide receptor interaction with αv integrin mediates astrocyte migration. J Neurochem 95:630–640 Available at: https://pubmed.ncbi.nlm.nih.gov/16135088/ [Accessed June 22, 2021].

Wyatt LR, Godar SC, Khoja S, Jakowec MW, Alkana RL, Bortolato M, Davies DL (2013) Sociocommunicative and sensorimotor impairments in male P2X4-deficient mice. Neuropsychopharmacology 38:1993–2002 Available at: /pmc/articles/PMC3746707/ [Accessed June 21, 2021].

Zamarbide M, Mossa A, Muñoz-Llancao P, Wilkinson MK, Pond HL, Oaks AW, Manzini MC (2019) Male-Specific cAMP Signaling in the Hippocampus Controls Spatial Memory Deficits in a Mouse Model of Autism and Intellectual Disability. Biol Psychiatry 85:760–768 Available at: https://pubmed.ncbi.nlm.nih.gov/30732858/ [Accessed June 21, 2021].

Zhao L, Liu YW, Yang T, Gan L, Yang N, Dai SS, He F (2015) The mutual regulation between miR-214 and A2AR signaling plays an important role in inflammatory response. Cell Signal 27:2026–2034.

Zimmermann FF, Gaspary KV, Siebel AM, Leite CE, Kist LW, Bogo MR, Bonan CD (2017) Analysis of Extracellular Nucleotide Metabolism in Adult Zebrafish After

Embryological Exposure to Valproic Acid. Mol Neurobiol 54:3542–3553 Available at: https://pubmed.ncbi.nlm.nih.gov/27189619/ [Accessed June 21, 2021].

Zolkipli-Cunningham Z, Naviaux JC, Nakayama T, Hirsch CM, Monk JM, Li K, Wang L, Le TP, Meinardi S, Blake DR, Naviaux RK (2021) Metabolic and behavioral features of acute hyperpurinergia and the maternal immune activation mouse model of autism spectrum disorder. PLoS One 16 Available at: https://pubmed.ncbi.nlm.nih.gov/33735311/ [Accessed June 21, 2021].

Legends of Figures

Figure 1. Main findings on purinergic system dysfunctions and autism-like features. Here we provide a clear overview of changes described in cell culture, in knockout animals for constituents of the purinergic system, and in animal models of ASD, as well as in humans diagnosed with ASD, emphasizing the important contribution of P2X4, P2X7, P2Y1, and A1 receptors in the pathophysiology of ASD. **1** Freitag et al., 2009; **2** Campbell et al., 2013; **3** Luo et al., 2018; **4** Takahashi et al., 2020; **5** Braun et al., 2007; **6** Stubbs et al., 1982; **7** Persico et al., 2000; **8** Bottini et al., 2001; **9** Avedaño et al., 2015; **10** Chávez et al., 2019; **11** Garré et al., 2020; **12** Horváth et al., 2019; **13** Trang et al., 2009; **14** Montilla et al., 2020; **15** Wyatt et al., 2013; **16** Mastrangelo et al., 2012; **17** Naviaux et al., 2013 ; **18** Hirsch et al., 2020; **19** Squillace et al., 2014; **20** Zimmermann et al., 2017; **21** López-Cruz et al., 2017

Figure 2. An integrative view of the changes described in ASD. Here, we show a compilation of alterations described both in patients with ASD and in animal models, evidencing the contribution of purinergic signaling in the most diverse biological processes. 1 Ahmad et al., 2017b; **2** Ahmad et al., 2018; **3** Ansari et al., 2017b **4** Ahmad et al., 2017a; **5** Ansari et al., 2017a; **6** Jimenez-Mateos et al., 2015; **7** García-Huerta et al., 2012; **8** Conte et al., 2020; **9** Reigada et al., 2019 **10** Giulivi et al., 2013 **11** Jyonouchi et al., 2019 **12** Abdel-Rahman et al., 2020**; 13** Singh et al., 2020**; 14** Ahn et al., 2020**; 15** Vandenberg et al., 2021; **16** Rossi et al., 2019; **17** Eltokhi et al., 2020; **18** Smith et al., 2020; **19** Stathopoulos et al., 2020; **20** Masino et al., 2009; **21** Bertelli et al., 2006; **22** Bottini et al., 2001; **23** Hettinger et al., 2008

Figure 3. An overview of the therapeutic approaches. Considering the important role of purinergic signaling in ASD pathophysiology, we summarize the main therapeutic approaches described both in ASD and associate disorders, emphasizing purinergic signaling modulation as a novel approach both in studies about pathophysiological mechanisms and innovative therapies. **ADC**: adenylate cyclase; **ENT**: Equilibrative Nucleoside Transporter; **PDE**: phosphodiesterase.
1 Ahmad et al., 2017b; **2** Ahmad et al., 2017a **3** Ahmad et al., 2018; **4** Ansari et al., 2017a **5** Ansari et al., 2017b; **6** Amodeo et al., 2018; **7** Lewis et al., 2020; **8** Behmanesh et al., 2019; **9** Naviaux et al., 2017; **10** Hirsch et al., 2020; **11** Naviaux et al., 2014; **12** Naviaux et al., 2015; **13** Tsimis et al., 2017; **14** Jimenez-Pacheco et al., 2016; **15** Engel et al., 2012; **16** Kim et al., 2011; **17** Sethna et al., 2017; **18** Mehan et al., 2020; **19** Matsuo et al., 2020; **20** Schmunk et al., 2017; **21** Reynolds et al., 2021 **22** Page et al., 1997

Table 1: Summary of all findings described in the section "7. Therapeutic Approaches and Purinergic System in ASD". In this table, the therapeutic

approaches are detailed, segregated by their functions in different biological tissues or structures, including descriptions of promising results in the context of ASD. Figure 3 illustrates these findings.

Therapeutic approach	Animal model	Outcome		Reference
Adenosine and P1 receptors modulators				
CGS 21680	BTBR mice	Splenic cells	↓ $CD4^+IL\text{-}21^+$, $CD4^+IL\text{-}22^+$, $CD4^+GATA3^+$, and $CD4^+T\text{-}bet^+$ ↓ $CD14^+TLR2^+$, $CD14^+TLR3^+$, $CD14^+TLR4^+$ ↑ $CD4^+CTLA\text{-}4$	(Ahmad et al., 2017a, 2017b)
		Splenic $CD8^+$ T cells	↓ $CCR3^+$, $CCR4^+$, $CCR5^+$, $CCR6^+$, $CCR7^+$, $CXCR3^+$, $CXCR4^+$, and $CXCR5^+$	(Ahmad et al., 2018)
		Total spleen and splenic $CD4^+$ T cells	↓ $IL\text{-}2^+$, $IL\text{-}6^+$, $IL\text{-}9^+$, $IFN\text{-}\gamma^+$, and $TNF\text{-}\alpha^+$ ↑ $TGF\text{-}\beta^+$	(Ansari et al., 2017a)
		$CD4^+$ cells	↓ IL-17A, RORγt, Stat3, and pStat3 ↑ $Foxp3^+$ and $IL\text{-}10^+$ (mRNA and protein expression)	(Ansari et al., 2017b)
		Brain tissue	↓ TLR2, TLR3, TLR4, and NF-κB mRNA and protein expression ↓ mRNA of C-C and C-X-C chemokine receptors ↓ IL-2, IL-6, IL-9, IFN-γ, and TNF-α ↑ TGF-β (mRNA and protein expression)	(Ahmad et al., 2017b, 2018; Ansari et al., 2017a)
		Behavior	Improvement in learning deficits, self-grooming behavior and response to the hot plate test	(Ansari et al., 2017a; Amodeo et al., 2018)
	C58 mice	Brain tissue	↑ BDNF mRNA expression (CGS, L-741,626, and CDPPB) ↑ Fos transcripts and Fos positive cells in dorsal striatum (CGS and CPA)	(Lewis et al., 2019; Muehlmann et al., 2020)
		Behavior	↓ repetitive motor behavior (CGS, L-741,626, and CDPPB) ↓ repetitive behavior (CGS and CPA)	(Lewis et al., 2019; Muehlmann et al., 2020)
	Deer mice	Behavior	↓ stereotypy behavior (CGS and CPA)	(Tanimura et al., 2010)
Propentofylline	Human	Behavior	↓ irritability (associated with risperidone)	(Behmanesh et al., 2019)
P2 receptors modulators				
Suramin	Human	Behavior	↓ repetitive behaviors Improvement in language and social interaction	(Naviaux et al., 2017)
	Rat ASD-model induced by VPA	Brain tissue	↓ IL-6 expression in medial prefrontal cortex	(Hirsch et al., 2020)
		Behavior	Improvement sociability behavior ↓ anxiety-like behavior	
	Rat ASD-model of MIA induced by poly(I:C)	Brain tissue	Normalization of metabolic pathways disturbed Improvement in the mitochondrial respiratory chain hyperactivity abnormalities Correction of phosphorylation of ERK1/2 and (CAMKII), Prevention of Purkinje cell loss	(Naviaux et al., 2013, 2014)

			Restoration of the diminished levels of P2X7 and P2Y2 immunocontent	
		Behavior	Amelioration in social behavior and the novelty preference Prevention in sensorimotor coordination deficits	(Naviaux et al., 2013, 2014)
	Fmr1 KO mice	Brain tissue	Normalization of abnormal synaptosomes and metabolomics alteration	(Naviaux et al., 2015)
		Behavior	Improvement in the animal performance in novelty preference, marble burying, and social behavior	
Brilliant Blue G	Rat ASD-model of MIA induced by LPS	Behavior	↓ preterm birth rate Improvement in neuromotor tests of the offspring Restoration of the density of cortical neurons	(Tsimis et al., 2017)
JNJ-47965567	*Status epilepticus* animal model	Behavior	JNJ-47965567: ↓ spontaneous seizures ↓ microgliosis and astrogliosis	(Jimenez-Pacheco et al., 2016)
A438079, OxATP, and A740003	*Status epilepticus* animal model	Behavior	A438079: ↓ seizure duration and the neuronal death A438079 (associated with OxATP and A740003): ↑ pilocarpine-induced seizure susceptibility	(Kim and Kang, 2011; Engel et al., 2012)
Adenylate cyclase modulators				
NB001	*Fmr1* KO mice	Behavior	Attenuation of social interaction deficits and stereotyped behaviors	(Sethna et al., 2017)
Diterpenoid Forskolin	Rat ASD-model induced by propionic acid	Brain tissue	Improvement in neuronal mitochondrial electron transport chain complexes Reduction in pro-inflammatory cytokines, oxidative stress, and lipid biomarkers levels	(Mehan et al., 2020)
		Behavior	Amelioration in memory dysfunction Decrease in muscle coordination and gait imbalance	
Other types of therapeutic molecules				
5-aminolevulinic acid	Rat ASD-model induced by VPA	Brain tissue	Amelioration in oxidative stress and mitochondrial dysfunction in the hippocampus Normalization of reduced parvalbumin-positive interneurons	(Matsuo et al., 2020)
		Behavior	Improvement in learning and memory	
Exogenous ATP and UTP	Primary astrocyte cultures derived from the Fmr1 KO mouse model		Elevation in intracellular Ca^{2+} responses and in synaptogenic protein TSP-1 expression	(Reynolds et al., 2021)
	Human primary skin fibroblasts from ASD patients		Decrease in Ca^{2+} release in ASD subjects	(Schmunk et al., 2017)
Exogenous UMP and CMP			Improvement in developmental delay and other autistic-associated characteristics.	(Page et al., 1997)

Figure 1

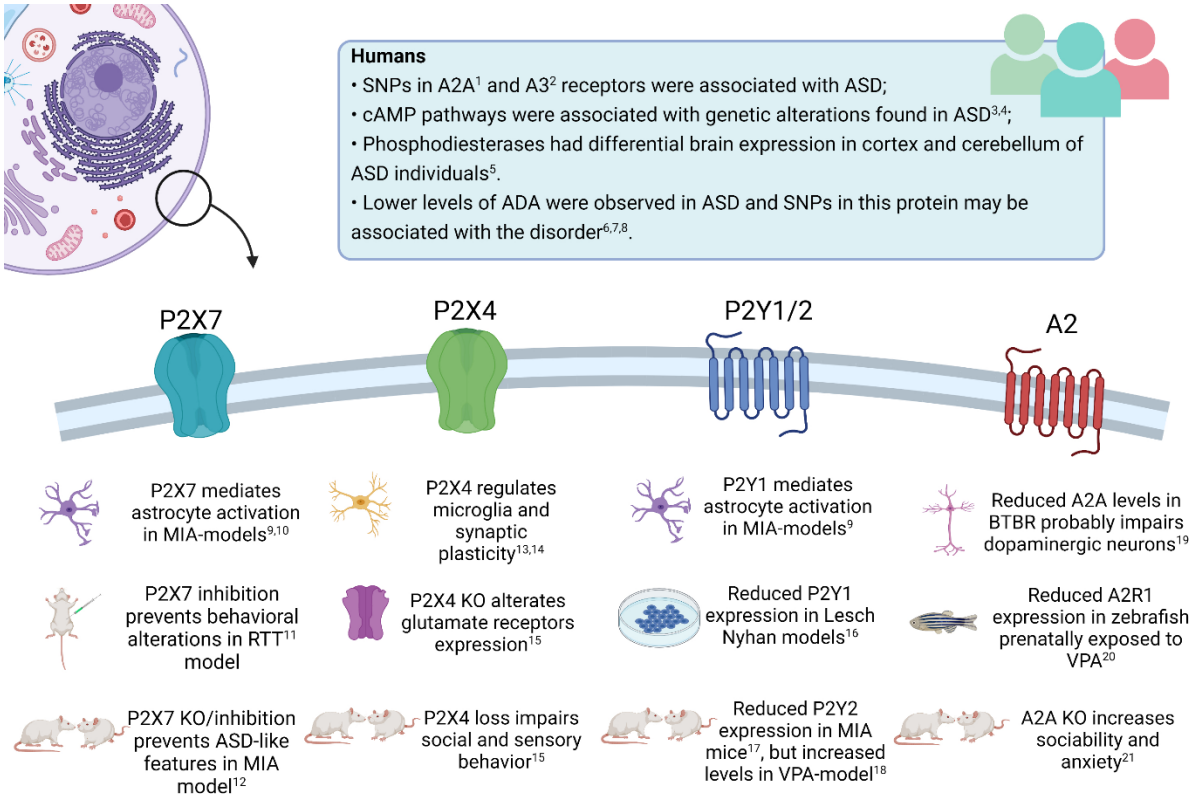
Humans
• SNPs in A2A[1] and A3[2] receptors were associated with ASD;
• cAMP pathways were associated with genetic alterations found in ASD[3,4];
• Phosphodiesterases had differential brain expression in cortex and cerebellum of ASD individuals[5].
• Lower levels of ADA were observed in ASD and SNPs in this protein may be associated with the disorder[6,7,8].
P2X7
P2X4
P2Y1/2
A2
P2X7 mediates astrocyte activation in MIA-models[9,10]
P2X4 regulates microglia and synaptic plasticity[13,14]
P2Y1 mediates astrocyte activation in MIA-models[9]
Reduced A2A levels in BTBR probably impairs dopaminergic neurons[19]
P2X7 inhibition prevents behavioral alterations in RTT[11] model
P2X4 KO alterates glutamate receptors expression[15]
Reduced P2Y1 expression in Lesch Nyhan models[16]
Reduced A2R1 expression in zebrafish prenatally exposed to VPA[20]
P2X7 KO/inhibition prevents ASD-like features in MIA model[12]
P2X4 loss impairs social and sensory behavior[15]
Reduced P2Y2 expression in MIA mice[17], but increased levels in VPA-model[18]
A2A KO increases sociability and anxiety[21]

Figure 2

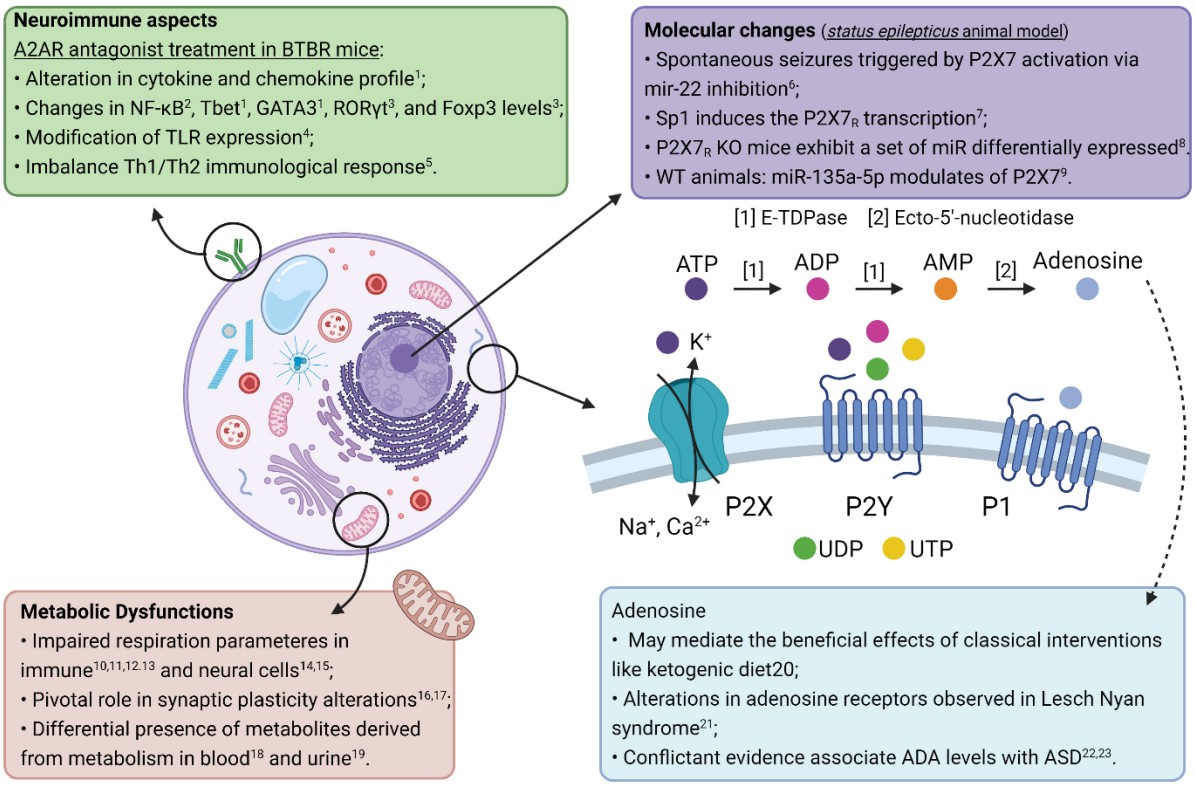
Neuroimmune aspects
A2AR antagonist treatment in BTBR mice:
• Alteration in cytokine and chemokine profile[1];
• Changes in NF-κB[2], Tbet[1], GATA3[1], RORγt[3], and Foxp3 levels[3];
• Modification of TLR expression[4];
• Imbalance Th1/Th2 immunological response[5].
Molecular changes (status epilepticus animal model)
• Spontaneous seizures triggered by P2X7 activation via mir-22 inhibition[6];
• Sp1 induces the P2X7R transcription[7];
• P2X7R KO mice exhibit a set of miR differentially expressed[8].
• WT animals: miR-135a-5p modulates of P2X7[9].
[1] E-TDPase [2] Ecto-5'-nucleotidase
ATP [1] ADP [1] AMP [2] Adenosine
K+
Na+, Ca2+
P2X
P2Y
P1
UDP
UTP
Metabolic Dysfunctions
• Impaired respiration parameteres in immune[10,11,12,13] and neural cells[14,15];
• Pivotal role in synaptic plasticity alterations[16,17];
• Differential presence of metabolites derived from metabolism in blood[18] and urine[19].
Adenosine
• May mediate the beneficial effects of classical interventions like ketogenic diet20;
• Alterations in adenosine receptors observed in Lesch Nyan syndrome[21];
• Conflictant evidence associate ADA levels with ASD[22,23].

Figure 3

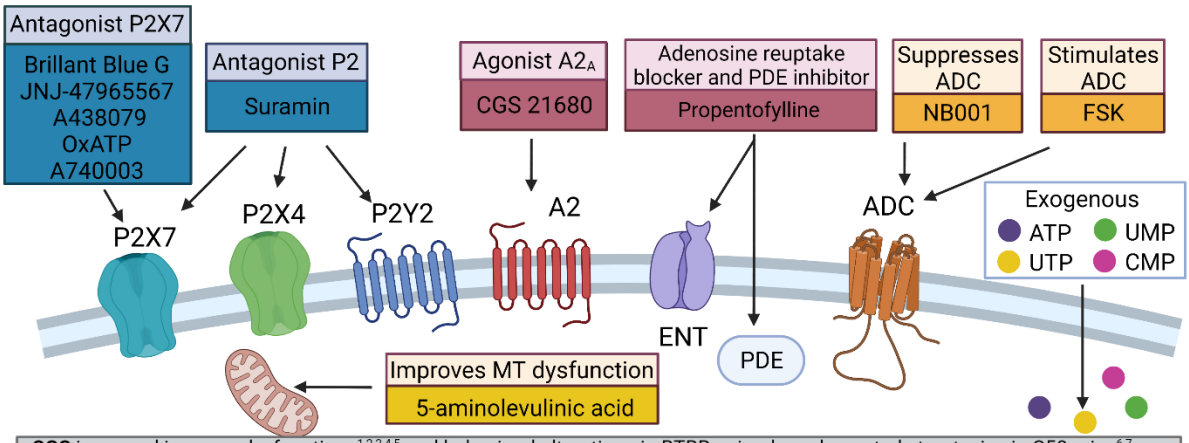

• **CGS** improved immune dysfunctions[1,2,3,4,5] and behavioral alterations in BTBR animals and reverted sterotypies in C58 mice[6,7].
• **Propentofylline*** + risperidone improved irritability in ASD[8].
• **Suramin*** improved ASD-like behaviors in humans[9] and in VPA[10], Poly(I:C)[11] and Fmr KO models[12], as well as immune and metabolic features.
• **BBG** prevented behavioral and cortical cytoarchitecture impairments induced by prenatal exposure to LPS[13].
• **JNJ-47965567**[14] and **A438079**[15] reduced seizure events in epileptic mice, while **OxATP**[16], **A438079**[16], and **A740003**[16] increased seizures in other model.
• **NB001** improved ASD-like traits in *Fmr* KO mice[17].
• **FSK** improved motor deficits, mitochondrial disfunctions and immune imbalance in an ASD model[18].
• **5-aminolevulinic Acid** improved behavioral and mitochondrial dysfunctions in the VPA model[19].
• Exogenous **ATP** and **UTP** modulated astrocyte function in *Fmr* KO mice[20,21].
• Exogenous **UMP*** and **CMP*** improved several features in patients with developmental delay[22].

*** These treatments presented promising effects in ASD individuals**

ANEXO 4 – Dados preliminares: expressão gênica de LHX6 e SOX6 em CPFm de animais de 30 dias

Método: RT-qPCR

A extração de RNA total foi realizada a partir das amostras de CPFm homogeneizadas em reagente Trizol®, utilizando clorofórmio, isopropanol e etanol. A síntese de DNA foi realizada a partir de quantidades iguais de RNA em todas as amostras utilizando a transcriptase reversa viral murina (MMLV). Em seguida, a amplificação do cDNA gerado foi utilizado para mensuração da expressão gênica relativa dos fatores de transcrição LHX6 e SOX6, finalizando a reação em cadeia da polimerase quantitativa em tempo real (RT-qPCR) conforme o protocolo descrito por Hirsch, MM *et al.*, 2018 adaptado para a mensuração de RNAm. Após essas análises, os valores de Ct (*Cycle Threshold*) serão utilizados para cálculo de expressão relativa de todos os RNA mensageiros, através do método $2^{-\Delta\Delta Ct}$ (PFAFFL, 2001), utilizando β3-tubulina como gene constitutivo. Análise estatística: test t student com correção de Welch.

Resultado: O grupo VPA apresentou aumento na expressão gênica relativa do fator LHX6 (Controle: 1,019±0,2105; VPA: 1,322±0,2723 p=0,0260). O fator SOX6 não apresentou diferenças significativas entre os grupos (p=0,5386).

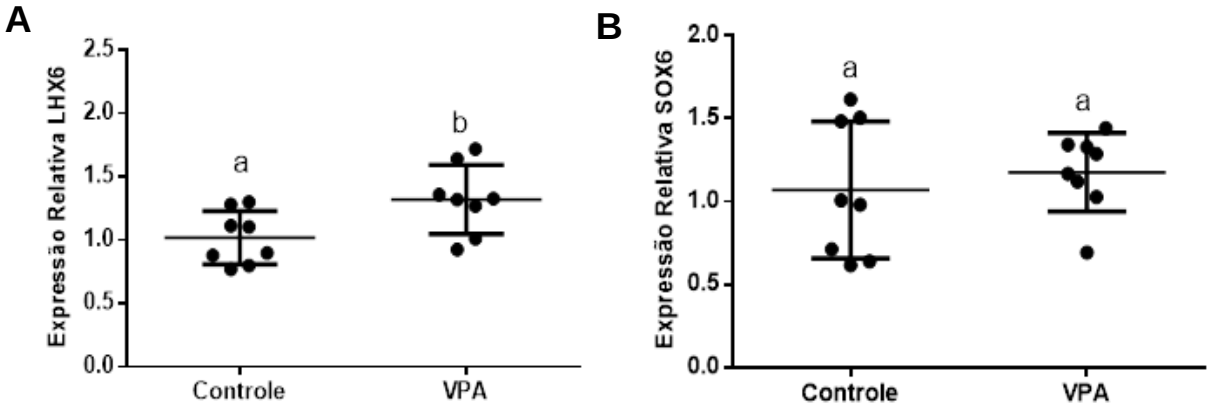

Figura 4: A exposição pré-natal ao VPA induz alterações na expressão gênica relativa do fator de transcrição LHX6, porém não de SOX6 em CPFm de animais jovens. A) VPA induziu aumento na expressão gênica relativa do fator LHX6. **B)** Não houve diferenças significativa na expressão gênica relativa de SOX6**.** Letras diferentes indicam diferenças significativas entre os grupos. Valores plotados no formato Média ± DP

ANEXO 5 – Dados preliminares: análise da composição neuronal em CPFm de animais de 120 dias.

Método: imunofluorescência indireta, conforme descrito no Capítulo II

Resultado; Análise histológica do córtex pré-frontal medial de animais adultos.

O grupo VPA demonstrou redução em número de interneurônios PV (Controle: 198±5,315; VPA: 162,5±20,04; RSV: 190,0+16,27 ; RSV+VPA: 184,0±2,000 p=0,0167 Cont-VPA F (3, 11) = 4,914) (Figura Anexo 5D), razão de interneurônios PV+ (Controle:0,07907±0,003429; RSV:0,07167±0,006449; VPA:0,05961±0,003564; RSV+VPA:0,06984±0,004641 p=0,0016 Cont-VPA F (3, 10) = 9,551) (Anexo 5E) números de interneurônios SOM+ (Controle:175,0±19,47; RSV:171,3±18,01; VPA: 138,5±6,455; RSV+VPA:149,7±15,89 F (3, 9) = 1,543) (Anexo 5G) e razão de interneurônios SOM+ (Controle:0,06828±0,006142;RSV:0,06539±0,007731; VPA:0,05789±0,007760; RSV+VPA:0,07690 ±0,004004 p=0,0324 F (3, 9) = 5,308) (Figura 7E). O grupo VPA não apresentou alterações no número de neurônios totais (pANOVA: 0,6656; F (3, 11) = 0,5386), no número de interneurônios CB+ (p=0,0673; F (3, 11) = 3,177) (Figura Anexo 5B) e na razão de interneurônios CB+ (p=0,1155 F (3, 11) = 0,5386) (Figura Anexo 5C). O número de neurônios totais não apresentou diferenças significativas nas subregiões e camadas (Figura Anexo 5A) (dados completos com médias, desvios e valores de p constam na Tabela 1 do Anexo 5). Os dados significativos referentes à distribuição de interneurônios ao longo das subregiões e camadas no CPFm foram compilados na Tabela 2 do Anexo 5

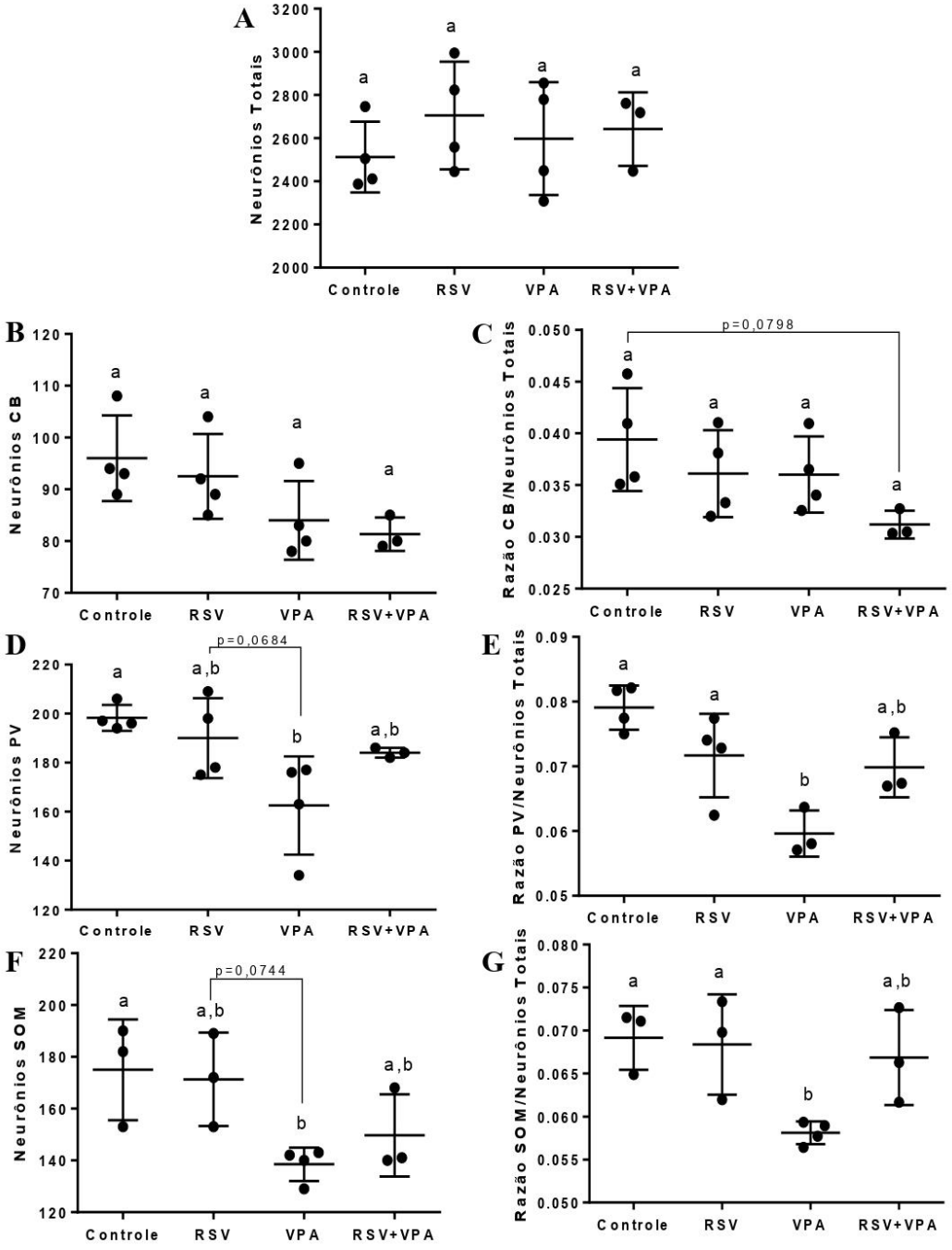

Figura Anexo 5: A exposição pré-natal ao VPA induziu alterações pontuais em parâmetros relativos aos interneurônios em CPFm de animais adultos. A) Não houve diferenças quantitativas em neurônios totais no CPFm **B,C)** Não houve diferenças quantitativas interneurônios CB+**. D,E)** VPA induz redução tanto no número quanto na razão de interneurônios PV+. **F,G)** VPA induz redução tanto no

número quanto na razão de interneurônios SOM+**.** Letras diferentes indicam diferenças significativas entre os grupos. Valores plotados no formato Média ± DP

Tabela 1, Anexo 5 : Análise quantitativa de neurônios totais nas diferentes subregiões do CPFm de animais adultos (total e segregada em camadas superiores e inferiores). Todas as subregiões e camadas replicaram o padrão de resultado identificado no CPFm total. Valores apresentados no formato Média ± DP

Região	Parâmetro	Grupos Experimentais	Valor de *p*
Camadas Superiores	Neurônios Totais	Controle 303,8 ± 34,71 a RSV 300,5 ± 32,55 a VPA 300,8 ± 21,93 a RSV+VPA 337,0 ± 40,63 a	>0,05
Camadas Profundas	Neurônios Totais	Controle 458,8 ± 30,41 a RSV 499,3 ± 61,17 a VPA 505,3 ± 80,34 a RSV+VPA 540,3 ± 58,05 a	>0,05
Córtex Cingulado Anterior	Neurônios Totais	Controle 762,5 ± 57,49 a RSV 799,8 ± 82,50 a VPA 806,0 ± 65,29 a RSV+VPA 877,3 ± 97,09 a	>0,05
Região	**Parâmetro**	**Grupos Experimentais**	**Valor de *p***
Camadas Superiores	Neurônios Totais	Controle 314,0 ± 42,76 a RSV 322,8 ± 32,94 a VPA 268,8 ± 45,83 a RSV+VPA 303,3 ± 56,89 a	>0,05
Camadas Profundas	Neurônios Totais	Controle 503,3 ± 23,07 a RSV 564,5 ± 128,3 a VPA 511,5 ± 17,21 a RSV+VPA 516,7 ± 44,11 a	>0,05
Córtex Pré Límbico	Neurônios Totais	Controle 817,3 ± 65,52 a RSV 887,3 ± 132,3 a VPA 780,3 ± 53,01 a RSV+VPA 820,0 ± 73,63 a	>0,05
Região	**Parâmetro**	**Grupos Experimentais**	**Valor de *p***
Camadas Superiores	Neurônios Totais	Controle 336,8 ± 81,54 a RSV 336,5 ± 35,03 a VPA 286,5 ± 46,32 a RSV+VPA 348,3 ± 17,90 a	>0,05
Camadas Profundas	Neurônios Totais	Controle 531,0 ± 16,55 a RSV 554,8 ± 54,71 a VPA 499,3 ± 84,87 a RSV+VPA 567,0 ± 73,51 a	>0,05
Córtex Infra Límbico	Neurônios Totais	Controle 867,8 ± 67,39 a RSV 891,3 ± 68,67 a VPA 785,8 ± 93,46 a RSV+VPA 915,3 ± 67,28 a	>0,05

Tabela 2, Anexo 5: descrição geral de parâmetros estatísticos associados à distribuição e proporção de interneurônios para subregiões e camadas do CPFm de animais adultos.

Região	Parâmetro	Grupos Experimentais	Valor de *p*
Camadas Superiores	Neurônios CB	Controle 13,75 ± 1,708 a RSV 12,25 ± 1,708 a VPA 15,50 ± 1,000 a RSV+VPA 11,67 ± 2,887 a	>0,05
	Razão CB/Neurônios Totais	Controle 0,04536 ± 0,003957 a,b RSV 0,04131 ± 0,008000 a,b VPA 0,05167 ± 0,003712 a RSV+VPA 0,0343 ± 0,004290 **b**	p=0,0060 (VPA-RSV+VPA)
Camadas Profundas	Neurônios CB	Controle 14,25 ± 2,986 a RSV 16,25 ± 2,754 a VPA 16,25 ± 6,752 a RSV+VPA 15,33 ± 3,055 a	>0,05
	Razão CB/Neurônios Totais	Controle 0,03109 ± 0,006538 a RSV 0,03267 ± 0,004932 a VPA 0,03172 ± 0,009782 a RSV+VPA 0,02819 ± 0,002827 a	>0,05
Córtex Cingulado Anterior	Neurônios CB	Controle 28,00 ± 4,243 a RSV 28,50 ± 2,887 a VPA 31,75 ± 6,185 a RSV+VPA 27,00 ± 5,568 a	>0,05
	Razão CB/Neurônios Totais	Controle 0,03677 ± 0,005281 a RSV 0,03576 ± 0,003281 a VPA 0,03930 ± 0,006012 a RSV+VPA 0,03056 ± 0,002893 a	>0,05

Região	Parâmetro	Grupos Experimentais	Valor de *p*
Camadas Superiores	Neurônios CB	Controle 17,50 ± 2,646 a RSV 13,00 ± 1,414 a,b VPA 11,25 ± 3,304 **b** RSV+VPA 13,00 ± 1,732 a,b	p=0,0182 (Cont-VPA)
	Razão CB/Neurônios Totais	Controle 0,05585 ± 0,005523 a RSV 0,04047 ± 0,004903 a VPA 0,04301 ± 0,01646 a RSV+VPA 0,04334 ± 0,005979 a	>0,05
Camadas Profundas	Neurônios CB	Controle 18,50 ± 2,380 a RSV 19,00 ± 3,162 a VPA 12,75 ± 1,500 **b** RSV+VPA 14,00 ± 2,000 a,b	p=0,0247 (Cont-VPA) p=0,0150 (RSV-VPA)
	Razão CB/Neurônios Totais	Controle 0,03698 ± 0,006362 a RSV 0,03452 ± 0,006771 a,b VPA 0,02493 ± 0,002832 **b** RSV+VPA 0,02745 ± 0,006316 a,b	p=0,0461 (Cont-VPA)
Córtex Pré-Límbico	Neurônios CB	Controle 36,00 ± 2,582 a RSV 32,00 ± 2,708 a,c VPA 24,00 ± 2,944 **b**,c RSV+VPA 27,00 ± 3,606 **c**	p=0,0006 (Cont-VPA) p=0,0091 (Cont-RSV+VPA) p=0,0119 (RSV-VPA)
	Razão CB/Neurônios Totais	Controle 0,04428 ± 0,005067 a RSV 0,03668 ± 0,006161 a,b VPA 0,03091 ± 0,004947 b RSV+VPA 0,03317 ± 0,006146 a,b	p=0,0259 (Cont-VPA)

Região	Parâmetro	Grupos Experimentais	Valor de *p*
Camadas Superiores	Neurônios CB	Controle 13,75 ± 2,062 a RSV 13,75 ± 1,500 a VPA 13,50 ± 1,732 a RSV+VPA 11,33 ± 1,155 a	>0,05
	Razão CB/Neurônios Totais	Controle 0,04175 ± 0,006157 a RSV 0,04096 ± 0,003463 a VPA 0,04844 ± 0,01279 a RSV+VPA 0,03251 ± 0,002429 a	>0,05
Camadas Profundas	Neurônios CB	Controle 18,25 ± 3,403 a RSV 18,25 ± 3,403 a VPA 16,25 ± 3,594 a RSV+VPA 16,00 ± 1,732 a	>0,05
	Razão CB/Neurônios Totais	Controle 0,03430 ± 0,005804 a RSV 0,03295 ± 0,005441 a VPA 0,03238 ± 0,002052 a RSV+VPA 0,02833 ± 0,002576 a	>0,05
Córtex Infra Límbico	Neurônios CB	Controle 32,00 ± 2,944 a RSV 32,00 ± 2,828 a VPA 29,75 ± 3,304 a RSV+VPA 27,33 ± 1,528 a	>0,05
	Razão CB/Neurônios Totais	Controle 0,03716 ± 0,005501 a RSV 0,03601 ± 0,003551 a VPA 0,03602 ± 0,001651 a RSV+VPA 0,02989 ± 0,0007889 a	>0,05

Região	Parâmetro	Grupos Experimentais	Valor de *p*
Camadas Superiores	Neurônios PV	Controle 22,75 ± 2,986 a RSV 24,75 ± 5,500 a VPA 22,50 ± 3,000 a RSV+VPA 23,33 ± 2,517 a	>0,05
	Razão PV/Neurônios Totais	Controle 0,07473 ± 0,003690 a RSV 0,07042 ± 0,006746 a VPA 0,06646 ± 0,008107 a RSV+VPA 0,06443 ± 0,01019 a	>0,05
Camadas Profundas	Neurônios PV	Controle 44,00 ± 7,165 a RSV 41,50 ± 5,447 a VPA 36,00 ± 11,97 a RSV+VPA 36,67 ± 6,807 a	>0,05
	Razão PV/Neurônios Totais	Controle 0,09362 ± 0,009725 a RSV 0,08354 ± 0,01430 a VPA 0,07397 ± 0,02118 a RSV+VPA 0,07349 ± 0,01193 a	>0,05
Córtex Cingulado Anterior	Neurônios PV	Controle 66,75 ± 9,069 a RSV 66,25 ± 9,215 a VPA 58,50 ± 10,66 a RSV+VPA 60,00 ± 8,000 a	>0,05
	Razão PV/Neurônios Totais	Controle 0,08623 ± 0,006285 a RSV 0,07820 ± 0,01037 a VPA 0,07119 ± 0,01504 a RSV+VPA 0,06976 ± 0,01056 a	>0,05

Região	Parâmetro	Grupos Experimentais	Valor de *p*
Camadas Superiores	Neurônios PV	Controle 22,50 ± 4,655 a RSV 26,50 ± 2,380 a VPA 23,50 ± 9,327 a RSV+VPA 24,67 ± 2,517 a	>0,05
	Razão PV/Neurônios Totais	Controle 0,06997 ± 0,004804 a RSV 0,06962 ± 0,009277 a VPA 0,06376 ± 0,01655 a RSV+VPA 0,07492 ± 0,009333 a	>0,05
Camadas Profundas	Neurônios PV	Controle 37,50 ± 4,203 a RSV 34,00 ± 1,414 a VPA 31,25 ± 8,995 a RSV+VPA 31,67 ± 6,807 a	>0,05
	Razão PV/Neurônios Totais	Controle 0,06927 ± 0,007092 a RSV 0,06446 ± 0,007745 a VPA 0,06011± 0,01693 a RSV+VPA 0,06036 ± 0,009731 a	>0,05
Córtex Pré Límbico	Neurônios PV	Controle 60,00 ± 7,118 a RSV 60,50 ± 3,317 a VPA 54,75 ± 14,31 a RSV+VPA 56,33 ± 4,619 a	>0,05
	Razão PV/Neurônios Totais	Controle 0,06958 ± 0,004594 a RSV 0,06639 ± 0,005972 a VPA 0,06212 ± 0,01381 a RSV+VPA 0,06608 ± 0,007713 a	>0,05

Região	Parâmetro	Grupos Experimentais	Valor de *p*
Camadas Superiores	Neurônios PV	Controle 20,50 ± 4,359 a RSV 23,50 ± 2,380 a VPA 18,50 ± 9,147 a RSV+VPA 25,00 ± 4,583 a	>0,05
	Razão PV/Neurônios Totais	Controle 0,06311 ± 0,01241 a RSV 0,06590 ± 0,007151 a VPA 0,05188 ± 0,02133 a RSV+VPA 0,06788 ± 0,006178 a	>0,05
Camadas Profundas	Neurônios PV	Controle 51,00 ± 3,559 a RSV 39,75 ± 7,411 a,b VPA 30,75 ± 10,78 **b** RSV+VPA 42,67 ± 4,933 a,b	p=0,0117 (Cont-VPA)
	Razão PV/Neurônios Totais	Controle 0,09290 ± 0,004066 a RSV 0,06968 ± 0,01757 a,b VPA 0,05617 ± 0,02071 **b** RSV+VPA 0,07764 ± 0,009229 a,b	p=0,0223 (Cont-VPA)
Córtex Infra Límbico	Neurônios PV	Controle 71,50 ± 7,416 a RSV 63,25 ± 8,500 a VPA 49,25 ± 17,00 a RSV+VPA 67,67 ± 9,452 a	>0,05
	Razão PV/Neurônios Totais	Controle 0,08164 ± 0,006639 a RSV 0,06812 ± 0,01271 a,b VPA 0,05510 ± 0,01865 **b** RSV+VPA 0,07328 ± 0,004988 a,b	p=0,0485 (Cont-VPA)

Região	Parâmetro	Grupos Experimentais	Valor de *p*
Camadas Superiores	Neurônios SOM	Controle 19,67 ± 4,163 a RSV 19,00 ± 3,606 a VPA 16,25 ± 1,258 a RSV+VPA 21,00 ± 3,000 a	>0,05
	Razão SOM/Neurônios Totais	Controle 0,06828 ± 0,006142 a RSV 0,06539 ± 0,007731 a VPA 0,05789 ± 0,007760 a RSV+VPA 0,07690 ± 0,004004 a	>0,05
Camadas Profundas	Neurônios SOM	Controle 37,33 ± 8,963 a RSV 38,67 ± 3,786 a VPA 27,50 ± 3,000 a RSV+VPA 28,67 ± 2,082 a	
	Razão SOM/Neurônios Totais	Controle 0,07232 ± 0,007257 a RSV 0,07849 ± 0,008329 a VPA 0,05626 ± 0,006632 **b** RSV+VPA 0,06444 ± 0,004962 a,b	p=0,0395 (Cont-VPA) p=0,0081 (RSV-VPA)
Córtex Cingulado Anterior	Neurônios SOM	Controle 57,00 ± 13,08 a RSV 57,67 ± 7,371 a VPA 43,75 ± 3,096 a RSV+VPA 49,67 ± 5,033 a	>0,05
	Razão SOM/Neurônios Totais	Controle 0,07079 ± 0,006398 a RSV 0,07353 ± 0,005973 a VPA 0,05663 ± 0,004197 **b** RSV+VPA 0,06913 ± 0,004454 a	p=0,0264 (Cont-VPA) p=0,0097 (RSV-VPA) p=0,0493 (RSV+VPA-VPA)
Região	**Parâmetro**	**Grupos Experimentais**	**Valor de *p***
Camadas Superiores	Neurônios SOM	Controle 19,33 ± 4,509 a RSV 20,33 ± 2,082 a VPA 18,00 ± 2,828 a RSV+VPA 18,00 ± 3,606 a	>0,05
	Razão SOM/Neurônios Totais	Controle 0,06676 ± 0,009146 a RSV 0,06680 ± 0,007617 a VPA 0,06271 ± 0,009601 a RSV+VPA 0,06719 ± 0,01386 a	>0,05
Camadas Profundas	Neurônios SOM	Controle 37,67 ± 4,933 a RSV 39,67 v 0,5774 a VPA 30,50 ± 2,887 a RSV+VPA 31,67 ± 5,033 a	>0,05
	Razão SOM/Neurônios Totais	Controle 0,07502 ± 0,001874 a RSV 0,07413 ± 0,01233 a VPA 0,06059 ± 0,005188 a RSV+VPA0,06701 ± 0,005013 a	>0,05
Córtex Pré-Límbico	Neurônios SOM	Controle 57,00 ± 8,888 a RSV 60,00 v 1,732 a VPA 48,50 ± 1,732 a RSV+VPA 49,67 ± 5,686 a	>0,05
	Razão SOM/Neurônios Totais	Controle 0,07200 ± 0,002774 a RSV 0,07113 ± 0,007633 a VPA 0,06145 ± 0,004613 a RSV+VPA 0,06717 ± 0,006318 a	>0,05

Região	Parâmetro	Grupos Experimentais	Valor de *p*
Camadas Superiores	Neurônios SOM	Controle 18,33 ± 1,528 a RSV 16,33 v 2,082 a VPA 17,75 ±2,062 a RSV+VPA 19,67 ± 0,5774 a	>0,05
	Razão SOM/Neurônios Totais	Controle 0,06369 ± 0,01016 a RSV 0,05573 ± 0,005235 a VPA 0,05851 ± 0,005078 a RSV+VPA 0,07162 ± 0,009008 a	>0,05
Camadas Profundas	Neurônios SOM	Controle 36,00 ± 8,888 a RSV 37,33 ± 8,021 a VPA 28,50 ± 3,416 a RSV+VPA 30,67 ± 7,095 a	>0,05
	Razão SOM/Neurônios Totais	Controle 0,06572 ± 0,009027 a RSV 0,06415 ± 0,01310 a VPA 0,05534 ± 0,007051 a RSV+VPA 0,06038 ± 0,007218 a	>0,05
Córtex Infra Límbico	Neurônios SOM	Controle 54,33 ± 8,963 a RSV 53,67 ± 9,713 a VPA 46,25 ± 5,439 a RSV+VPA 50,33 ± 7,024 a	>0,05
	Razão SOM/Neurônios Totais	Controle 0,06499 ± 0,004196 a RSV 0,06133 ± 0,01035 a VPA 0,05650 ± 0,006323 a RSV+VPA 0,06447 ± 0,005984 a	>0,05